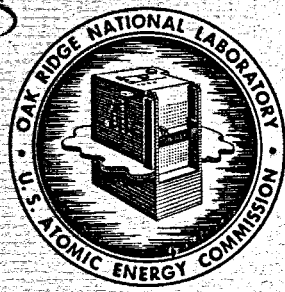


SEP 15 1965



OAK RIDGE NATIONAL LABORATORY
operated by
UNION CARBIDE CORPORATION
for the
U.S. ATOMIC ENERGY COMMISSION



ORNL-TM- 1060

171

MOLTEN SALT CONVERTER REACTOR
DESIGN STUDY AND POWER COST ESTIMATES FOR A
1000 Mwe STATION

L. G. Alexander
W. L. Carter
C. W. Craven
D. B. Janney
T. W. Kerlin
R. Van Winkle

RELEASED FOR ANNOUNCEMENT
IN NUCLEAR SCIENCE ABSTRACTS

NOTICE This document contains information of a preliminary nature and was prepared primarily for internal use at the Oak Ridge National Laboratory. It is subject to revision or correction and therefore does not represent a final report.

LEGAL NOTICE

This report was prepared as an account of Government sponsored work. Neither the United States, nor the Commission, nor any person acting on behalf of the Commission:

- A. Makes any warranty or representation, expressed or implied, with respect to the accuracy, completeness, or usefulness of the information contained in this report, or that the use of any information, apparatus, method, or process disclosed in this report may not infringe privately owned rights; or
- B. Assumes any liabilities with respect to the use of, or for damages resulting from the use of any information, apparatus, method, or process disclosed in this report.

As used in the above, "person acting on behalf of the Commission" includes any employee or contractor of the Commission, or employee of such contractor, to the extent that such employee or contractor of the Commission, or employee of such contractor prepares, disseminates, or provides access to, any information pursuant to his employment or contract with the Commission, or his employment with such contractor.

ORNL TM-1060

Contract No. W-7405-eng-26

REACTOR DIVISION

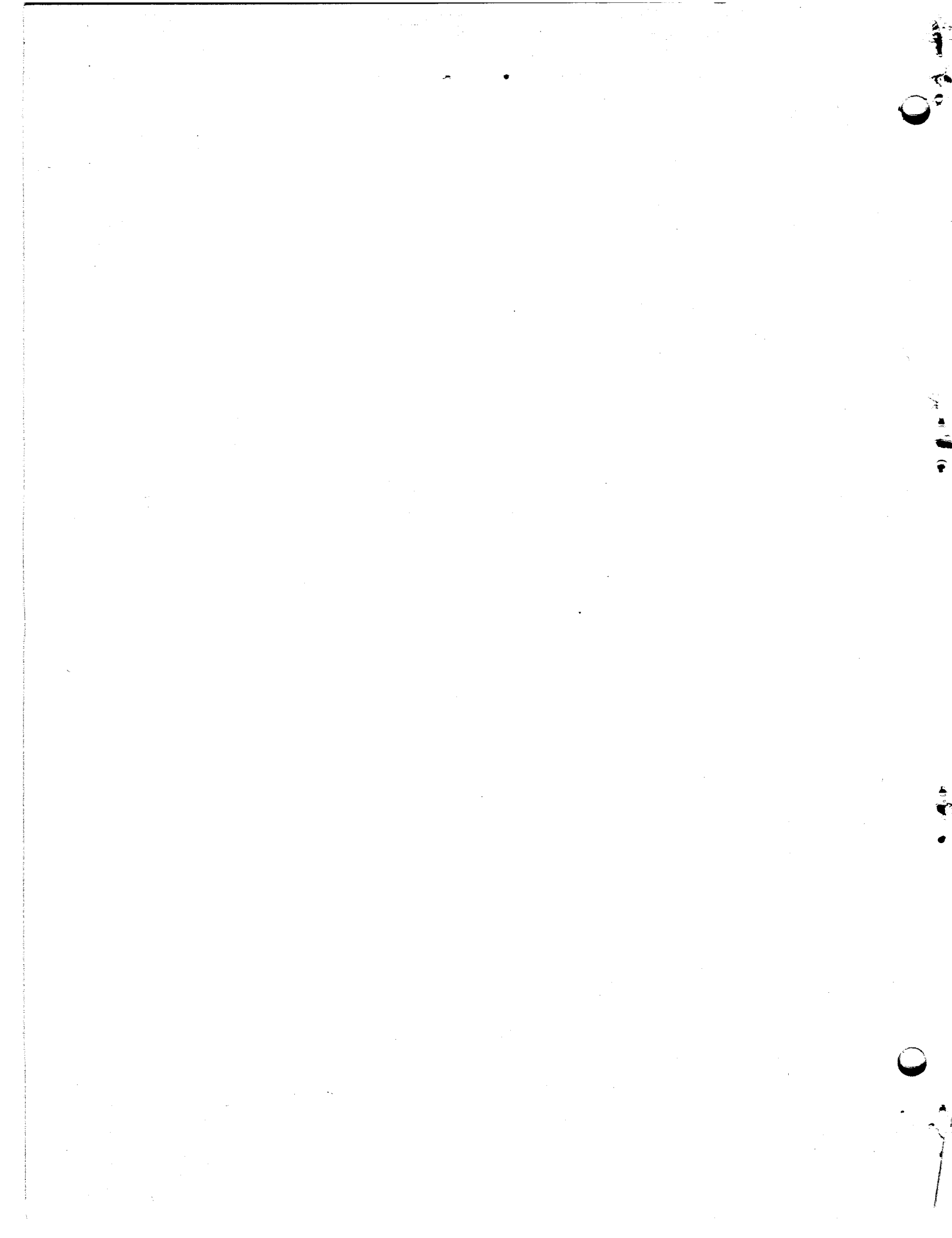
MOLTEN SALT CONVERTER REACTOR

Design Study and Power Cost Estimates for a
1000 Mwe Station

L. G. Alexander, W. L. Carter, C. W. Craven, D. B. Janney,
T. W. Kerlin, and R. Van Winkle

SEPTEMBER 1965

OAK RIDGE NATIONAL LABORATORY
Oak Ridge, Tennessee
Operated by
UNION CARBIDE CORPORATION
for the
U. S. ATOMIC ENERGY COMMISSION



FOREWORD

A molten-salt-breeder reactor was evaluated at the Oak Ridge National Laboratory beginning in 1959. Because a number of the features postulated had not been demonstrated at that time, the realization of a breeder appeared to lie rather far in the future. Accordingly, the study of the near-term, one-region, one-fluid molten-salt converter described in this report was begun in July 1961 and completed in December 1962. Since then, several advances have been made in molten-salt technology which make the breeder reactor much less remote and modify some of the conclusions in this report.

Briefly, these advances include:

1. Progress in core graphite design which greatly simplifies previous problems of separating the core into two regions — one for the uranium-bearing fuel salt and one for the thorium-bearing blanket salt. The new design utilizes a liquid-lead seal around the tops of graphite tubes containing fuel salt that allows the tubes to expand or contract freely while maintaining an absolute seal between fuel and blanket fluids.* The addition of a blanket results in a much better conversion than obtained in this report and leads directly to an attractive breeder.

2. Thermal engineering studies which show that the Loeffler boiler system can advantageously be replaced by a supercritical boiler. Thermal stress problems are reduced, overall thermodynamic efficiency is increased, and capital costs are considerably reduced. In addition, studies of sodium metal and of mixtures of alkali carbonates show that if either of these inexpensive materials can be safely used for the intermediate coolant in place of the costly lithium-beryllium fluoride mixtures postulated in this study, then further large cost reductions can be realized.[†]

*E. S. Bettis, Oak Ridge National Laboratory, personal communication with L. G. Alexander, Oak Ridge National Laboratory, January 1965.

[†]C. W. Collins, Oak Ridge National Laboratory, personal communication with L. G. Alexander, Oak Ridge National Laboratory, January 1965.

3. A fuel purification process based on simple distillation^f which not only reduces processing costs[§] but permits reuse of the carrier salts - an advantage not assumed in this study.

As a result of these developments, we believe that fuel cycle costs for a two-region breeder based on 1965 technology will be only 0.3 to 0.4 mill** compared to the 0.68 mill/kwhr shown in Table 6.10 for the MSCR.

^fM. J. Kelley, Oak Ridge National Laboratory, personal communication with L. G. Alexander, Oak Ridge National Laboratory, January 1965.

[§]W. L. Carter, Oak Ridge National Laboratory, personal communication with L. G. Alexander, Oak Ridge National Laboratory, January 1965.

**H. F. Bauman, Oak Ridge National Laboratory, personal communication with L. G. Alexander, Oak Ridge National Laboratory, January 1965.

CONTENTS

	<u>Page</u>
ABSTRACT	1
1. SUMMARY	1
1.1 Description	3
1.2 Fuel Reprocessing	3
1.3 Nuclear and Thermal Performance	3
1.4 Fuel Cycle Cost	4
1.5 Power Costs	5
1.6 Advanced MSCR	6
1.7 Post Script - January 1965	7
2. INTRODUCTION	8
2.1 Purpose, Scope, and Method of Approach	8
2.1.1 Figure of Merit	8
2.1.2 Reactor Concept	8
2.1.3 Procedure	8
2.2 Status of Molten Salt Reactor Development	9
2.2.1 Early Work	9
2.2.2 The Molten Salt Reactor Program	10
2.2.3 Fuel Development	10
2.2.4 Container Development	12
2.2.5 Moderator Development	13
2.2.6 Component Development	14
2.2.7 Reactor Vessel	14
2.2.8 Molten Salt Pumps	14
2.2.9 Molten Salt Heat Exchangers and Steam Boilers	14
2.2.10 Freeze Valves and Freeze Flanges	15
2.2.11 Molten Salt Instrumentation and Special Equipment	16
2.2.12 Remote Maintenance	16
2.2.13 Chemical Processing of Molten Salt Fuels	18
2.2.14 Fluoride Volatility and HF Solution Processes	18
2.2.15 Thorex Process	19

CONTENTS (continued)

	<u>Page</u>
2.2.16 Fractional Crystallization Process	20
2.2.17 Other Processes	20
2.2.18 Molten Salt Reactor Studies	21
2.3 Molten Salt Reactor Experiment	22
3. BASES AND ASSUMPTIONS	23
3.1 Design Bases	23
3.1.1 Reactor Concept	23
3.1.2 Design Calculations	23
3.1.3 Station Power	23
3.1.4 Plant Utilization Factor	24
3.1.5 Thermal Efficiency	24
3.1.6 Fueling Cycle	24
3.1.7 Processing	24
3.1.8 Feed and Recycle	25
3.1.9 Isotopic Composition of Lithium	25
3.1.10 Energy Conversion System	25
3.1.11 Primary Heat Exchanger Requirements	26
3.1.12 Minimum Salt Temperatures	26
3.2 Cost Bases	26
3.2.1 Value of Fissile Isotopes	26
3.2.2 Value of Thorium	27
3.2.3 Value of LiF(99.995% ⁷ Li)	27
3.2.4 Value of BeF ₂	27
3.2.5 Value of Base Salt	27
3.2.6 Cost of Compounding and Purifying Fuel Salt	27
3.2.7 INOR-8 Cost	27
3.2.8 Moderator Graphite Cost	28
3.2.9 Annual Fixed Charges	28
3.2.10 Central Fluoride Volatility Plant Processing Charges	29
3.3 Special Assumptions	29
3.3.1 Permeation of Graphite by Salt	29

CONTENTS (continued)

	<u>Page</u>
3.3.2 Permeation of Graphite by $^{135}\text{Xenon}$	30
3.3.3 Corrosion Products	30
3.3.4 Approach to Equilibrium	31
4. DESCRIPTION OF MSCR CONCEPT	32
4.1 General Description	32
4.2 Site Plan	32
4.3 Structures	40
4.4 Primary System Components	44
4.4.1 Reactor Vessel	44
4.4.2 Moderator Structure	45
4.4.3 Fuel-Salt Circulating Pumps	45
4.4.4 Primary Heat Exchanger	48
4.5 Intermediate Cooling System	51
4.5.1 Introduction	51
4.5.2 Coolant Salt Pumps	51
4.5.3 Steam Superheaters	51
4.5.4 Steam Reheaters	53
4.6 Power Generation System	53
4.6.1 Introduction	53
4.6.2 Loeffler Boiler System	54
4.6.3 Steam Circulators	55
4.6.4 Turbogenerator	57
4.7 Reactor Control System	57
4.7.1 Introduction	57
4.7.2 Shim Control	58
4.7.3 Emergency Control	58
4.8 Salt Handling Systems	59
4.8.1 Introduction	59
4.8.2 Fuel Salt Preparation	59
4.8.3 Coolant Salt Preparation	61
4.8.4 Reactor Salt Purification	61
4.8.5 Coolant-Salt Purification	62

CONTENTS (continued)

	<u>Page</u>
4.8.6 Reactor Salt Charging System	63
4.8.7 Intermediate Coolant Charging System	63
4.8.8 UF ₄ Addition Facility	63
4.8.9 Fuel Salt Drain and Storage System	64
4.8.10 Coolant Salt Drain System	66
4.8.11 Spent Fuel Withdrawal System	66
4.8.12 High Level Radioactive Salt Sampler	67
4.8.13 Coolant Salt Sampling	69
4.8.14 Freeze Valves	69
4.9 Auxiliary Services and Equipment	70
4.9.1 Introduction	70
4.9.2 Helium Cover Gas Supply and Distribution System	70
4.9.3 Reagent Gas Supply and Disposal System	72
4.9.4 Waste Gas System	72
4.9.5 Liquid Waste Disposal System	73
4.9.6 Coolant Pump Lubricating Oil Systems	74
4.9.7 Preheating System	74
4.9.8 Auxiliary Power	74
4.9.9 Service Water System	75
4.9.10 Control and Station Air Systems	75
4.9.11 Cranes and Hoists	75
4.9.12 Instrumentation and Control	76
4.9.13 Plant Utilities	76
4.10 MSCR Design Specifications	77
5. FUEL PROCESSING	91
5.1 Reprocessing System	91
5.2 Fluoride Volatility Central Plant	91
5.2.1 Process Design	92
5.2.2 Shipping	94
5.2.3 Prefluorination Storage Tanks	94
5.2.4 Fluorinator	96
5.2.5 CRP Trap and NaF Absorbers	98

CONTENTS (continued)

	<u>Page</u>
5.2.6 Cold Traps	100
5.2.7 Reduction Reactor	100
5.2.8 Transfer Tanks	100
5.2.9 Waste Storage Tanks	100
5.2.10 Freeze Valves	102
5.2.11 Samplers	102
5.2.12 Biological Shield	102
5.2.13 Process Equipment Layout	102
5.2.14 Plant Layout	105
5.2.15 Capital Cost Estimate	105
5.2.16 Operating and Maintenance Cost Estimates	113
5.2.17 MSCR Irradiated Fuel Shipping Cost	113
5.2.18 MSCR Unit Processing Cost	117
5.3 Thorex Central Plant	118
5.3.1 Head-End Treatment	119
5.3.2 Solvent Extraction	121
5.3.3 Tail-End Treatment	121
5.3.4 Processing Costs	123
5.4 Comparison of Processing Cost Estimates	125
6. FUEL CYCLE ANALYSIS	127
6.1 Analysis of Nuclear System	127
6.1.1 Computer Programs	127
6.1.2 Reactor Physics Model	129
6.1.3 Cross Section Data	129
6.2 Analysis of Thermal and Mechanical System	130
6.2.1 Maximum Fuel Temperature	131
6.2.2 Minimum Fuel Temperature	131
6.2.3 Velocity	131
6.2.4 Fuel Volume	133
6.3 Analysis of Chemical System	134
6.3.1 Thorium-232	134
6.3.2 Protactinium-233	135

CONTENTS (continued)

	<u>Page</u>
6.3.3 Uranium-233	135
6.3.4 Uranium-234	135
6.3.5 Uranium-235	136
6.3.6 Uranium-236	136
6.3.7 Neptunium-237	136
6.3.8 Uranium-238	136
6.3.9 Neptunium-239 and Plutonium Isotopes	136
6.3.10 Salt	136
6.3.11 Xenon-135 and Related Isotopes	137
6.3.12 Noble Metal Fission Products	137
6.3.13 Other Fission Products	137
6.3.14 Corrosion Products	137
6.4 Fuel Cycle Optimization	138
6.5 Reference Design Reactor	141
6.5.1 Specifications	142
6.5.2 Neutron Economy	143
6.5.3 Inventories and Processing Rates	147
6.5.4 Fuel Cycle Cost	148
6.6 Parameter Studies	150
6.6.1 Processing Cost as Parameter	150
6.6.2 Effect of Xenon Removal	152
6.6.3 Effect of Product Sale Without Recycle	153
6.7 Alternative Design and Cost Bases	154
6.7.1 Thorex Processing Cost Estimates	154
6.7.2 Reactor-Integrated Fluoride Volatility Processing ...	155
6.7.3 Reactor-Integrated Precipitation Process	156
6.8 Evolution of a Self-Sustaining MSCR	156
6.8.1 Reduction of Leakage	157
6.8.2 Reduction of Xenon Captures	157
6.8.3 Reduction of Fission Product Poisoning	158
6.8.4 Improvement of Mean Eta and Reduction of ^{236}U Captures	158

CONTENTS (continued)

	<u>Page</u>
6.8.5 Ultimate Breeding Potential of MSCR	158
7. MSCR CAPITAL INVESTMENT, FIXED CHARGES, AND OPERATING EXPENSE	160
7.1 Introduction	160
7.2 Summary of MSCR Capital Investment	160
7.3 MSCR Fixed Charges	162
7.4 MSCR Operating and Maintenance Cost Estimate	164
7.4.1 Labor and Materials	164
7.4.2 Operation and Maintenance Cost	165
8. RESULTS AND CONCLUSIONS	168
8.1 Fuel Cost	168
8.2 Fixed Charges	169
8.3 Operation and Maintenance Expense	170
8.4 Cost of Power	170
8.5 Breeding Potential of the MSCR	171
8.6 Conclusions	173
8.7 Recommendations	173
8.7.1 Title 1 Design Study of MSCR	173
8.7.2 Conceptual Design Studies of Advanced Breeder Reactors	174
8.7.3 Fundamental Studies of Alternative Chemical Processes	174
8.7.4 Engineering Laboratory Study of Precipitation Processing	174
8.7.5 Pilot Plant Study of HF Dissolution Process	175
APPENDICES	177
Appendix A - MULTIGROUP CROSS SECTIONS FOR MSCR CALCULATIONS	179
Appendix B - EFFECTIVE THORIUM RESONANCE INTEGRALS	196
Introduction	196
Analysis	197
Sample Calculation	200
Results	201
Symbols	201
References	204

CONTENTS (continued)

	<u>Page</u>
Appendix C - ENERGY DEPENDENCE OF ETA OF ^{233}U	205
Summary	205
References	208
Appendix D - THE MERC-1 EQUILIBRIUM REACTOR CODE	209
Introduction	209
Theory	209
References	220
Appendix E - FISSION PRODUCT NUCLEAR DATA	221
References	224
Appendix F - TREATMENT OF DELAYED NEUTRONS	225
Summary	225
References	229
Appendix G - TREATMENT OF XENON ABSORPTION IN GRAPHITE	230
Introduction	230
Analysis	231
Reference	234
Appendix H - THE EQUILIBRIUM STATE AS A BASIS FOR ECONOMIC EVALUATION OF THORIUM REACTORS	235
Introduction	235
Methods	236
1. Fission Products	236
2. Uranium-233	237
3. Uranium-234	239
4. Uranium-235	239
5. Uranium-236	240
6. Uranium-238	241
Results and Conclusions	242
1. Fission Products	242
2. Uranium-233	249
3. Uranium-234	249
4. Uranium-235	249
5. Uranium-236	249
6. Uranium-238	249

CONTENTS (continued)

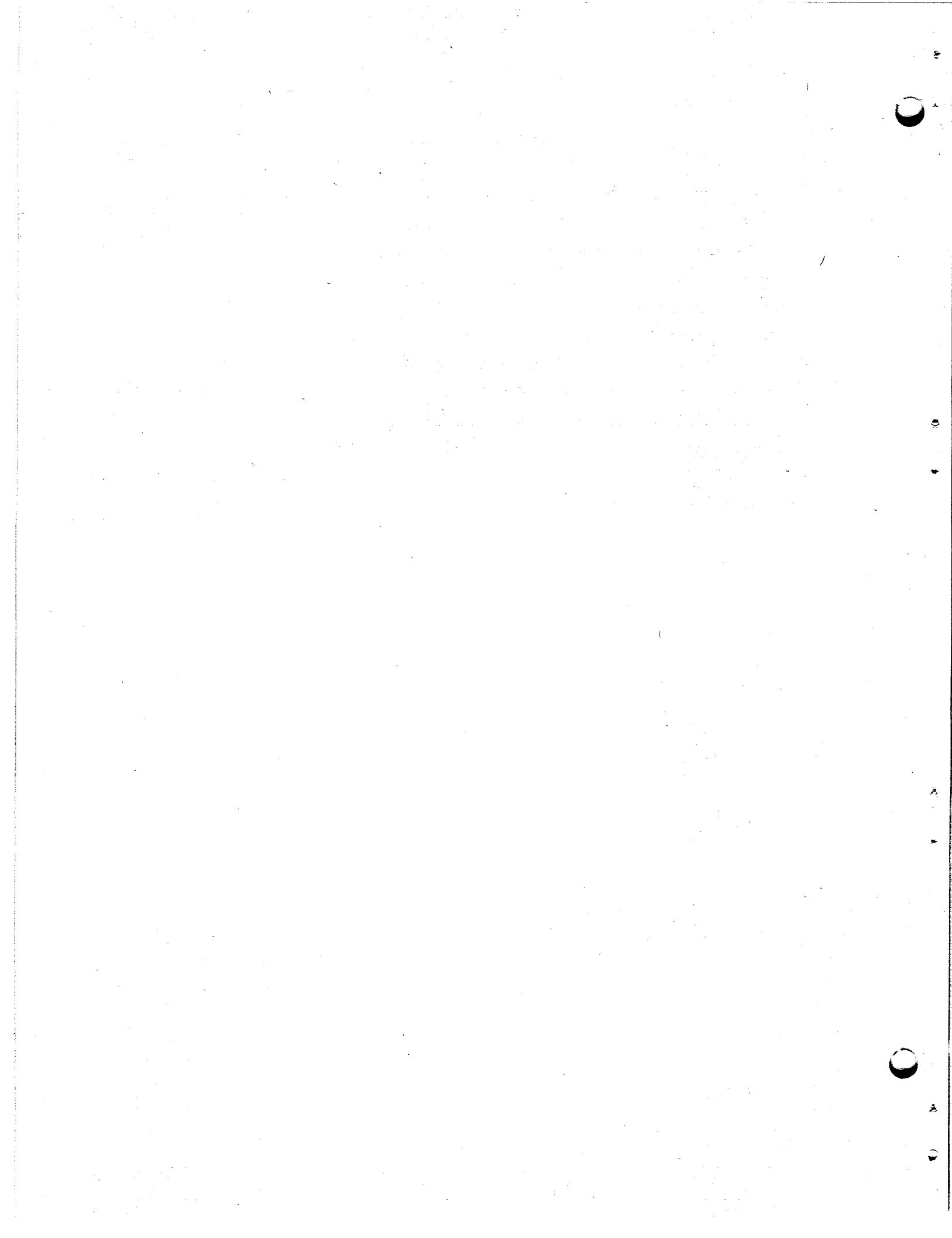
	<u>Page</u>
Appendix I - ESTIMATES OF PHYSICAL PROPERTIES OF LITHIUM-BERYLLIUM MSCR FUEL AND COOLANT SALTS	252
Introduction	252
Viscosity	253
Heat Capacity	256
Thermal Conductivity	256
Density	258
Liquidus Temperature	258
References	260
Appendix J - FUEL AND CARRIER SALT COST BASES	261
Introduction	261
Bases for Establishing Prices	269
General Comments on Price Quotations	269
Thorium Fluoride	269
Zirconium Fluoride	269
Beryllium Fluoride	270
Sodium Fluoride	270
Thorium Oxide	270
Lithium Fluoride	270
Recommended Values for Molten Salt Fuel	271
References	272
Appendix K - MSCR POWER LIMITATION RESULTING FROM MODERATOR THERMAL STRESS	273
Summary	273
References	279
Appendix L - VOLUMES OF FUEL SALT AND INTERMEDIATE COOLANT SALT FOR 1000 Mwe MOLTEN SALT CONVERTER REACTOR	280
Introduction	280
Fuel Salt Volume	280
Coolant Salt Volume	282
Appendix M - EVALUATION OF A GRAPHITE REFLECTOR FOR THE MOLTEN SALT CONVERTER REACTOR	285
Introduction	285

CONTENTS (continued)

	<u>Page</u>
Results	286
Conclusions	288
Appendix N - DETAILED ESTIMATE OF 1000 Mwe MSCR CAPITAL INVESTMENT	289
Summary	289
Investment Requirements	290
Appendix O - DESIGN REQUIREMENTS FOR THE MSCR MODERATOR	328
Introduction	328
Moderator	330
Void Fraction	330
Permeation of Graphite by Salt	331
Graphite Shrinkage	332
Graphite Replacement	333
Differential Expansion	335
References	336
BIBLIOGRAPHY	337

ACKNOWLEDGMENTS

The comments, suggestions, and critical reviews of R. B. Briggs, P. R. Kasten, J. A. Lane, H. G. MacPherson, E. S. Bettis, A. M. Perry, and S. E. Beall are gratefully acknowledged. The computer programming was performed by J. Lucius, ORGDP Computing Center, and many of the drawings were prepared by H. MacColl. The capital costs were estimated by C. A. Hatstat of Sargent and Lundy, Engineers. R. P. Milford and W. G. Stockdale, ORNL Chemical Technology Division, assisted the chemical processing cost studies. Roy Robertson and I. Spiewak, ORNL Reactor Division, assisted the design and analysis of the energy conversion systems. Special studies reported in the Appendix were performed by R. H. Chapman, J. W. Miller, and C. W. Nestor of the ORNL Reactor Division, and D. B. Janney of ORGDP.



MOLTEN SALT CONVERTER REACTOR

Design Study and Power Cost Estimates for a 1000 Mwe Station

L. G. Alexander, W. L. Carter, C. W. Craven, D. B. Janney,
T. W. Kerlin, and R. Van Winkle

ABSTRACT

The MSCR is a one-region, one-fluid, graphite-moderated converter reactor fueled with a mixture of the fluorides of thorium uranium, lithium-7, and beryllium which is circulated through the 20-ft-diam core to an external heat exchanger. Heat is transferred through an intermediate salt-coolant to steam at 2400 psi, 1000°F in a Loeffler boiler system having a net thermal efficiency of 41.5%. Spent fuel is processed by fluorination (at 0.08 mill/kwhe) for recycle of isotopes of uranium. The stripped salt is discarded.

A capital investment of \$143/kwe (3.0 mills/kwhe), an operation and maintenance annual expense of \$2.1 million (0.3 mill/kwhe), and a minimum fuel cycle cost of 0.7 mill/kwhe (optimum conversion ratio is ~0.9) were estimated, giving a net power cost of 4.0 mills/kwhe. All costs were based on 1962 bases ground rules.

Second generation plants may have capital costs as low as \$125/kwe. Conversion ratios slightly greater than one can be obtained in advanced designs.

This study was completed in December 1962 and does not reflect increased feasibility and superior performance of two-region, two-fluid molten salt breeder reactors made possible by recent (January 1965) advances in core design, heat transfer, and fuel-salt processing.

1. SUMMARY

The Molten Salt Converter Reactor (MSCR) is a one-region, one-fluid, near-term reactor that does not require any technology beyond the scale-up of that already developed at ORNL or to be demonstrated in the MSRE. Salient characteristics are given in Table 1.1.

Table 1.1. Characteristics of the Molten Salt Converter Reactor

Thermal capability	2500 Mw
Net thermal efficiency	41.5%
Diameter and height of core	20 x 20 ft
Moderator	Graphite
Volume fraction of fuel in core	0.10
Composition of fuel carrier salt (mole-percentages)	68-LiF, 22-BeF ₂ , 9-ThF ₄ , 1-UF ₄
Density of fuel salt	190 lb/ft ³
Heat capacity of fuel salt	0.35 Btu/lb·°F
Velocity of fuel salt	6 fps
Inlet temperature	1100°F
Outlet temperature	1300°F
Flow rate	160 ft ³ /sec
Volume of circulating stream	2500 ft ³
Power density in core (av)	14 w/cm ³
Power density in fuel salt (av)	35 w/cm ³
Thorium specific power	30 Mwt/tonne
Fissile material specific power	0.9 Mwt/kg
Fertile material exposure	47 Mw days/kg
Intermediate coolant (mole-percentages)	63-LiF, 37-BeF ₂
Steam conditions	2400 psi, 1000°F
C: Th atom ratio	~300
Th: U atom ratio	~30
Mean neutron productions ($\bar{\eta}\epsilon$)	2.21
Optimum conversion ratio	0.9

1.1 Description

The reactor vessel is fabricated of INOR-8 alloy and is filled with cylindrical graphite logs 8 inches in diameter and 24 inches long. The fuel, a mixture of the fluorides of ^7Li , Be, Th, and U flows upward through the passages around the logs and is discharged through eight pumps to an equal number of heat exchangers where the heat is transferred to an intermediate-salt coolant. Saturated steam is superheated in a shell-and-tube exchanger; part of the steam is routed to the turbines; the rest is recirculated to Loeffler boilers where saturated steam is generated by injecting the superheated steam into water. Thus, thermal contact of the coolant salt with subcooled, boiling water is avoided, and thermal stress in the tube walls is tolerable. The thermal efficiency is in excess of 40%. Twenty-five hundred Mw of heat are extracted from a single core at average power densities in the fuel salt of not more than 35 w/cm^3 .

1.2 Fuel Reprocessing

Irradiated fuel is removed from the reactor daily, collected into processing batches, and treated with fluorine for recovery of isotopes of uranium (fully decontaminated) as the hexafluoride. The stripped salt is discarded. Recovered UF_6 is reduced to UF_4 , blended with fresh salt, and recycled to the reactor. Net burnup and loss of fissile material are compensated by addition of 95% enriched ^{235}U .

1.3 Nuclear and Thermal Performance

The limiting criteria (e.g., maximum allowable fuel temperature, maximum allowable thermal stress in graphite, etc.) were chosen conservatively throughout, and provide considerable margin for improvement in later designs. The key variables (core diameter, volume fraction of fuel in core, carbon/thorium ratio, and processing rate) were optimized with respect to the fuel cycle cost. Characteristics of the optimized system are listed in Table 1.1 where it is seen that the optimum conversion ratio is 0.9, with slightly permeable graphite that absorbs ^{135}Xe only slowly.

1.4 Fuel Cycle Cost

The estimation of inventory and replacement charges for the MSCR is straightforward. Processing costs are less well defined; however, the processing contributes only a small part of the total fuel cost, and the aggregate is not sensitive to large errors in the processing cost estimates.

A central Fluoride Volatility facility capable of processing 30 ft³/day of salt was designed and costed. Only isotopes of uranium are recovered; carrier salt and thorium are discarded along with fission products. Unit costs and the components of the fuel cycle cost are listed in Table 1.2.

Table 1.2. Fuel Cycle Cost in 1000 Mwe Molten Salt Converter Reactor Plant

Cost Bases

Capital investment in processing plant: \$26 million
 Annual operating expense: \$2 million
 Turn-around-time: 2 days
 Batch size: 6000 kg
 Unit processing cost: \$27/kg Th
 Shipping costs: \$10/kg Th
 Purchase price ThF₄: \$19/kg Th
 Carrier salt purchase price: \$1130/ft³
 Fissile isotopes: \$12/gram

Material	Charges, mills/kwhre			Total
	Inventory	Replacement	Processing	
Th ²³²	0.033	0.043		
Pa ²³³	0.008			
U ²³³	0.183		0.082	
U ²³⁵	0.037	0.156		
Total	0.262	0.199	0.082	0.54
Salt	0.062	0.079		0.14
Total charges, mills/kwhre				0.7

1.5 Power Costs

The cost of power was obtained by combining fuel-cycle costs with estimates of capital charges prepared by Sargent and Lundy, Engineers (95,96), from a design study conducted at ORNL. Equipment was sized and specified in sufficient detail that costs might be estimated by usual procedures. Plant arrangement drawings were prepared from which costs of buildings, piping, services, etc. were estimated. Operation and maintenance costs were estimated according to standard procedures (52). A summary of the principal items is given in Table 1.3.

Table 1.3. 1000-Mwe Molten Salt Converter Reactor
Construction Costs

Direct construction costs	
Structures and improvements	\$ 5,997,950
Reactor plant equipment	51,324,350
Turbine-generator units	26,843,700
Accessory electric equipment	4,375,300
Miscellaneous power plant equipment	<u>799,900</u>
Total direct construction costs	89,341,200
Indirect costs	9,083,300
Engineering design and inspection costs	15,080,300
Miscellaneous charges	<u>35,370,800</u>
GRAND TOTAL	\$148,875,600
Net station power	1038 Mwe
Unit capital cost	\$143/Kwe

The fixed charges (14.46%) on the capital investment contribute 3.0 mills/kwhre to the power cost.

The uncertainty in this cost might run as high as 15-20%, and the fixed charges might range up to 3.5 mills/kwhre.

Operation and maintenance contribute 0.3 mills/kwhre to the total power cost (Table 1.4). Because of the many uncertainties, this estimate may be low, and the cost might run as high as 0.5 mills/kwhre.

Table 1.4. 1000-Mwe Molten Salt
Converter Reactor Operating
and Maintenance Cost

Wages and salaries	\$ 872,000
Routine materials	220,000
Maintenance	800,000
Management	<u>262,000</u>
Total	\$2,154,000

The various contributions to the cost of power have been summed in Table 1.5.

Table 1.5. Cost of Power in a 1000-Mwe
Molten Salt Converter Reactor

Item	Charge, mills/kwhre
Fuel cycle cost	0.7
Fixed charges	3.0
Operation and maintenance	<u>0.3</u>
Cost of power, mills/kwhre	4.0

Taking the upper bound on these three items estimated above (fuel cost ~1.0, fixed charges ~3.5, operation and maintenance ~0.5) gives an upper limit on the cost of power of 5.0 mills/kwhre.

1.6 Advanced MSCR

The system evaluated above was based on the scale-up of current technology, and was conservatively designed in every respect. There are several obvious improvements that could be incorporated into a "second generation" design. If the design criteria were relaxed, metallic sodium could be substituted for the intermediate salt coolant (saving about \$10 million in capital costs. This would also permit the use of "conventional"

once-through sodium-heated boilers and reduce the cost of the energy conversion system by about another \$10 million. The total cost would then be ~\$125/kwe. By careful design and development the fuel volume might be reduced from 2500 ft³ to 1800 ft³. Separated ⁹²Mo could be used to clad the graphite and so reduce absorption of xenon therein and also as a structural material by means of which a blanket of ThF₄ bearing salt could be added at the periphery of the core to reduce neutron leakage. The use of Fluoride Volatility coupled with the HF Solution Process to remove rare earths could reduce the fission product poisoning to very low levels while permitting recycle of carrier salt (but not thorium). Preliminary calculations show that these improvements (all within reach of modest development programs) might increase the conversion ratio above 1.0, and, with the reduction in capital costs noted, result in a power cost of 3.4 mills/kwhre.

1.7 Post Script - January 1965

This study was completed in December 1962, and does not reflect increased feasibility and superior performance of two-region, two-fluid molten salt breeders made possible by the recent advances (January 1965) in core design, heat transfer, and fuel-salt processing alluded to in the Foreword.

2. INTRODUCTION

2.1 Purpose, Scope, and Method of Approach

The purpose of this study was to evaluate the economic potential of a near-term molten salt power reactor. "Near-term" characterizes a system which utilizes only techniques or equipment currently under development.

2.1.1 Figure of Merit

The economic potential of power reactors is measured by the net cost of electric power.

Fuel cycle cost, although not definitive, is also an important index of economic potential. Moreover, the optimization of the fuel cycle is a required first step in the detailed design of both reactor and electric plants. In this study, the reactor and its associated heat transfer system, the energy conversion system, and the fuel reprocessing plant were designed in detail sufficient to permit the optimization of the fuel cycle.

2.1.2 Reactor Concept

A concept was selected for evaluation, which, judging from previous experience, would satisfy the "near-term" requirement and yet would exhibit attractive fuel costs: A single-fluid, single-region, graphite-moderated molten-salt reactor generically related to the Molten Salt Reactor Experiment. Since the breeding ratio was expected to be less than unity, the system was designated the "Molten Salt Converter Reactor" (MSCR).

2.1.3 Procedure

In a series of preliminary calculations, the limitations on reactor design imposed by consideration of allowable temperature, pressures, velocities, thermal stress, etc., were determined. Design and cost bases were established, and the fuel cycle cost was minimized by optimization of the key variables, which in the MSCR are the core diameter, carbon/thorium ratio, volume fraction of fuel in the core, and spent fuel

processing rate. For the optimum conditions, the fuel cycle costs resulting from alternate bases and assumptions (e.g., removal of xenon) were determined. Finally, the ultimate performance resulting from a concatenation of all favorable assumptions and potentially low processing costs was estimated.

2.2 Status of Molten Salt Reactor Development

2.2.1 Early Work

Molten salt fuels were conceived originally as a means of satisfying the requirements for very high temperature and extremely high power density necessary for aircraft propulsion. A very large amount of work on the physical, chemical, and engineering characteristics of uranium and thorium bearing molten fluorides was carried out as part of the ANP program at Oak Ridge National Laboratory.

The technology of molten salt reactors was first introduced into the open literature in 1957 by Briant and Weinberg (14). Papers by Bettis et al. (6,7) and Ergen et al. (31) reported the Aircraft Reactor Experiment, a beryllium-moderated reactor fueled with UF_4 dissolved in a mixture of the fluorides of sodium and zirconium, and contained in Inconel. The reactor was successfully operated in 1954 for about 90,000 kwhr without incident at powers up to 2.5 Mwt and temperatures as high as 1650°F.

The potential usefulness of molten salt fuels for civilian power was recognized from the start. The features that attracted attention were the high temperature of the fuel (permitting use of modern steam technology and attainment of high thermal efficiency) combined with a low vapor pressure, the high stability of halide salts under radiation, and the advantages that a fluid fuel provides. These include a negative temperature coefficient of reactivity, absence of the need for initial excess reactivity and of neutron wastage in control elements, no limitation to fuel exposure due to radiation damage or fuel burnup, the absence of a complicated structure in the reactor core, removal of the heat transfer operation from the core to an external heat exchanger, and the potential for a low-cost fuel cycle. In addition, suitable molten salt mixtures exhibit a

solubility for thorium fluoride sufficient for all reactor applications; moreover, these mixtures may be economically and rapidly processed for the recovery of ^{233}U by means of the well-developed Fluoride Volatility Process.

Studies of power reactors utilizing molten salts have been reported by Wehmeyer (109), Jarvis (49), Davies (27), and Bulmer (15). Davidson and Robb (26) conceived many of the features of one-region thorium converter reactors and anticipated some of the development problems.

2.2.2 The Molten Salt Reactor Program

The molten salt reactor program was inaugurated at ORNL in 1956 (57, 58) to exploit the technology of molten salt fuels for purposes of economic civilian power. Several parts of the program were: (a) a reactor evaluation study to select the most promising concepts for civilian power and to pinpoint specific development problems; (b) an extensive materials development program for fuels, containers, and moderators; (c) an equally extensive program for the development of components, especially pumps, valves, and flanges suitable for extended use with molten salts at 1300°F; (d) a modest program for the discovery of supplementary chemical processes for recovering valuable components (other than uranium) from spent fuel; (e) a program for the development and definitive demonstration of the feasibility of completely remote maintenance of molten salt reactor systems; and presently (f) the Molten Salt Reactor Experiment (MSRE).

2.2.3 Fuel Development

The program for the development of molten salt fuels in the Reactor Chemistry Division at ORNL has been highly successful (56). The five-component mixtures (fluorides of Li, Be, Th, U, and Zr) developed for the MSRE (12) have many exceptional features. They have melting points well below 1000°F, with ample solubility for UF_4 , ThF_4 , and fission product fluorides. They are thermodynamically stable with vapor pressures less than 0.1 atm at temperatures well above 2000°F, and, being ionic liquids, are not subject to permanent radiation damage (e.g., radiolytic dissociation) when in the liquid state. The parasitic capture cross sections of the base elements (^7Li , ^9Be , and ^{19}F) are satisfactorily low, and ^7Li

is available at attractive prices in grades containing as little as 0.005% Li-6. The high volumetric heat capacities of salt mixtures make them better heat transfer media than most liquid metals in spite of the higher film conductances obtainable with the latter.

These mixtures do not appreciably attack the container material (INOR-8), corrosion rates being less than 1 mil/year (possibly as low as 1/2 mil/year) at temperatures below 1300°F (28). Although it is not now anticipated that it will be necessary to use INOR in the neutron active zone, since the moderator material (graphite) is suitably self-supporting, experiments have shown that the corrosion is not appreciably accelerated by radiation. A long life (10-30 years) is predicted for all components constructed of INOR (reactor vessel, pumps, heat exchangers, etc.) because resistance to corrosion does not depend on maintenance of a protective film but stems from the inertness of the base metal toward the salt.

Molten salt fuel mixtures are compatible with graphite. Tests of a typical grade show that the salt does not wet the graphite and penetration is mostly confined to the surface layers (84, p. 93). Some CF₄ has been observed in post-irradiation examination of in-pile experiments. Since CF₄ is thermodynamically unstable with respect to the salt, it is thought that its formation resulted from attack on graphite by free fluorine produced by radiolysis of solid salt. Since the fuel-salt must be maintained in the liquid state for other reasons, free fluorine would not normally be present in the circulating stream.

Xenon is not adsorbed appreciably on graphite (17) at reactor temperatures, though it will saturate the voids present because of its extremely low solubility in salt (107). However, it may be possible to exclude Xe from the graphite by treating the surface to close the pores there and render interior pores inaccessible (5). Purging the salt with a stream of helium in the pump bowl or in a special contactor would then maintain the Xe concentration at a very low level (Section 6.8). Iodine remains in the ionic state and is not absorbed. Noble metal fission products are expected to be reduced by INOR outside the core.

The phase behavior of a great many mixtures has been investigated (108). Proposed mixtures containing up to 40 mole % BeF₂ have viscosities

adequately low and dissolve heavy metal fluorides (UF_4 , ThF_4 , or ZrF_4) in concentrations up to 15 mole % with liquidus temperatures less than 1000°F (56). Additions of 5 mole % of ZrF_4 to the base salt satisfactorily reduces the sensitivity of the fuel mixture toward precipitation of UO_2 by oxygenated contaminants (e.g., air, water, lubricating oils) which will be difficult to exclude entirely from a large reactor system. Graphite is readily de-oxygenated by in situ decomposition of $\text{NH}_4\text{F-HF}$ vapor, which shows negligible attack on the INOR.

Thermophysical properties of the important salt mixtures have been measured (8,24) in detail sufficient to permit reliable calculation of pumping and heat transfer characteristics, which are good. No evidence of the deposition of scale or dendrites in the heat exchangers has been found.

2.2.4 Container Development

The development of nickel-molybdenum base alloys (INOR series) for containment of molten fluorides was conducted jointly by ORNL and International Nickel Company. In addition to the resistance to corrosion mentioned above, the alloys have good-to-excellent mechanical and thermal characteristics, (superior to those of many austenitic stainless steels) and are virtually unaffected by long-term exposure to salts or to air at 1300°F (12). The alloy has been made by several major manufacturing companies, and it is presently available on a limited commercial basis in the form of tubing, plates, bars, forgings, and castings. Exhaustive tests at ORNL have shown that its tensile properties, ductility, creep strength, cyclic fatigue strength (both thermal and mechanical) are adequate for molten salt reactor applications when judged in accordance with criteria used in the ASME Boiler Code (75-87). INOR is weldable by conventional techniques using welding rods of the same composition as the base metal. A gold-nickel alloy has been developed at ORNL suitable for remote brazing of reactor components. INOR begins to soften above 2000°F and melts at 2500°F . The thermal conductivity is about $12 \text{ Btu/hr}\cdot\text{ft}\cdot{}^{\circ}\text{F}$ at 1200°F . No major difficulties have been encountered in the design and fabrication of reactor components, including pumps and heat exchangers (12).

2.2.5 Moderator Development

Graphite, because of its good moderating properties, low neutron capture cross section, compatibility with fluoride salts and INOR, and excellent high-temperature physical properties is a superior moderator for molten salt reactors. The graphite proposed for use in the MSRE has a density of 1.8 g/cc and a kerosene-accessible porosity of 6%. About half the pore volume is accessible from the surface. However, as mentioned above, molten fluorides do not wet graphite and permeation of MSRE grade graphite by the salt is less than 0.5% by volume at 150 psi (84, p. 93). The coefficient of permeability by helium at 30°C is 10^{-5} cm²/sec, and Xe will be adsorbed rapidly. However, techniques for reducing permeability are being developed. Samples of high-density graphite having permeabilities at least two orders of magnitude lower have been made (107).

Development of graphites and graphite bodies is being carried out cooperatively with National Carbon Company. Pieces of graphite are presently available in sections up to 20 in. square and 20 ft long. Graphite having outstanding mechanical properties is available in the form of readily machinable rods, tubes, slabs, and spheres. The effects of nuclear radiations on this material are not fully known. The thermal conductivity declines, but probably not below 15 Btu/hr·ft·°F. Thermal stress considerations thus affect the design of moderator elements; the allowable stress is thought to be at least 2000 psi and the allowable strain at least 0.1%. These limits appear to be compatible with the thermal and nuclear requirements of optimum core design. However, experimental verification of these values is needed.

At the temperatures encountered in molten salt reactors, graphite will shrink during exposure to fast neutrons. Where large gradients in the fast neutron flux exist, the resulting differential shrinkage will result in deformations, or, if these are restrained, in stresses. The problem of designing a long-lived core structure of large pieces of graphite is presently unresolved. The bowing of graphite stringers might be restrained by use of molybdenum hoops, but this solution may not be suitable for large power reactors.

2.2.6 Component Development

Development of components for molten salt reactors has been in progress for over ten years. The most notable achievements to date are the demonstration of the long-term reliability of pumps operating at 1300°F, including pumps having molten-salt-lubricated bearings, and the demonstration of the reliability and maintainability of remotely operated freeze flanges and freeze valves.

2.2.7 Reactor Vessel

No difficulties were encountered in the design or fabrication of the reactor vessel for the MSRE. In large power reactors provision to limit thermal stress by means of thermal shields may be necessary, but mechanical stresses are not important because pressures greater than 200 psi are not encountered anywhere in the systems. Corrosion does not appear to be a problem.

2.2.8 Molten Salt Pumps

Molten salt pumps have been operated continuously for 33 months at temperatures above 1200°F. A sump-type pump having one salt-lubricated journal bearing has logged more than 12,000 hours of operation at 1225°F, 1200 rpm, and 75 gpm. After it was stopped and restarted 82 times, examination of the bearings disclosed no discernible attack. The use of salt-lubricated bearings will enable the shaft to be lengthened so that shielding may be interposed between the pump bowl and the motor with its oil-lubricated bearings. The impellers of these pumps also withstand attack indefinitely under operating conditions. It is believed that pumps of the types developed can be made in large sizes for use in large molten salt reactor plants and that these can operate at the temperatures required.

2.2.9 Molten Salt Heat Exchangers and Steam Boilers

The design and fabrication of exchangers for transferring heat from fuel salt to an intermediate coolant salt are straightforward. Heat

transfer experiments conducted at ORNL with unirradiated salt verify the correlations used to predict the performance. Scale did not form on the heat transfer surfaces.

The Loeffler boiler seems especially suited for use with molten salts. Here dry saturated steam is superheated in a salt-to-steam exchanger; part of the superheated steam is routed to the turbines, and part is recirculated through an evaporator producing saturated steam for recycle to the exchanger. Problems in boiling burnout, thermal stress in the exchanger tubes, and freezing of the salt are thus avoided.

However, a fuel-salt boiler presently in the conceptual stage has many potential advantages. In this concept, the fuel downcomer annulus inside the reactor vessel is widened to accommodate several hundred INOR thimbles. Bayonet tubes, into which water is introduced, are inserted into the thimbles, but are separated from the thimble walls by a narrow annulus filled with an inert salt. Calculations show that the heat transfer is adequate to produce steam at 1000°F and 2000 psi. Yet the salt and steam systems are isolated from direct contact and the salt system is under negligible pressure. Should either system leak, this would be detected immediately by monitors in the inert salt system.

Such a boiler has many advantages, including the complete elimination of one cooling loop and its associated pumps, heat exchanger, etc. In addition, the fuel circuit is appreciably shortened in comparison to a "spread-out" system. The steam produced will be considerably less radioactive than that produced in a direct cycle boiling-water reactor.

2.2.10 Freeze Valves and Freeze Flanges

Although the high melting point of a molten salt reactor fuel (800-1000°F) is a disadvantage in that the system must be preheated before filling and provision must be made to avoid freezing, there are also benefits that accrue. Among these is the fact that if a leak does occur there is little tendency for the material to disperse rapidly. Noble gas fission products do not accumulate in the liquid, and the fluorides of the remaining fission products have negligible vapor pressure and are retained.

The ready solidification of salts has also been put to use in the development of flanges and valves. The remote manipulation of reliable freeze flanges has been successfully demonstrated in many tests and in a remote maintenance development facility. Freeze valves have no moving parts, no seals, and have been demonstrated to be satisfactory in salt transfer and drain pipes.

2.2.11 Molten Salt Instrumentation and Special Equipment

Conventional equipment is adequate for measuring the nuclear behavior of molten salt reactors; however, special equipment for handling molten salts was developed at ORNL for the MSRE. For measuring liquid level in the pump bowls, for example, a ball-float suspending an iron bob whose position is sensed by an external induction coil was developed. A single point electrical probe device has also been developed for use in the fill-and-drain tanks to calibrate the weighing system.

A sampler-enricher device is being tested whereby fresh fuel may be added to the fuel stream during operation, and a sample of spent fuel may be removed without contamination of the fuel stream by air or water vapor and without the uncontrolled escape of any radioactive material from the reactor.

Clam-shell electrical pipe heaters for lines carrying molten salt have been developed.

2.2.12 Remote Maintenance

Because of fission-product contamination and induced activity in components and piping, the fuel-containing portions of molten salt reactors cannot be approached for direct maintenance even after draining and flushing. Semi-direct maintenance through a shield plug with long-handled tools is possible for some items, but it is necessary to develop completely remote tools and methods for many of the larger components. These include tools, techniques, and procedures for removing and replacing all major reactor components, including the heat exchanger, primary fuel-pump and motor, reactor vessel, and fill-and-drain tank. Such equipment and techniques successfully demonstrated in the Molten Salt Remote Maintenance Development Facility at ORNL (65). This facility simulated a

20-Mwt molten salt reactor system and comprised a mockup of the reactor vessel, a mockup of the heat exchanger, together with full-scale pumps, flanges, valves, electrical heaters, thermocouples, etc. All maintenance operations were performed by a single operator from a remotely located control center, using closed-circuit stereo-television for viewing. The manipulator was a general purpose, medium duty, electro-mechanical "arm" which performed a variety of functions easily and efficiently. It was used to connect and disconnect tube and electrical connections, to carry loads weighing up to 750 lbs and to manipulate tools. Eight basic motions, five for the arm and three for the crane bridge, were controlled independently by two pistol-grip handles on the control console. Two types of remotely interchangeable grasping devices permitted a variety of objects to be handled.

Tools developed for remote manipulation included impact wrenches, a torque tool and bolt runner, screw jacks on the heat exchanger for working the freeze flanges, and miscellaneous devices such as lifting slings, socket extensions, hooks, fingers, etc. All these were operated by the manipulator. In addition, a reactor-lifting jig, a pump-lifting eye, and socket extensions for the torque tool and bolt runner were positioned by the manipulator, but operated by the crane or by their own power.

The installation of microphones at strategic locations inside the reactor cell to enable the operator to listen to pneumatic and electric motor sounds was found to be helpful.

Reliable, quickly acting disconnects for electric, pneumatic, oil, and other services were adapted or developed.

The components of the Remote Maintenance Facility were removed and replaced several times before the system was filled with salt in order to develop procedures and test the tools. Finally, the system was filled with salt, brought to temperature with salt circulating freely, then shut down and drained. All equipment was then removed and replaced remotely, and tested. The salt was replaced and brought to temperature again. Items "maintained" in this way included the pump motor, the fuel pump, the reactor vessel, the heat exchanger, the fill-and-drain tank, electrical pipe heaters, and thermocouples. The demonstration was entirely successful.

Maintenance of the MSRE will be accomplished by means of the techniques and tools developed and supplemented with some semi-direct maintenance operations through a portable shield having a rotatable plug. Long-handled tools may be inserted through this plug and manipulated by hand. These means of maintenance will be thoroughly tested in a full-scale mockup of the MSRE now being constructed at ORNL.

2.2.13 Chemical Processing of Molten Salt Fuels

The use of fluid fuels in nuclear reactors provides an opportunity for continuously removing fission products and replacing fissile isotopes at power. Thus, it is possible to hold fission-product neutron losses to low levels and to eliminate capture of neutrons in control rods.

The "Fluoride Volatility Process" is in an advanced stage of development; a pilot plant for general application is now in operation at ORNL. Other processes are being sought, and prospects are good that simple and economic means can be found to separate fission products continuously from spent fuel salt.

2.2.14 Fluoride Volatility and HF Solution Processes

While the fluoride volatility process was not developed specifically for use with molten salt fuels, it has been verified in laboratory experiments conducted at ORNL that it is applicable for removal of uranium from fluoride mixtures containing ThF_4 (16). In this process, elemental fluorine, diluted with an inert gas, is bubbled through the salt. UF_4 is converted to UF_6 which is volatile at the temperature of operation (500–700°C) and passes out of the contactor to be absorbed reversibly in a bed of sodium fluoride. The off-gas is cooled, stripped of F_2 in a scrubber, and passed through charcoal beds where fission product gases are absorbed.

The fluorides of a few of the fission products are also volatile but these are irreversibly absorbed in the sodium fluoride beds. Thus, by heating the beds, UF_6 is brought over in a very pure state, completely decontaminated and with losses less than 0.1%.

The UF_6 is reduced to UF_4 in a hydrogen-fluorine flame, and is collected as a powder in a cyclone separator backed up by gas filters. Losses

routinely are smaller than random errors in the assays, and the process has been used successfully for many years in the manufacture of enriched ^{235}U from natural uranium in the production plants at Oak Ridge.

The Fluoride Volatility Process alone is sufficient for the economical operation of a molten salt converter reactor. Spent fuel containing UF_4 , ThF_4 , ^{233}Pa , as well as fission products is removed from the reactor periodically and fluorinated for recovery of uranium isotopes. The stripped salt is discarded (stored in INOR cylinders indefinitely) to purge the system of fission products. Although the discarded salt contains valuable components (^7Li , Be , ^{232}Th , ^{233}Pa), the cost of discarding these is offset by the improvement in conversion ratio.

The steps described above appear to be especially attractive for integration with the reactor plant. That is, they are all high-temperature, non-aqueous processes, and could conveniently be carried out in the reactor cell, utilizing the same shielding and sharing in the use of remote maintenance equipment. The waste product (fuel salt stripped of isotopes of uranium) is in a form conveniently stored for decay of radioactivity. After a period measured in years, the waste could conveniently be removed to another location for recovery of thorium, lithium, beryllium, and other valuable components in a relatively low-level-radiation facility.

The HF Solution Process (16) under study at ORNL provides one means of separating rare earths (which constitute the bulk of important non-volatile fission products, including isotopes of samarium) from the base salt, after uranium has been removed. The separation is effected by dissolving solidified salt in liquid HF containing up to 10% water. The rare earths, thorium, and related materials precipitate and may be separated by filtration or decantation, permitting reuse of the salt. The HF Solution Process is presently in the laboratory stage of development.

2.2.15 Thorex Process

While the Fluoride Volatility process appears attractive if integrated with the reactor plant, it is not obvious that it is superior in a central facility to alternative modes of processing, such as Thorex.

This uncertainty is due in part to paucity of reliable information on costs of on-site and central Fluoride Volatility process plants, and in part to the limitations of the method in respect to recovery of lithium and thorium. On the other hand, the costs of Thorex plants are rather better known, and, with suitable modifications, Thorex appears to permit economic recovery of all valuable components of the fuel salt only moderately contaminated with certain fission products (e.g., cesium). The costs associated with a modified Thorex process as described in Section 5.3 were used in an alternate evaluation of the MSCR.

2.2.16 Fractional Crystallization Process

Studies by Ward et al. (108, 106, 80, p. 80) provide a basis for evaluating the feasibility of removing rare earth fluorides from the fuel salt by partial freezing. A brief description is given in Section 6.7.3. The process is not suitable for a breeder reactor inasmuch as the fission product concentration cannot be lowered much below 0.2 mole %; however, much higher concentrations can be tolerated in a converter. In the reference design studied here, the concentration is approximately 0.5 mole %.

2.2.17 Other Processes

Solvents which will selectively dissolve either ThF_4 or rare earth fluorides are being sought at ORNL. Solutions of SbF_5 in HF show some promise.

The capture of a neutron by an atom of ^{233}Pa results in a double loss — that of the neutron and of the fissile atom of ^{233}U that would have been formed by decay of the Pa. A process is needed that can quickly and economically remove ^{233}Pa from the circulating salt stream so that it may be held outside the reactor until it decays to ^{233}U . There is a possibility that exposing the fertile stream to beds of ThO_2 pellets might accomplish this. There is some evidence that thorium from the beds will exchange with Pa in the solution, and the latter will be immobilized until it decays, after which it might, as ^{233}U , exchange with thorium in the salt, and so become available for recovery by fluorination. Other oxides, e.g., BeO , are also under study.

2.2.18 Molten Salt Reactor Studies

The status of the Molten Salt Reactor Program was reviewed in 1958 for the second Geneva Conference by MacPherson et al. (56). At that time a homogeneous molten salt reactor having only a limited capability for fuel regeneration was under consideration. Further studies of this system were reported by Alexander et al. (1), and a 30-Mwt experimental reactor was described (2).

Also, in 1958, good indications were obtained that the system INOR-graphite-salt is chemically stable in radiation fields and attention was accordingly shifted to graphite-moderated systems. MacPherson et al. (60) described a one-region single-fluid reactor utilizing slightly enriched uranium and a highly enriched feed. Many features of his concept were incorporated in the present study.

The potential of graphite-moderated molten-salt reactors for breeding in the Th-²³³U cycle was investigated and the associated development problems were identified by MacPherson in a series of papers (61-63). Several conceptual designs for one- and two-region breeders were proposed. One of these (the MSBR) was evaluated in comparison with four other thermal breeders by the Thorium Breeder Reactor Evaluation Group at ORNL (3); this system employed a fuel salt (contained in graphite bayonet tubes and circulated through external heat exchangers) together with a fertile salt stream (containing all the thorium) surrounding the moderated core region. The major problems associated with this concept were the development of a reliable graphite-metal joint for connecting the bayonet tubes to an INOR header and the uncertain behavior of the core structure for long periods under irradiation at high power densities.

It was estimated that the MSBR could achieve fuel yields up to about 7%/year (doubling time about 14 years) at fuel cycle costs not greater than 1.5 mills/kwhr; and that fuel costs as low as 0.7 mills/kwhr could be achieved by sacrificing the fuel yield in favor of lower processing costs (3).

2.3 Molten Salt Reactor Experiment

The favorable results obtained in the various evaluation and development programs led to the initiation in May 1960 of preliminary design of the Molten Salt Reactor Experiment (12,5). Construction and installation of the entire system are scheduled for completion in mid-1964 and criticality late in 1964, or early 1965.

The MSRE is expected to demonstrate the long-term reliability of components and the compatibility of materials under actual operating conditions, including the dimensional stability of the graphite and its resistance to permeation by fuel salt in the presence of radiations and the maintainability of the system after operation at power.

The reactor will produce up to 10 megawatts of heat in a fuel consisting of a solution of highly enriched $^{235}\text{UF}_4$ dissolved in a mixture of the fluorides of lithium (99.990% ^7Li), beryllium, and zirconium having a liquidus temperature of 842°F. The salt enters a volute around the upper part of the cylindrical vessel at 1175°F and flows at the rate of 1200 gpm down through an annular plenum between the wall of the vessel and up the graphite core-matrix. This is constructed by pinning 2-in. square bars loosely to INOR beams lying across the bottom of the vessel. The salt flows up among the bars at a velocity of 0.7 ft/sec. (Reynolds number 1000) and exits at 1225°F.

The fuel pump, a sump-type having a bowl 36 in. in diameter and 12 in. high, is driven by a 75 hp motor and develops a head of 48.5 ft at 1200 gpm. All parts are constructed of INOR.

The heat exchanger, also constructed of INOR, has 165 tubes 14 ft long by 1/2 in. OD with walls 0.042 in. thick, and provides 259 ft² of heat transfer surface (heat flux 130,000 Btu/hr·ft² at a LMTD of 133°F). The reactor heat is transferred to a secondary salt coolant from whence it is discharged to the atmosphere in an air-cooled radiator.

Initially, the MSRE will contain no thorium, since the power level is too low for significant amounts of ^{233}U to be produced in a reasonable time. Thorium may be added later to permit verification of nuclear calculations of critical mass, etc., and to discover if there are any unforeseen compatibility or stability problems.

3. BASES AND ASSUMPTIONS

3.1 Design Bases

3.1.1 Reactor Concept

The concept selected for study was modeled closely after that proposed by MacPherson et al. (60), and is essentially a scale-up of the Molten Salt Reactor Experiment (12,5) plus necessary auxiliary equipment for generation of electricity, etc. Briefly, the core consists of a vertical bundle of unclad graphite logs contained in an INOR vessel. Fuel salt containing thorium and uranium flows up through the bundle into a plenum, thence through several pumps in parallel to the shell side of multiple shell-and-tube heat exchangers, and then back to the reactor.

3.1.2 Design Calculations

These were performed only in sufficient detail to permit the estimation of the capital cost. Problems of control, shielding, hazards analysis, etc., were ignored. Attention was centered on the nuclear performance and processing costs. The energy conversion system was designed to provide a basis for estimating the volume of the fuel salt circulating in the primary heat system, the net thermal efficiency, and the capital investment.

3.1.3 Station Power

An electrical capability of 1000 Mw was selected to permit direct comparison with systems previously evaluated at the same plant capacity. Preliminary calculations indicated that the core should be ~20 ft in diameter for satisfactory nuclear performance. At a power of 1000 Mwe, power densities are only 14 kw/liter of core and 35 kw/liter of salt (average). A lower plant output would result in inefficient utilization of the fuel inventory.

3.1.4 Plant Utilization Factor

The standard factor of 0.8 was used as recommended in the "Guide" (52).

3.1.5 Thermal Efficiency

Several different energy conversion schemes were considered in sufficient detail (see Section 4.3) to show that even the least efficient system (Loeffler boiler) would have, when fully optimized, a thermal efficiency not less than 40%. This efficiency was therefore adopted for use in the fuel cost optimization calculations.

3.1.6 Fueling Cycle

For the purposes of optimization calculations, it was assumed that make-up fuel was added and spent fuel was removed quasi-continuously, and that, with three exceptions, the concentrations of the various nuclides in the circulating salt system were in equilibrium with respect to feed rates, nuclear reactions, and processing rates. The exceptions were ^{234}U and ^{238}U (which are initially present in amounts substantially lower than the equilibrium value, and whose concentrations increase with time) and ^{236}U (the concentration of which starts at zero and reaches only about 3/4 of its equilibrium values in 30 years). For these three isotopes, concentrations that approximated the average over a life of 30 years starting with the reactor charged with ^{235}U (95% enrichment) were used. Other important isotopes appear to approach their equilibrium concentrations in times short compared to the reactor life. The use of equilibrium concentrations for these, especially for slowly equilibrating fission products, is discussed in Appendix H.

3.1.7 Processing

The processing rate was optimized with respect to the fuel cycle cost. In the selected process, spent fuel is accumulated, shipped to a central Fluoride Volatility Plant, cooled for a minimum of 90 days, and treated for recovery of uranium. Undecayed ^{233}Pa , along with ^{232}Th , ^7Li , and ^9Be are lost in the waste.

3.1.8 Feed and Recycle

In the optimization calculations, it was assumed that isotopes of uranium recovered from irradiated fuel are recycled, and that deficiencies in the breeding ratio are compensated by additions of 95%-enriched ^{235}U .

The effects of a few feed and recycle schemes on the optimum reactor were studied (Section 6.9), such as the use of feeds containing a mixture of uranium isotopes (e.g., spent fuel from the Consolidated Edison Reactor at Indian Point, New York). The sale of irradiated fuel to the AEC as an alternate to recycle was also investigated.

3.1.9 Isotopic Composition of Lithium

It was assumed that lithium (as the hydroxide) would be available in grades containing up to 99.995% ^7Li at a price no greater than that quoted in reference 67 (\$120/kg of lithium). The choice of this composition (rather than one having a lower cost) resulted from a compromise between cost of neutron losses to ^6Li and the cost of discarding the salt enriched in ^7Li with a processing rate of about 2 ft³/day.

3.1.10 Energy Conversion System

Although it would be difficult to establish a complete set of requirements for coupling of the reactor system with the energy conversion system prior to the preparation of a detailed design, nevertheless, it is necessary to fix some of these in order that the fuel cycle cost may be estimated. The most important requirement appears to be a necessity to isolate the fuel salt from the thermodynamic fluid, at least when that fluid is water. The hazards associated with the possibility that high pressure steam might leak into the fuel system cannot be tolerated, since such leakage would result in the rapid formation of UO_2 (81, p. 63). This is only slightly soluble in the base salt, although its solubility can be increased somewhat by additions of ZrF_4 and of ThF_4 (84, p. 96). Isolation of the steam and fuel systems is achieved by interposing a compatible third fluid, either as a stagnant layer or as a separate stream circulated between primary and secondary heat exchangers.

The intermediate coolant (third fluid) must be chemically compatible with fuel salt, and in addition, it is desirable that it be inert with respect to steam. Also, it should either not be a nuclear poison, or else it should be readily removable from fuel salt. For the reference design, a salt 66 mole % LiF (99.995% ^7Li) and 34 mole % BeF_2 was selected (Table 3.4) as the intermediate fluid.

3.1.11 Primary Heat Exchanger Requirements

It is important that the external portion of the fuel salt circulating system shall have as small a volume as possible in order to reduce the inventory of valuable materials. However, the reliability and maintainability of the system cannot be compromised in favor of small volume. A requirement for maintainability, which includes replaceability, implies that the primary heat exchanger shall be drainable of fuel salt. This requirement is most easily and certainly met by putting the fuel salt in the shell-sides of the heat exchangers and grouping these about the reactor in a vertical position so that the heads may be removed and the tube bundles lifted out easily.

3.1.12 Minimum Salt Temperatures

To provide a margin of safety in regard to possible freezing of both fuel salt and intermediate coolant salt, it was decided that the operating temperature of any salt stream should not be at a temperature less than the liquidus temperature of the fuel salt.

3.2 Cost Bases

3.2.1 Value of Fissile Isotopes

Unirradiated, highly enriched ^{235}U was valued at \$12.01/gram of contained ^{235}U (52). Mixtures of isotopes were valued according to the formula $V = f(E) \$12/\text{gram}$ of contained fissile isotope (^{233}U , ^{235}U), where $f(E)$ is an enrichment factor found by dividing the value of enriched ^{235}U having the same composition as the mixture in question by \$12.01/gram. The enrichment, E , of the mixture is found by dividing the sum of the

atomic concentrations of ^{235}U and ^{233}U (and ^{233}Pa , if any) by the sum of atomic concentrations of all isotopes of uranium in the mixture (thus lumping ^{234}U and ^{236}U with ^{238}U as diluents).

3.2.2 Value of Thorium

Inquiries directed to several vendors elicited only one reply (Appendix J); however, the quotation given (\$6/lb of ThF_4) agreed well with a 1959 estimate by Orrosion (89) and led to the adoption of a price of \$19.00/kg of thorium as ThF_4 (\$6.50/lb ThF_4).

3.2.3 Value of LiF(99.995% ^7Li)

This was taken to be \$120/kg of contained lithium (Appendix J) or \$32.30/kg of LiF.

3.2.4 Value of BeF_2

Inquiries cited in Appendix J led to adoption of a price of \$15.40/kg of BeF_2 .

3.2.5 Value of Base Salt

This varied with the composition, but the base salt in the optimum reactor contained 68 moles of LiF per 23 moles of BeF_2 giving a value of \$25.97/kg.

3.2.6 Cost of Compounding and Purifying Fuel Salt

The operation of blending recycle uranium with make-up uranium and fresh lithium, beryllium, and thorium fluoride and purifying is to be performed on-site. The cost was therefore excluded from the operating and capital charges of the processing plant and included in the capital and operating charges of the reactor plant.

3.2.7 INOR-8 Cost

The following cost information supplied by A. Taboada of ORNL is based on quantity production. Manufacturing experience to date with fabrication of the listed forms has not indicated the existence of any

serious problems and therefore pricing safety factors in the costs shown may be pessimistic.

Plate	\$3 per lb
Round Rod	\$4.25 per lb
Welding Rod	\$8 per lb
Pipe (Seamless)	\$10 per lb
Pipe (Welded)	\$5 per lb
Tubing (Seamless)	\$12 per lb
Tubing (Welded)	\$6 per lb
Simple forgings	\$4.50 per lb (e.g., tube sheets)
Fabricated Plate	\$10 per lb (e.g., pressure vessel shells)
Dished Heads	\$5.50 per lb
Forged Pipe Fittings	\$50 per lb
Castings	\$2 per lb

3.2.8 Moderator Graphite Cost

The cost of graphite such as would be used in the MSCR core has been established at \$6.00 per lb. This is from informal discussion with vendors.

3.2.9 Annual Fixed Charges

For fissile isotopes, the use charge was taken at 4.75%/yr in accordance with the "Guide" (52). Other components of the fuel mixture were carried as depreciating assets (since only the isotopes of uranium and thorium are recoverable). For such the "Guide" recommends (Table 3.1) an annual rate of 14.46% for an investor-owned public utility (IOPU). This rate, however, includes 0.35% for interim replacement when the rate of replacement is not known. In the present instance, the replacement rates for base salt were calculated and the corresponding costs listed separately; therefore, the annual charge for the above items was set at 14.11%/yr. This included also 1.11%/yr for amortization by means of a 30-yr sinking fund with cost of money at 6.75%/yr; hence, a charge for replacement of salt at the end of 30 years was not made either separately or as part of the final processing to recover the uranium inventory.

3.2.10 Central Fluoride Volatility Plant Processing Charges

The schedule given below was extracted from the estimates presented in Table 5.9 and apply to a plant capable of processing 30 ft³ of salt per day (about 1000/kg day of thorium for the reference design salt) for recovery of isotopes of uranium. The barren salt is discarded. Capital investment (\$25.5 million) was estimated by scaling from a study by Carter, Milford, and Stockdale (21) of two smaller on-site plants (1.2 and 12 ft³/day), and adding costs of other facilities required in a central plant (receiving, outside utilities, land improvements, etc.). The plant is large enough to service about fifteen 1000 Mwe molten salt converter reactor plants. A turn-around-time of two days was allowed. Shipping charges (\$10.30/kg thorium) were estimated separately (Table 5.8).

Table 3.1. MSCR Reference Design One
Ton/Day Central Fluoride Volatility
Plant Cost Schedule

Production Rate kg/day of Thorium from Reactor	Processing Cost* \$/kg Thorium
320	23.0
160	24.0
80	25.3
40	26.1
53.3	26.6
40	27.6
26.7	30.0

*Excluding shipping.

3.3 Special Assumptions

3.3.1 Permeation of Graphite by Salt

Tests with MSRE fuel salt at 1300°F and 150 psi in MSRE graphite showed penetrations of the order of 0.02% in 100 hours (86, p. 93). Most of the absorbed salt was contained in pockets lying at the surface of the graphite, and presumably in communication with bulk liquid. From a metallographic examination of thin sections, it was concluded that penetrations

considerably less than 0.12% would be encountered in the MSRE at the maximum pressure of 65 psia. For the purposes of evaluating the MSCR, it was assumed the penetration would be 0.1%, and that only pores lying at the surface would contain salt. Thus, in a core 90 volume % graphite the volume of salt absorbed in the graphite would be slightly less than 1% of the volume of salt in the core. This absorbed salt was assumed to have the same composition as the circulating stream.

3.3.2 Permeation of Graphite by $^{135}\text{Xenon}$

The solubility of xenon and other noble fission product gases in fuel salt is very low (107); also, their adsorption on graphite at 1200°F appears to be negligible (17). However, there remains the possibility that gaseous xenon may diffuse into the pores in graphite at a rate large compared to that at which it can be removed from the salt by sparging or spraying. The mathematical treatment of the case at hand has been presented by Watson, et. al. (107), who also established probable ranges for the diffusion coefficient. For the purposes of a reference calculation having a reasonable degree of plausibility, a value of 10^{-6} (cm^2/sec) was selected for the diffusion coefficient and a value of 0.01 for the porosity of graphite to noble gases. Further, it was assumed to be feasible to by-pass 10% of the fuel salt ($16 \text{ ft}^3/\text{sec}$) through the pump bowls or through a sparge chamber, and that this by-pass steam would give up substantially all of its xenon to the sweep gas.

3.3.3 Corrosion Products

Tests in a forced convection INOR loop using a salt (62-LiF, 36.5-BeF₂, 0.5-UF₄, 1.0-ThF₄) very similar (except for thorium content) to that proposed for the MSCR, show that after a period of initial attack (occurring generally in the equipment in which the batch of salt is prepared) the concentration of structural-element cations reaches equilibrium values (84, p. 79). The temperature of the salt was 1300°F in the hot leg, 1100°F in the cold leg, and was circulated for a total of almost 15,000 hours. The concentration of nickel, after rising to a maximum of 80 ppm in about a thousand hours, reached an equilibrium value of about

50 ppm at 2000 hours. Chromium concentration fluctuated between 400 and 600 ppm, averaging about 500 ppm, while iron averaged about 250 ppm. Molybdenum was said to be negligible and was not reported.

Apparently the concentration of chromium is in equilibrium with respect to the rate with which chromium is oxidized by UF_4 to CrF_2 at the hot metal surfaces and the rate with which it is reduced to ^{60}Cr at the cold surfaces (75, p. 39). In the MSCR, large areas of INOR are exposed to the salt at all temperatures between 1100°F and 1300°F . Although the rate of diffusion of chromium in INOR has been determined at various temperatures, it is not possible to calculate the chromium concentration in the salt until the temperature profile is known.

In the calculations performed here, a neutron-poison allowance was made for corrosion products, amounting to 0.008 neutrons per atom of fuel destroyed. This loss is comparable to the loss that would result if the concentrations of Ni, Cr, and Fe were 50, 500, and 250 ppm, as in the loop-corrosion test cited above (Section 6.3).

3.3.4 Approach to Equilibrium

The nuclear performance was calculated by means of MERC-1, an equilibrium reactor code. Thus the performance of the reactor during the approach to equilibrium, when concentrations of isotopes of uranium and of fission products are changing, was not considered, except in regard to ^{234}U , ^{236}U , and ^{238}U . These were averaged over a fuel lifetime of 30 years; ^{233}U , ^{235}U , and fission products were taken at their equilibrium values.

In cases where adequate supplies of ^{233}U are unavailable the reactor would be fueled initially with enriched ^{235}U . This is inferior to ^{233}U in respect to eta and also forms a non-fertile daughter, ^{236}U . These disadvantages are offset by initially-low concentrations of fission products and ^{236}U . While a calculation of the time-dependent behavior is desirable in such cases, it does not appear that the error introduced by assuming equilibrium conditions is important. The matter is explored further in Appendix H.

4. DESCRIPTION OF MSCR CONCEPT

4.1 General Description

The MSCR is a single-region, unreflected, graphite-moderated fluid-fuel reactor utilizing a mixture of molten fluorides of lithium, beryllium, thorium, and uranium as the fuel and primary coolant. A sketch of the reference design reactor is shown in Fig. 4.1. As seen in this figure, the reactor consists of a 20-ft-diam by 20-ft-high cylindrical core made up of 8-in.-diam graphite cylinders. The fuel salt enters through a bottom grid, flows upward through the spaces between the cylinders and is discharged into one of eight primary heat removal circuits located around the reactor. The arrangement of these circuits is shown in Fig. 4.2. The heat generated in fuel salt is transferred to an intermediate coolant salt consisting of a mixture of barren lithium and beryllium fluoride containing no uranium or thorium. The coolant salt is used to superheat saturated steam produced in a Loeffler boiler and also to reheat steam from the turbogenerators. The reactor vessel, internals and all primary and secondary system components in contact with fuel salt and coolant salt are constructed of INOR-8. The specifications are tabulated in section 4.10. Part of the superheated steam is sent to a high-pressure turbine and the rest is injected into the Loeffler boilers to generate saturated steam. This saturated steam is recirculated to the superheater by steam-driven axial compressors using steam drawn from the high-pressure turbine discharge. A flowsheet of this heat removal-power generation system is shown in Fig. 4.3.

Design data and operating characteristics for the reference design are given in Table 4.1.

4.2 Site Plan

The site plan of the MSCR plant is shown in Fig. 4.4 based on conditions specified in the AEC Cost Evaluation Guide (52). The 1200-acre grass-covered site has level terrain and is located on the bank of a river. Grade level of the site is 40 ft above the river low water level

ORNL-DWG. 63-2801RL

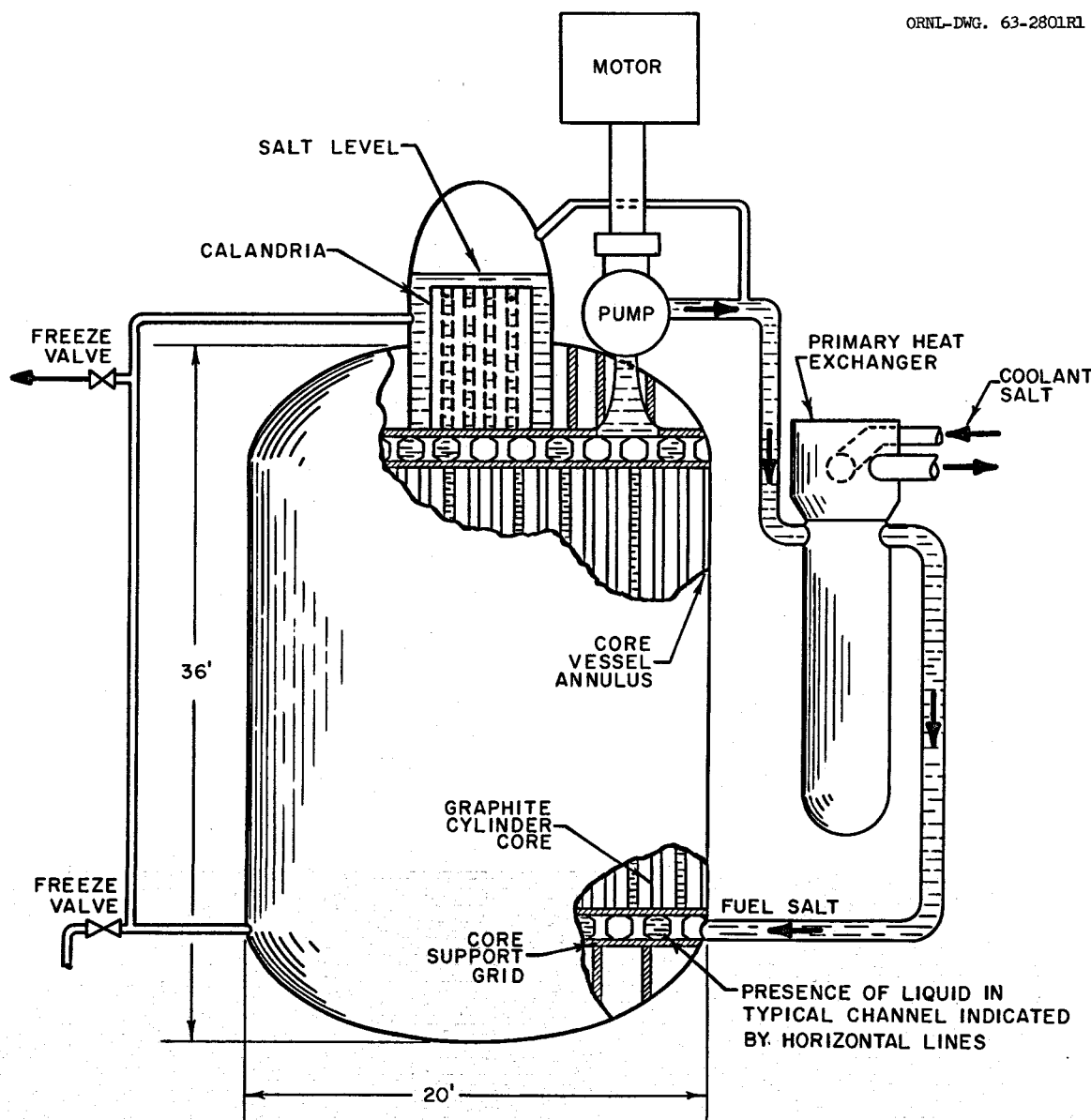


Fig. 4.1. MSCR Vessel and Heat Exchanger.

ORNL-DWG. 65-7906

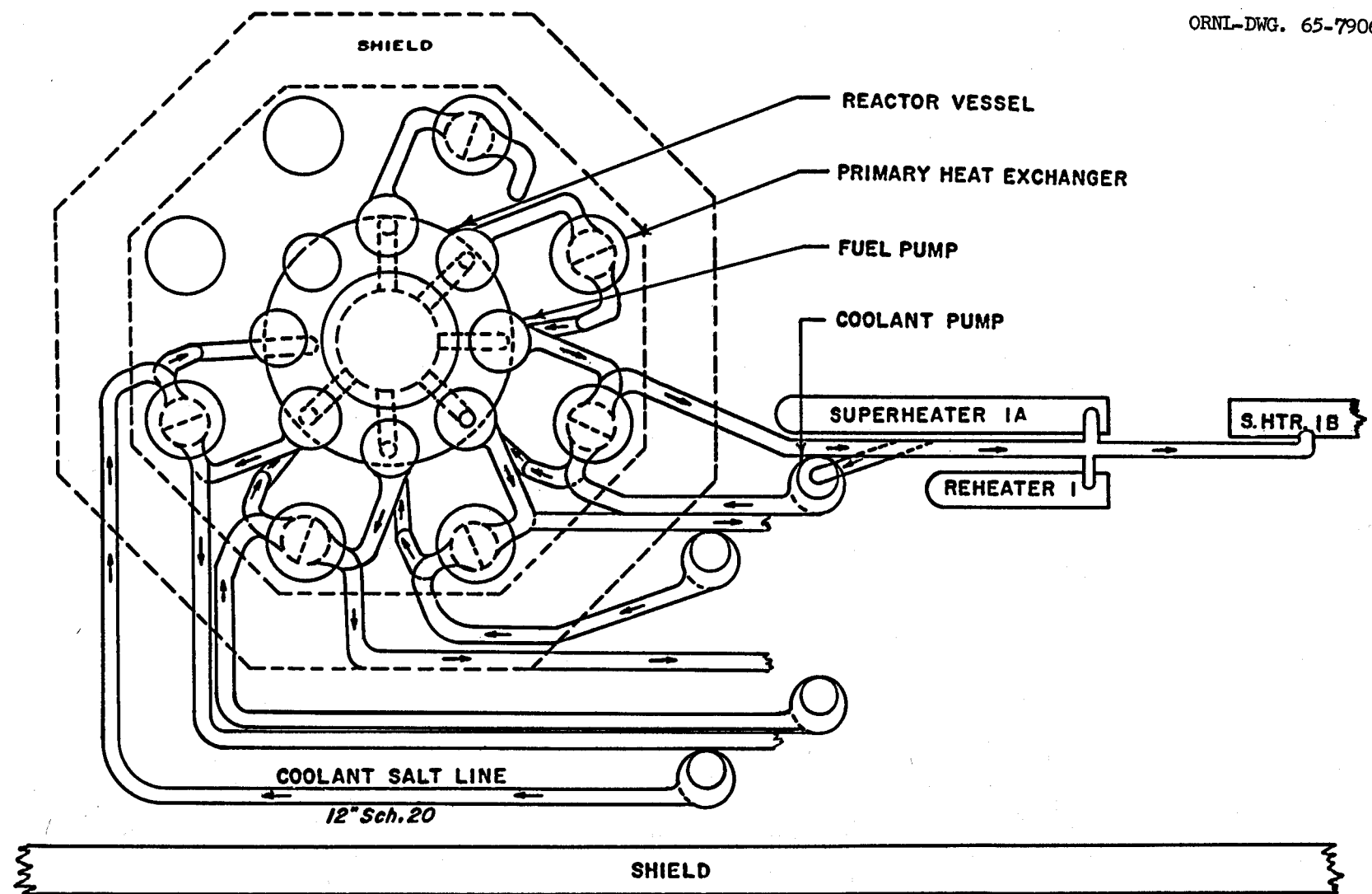


Fig. 4.2. MSCR Heat Transfer Flow Diagram.

ORNL-DWG. 65-79C

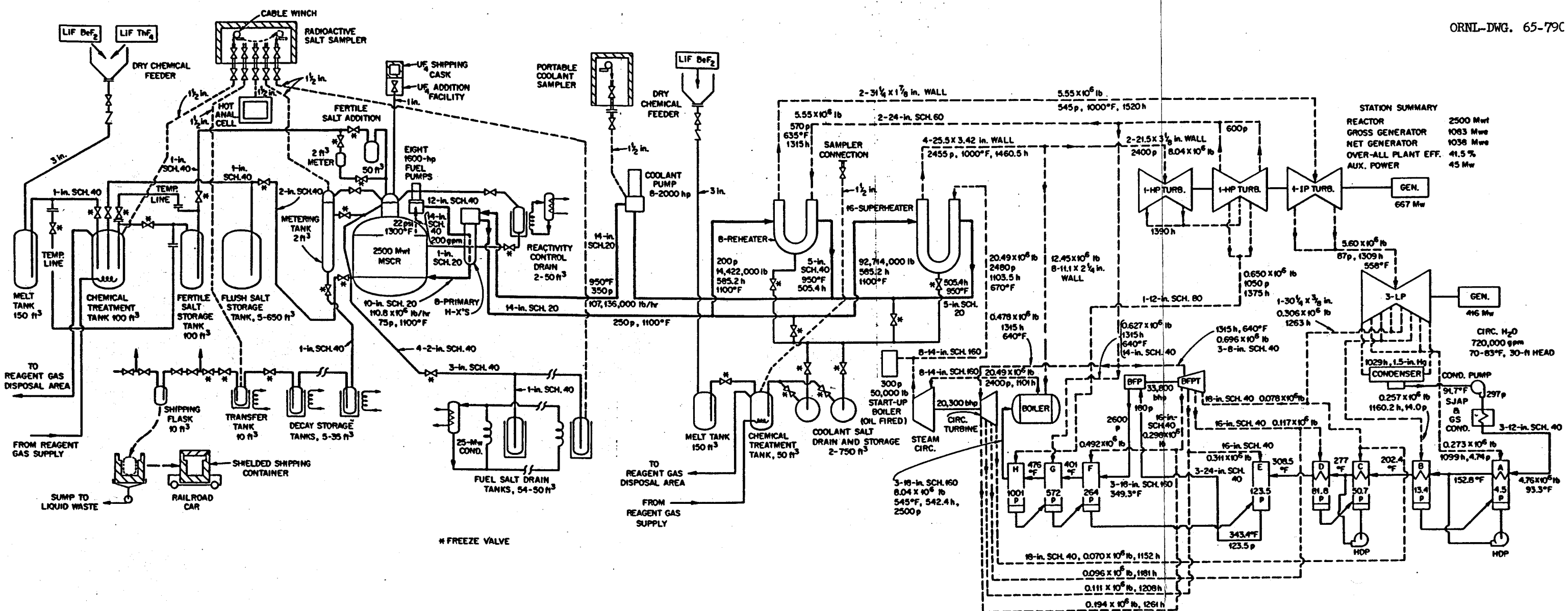


Fig. 4.3. MSCR Composite Flow Diagram

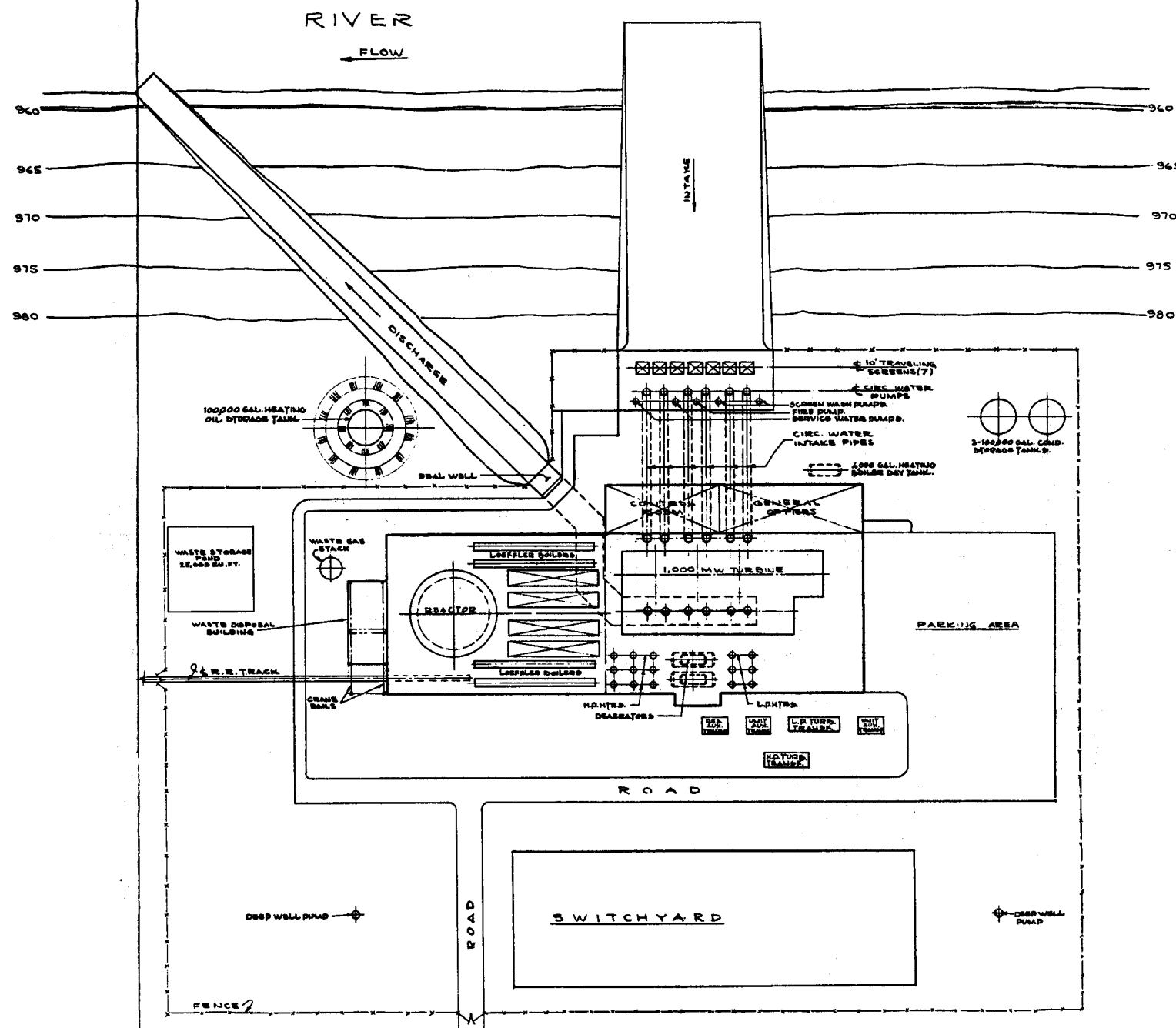


Fig. 4.4. MSCR Plant Plot Plan. (Sargent and Lundy Drawing)

Table 4.1. Design Characteristics of the 1000 Mwe
Molten Salt Converter Reference Reactor

General	
Thermal power	2500 Mw
Net thermal efficiency	41.5%
Net electrical power	1038 Mw
Core geometry	Cylindrical, 20 ft × 20 ft
Moderator	Unclad graphite
Form	Cylinders
Dimensions	8 in. diam, 24 in. long
Weight	335 tons
Volume fraction in core	0.9
Porosity accessible to salt (assumed)	0.1%
Porosity accessible to gas (assumed)	1.0%
Gas diffusion coefficient (assumed)	10 ⁻⁶ cm ² /sec
Graphite density	1.9 g/cm ³
Radiation heating (max.)	5.2 watts/cm ³
Maximum temperature rise	520°F
Reactor vessel	
Inside diameter	20 ft-2 in.
Thickness	1.7 in.
Maximum temperature	1400°F
Weight, including internals	125 tons
Radiation heating in support plates	2 watts/cm ³
Radiation heating in vessel wall	0.6 watts/cm ³
Maximum temperature rise in wall	40°F
Fuel stream	
Composition	
Base salt (LiF-BeF ₂ -ThF ₄)	68-22-9 mole %
UF ₄ (fissile)	0.3 mole %
Fission products	0.5 mole %
Corrosion products	750 ppm
Liquidus temperature of base salt	887°F
Density of base salt at 1200°F	3.045 g/cc
Mean heat capacity of base salt at 1200°F	0.383 Btu/lb.°F
Fraction of core occupied by fuel salt	0.1
Fuel stream inlet temperature	1100°F
Fuel stream outlet temperature	1300°F
Flow rate	160 ft ³ /sec
Velocity in channels in core (avg.)	6 ft/sec
Velocity in piping	35 ft/sec
Velocity in heat exchanger	
Shell side	20 ft/sec
Tube side	31 ft/sec

Table 4.1 (continued)

Fuel Stream (continued)

Pressure, psia	
Pump discharge	190
Heat exchanger inlet	185
Heat exchanger outlet	95
Reactor inlet	80
Reactor outlet	35
Pump suction	22.5
Power density in fuel salt	
In core (max.)	510 w/cc
Average over entire fuel volume	35 w/cc
Volume of fuel salt	
In active core	630 ft ³
In top and bottom plena	540 ft ³
In fuel annulus adjacent to vessel wall	105 ft ³
In surge tank	85 ft ³
In pumps	130 ft ³
In heat exchangers	575 ft ³
In connective piping	320 ft ³
In dump tanks and reactivity control tanks	115 ft ³
TOTAL	2500 ft ³
Volume of fuel in active core	650 ft ³
Primary heat transfer loop	
Primary pumps; number and type	8 - Salt Lubricated
Pressure at pump discharge	200 psi
Primary heat exchangers	8 - Shell and Tube
Total heat transfer area	53,000 ft ²
Average heat flux	160,000 Btu/hr·ft ²
Material	INOR-8
Weight	36,000 lb each
Secondary heat transfer loop	
Coolant salt composition (mole %)	66-LiF; 34-BeF ₂
Coolant salt inlet temperature	950°F
Coolant salt outer temperature	1100°F
Coolant salt flow rate	203 ft ³ /sec
Coolant salt pump discharge pressure	350 psi
Coolant salt volume	5600 ft ³

Table 4.1 (continued)

Energy conversion loop

Superheaters	16 - U-Shell and U-Tube
Materials	INOR-8 and alloy steel
Heat flux	52,440 Btu/hr·ft ²
Heat transfer area	8,850 ft ²
Weight	~50,000 lbs
Inlet steam temperature	670°F
Steam flow rate	1.3×10^6 lb/hr
Reheaters	8 - Shell and U-Tube
Materials	INOR-8 and alloy steel
Heat flux	37,250 Btu/hr·ft ²
Heat transfer area	3,543 ft ²
Weight (approx.)	22,000 lbs
Inlet steam temperature	635°F
Steam flow rate	0.7×10^6 lb/hr
Loeffler boilers	4
Length	100 ft
Diameter (ID)	6 ft
Weight (approx.)	600,000 lbs
Inlet steam conditions	2430 psia/1000°F
Steam flow rate	3.1×10^6 lb/hr
Inlet feedwater conditions	2520 psia/545°F
Feedwater flow rate	2.0×10^6 lb/hr
Discharge steam conditions	2400 psia/662°F (sat.)
Steam circulators	4 (turbine driven)
Flow rate	20.5×10^6 lb/hr
Power	5,100 BHP
Steam temperature	670°F
Steam pressure	2,480 psia
Turbine	1 (CC6F-RH)
Flow rate	8.04×10^6 lb/hr
Generator output	1083 Mw
Steam temperature	1000/1000°F
Steam pressure	2400/545 psia
Exhaust	1.5 in. Hg
Processing system	Central Fluoride Volatility
Processing method	1.67 ft ³ /day
Salt processing rate	53.3 kg Thorium/day
Production rate	~90 days
Cooling time (average)	

Table 4.1 (continued)

Processing system (continued)

Hold-up time (total)	116 days
Processing batch size	~6,000 kg Thorium
Processing plant capacity	1,000 kg/day
Turn-around time	2 days

and 20 ft above the high water level. An adequate source of raw water for the ultimate station capacity is assumed to be provided by the river with an average maximum temperature of 75°F and an average minimum temperature of 40°F.

4.3 Structures

Plan views of the reactor and turbine building are shown in Figs. 4.5 and 4.6 and vertical sections in Fig. 4.7. As seen in these figures, the reactor building and turbine building are adjacent, the secondary shield wall forming a separation from grade to the main floor. The buildings are two-level structures with the grade floors of the turbine and reactor buildings at an elevation of one foot above grade, and the main floor at 36 feet above grade. The secondary shield wall extends to the main floor and forms the walls of the lower part of the reactor and auxiliary building.

The turbine building and the upper level of the reactor and auxiliary buildings are steel frame structures, with insulated metal panel siding. The arrangement of the equipment within the buildings is indicated on the general arrangement drawings, Figs. 4.5 and 4.7.

A three-level steel frame and insulated metal-panel structure adjoining the turbine building houses the administrative offices, control room, switchgear, batteries, plant heating boiler and makeup water demineralization plant. Lockers, showers, and toilets for plant personnel are also located in this building.

A 200-ft waste gas stack is provided for dispersal of plant ventilating air and waste gases from the various reactor and reactor equipment rooms.

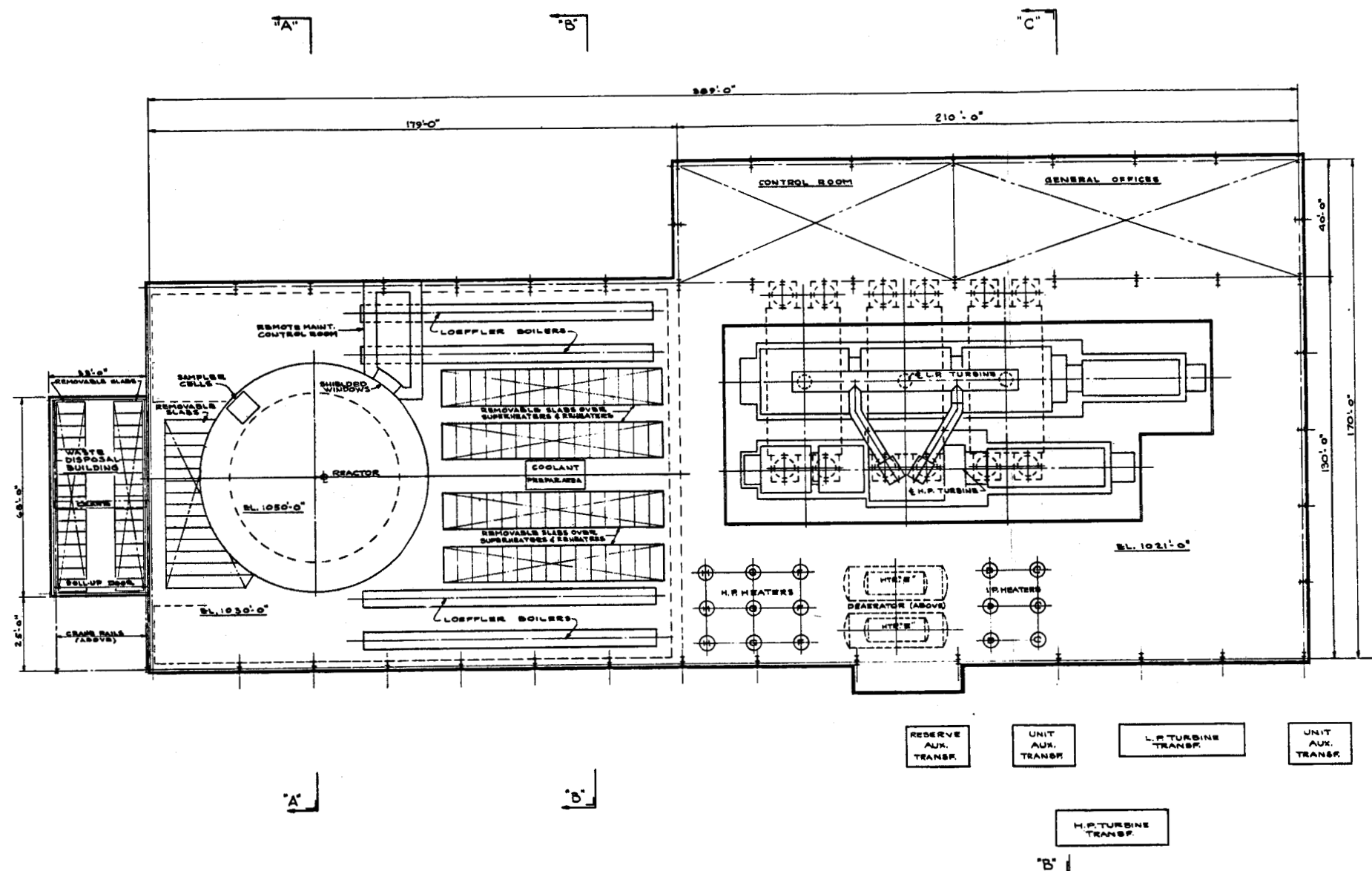


Fig. 4.5. MSCR Plant General Arrangement. (Sargent and Lundy Drawing)

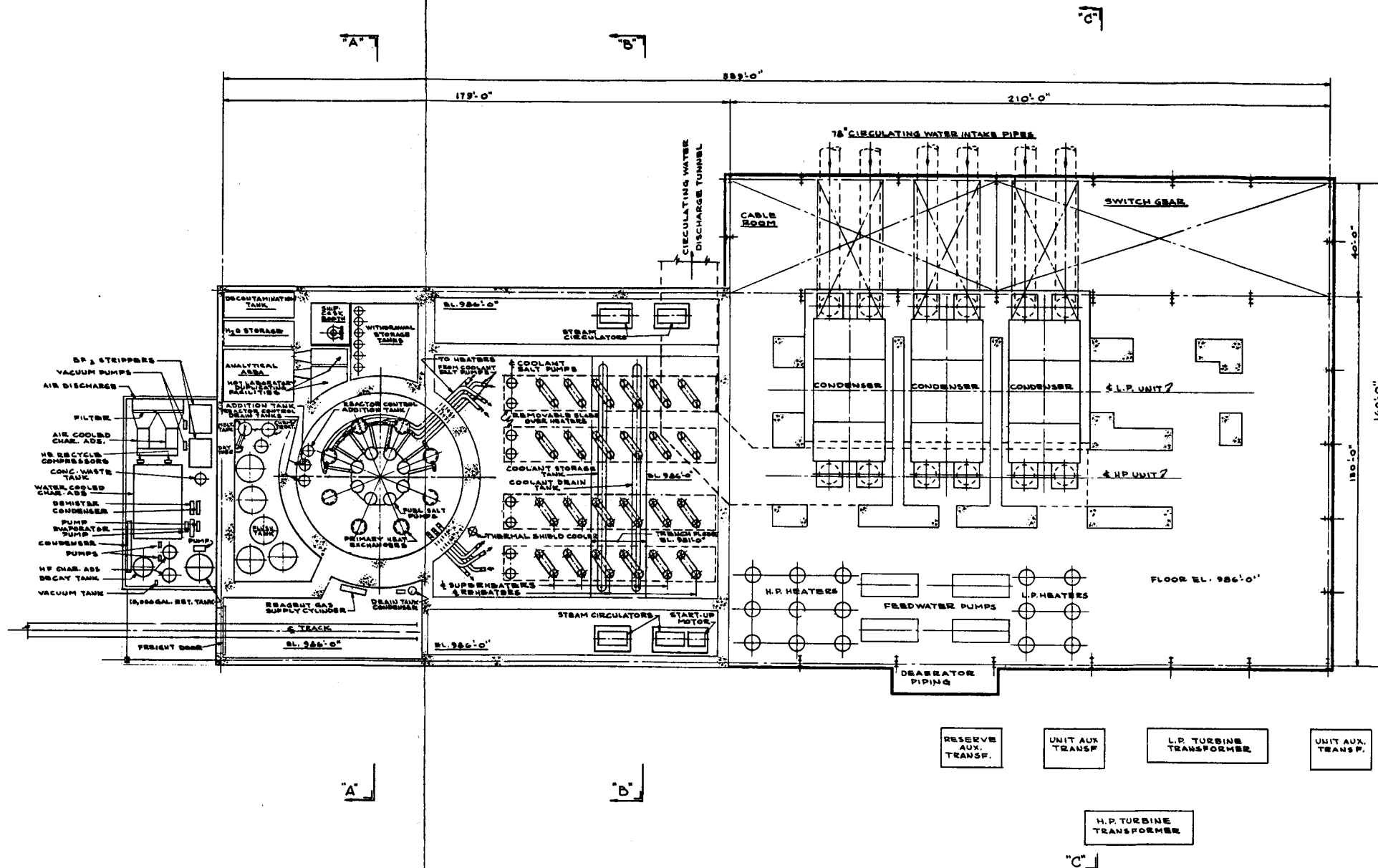


Fig. 4.6. MSCR Plant - Plan. (Sargent and Lundy Drawing)

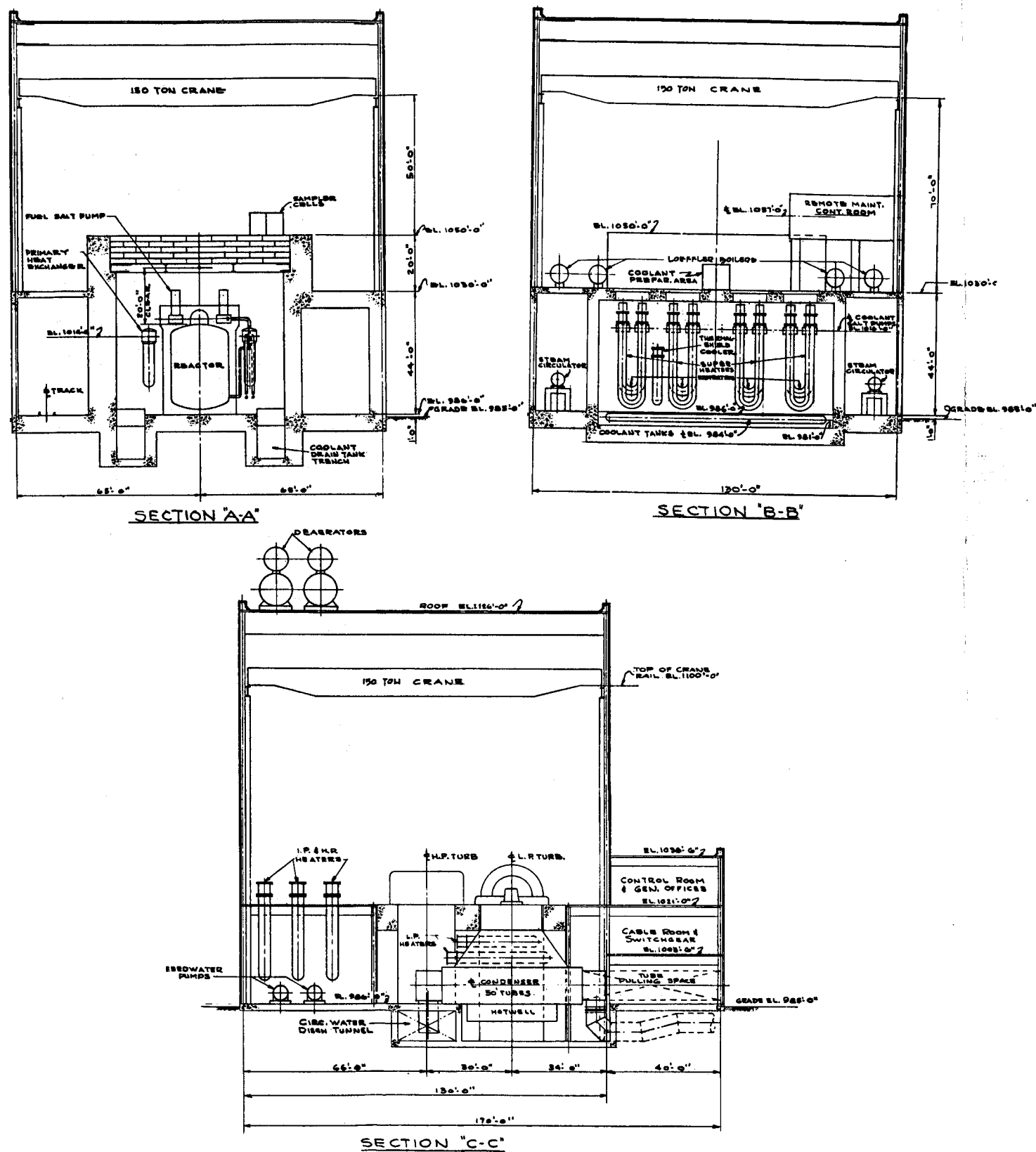


Fig. 4.7. MSCR Plant - Elevation. (Sargent and Lundy Drawing)

4.4 Primary System Components

The primary system components consist of the reactor vessel, moderator, fuel salt pumps and fuel salt-to-intermediate coolant salt heat exchanger. The arrangement of these components is shown in Figs. 4.1 and 4.2. Design and performance characteristics are summarized in the following paragraphs.

4.4.1 Reactor Vessel

The reactor vessel is 20 ft in diameter and 37 ft high (including expansion dome) as shown in Fig. 4.1. The vessel wall is fabricated of 2-in.-thick INOR-8. No thermal shield is required since the gamma heating of the vessel wall does not exceed 0.6 w/cc. The thickness of the external vessel insulation and salt flow through the core-vessel annulus can be adjusted as necessary to avoid excessive thermal stresses in the vessel wall and at the same time minimize heat loss to the external containment space.

A 6-ft diam expansion dome at the top of the reactor vessel not only provides surge volume but serves as the fuel salt volatiles purge location, the UF₄ pellet injection point and salt sampler location. Circulation of fuel salt in the dome is accomplished by recirculation of salt from each pump discharge through an orificed 2-in. line to a point below the normal liquid level in the dome. This level is maintained by adjusting the pressure of the helium cover gas. To minimize holdup of salt, 50% of the volume of the dome is occupied by 2-in. diam sealed INOR-8 tubes.

The reactor vessel is provided with eight inlet nozzles which discharge fuel salt radially into the bottom plenum, eight outlet nozzles leading to the pumps, together with bottom and top INOR-8 grids for support and restraint of the graphite core. These grids in turn are supported by columns or stanchions attached to the reactor vessel.

The reactor vessel specifications are given in Section 4.10.

4.4.2 Moderator Structure

The graphite matrix is composed of cylindrical logs 8 in. in diameter and 24 in. long, as shown in Fig. 4.8. These are stacked in a vertical position and alligned by means of axial pins and sockets. Fuel-salt flows up through the cusp-shaped passages between logs.

The "pile" is centered in the vessel by metal pins protruding from the support plates at the bottom and top of the vessel. These are located near the axis of the vessel and mate with a corresponding moderator log. Initially the pile rests on the lower support grid; as the reactor is filled with salt, the pile floats up against the upper grid. The pins, while allowing this vertical motion, keep the central logs centered in the vessel. The remaining logs are bound to these by means of metal hoops passing around the peripheral logs. These hoops are fabricated from molybdenum, which has about the same coefficient of expansium as graphite. This arrangement allows the support grids to expand independently of the moderator as the reactor is brought to operating temperature. Also, the increase in height of the vessel on expansion is accommodated.

The radial profile of temperature in the fuel-salt is flattened by proper distribution of the flow, which is accomplished by orificing the flow channels. The bottom row of moderator logs is machined from hexagonal pieces. A 4-in. section of the end in contact with the support grid is not machined. If close-packed in a triangular lattice, these ends would block completely the flow path of the fuel salt. Therefore, the corners of the hexagons are cut away to provide orifices of appropriate diameter for each channel.

4.4.3 Fuel-Salt Circulating Pumps

Circulation of the fuel salt flowing at 9075 gpm is maintained by a centrifugal pump as shown in Fig. 4.9 in each of the eight independent heat exchange circuits. Because the system has no valves or other means of equipment isolation, the pumps are installed at the highest elevation (and the highest temperature region) of the circuit between the reactor and the primary heat exchanger. By this means it is possible to avoid the hazard of seal flooding and reverse rotation at standstill and to

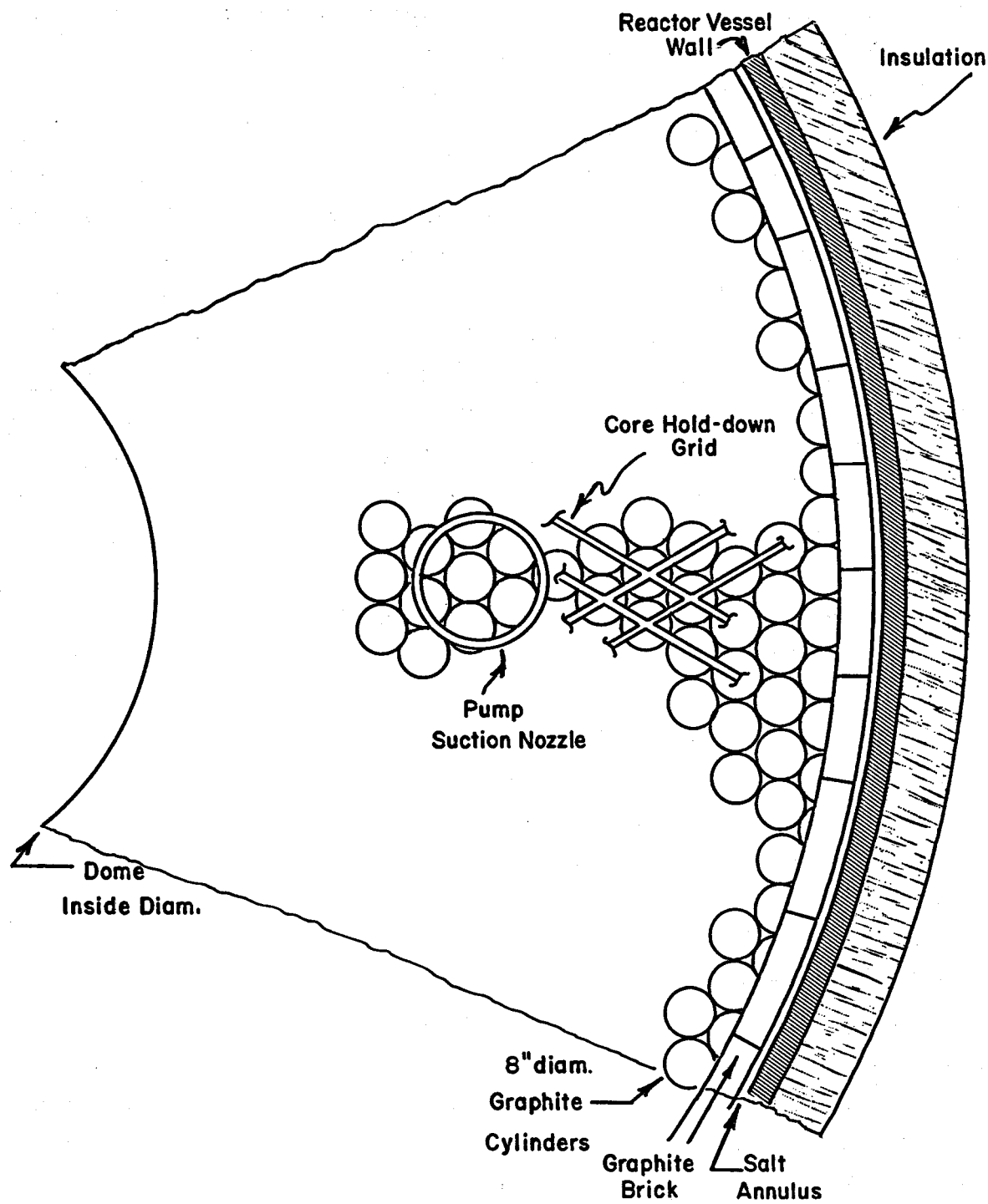


Fig. 4.8. MSCR Core Configuration.

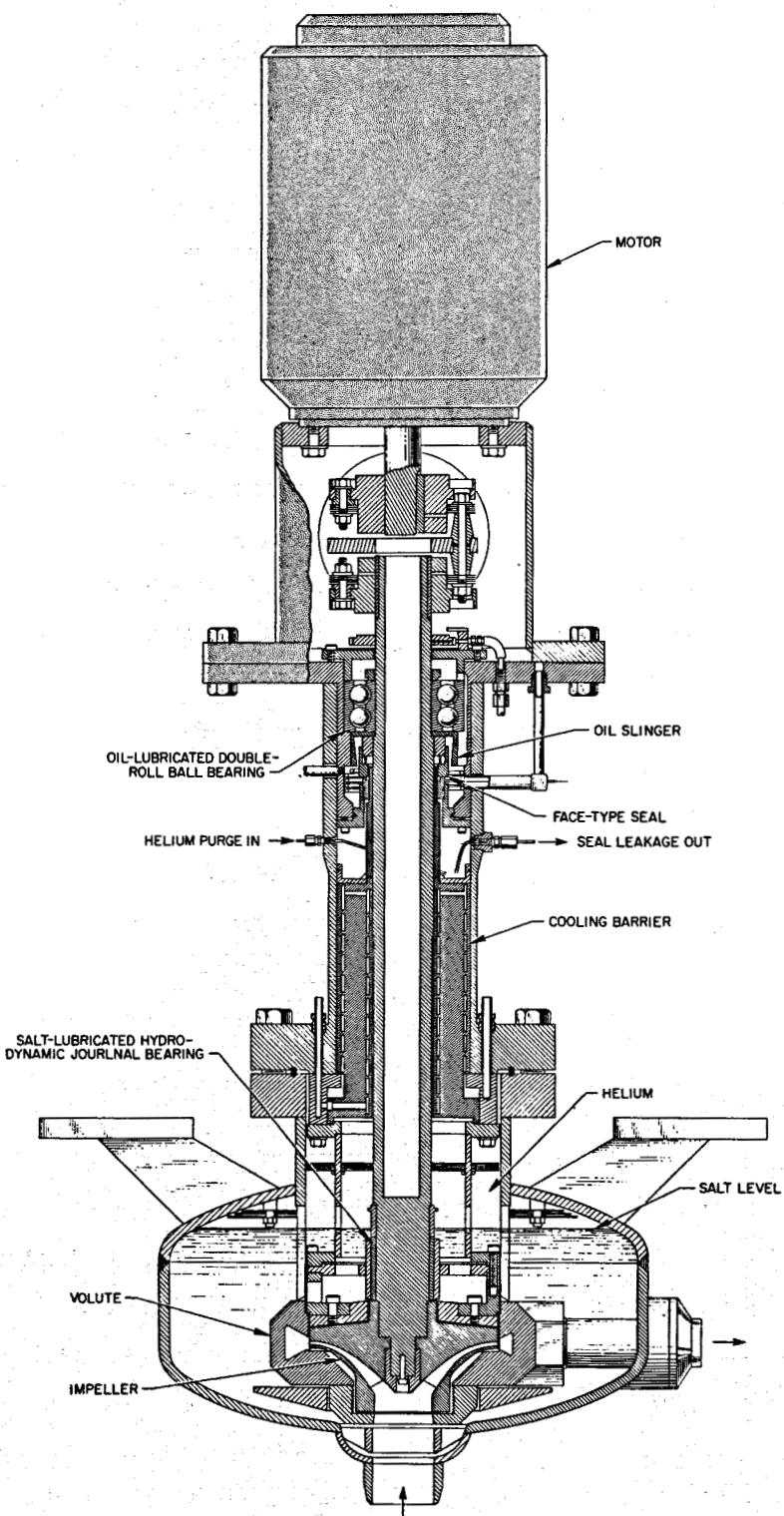


Fig. 4.9. Molten Salt Journal Bearing Pump.

minimize some design problems related to thermal expansion, shaft seal and guide bearings, and maintenance accessibility. Locating the pumps so close to the reactor, however, introduces the problem that the organic materials used in the motor winding insulation and bearing lubricant must be shielded from radiation. Also the pump motor and oil-lubricated bearings must be located at some distance from the salt region. In the design shown, the motor and oil-bearings are positioned above the pumps for easy maintenance and a lower salt lubricated bearing provided to take the radial thrust. Circulation of salt through this bearing is accomplished by allowing salt to leak upwards around the shaft and out a small vent line. A cylindrical casing above the impeller provides expansion volume and a volatile fission product purging surface. The surface of salt in this casing is maintained at the same level as that in the expansion dome under a helium cover gas at 22 psi. This gas overpressure also helps prevent impeller cavitation.

Detailed specifications of the MSCR pumps are given in Section 4.10.

4.4.4 Primary Heat Exchanger

The design of the heat exchanger for transferring heat from the fuel salt to the intermediate coolant salt is shown in Fig. 4.10. This shell and tube heat exchanger is of a U tube configuration designed particularly for accessibility to the tube sheet from above without disturbing connecting piping. Removal of the tube bundle through the top head is also possible with the given design. With this configuration, however, the more valuable fuel salt, which normally would be circulated through the tubes, is put on the shell side to permit ready drainage. The tube bundle and associated baffles, which can slide into the shell from above, hang from the tube-sheet which rests on a shelf machined into the shell. A circumferential seal weld joins the tube sheet to the shell and separates the coolant from the fuel salt. A hold-down ring keeps the tube sheet in place in case pressure on the shell side should exceed pressure on the tube side. Normal design conditions require that the coolant salt (tube side) be kept at a pressure higher than that of the fuel salt.

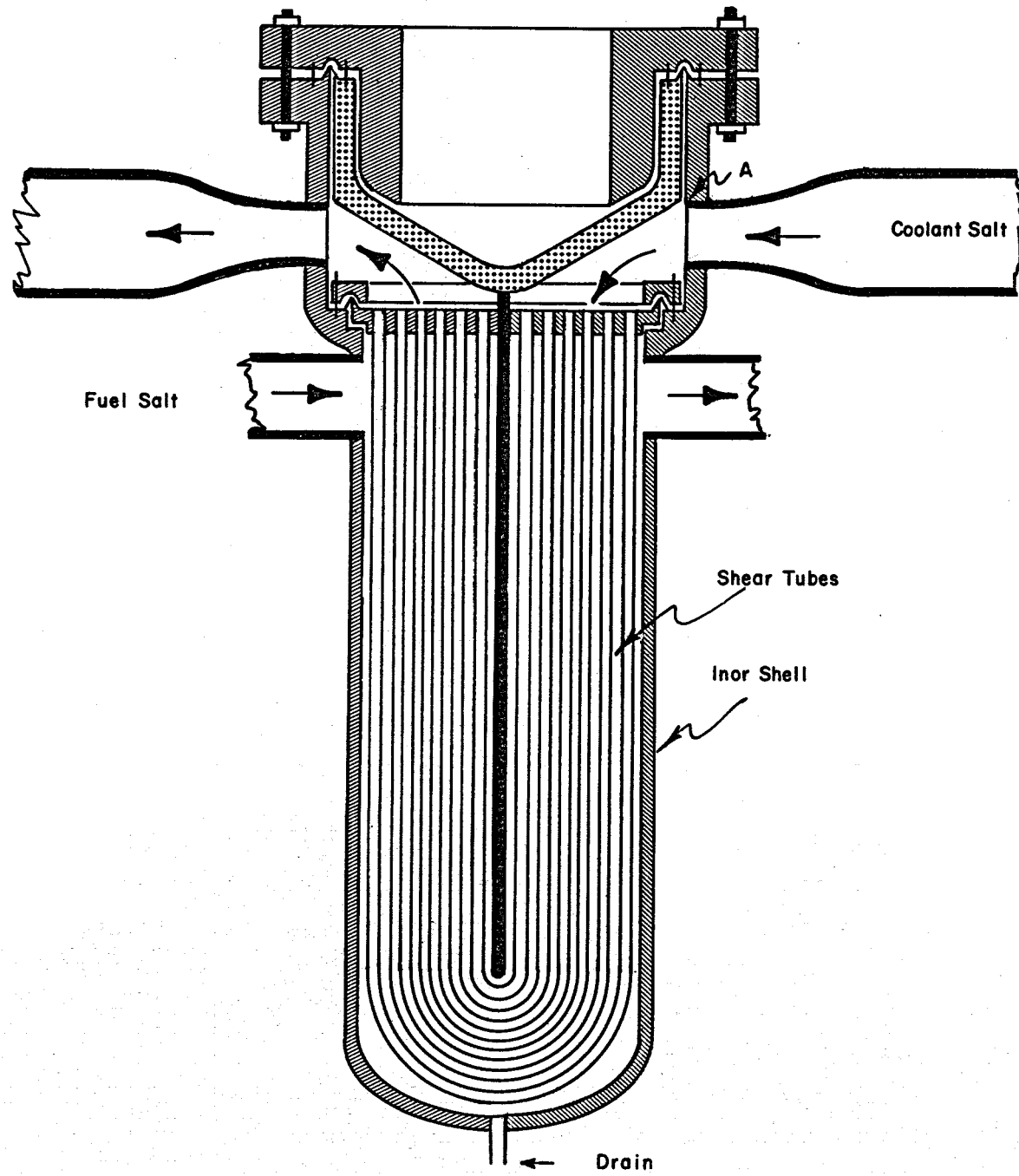


Fig. 4.10. MSCR Primary Heat Exchanger.

The end-closure may be sealed against leakage of coolant salt to the outside in several ways. A bearing and sealing surface (much like a valve seat) is provided at point "A" shown on Fig. 4.10. A frozen salt seal is maintained in the annulus above "A". A seal weld could be made at the top between the flange on the shell side and the inverted head. Or lastly, double-gaskets on circles inside and outside of the seal weld lip could confine leakage if the seal weld, or other seals ahead of the seal weld, should fail. A massive hold-down flange bolted to the top flange provides the strength necessary to hold the inverted head against the several hundred pound pressure of the coolant salt.

A partition attached to the inverted heat fits closely into a diametrical slot in the tube sheet to separate the inlet coolant salt plenum from the outlet plenum. A small amount of by-pass flow may occur through the very small gap between the slot and the partition. The inverted head is shaped so as to minimize the volume of coolant salt in the tube-sheet distribution plenums. The inlet and outlet coolant nozzles are noncircular in cross section (flattened and broadened so as to minimize head-space without sacrificing flow area).

Not shown are cooling and heating provisions for the top head, heating provisions for the shell or the insulation which must be provided.

In order to avoid excessive thermal stresses in the tube sheet it may be necessary to reduce the thermal gradient across the tube sheet by providing insulation between it and the fuel salt.

An appreciable heel of coolant salt will remain in the tubes after draining. In order that the salt-containing internals of the heat exchanger be exposed only to inert atmospheres when the top closure is removed, the upper portion of the heat exchanger (above the coolant nozzle) is provided with a gas-tight caisson that extends from the heat exchanger to the locality of the maintenance equipment.

The specifications given in Section 4.10 are based on eight heat exchangers per reactor, each with a heat load of 1.006×10^9 Btu/hr per unit.

4.5 Intermediate Cooling System

4.5.1 Introduction

Leakage of steam into the fuel salt would result in precipitation of uranium; therefore, a material which has good heat transfer properties and is compatible with both fuel salt and steam must be interposed between these two materials. Of the various possible choices, a barren salt of LiF-BeF₂ appears to be the most promising and is used as a basis for the present MSCR design involving a Loeffler steam generation system. In this design the intermediate cooling system consists of the heat exchanger already described, coolant salt pumps, steam superheaters and steam reheaters.

4.5.2 Coolant Salt Pumps

The coolant salt pumps are similar in design to the fuel salt pumps but have a higher capacity and head. Eight pumps serve the sixteen superheaters and four reheaters and each pump circulates 13,900 gpm of coolant salt at a temperature of 950°F and the primary heat exchanger inlet pressure of 300 psia. The developed head of the pump is approximately 270 ft. Additional specifications for the coolant pumps are given in Section 4.10.

4.5.3 Steam Superheaters

Steam from the superheaters is divided among several streams. About 20% is used to drive the turbogenerators for the production of electricity; a much smaller fraction is used to drive other turbines which power feedwater pumps and the steam circulators. The balance is mixed with feedwater in the Loeffler boiler to produce saturated steam required in the superheater.

A U-tube in U-shell arrangement with fixed tube sheets and counter-current flow of coolant salt and steam is shown in Fig. 4.11. Coolant salt is on the shell-side, and steam flows through the tubes. The unit is mounted on its side to minimize floor space. The shell-side is unbaffled to minimize pressure drop. The heat transfer coefficient with near-laminar flow of coolant salt is about 15% less than for baffled flow, and requires

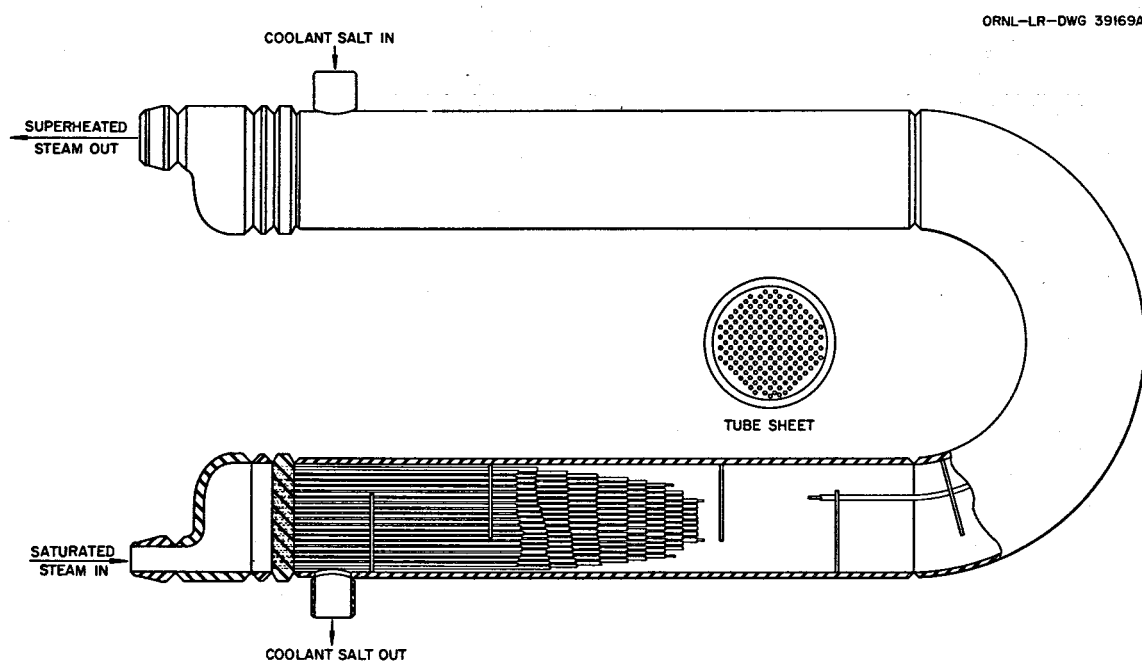


Fig. 4.11. MSCR Steam Superheater.

more tubing. To prevent freezing of the salt, the superheater is brought up to operating temperature by steam generated in an auxiliary, oil-fired boiler.

Coolant salt operating between 950 and 1100°F circulates through the shell-side. Steam enters at 670°F and 2490 psi, and leaves at 1000°F and 2465 psi.

4.5.4 Steam Reheaters

In order to provide greater energy availability for the turbine work cycle and to provide lower pressure steam to drive auxiliary turbines, the high pressure turbine exhaust steam is directed to the reheaters, the auxiliary turbines, and the second feedwater heaters. The same general design criteria apply to the reheaters as to the superheaters, although the steam is at a lower pressure.

As with the superheaters, the reheaters are constructed of INOR-8 and alloy steel. Eight units provide the desired heat transfer surface. Again, the coolant salt flows in the shell countercurrently to the steam passing through the tubes. Comparable pressure drop and heat transfer conditions exist in the reheater as in the superheaters, although baffling (to improve heat transfer) on the shell introduces a pressure drop of about 40 psi.

4.6 Power Generation System

4.6.1 Introduction

Before selecting the power generation system for the MSCR a number of alternative approaches were considered in some detail. These included the use of (a) a mercury boiler, (b) a "Kinyon" boiler, (c) a "Bettis" boiler, and (d) a "Loeffler" boiler. The characteristics of these alternative steam generation systems are summarized as follows.

The use of binary mercury-steam power cycles for power generation from solid fuel reactors has been studied by Bradfute et al. (13) and Randall et al. (92). Kinyon and Romie (55) considered application of the binary cycle to molten salt reactors. The binary system, in addition to

mitigating the thermal stress problem, has the further advantage of a higher thermal efficiency (95). On the other hand, bimetallic heat exchangers are required at the high temperature end, and it is not obvious that the fuel salt volume will be small compared to that involved in the Loeffler system.

The "Kinyon" boiler (53) employs bayonet elements composed of three concentric tubes. Water is introduced in the annular passage surrounding the innermost tube and is boiled by heat transferred from superheated steam flowing downward in the outer annulus. Vapor is separated from the liquid at the top of the inner annulus; the liquid is routed down the central tube to a plenum from which it is recycled to the boiling annulus. Vapor passes down the outer annulus; it is superheated by salt surrounding the bayonet element and in turn boils the water rising in the inner annulus. This arrangement results in tolerable thermal stresses in the tubing. The system avoids the use of steam recirculators. Furthermore, the bayonet tube boiler may be more compact and less expensive than the equivalent superheaters and boilers in the Loeffler system. It is not clear, however, that the required rate of vapor-liquid separation can be achieved with present technology.

The "Bettis" boiler is a modification of the "Lewis" boiler (59,55) wherein a bayonet tube containing water and steam is inserted into a thimble extending down into the fuel salt. An inert buffer salt occupies the annular space between the pressure tube and the thimble, providing thermal contact along with physical isolation. This system avoids use of steam circulators and also eliminates the necessity for pumping the intermediate salt.

4.6.2 Loeffler Boiler System

In the system selected for the reference design, four boilers generate steam by direct contact between the steam from the superheaters and the feed water from the turbine cycle. Four steam compressors circulate the saturated steam from the boilers through the superheaters of the inert salt system, providing steam at 2400 psia, 1000°F at the turbine throttle and at the superheated steam inlet of the Loeffler boilers.

These boilers, shown in Fig. 4.12, consist of cylindrical drums with an inside diameter of about 72 in., with distribution pipes for superheated steam and feed water located on the vertical centerline and below the horizontal centerline of each drum. Conventional cyclone steam separators, located above the horizontal centerline and arranged in four parallel rows along the inside of the drum, separate the steam from the boiling water. A system of scrubber-type steam driers occupies the upper part of the drum. In operation, superheated steam and feed water are mixed as they leave the two distribution pipes and boiling occurs. The boiling water is guided by internal baffles through the cyclone separators where the water is removed by centrifugal force. Steam and a small amount of moisture flow through the scrubbers, where the steam is dried to approximately 99.7 quality. The drums are fabricated of carbon steel and are designed for a pressure of 2625 psia. A wall thickness of 7 in. is required for an inside diameter of 72 in. and a temperature of 650°F. Each drum is about 100 ft in length and has hemiellipsoidal heads.

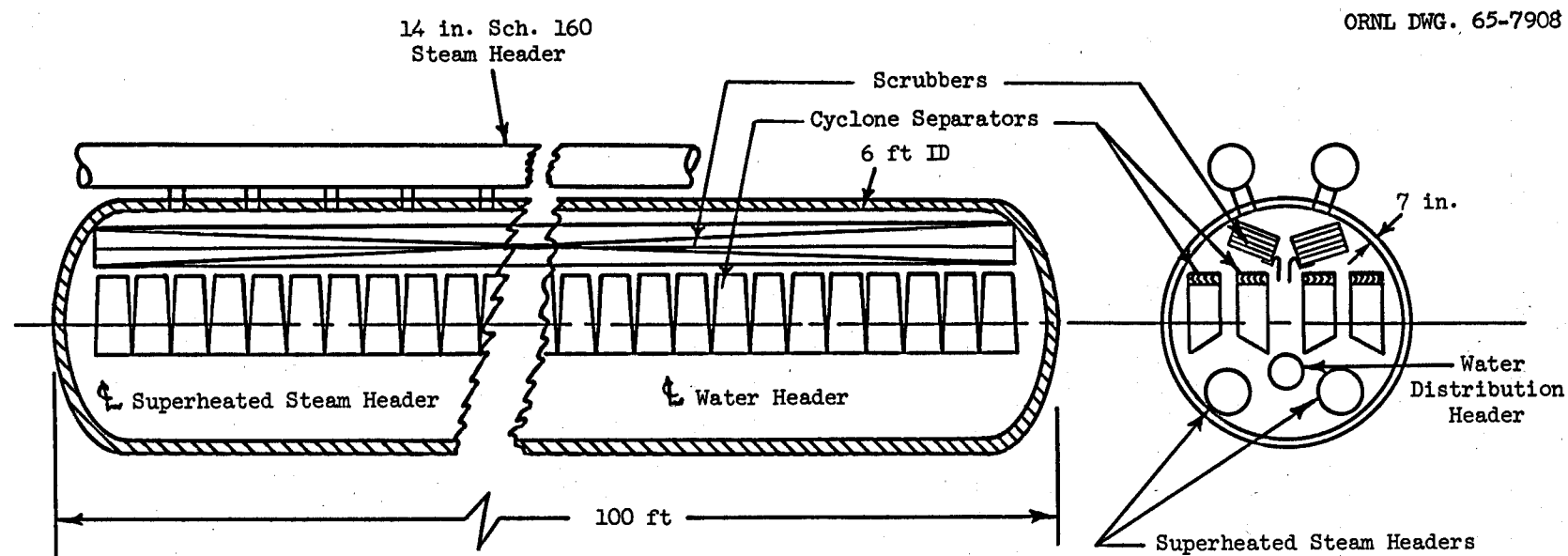
4.6.3 Steam Circulators

The steam circulators are single-stage axial compressors suitable for a steam flow of approximately five million lb/hr at a discharge pressure of 2480 psia. The circulators are driven by steam turbines, using steam from the cold reheat lines of the main turbine-generator. At design conditions, each circulator requires a power input of 4750 BHP. Steam from the turbines is returned to the cycle through the feed-water heaters. One circulator has a motor drive suitable for full flow at design pressure to be used during start-up shutdown. An oil-fired package boiler, designed for a saturated steam flow of 50,000 lb/hr at 300 psia, is provided for startup purposes.

The system is designed to operate as four 1/4 capacity units; each unit consists of one Loeffler boiler, one steam circulator and four superheaters. Valves are located according to this philosophy. Interconnections between various units are not provided except at the inlet to the boilers and the discharge from the superheaters.

ORNL DWG. 65-7908

56



Operating Conditions (one unit):

Inlet Water 2×10^6 lb/hr @ 545°F, 2500 psi

Inlet Steam 3.1×10^6 lb/hr @ 1000°F, 2450 psi

Outlet Steam 5.1×10^6 lb/hr, sat. @ 2400 psi

Fig. 4.12. MSCR Loeffler Boiler.

4.6.4 Turbogenerator

The turbogenerator is a standard CC6F-RH unit operating at 2400 psia 1000°F and producing a gross electrical output of 1083 Mw. As shown in Fig. 4.3 the units consist of three turbines: two double-flow high pressure units and one double-flow intermediate pressure unit on one shaft with a 667 Mw net output plus three double-flow low pressure units on another shaft with a 416 Mw net output.

The plant auxiliaries have a maximum coincidental loading of 45,000 kw; this power results in a net station output of 1038 Mwe to the station main power transformers.

Other characteristics of the power generation system are given in Fig. 4.3 and summarized in Section 4.10.

4.7 Reactor Control System

4.7.1 Introduction

The specifications for the MSCR control system depend on the unique properties of its fluid-fuel. The main mode of shim control is by adding UF₄ to increase reactivity and by replacement of fuel salt with a salt containing no fissile isotopes to decrease reactivity. This control is supplemented by operational control with BF₃ gas, which is sufficiently soluble that adequate concentrations may be obtained in the salt by regulating the partial pressure of BF₃ over the salt surface in the dome.

Fuel is added to compensate burnup and fission product accumulation. Greater reactivity control is required during startup and shutdown. The startup procedure involves a gradual increase in power, during which the rising xenon poisoning (controlled by the flux level) is compensated by the addition of new fuel. After shutdown, the reactor is sub-critical for forty hours while ¹³⁵Xe grows in. If longer shutdown is required, then fifty cubic feet of fuel salt must be removed and replaced by non-fissile salt.

Emergency shutdown, such as that required in a loss-of-flow accident, is provided by injecting BF₃ gas through tubes opening into the core just above the bottom support grid. The BF₃ will displace fuel, will rapidly

dissolve in the salt, and will diffuse into the graphite. All of these processes will result in a rapid and large decrease in reactivity.

4.7.2 Shim Control

For shim control by fuel addition or removal, two reactivity-control drain tanks of 50 cubic ft capacity each and a shim-control salt-addition tank of 50 cubic ft capacity are located in the reactor containment cell. All tanks are provided with vents to the reactor dome, gas connections to the helium pressurizing system, and several 100 kw electric heaters for initial vessel heating and maintaining stored salt temperature. The addition tank is essentially in parallel with the 2 cubic ft salt-addition metering tank. The drain tank is connected to the reactor vessel upper plenum and is installed with respect to the reactor dome liquid level so that overfilling will not be possible. Freeze valves are used to isolate the tanks from the reactor. The reactivity control drain tanks must have, in addition to heating coils, decay heat removal facilities similar to the fuel salt drain tanks. They have an independent steam condenser and heat removal system which will be 1/20 the size of the fuel drain tank heat removal system.

4.7.3 Emergency Control

The BF₃ addition system comprises pressure cylinders manifolded to a heater. BF₃ flow control and quick-acting injection valves are incorporated in the supply line connected to the bottom plenum of the reactor vessel. The flow control facility is operated from the shim control instrumentation and the quick-acting injection system is operated from the "scram" circuits.

The BF₃ gas is stored in six 330 cubic ft, 2000 psi cylinders located outside and adjacent to the east wall of the reactor building. The specifications for the reactivity-control drain tanks and the reactivity-control salt-addition tank are given in Section 4.10.

4.8 Salt Handling Systems

4.8.1 Introduction

Facilities for handling both fresh and spent fuel salt and intermediate coolant salt constitute the heart of the MSCR complex. The functions which must be performed include melting, purifying, charging, removal, storage, and sampling of the salt. These are accomplished by means of the following systems and facilities shown in Fig. 4.13.

- a. Fuel salt preparation
- b. Coolant salt preparation
- c. Reactor salt purification
- d. Coolant salt purification
- e. Reactor salt charging system
- f. UF_4 addition facility
- g. Fuel salt drain and storage system
- h. Coolant salt drain system
- i. Spent fuel withdrawal system
- j. High level radioactive sampling
- k. Coolant salt sampling

4.8.2 Fuel Salt Preparation

Fuel salt is received in solid form and must be liquified prior to processing. Barren salt, having the same composition as the intermediate coolant salt, i.e., 66% LiF and 34% BeF_2 , with a liquidus temperature of 851°F is used for preoperational testing and system flushing before and after maintenance activity. A solid mixture having this composition is charged initially. Sufficient LiF and ThF_4 are added to form composition 68% LiF, 23% BeF_2 and 9% ThF_4 . All mixtures are processed through the same equipment. After routine operation is established, flush salt is the base material for the lithium/thorium addition process. In this manner, flush salt contaminated by fission products may be consumed and special treatment for removal of fission products will be unnecessary.

A 12-ft-high, 150 cubic ft tank enclosed by an 8-ft-high, 150 kw furnace receives solid salt for melting. The furnace, located in the

ORNL-DWG. 65-7909

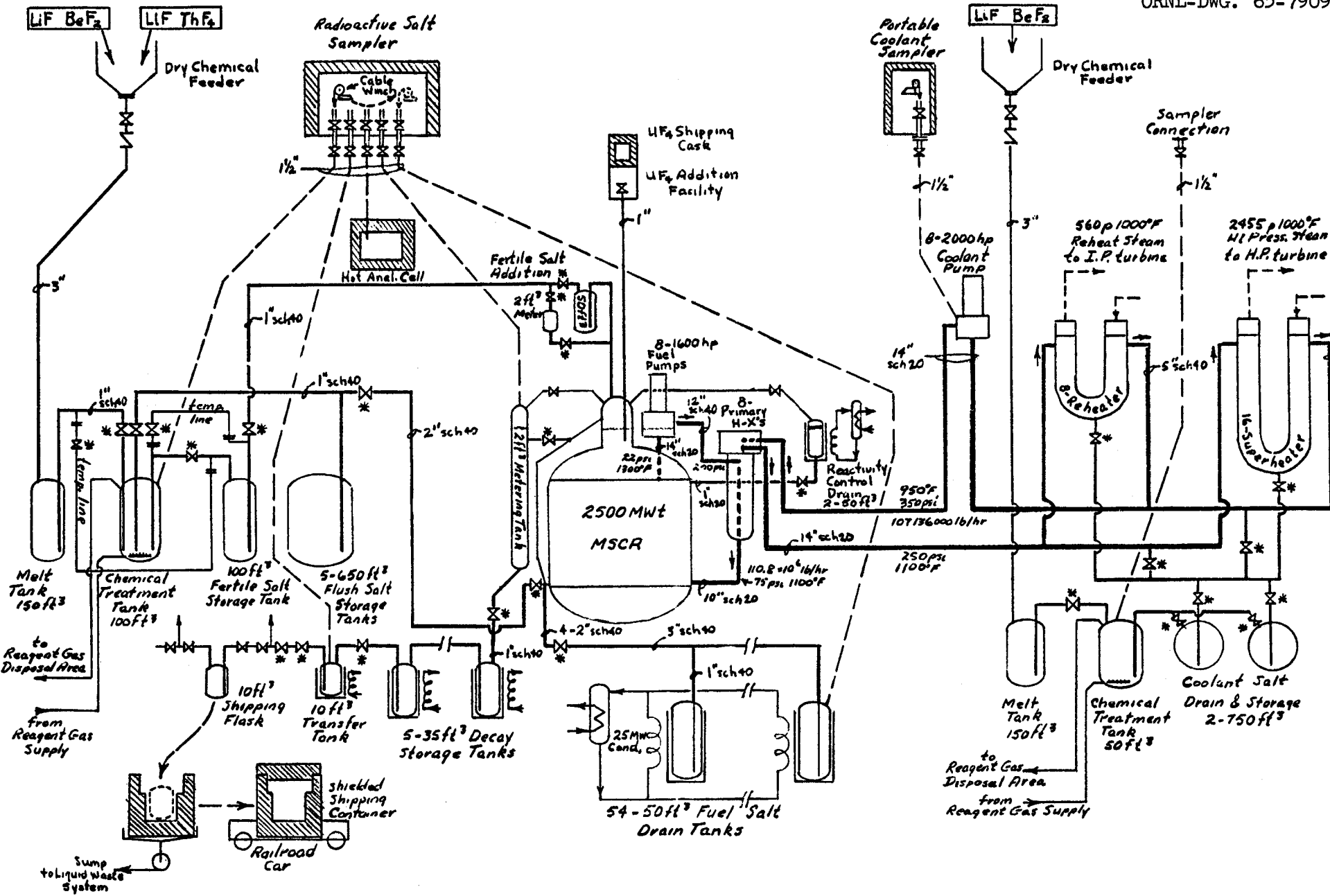


Fig. 4.13. MSCR Fuel Handling Storage Diagram.

flush-salt storage area, is designed for melting approximately 7 ft³/hr. Molten salt is transferred by pressure siphoning.

Solid salt is added by means of a tube extending from the floor above the storage area to the melt tank. The top of the tube is flanged and sealed. A valve is located just below the flange. The tube takes a devious route and is provided with a helium purge to prevent back-flow of radioactive material and intolerable radiation levels at the open feed point. A check valve just below the flange allows purge gas to be directed into the melt tank. A portable hopper is connected to the flange face to receive salt from the shipping containers. A portable shed covers the work area to prevent the spread of toxic dust resulting from the feed operation.

4.8.3 Coolant Salt Preparation

Equipment and system design are similar to that of fuel-salt melt tank and solid salt feed. The melt tank is located in the heat exchanger room near the chemical treatment tank. Solid salt is fed from the floor above.

4.8.4 Reactor Salt Purification

The reactor fuel and flush salts are purified in the molten state prior to charging or storing. This is done initially to remove oxides, and subsequently, to remove oxides and other contaminants.

In normal operation, a chemical treatment tank of 100 cubic ft capacity located in the flush-salt storage area receives the molten salt. After a one-day holdup for purification, the salt is transferred to storage tanks. By the addition of LiF and ThF₄ to flush salt in the melt tank, fertile salt is formed; this is then transferred to the fertile salt purification tank where gaseous HF and H₂ are bubbled through the liquid to remove oxides. Subsequently, the treated salt is transferred to the 100 cubic ft salt-storage tank installed at the same location. Flush-salt make-up is processed in the same manner, and through the same equipment. After treatment, it is transferred to a spare flush-salt tank.

For the initial charges of flush salt and fertile salt for the reactor system, greater purifying capacity is required in order to avoid delay

in preoperational testing and power production. To fulfill this condition, HF and H₂ bubbling facilities are provided in the fertile salt storage tank and temporary flanged lines arranged so that the fertile salt tank may receive molten salt from the melt tank, perform partial purification and allow transfer of the salt to the normal treatment tank. In this manner the two tanks, fertile storage and chemical treatment, are placed in series to double both the purification rate and the system salt charging rate. This procedure does not increase the sampling or analysis requirements over those necessary for normal operation.

4.8.5 Coolant-Salt Purification

The purpose of the coolant salt purification system is to remove impurities such as corrosion products or oxides which could cause fouling of surfaces and plugging of lines and tubes if allowed to accumulate.

It is unlikely that a single coolant charge could be used for the whole lifetime of the reactor without exceeding permissible concentrations of oxides or corrosion products; however, it probably will not be necessary to employ a continuous treatment of coolant salt. Oxides may get into the coolant salt by accidental exposure to air or water vapor, or from oxygen present as an impurity in the cover gas used to pressurize the coolant-salt systems. Although the rate of corrosion of INOR-8 surfaces by coolant salt is low, the area of metal surface in contact with coolant salt is very large, so that corrosion products are certain to accumulate. When it becomes necessary to repurify the coolant salt, it is done batch-wise, one coolant circuit per batch, at infrequent intervals during periods of reactor shutdown.

If the coolant salt should become contaminated with fission products or uranium as a result of a leak in the primary heat exchanger (an event not likely to occur because the coolant salt system is kept at a pressure higher than that of the fuel salt), the contaminated coolant salt is drained from the affected circuit to a drain tank, and then transferred to the chemical processing plant for disposal.

4.8.6 Reactor Salt Charging System

Fuel salt without uranium is injected into the primary reactor circuit by manual control from a small salt addition tank to replenish the fuel salt withdrawn for chemical processing (two cubic ft per day). This addition is made remotely and with assurance that fuel salt will not flow back into the addition system. The make-up is fed into the reactor in a molten condition by gravity flow or under pressure. Sufficient electrical heating to maintain the salt in a molten condition prior to injection is provided.

A two-cubic-ft salt addition tank (metering tank) is located on the wall of the biological shield at a level somewhat above the liquid level in the reactor. The tank is supplied from the fertile-salt storage tank situated in the flush salt storage area. Makeup is accomplished by opening the freeze valve and the vent valve between the tank and reactor dome. The freeze-valve in the line leading to the reactor dome must be placed at the bottom of a loop so that when the tank is empty a heel of salt will remain in the valve.

4.8.7 Intermediate Coolant Charging System

Molten coolant salt is injected into any one of the eight intermediate coolant loops from the coolant drain tanks at a rate up to 600 ft³/hr. The drain lines from several locations in each of the eight intermediate coolant loops also serve as charging lines for this operation.

4.8.8 UF₄ Addition Facility

During steady-state operation at equilibrium, about 6 kg/day of UF₄ are added to the reactor to compensate for burnup and a fuel withdrawal of 2 ft³/day. The amount and rate of addition of UF₄ to the reactor is governed by reactivity and temperature requirements. Valves in the UF₄ addition system must be kept gas-tight when closed even though they must pass solids when opened, but since they will be in a region of relatively low radiation level, plastic seats (for non-scoring properties) may be used.

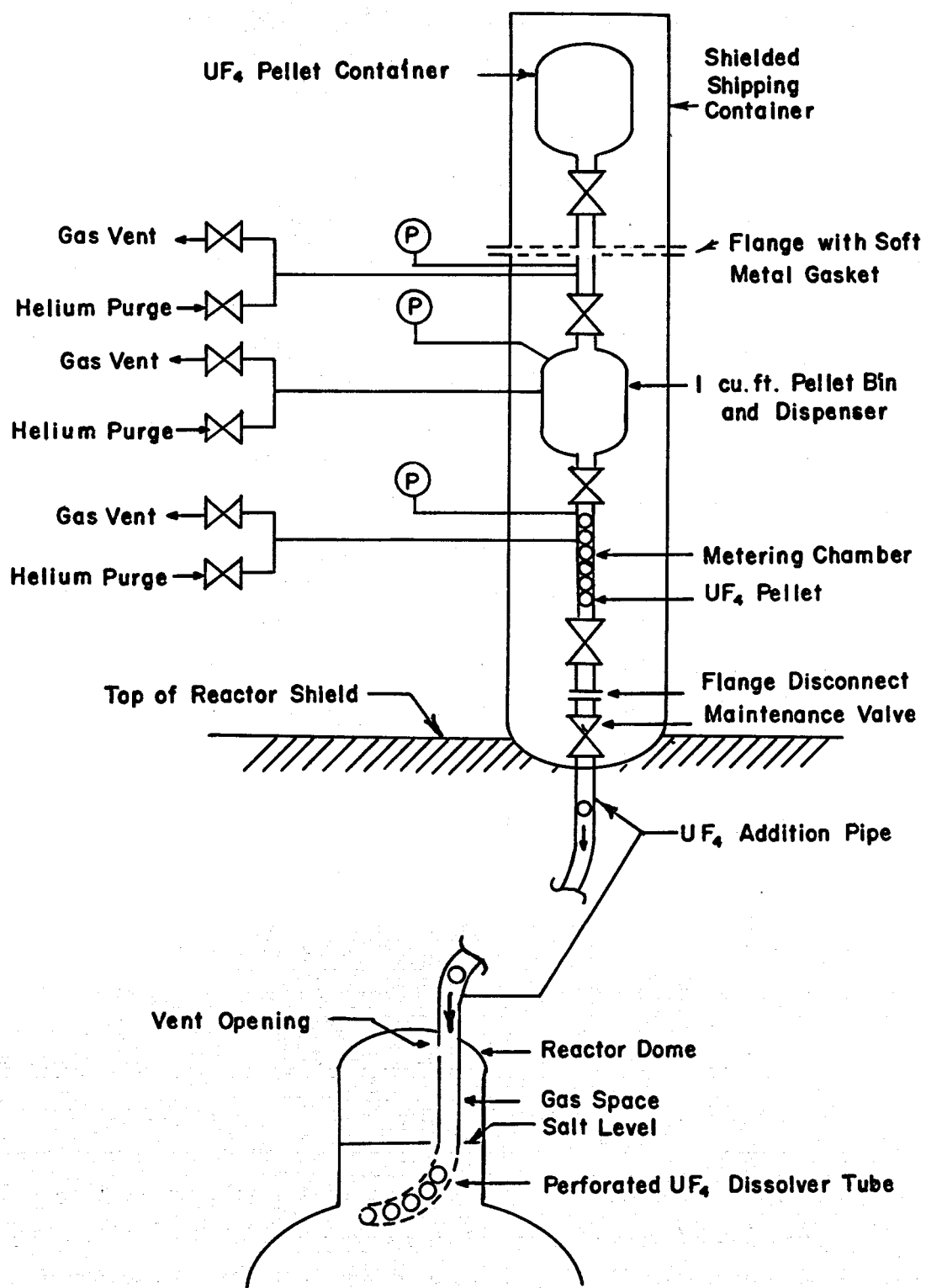
The UF₄ charged into the reactor system is prepared by mixing recycled uranium with fresh uranium. Pellets about 0.75-in. in diam, fabricated by casting UF₄ in an inert atmosphere, are charged into a gas-tight shielded shipping container, containing an atmosphere of dry helium at approximately 1 atmosphere absolute pressure. At the reactor, the shielded shipping container is mounted on the fuel charging machine (which is located above the reactor), and the mated assembly of the shipping container and fuel charging machine is made gas-tight by bolting a gasketed flange. Figure 4.14 shows a schematic sketch of the UF₄ addition facility.

4.8.9 Fuel Salt Drain and Storage System

Facilities are provided for the drainage and storage of fuel salt during periods of maintenance and emergency shutdown. The system is shown on the flow diagram in Fig. 4.2. All salt circuits have drain connections; this includes the primary heat exchangers as well as the reactor vessel. The draining of the fuel salt is accomplished quickly, even under emergency condition without steam flow and auxiliary power, since without heat removal the salt temperatures rise 300-400°F in the first half hour. Four equally spaced 2-in. drain lines connected radially to the bottom plenum of the reactor vessel, with 1-in. interconnections to the primary heat exchangers drain connections, will drain the reactor system in approximately one-half hour after the freeze valves are opened.

The tanks are capable of receiving the full inventory of the reactor within half an hour, maintaining the stored volume of salt at a temperature of less than 1400°F, and recharging it to the reactor. Gravity drain and gas pressure are used for transferring salt.

Because forced circulation may not be available under emergency conditions, natural convection cooling is provided in small-diam cylindrical vessels. Fifty-four vertically mounted 35-in. ID cylinders 8 ft long are located in a 10-ft trench around the inside periphery of the reactor containment cell. Each cylinder is immersed in a molten alkali metal carbonate bath. The carbonate mixture is contained in a double-walled tank which serves as a boiler for the removal of decay heat from the fuel salt. Fifteen-kilowatt electric heaters are arranged within the carbonate mixture annulus for fuel-salt melting following long storage periods and

Fig. 4.14. MSCR UF₄ Addition Facility.

temperature maintenance during shorter periods. The heaters are sized to bring the salt to 1100°F in four days.

4.8.10 Coolant Salt Drain System

These drain tanks have several purposes: (a) to provide storage space for the complete volume of coolant contained in two (out of eight) coolant circuits during periods when it is necessary to drain the coolant from one circuit for maintenance; (b) to provide the reservoir and the application of motive force for transferring coolant salt into the reactor coolant circuits during initial salt-charging; and (c) to serve as a transfer point from which coolant salt may be removed from the system and transferred to shipping containers in case it should become necessary to process contaminated coolant salt.

The drain tanks are located at an elevation which permits the coolant salt to flow by gravity from the reactor coolant system into the drain tanks. The transfer lines are valved with freeze-valves to permit flow to or from any one of the 8 coolant circuits. The transfer lines are large enough to fill one coolant circuit in one hour, using a gas pressure of 50 psig.

4.8.11 Spent Fuel Withdrawal System

Fuel salt is drawn from the reactor vessel drain line at about 30 psia into the vented metering tank. The metering tank is a 4-in. (ID) by 25-ft-long cylindrical vessel located at an elevation such that when flow stops it contains two cubic ft of fuel salt. Vent connections above the salt in the tank lead to the dome on the reactor vessel. Decay-heat removal is accomplished by radiation and convection to the reactor containment cell atmosphere. Because the heat generation rate diminishes rapidly, the rate of removal is controlled by means of an insulated jacket 4 in. thick surrounding the tank, and separated from it by a small air gap. A temperature-actuated bellows opens the jacket to allow excess heat to be radiated to the room. A 12-kw electric heater provides preheating and aids in maintaining desired salt temperature when the tank is full.

After a 24-hr holdup, the salt is released by gravity drain to a transfer tank. When a 10 ft³ batch of salt is accumulated, the salt is

transferred to a shipping flask, which is placed in a shielded cask and shipped by rail to a central processing plant. Spent fuel is accumulated for about 120 days at the processing plant, and is then processed in about 6 days.

Should it be necessary or desirable to hold spent fuel at the reactor site (Section 5.3.4), five 35 ft³ intermediate storage tanks are provided. Heat is removed by boiling water in steam jackets; the steam generated is condensed in water-cooled condensers.

4.8.12 High Level Radioactive Salt Sampler

The high level radioactive salt sampler shown in Fig. 4.15 is used to obtain samples of fuel or flush salt from several points such as the reactor (via the fuel withdrawal tank), the transfer tank in the shipping area, the fuel drain tanks, or the flush-salt chemical treatment tank, and to deliver these samples to an adjoining hot cell for chemical analysis.

Sampling is accomplished by means of access ducts located at appropriate points. These are mounted vertically with no pitch less than 50° from the horizontal. They are large enough to allow the free passage of the sample capsule, and are equipped with a sample capsule cage at the sampling point to limit the depth in the salt melt reached by the capsule and prevent the end of the cable from dipping in the salt.

The thief sampler principle is employed wherein an open sample capsule made in the form of a thick-walled, round-bottomed bucket hanging on a flexible cable is lowered into the salt-containing vessel. The capsule sinks below the surface and is filled with salt which solidifies when the sample capsule is withdrawn to a cooler region above the sample point. After solidification, the capsule is pulled up through the sampler access duct into the sampler cavity in which is located the cable drive mechanism. Once in the sampler cavity, the capsule is positioned over a second duct leading to a hot analytical cell. The sample capsule is lowered through the second duct and deposited in the hot cell. Using a suitable manipulator, which is part of the hot cell equipment, the sample capsule is detached from the end of the cable, and a new sample capsule is attached. The new sample capsule is then pulled up into the sampler cavity in readiness for another sampling operation.

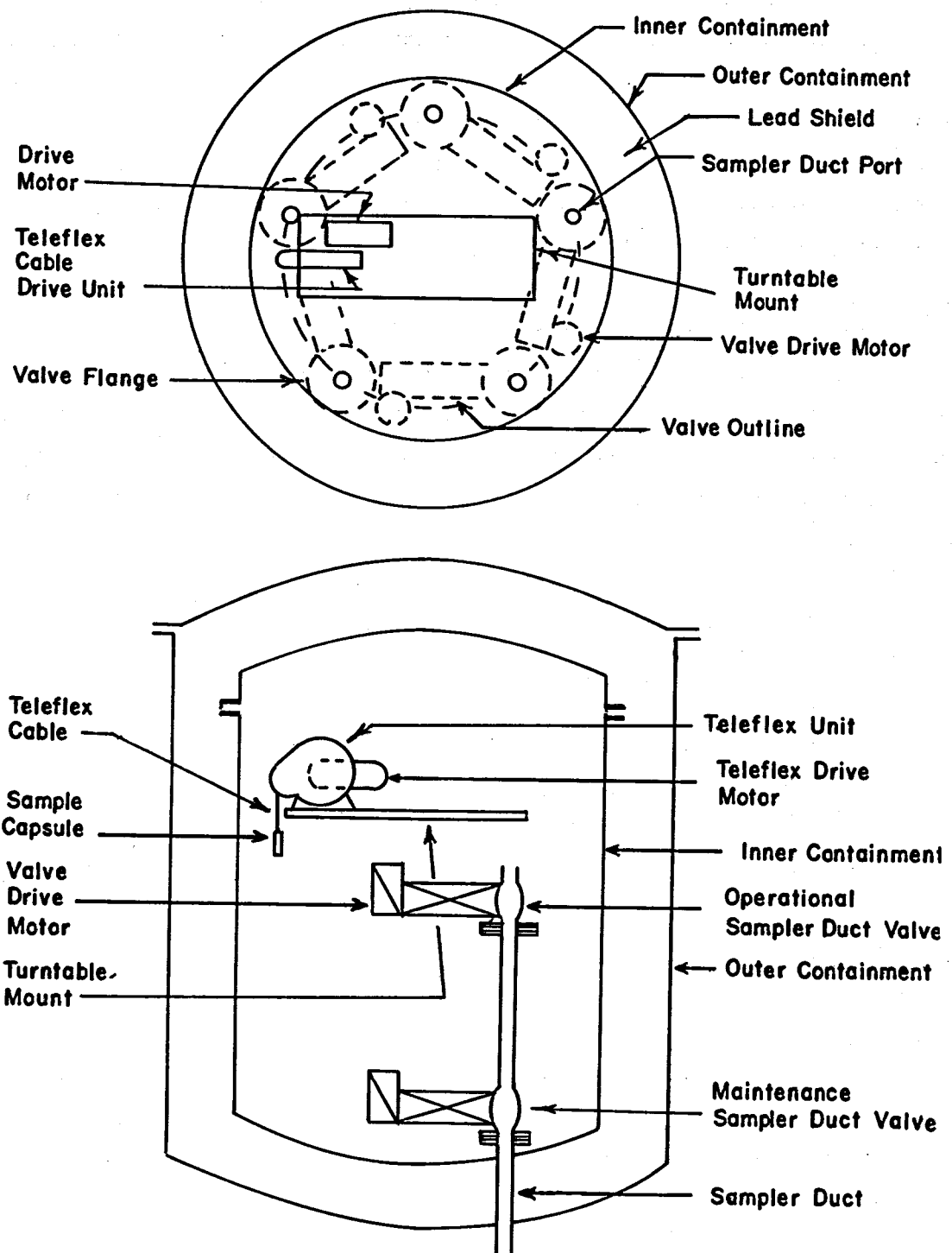


Fig. 4.15. Radioactive Salt Sampler.

The sampler cavity is connected to the hot cell and to each of the four sample points by five separate sample access ducts. Each duct is made of 1 1/2-in. Sch. 40 pipe and contains two 1 1/2-in. double-disc gate valves. The bottom valve is closed only in the event the upper valve is removed for repair or replacement.

4.8.13 Coolant Salt Sampling

Coolant salt sampling connections for a portable sampling device are provided on the eight coolant loops and the chemical treatment tank. Samples are also drawn from the eight coolant-salt pump bowls and from the make-up salt chemical-treatment tank. A portable, single-sample holding device receives the sample in a manner similar to that of the high level radioactive salt sampler, transports the sample to the hot cell area, deposits the sample capsule in the hot cell, and receives a fresh capsule from the hot cell. The connection between the portable sampler and coolant salt system is of a lock type, has a gas-tight fitting and operates in an inert atmosphere (possibly radioactive) from full vacuum to 200 psia at 100°F.

4.8.14 Freeze Valves

Freeze valves are used to close off all lines used for transferring salt from one location to another. These valves are formed in any size of pipe up to 2 in. in diam by pinching the pipe to form a rectangular shaped flow passage. In a 2-in. pipe, the flattened section is about 0.5 in. thick and 2 in. long. Closure of the valve is accomplished by freezing salt inside the pipe. This is done by directing jets of cold air against the top and bottom surfaces of the flattened portion. The air, supplied by a Roots-Connersville blower, is controlled to regulate the rate of freezing. Subsequent thawing of the salt plug is achieved in a few minutes by means of a Calrod electric heater (3000 watts for a 2-in. line) bent in a saddle-shaped series of turns conformal to the flat section. This heater is easily removed for maintenance.

4.9 Auxiliary Services and Equipment

4.9.1 Introduction

Auxiliary services necessary for the MSCR plant are as follows:

- a. Helium cover gas supply and distribution
- b. Reagent gas supply and disposal
- c. Waste gas disposal
- d. Liquid waste disposal
- e. Coolant pump lubricating oil system
- f. Preheating system
- g. Auxiliary power supply
- h. Service water system
- i. Control and station air systems
- j. Cranes and hoists
- k. Instrumentation and control system
- l. Plant utilities

4.9.2 Helium Cover Gas Supply and Distribution System

The helium inert cover gas system serves a number of functions, viz: (a) as a pressurizing gas in various salt containing vessels for the transfer of salt from one place to another; (b) as a carrier gas for the removal of volatile fission products from the recycle gas purge system; (c) as an inert atmosphere to protect against contamination of the salt in places such as the UF₄ system, samplers, melt tank atmospheres, etc., which are occasionally opened to the atmosphere; (d) as a gas seal and bearing lubricant in molten salt pumps; (e) to provide the pressures required in the fuel salt and coolant salt circuits to prevent pump cavitation, and to avoid leakage of fuel salt into the coolant salt in case of a leak in the primary heat exchangers; and (f) to pressurize leak-detection devices at various flanged joints and disconnects.

Since the helium comes into contact with fuel salt or with intermediate coolant salt it must be free from oxide-containing impurities such as H₂O, SO₂, etc; therefore, a purification system is necessary as shown in Fig. 4.16. The raw helium is supplied from a trailer having a capacity

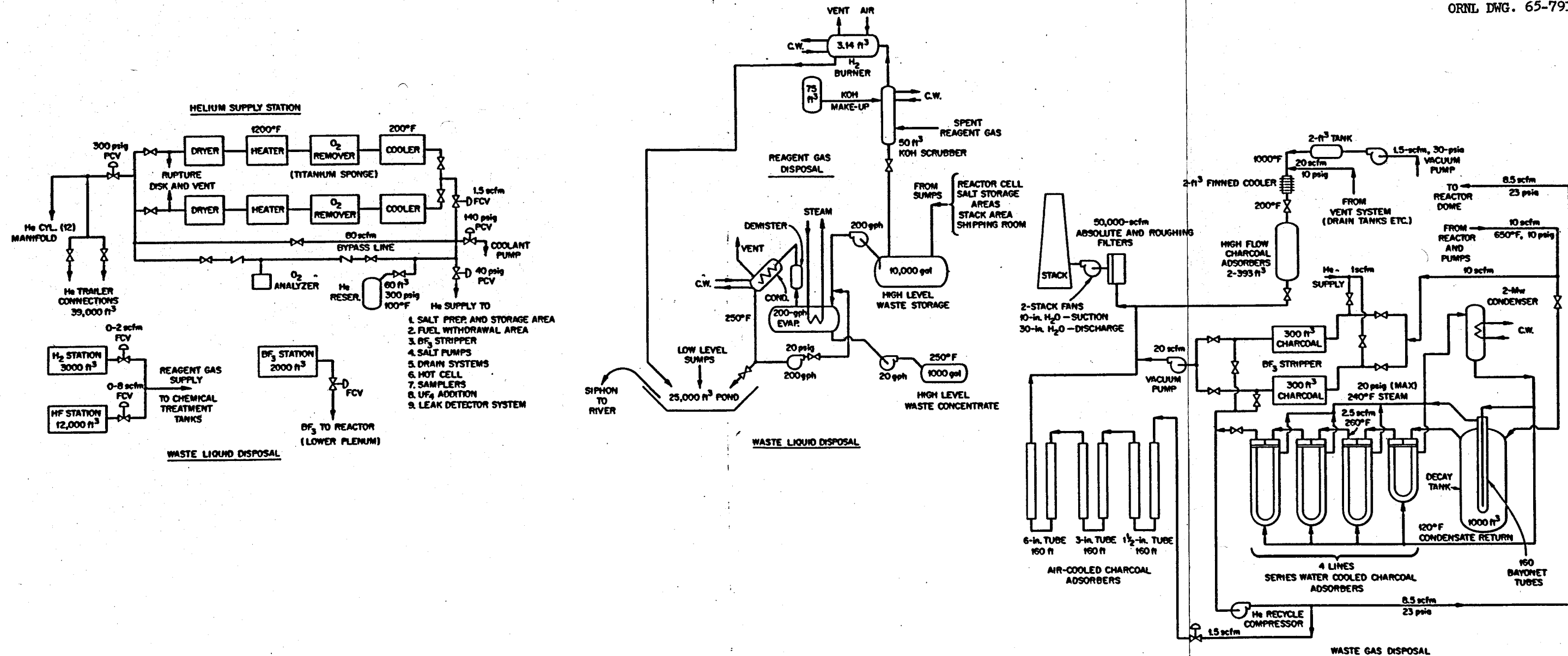


Fig. 4.16. MSCR Auxiliary Services

of 39,000 std. cubic ft in 30 cylinders at 2400 psi. An emergency supply of 2400 std. cubic ft is supplied from twelve 200 std. cubic ft cylinders. As shown in the flow diagram duplicate lines of helium purification units are provided. Each has a capacity of 1.5 scfm.

4.9.3 Reagent Gas Supply and Disposal System

A reagent mixture consisting of 80% anhydrous hydrogen fluoride and 20% hydrogen is used to remove oxide impurities from reactor and intermediate coolant salts. Unreacted reagent gas may contain radioactive material, and thus must be handled by both the gaseous and liquid waste disposal systems.

The reagent gases are supplied from high pressure cylinders provided with pressure reducers and flow control instruments so that the flow may be adjusted (Fig. 4.16). The mixed reagent gas is bubbled through molten salt contained in the fuel-salt and the coolant-salt chemical treatment tanks. Unreacted reagent gas passes through a potassium hydroxide (KOH) scrubber to remove HF, and through a hydrogen burner to remove hydrogen. Spent caustic and condensate from the hydrogen burner may contain radioactive material and thus must be sent to the liquid waste disposal system for concentration and ultimate shipment to a remote disposal area. Non-condensibles from the hydrogen burner are cooled and vented from the system through the gaseous waste disposal system.

4.9.4 Waste Gas System

As mentioned previously, helium is passed through the dome above the core to carry away xenon and other volatile fission products. In addition, purge gas is passed down around the shafts of the fuel pumps to sweep away fission products diffusing toward the upper, oil-lubricated bearings. Also, there is helium cover gas in the bowls of the pumps, in the dump tanks, in the fuel handling system, etc., and all of these must be purged to some extent. In order to limit radioactivity in the atmosphere surrounding the reactor site, the off-gas from these various systems is passed through charcoal beds to trap the fission products until they have decayed, as shown in Fig. 4.16. A few long-lived isotopes,

particularly ^{85}Kr , decay but little in the charcoal beds, and hence considerable dilution with air is required to limit the concentration of these in the stack discharge.

If the BF_3 addition system is ever used to effect a "scram" of the reactor, it will be necessary to remove the BF_3 from the reactor system before normal reactor operation can be restored. A stripped unit removes BF_3 from the recycle helium stream to avoid saturating the off-gas adsorber as shown in the flow diagram (Fig. 4.16).

4.9.5 Liquid Waste Disposal System

Liquid wastes originate in the drains and sumps of the various equipment cells. Typical sources are hot sinks in the analytical laboratory, cell drains in the shipping area where the shipping cask will be flushed with decontaminants, the contaminated equipment storage and decontamination cell, and spent caustic solutions from the reagent-gas disposal system. The liquid waste system shown in Fig. 4.16 provides for holdup, concentration, and storage of active wastes on-site. High level wastes are concentrated by evaporation and stored in underground tanks. Low-level wastes may be held in underground tanks or in a low-level activity pond until they have decayed sufficiently for discharge into the river. The capacity of this pond is approximately 25,000 cubic ft (nearly twice the volume of the contaminated equipment storage cell).

Intermediate wastes are sent to ten 10,000-gallon stainless steel retention tanks, which are used for temporary storage until it is possible to send the waste to an evaporator for concentration.

High level wastes from the plant and from the evaporator are sent to a 10,000-gallon waste-storage tank which provides semi-permanent storage of these wastes, which will ultimately be transferred to shielded shipping containers for shipment to a permanent disposal area.

Spent caustic wastes from the reagent gas disposal system are sent to the intermediate-level storage tank for further concentration and ultimate disposal off-site.

Pumps (mechanical, air jet, or steam jet) are provided at every sump, at the pond, at the 10,000-gallon tanks, at the evaporator tank, and at the 1000-gallon tanks to transfer the liquids.

The waste evaporator is capable of evaporating 200 gallons of water per hour using the plant heating steam. The condenser drains either to the retention tank or to the low level waste pond, depending on the activity. A vent on the shell side allows noncondensables to be vented to the charcoal beds.

4.9.6 Coolant Pump Lubricating Oil Systems

These systems supply oil to the bearings of eight pumps in the fuel circuits and to eight pumps in the intermediate coolant loops. The two groups of eight pumps each are supplied by two independent systems. The lubricant is circulated under oxygen-free conditions, 120 gpm to each pump group. The systems are designed to 120°F supply with an expected oil temperature rise of 20°F.

4.9.7 Preheating System

Prior to the admission of salt, all salt-containing piping and equipment must be preheated to 900°F. This is accomplished by the use of several types of resistance heating. In sizes up to about 2 in., piping is heated by passing an alternating current through the piping itself. All pipes heated this way are electrically insulated. Larger diameter salt-containing pipes are heated by hinged resistance heaters (2000 w/ft) surrounding the pipe. For large pipes (above 10 in.) a three-section heater assembly is used. Piping fittings are covered by prefabricated heating units. Heaters for pumps are field-fabricated.

The reactor vessel and primary heat exchangers are heated by tubular resistance heaters attached to the outer surfaces by means of clips on welded studs.

4.9.8 Auxiliary Power

Auxiliary power is supplied at 4160 volts by a pair of auxiliary power transformers, type OA/FA, 24-4.16 kv with a maximum fan-cooled rating of 25 Mva. A reserve transformer, fed from the switchyard bus, serves as a standby unit. The loads fed at 4160 volts include all motors rated at 150 horsepower or more, and the auxiliary power transformers

required for station lighting, 480 volt auxiliaries, and the fuel melting and preheating system.

Smaller auxiliaries, of 30 horsepower or less, and those whose continuous operation is not considered vital to station operation, are fed from motor control centers in the vicinity of the load. Two 15 kva 480-120 volt transformers supply a 115 volt a-c control and instrumentation bus for each unit. An emergency supply to this bus is provided from a 15 kva inverter motor-generator set which is driven by the unit 250-volt battery.

4.9.9 Service Water System

The service water system supplies river water for cooling purposes throughout the plant, including the reactor auxiliaries and the turbine plant components.

Water is supplied by three 15,000 gpm, half-capacity, vertical centrifugal pumps. Each pump is driven by a 1250-horsepower motor, and is located in the circulating water intake structure. During normal operation two pumps supply the system with water at 100 psig, with the third pump employed as a standby.

4.9.10 Control and Station Air Systems

The compressed air system for the plant consists of separate, interconnected air supplies for the station and for control purposes. The station air system supplies hose valves for operating and maintenance requirements throughout the station. Control air is used primarily for instrument transmitters and air-operated valves. The two air systems are cross connected so that compressed air may be supplied to the control air system in event of a compressor failure.

The control air system of the plant supplies air-operated control devices at a header pressure of 115 psia and is reduced to 55 psia and 45 psia for supply to various drive units and instrument transmitters.

4.9.11 Cranes and Hoists

A single traveling bridge crane serves the reactor and steam turbine buildings. Its lifting capacity is based on handling the rotor of the

low pressure steam turbine-generator, which weighs about 150 tons. The bridge span is 130 ft, and the crane lift is sufficient to reach the lowest portion of the building. All heavy equipment coming into the building by rail may be handled by the crane. Its capacity is sufficient to allow removal of all components within the reactor primary shield except the reactor.

4.9.12 Instrumentation and Control

The requirements for instrumentation and control of the turbine systems are similar to those of the turbine system in a conventional fossil-fuel power plant.

Instrumentation for the reactor system monitors the reactor neutron flux, primary system pressures, temperatures, levels, and flow rates, and provides control and alarm signals to actuate the appropriate device or to call for operator action when changes occur in the measured quantities, through either changes in load or malfunction of system components.

Control and instrumentation panels are located in the control room, for convenience of reading, recording and operating the most important quantities and components. Other auxiliary control panels or isolated instruments may be located at appropriate places in the plant; area radiation monitors, alarm or warning signals, hydrogen and seal oil controls for the generators, etc.

4.9.13 Plant Utilities

The plant utilities include those systems that are provided for monitoring plant equipment, disposing of nonradioactive wastes, safety of personnel, protection of equipment and for heating, ventilating and air-conditioning the plant buildings. These systems do not differ appreciably from those provided for conventional plants.

4.10 MSCR Design Specifications

The significant specifications for the MSCR equipment and materials are listed in Tables 4.2 through 4.6. The vessels are described in Table 4.2, heat-transfer equipment in Table 4.3, pumps and circulators in Table 4.4, miscellaneous equipment in Table 4.5, and materials in Table 4.6.

Table 4.2. INOR-8 Salt-Containing Vessels

	Number of Units	Volume of Each Unit ft ³	Diameter in.	Height in.	Wall Thickness in.	Heater Capacity (each unit) kw	Design Temp. °F	Design Pressure psi	Weight (each) lb gross, lb tare
1. Reactor Vessel	1	630 fuel	241	240	1.7		1100 inlet 1300 outlet	100 in 50 out	1,100,000
2. Fuel Salt Drain Tanks	54	50	35	96	1/2	15	1300	100	
3. Fertile Salt Melt Tank	1	150	42	144	1/4	150	1200	50	
4. Fertile Salt Chemical Treatment Tank	1	100	36	168	5/8	15	1300	100	25,000 g
5. Fertile Salt Storage Tank	1	100	36	168	3/8	12	1200	100	23,000 g
6. Fertile Salt Small Addition Metering Tank	1	2	12	32	3/16	1	1300	50	500 g
7. Fertile Salt Large Addition Metering Tank	1	50	36	90	1/8	10	1000	100	
8. Fuel Salt Small Withdrawal Metering Tank	1	2	4	300	0.4	12	1300	150	
9. Fuel Salt Reactivity Control Drain Tanks	2	50	36	96	1/2	10	1300	100	
10. Fuel Salt Decay Storage Tanks	5	35	30	90	1/4	10	1300	25	7360 g 900 t
11. Fuel Salt Withdrawal Transfer Tank	1	10	30	27	1/4	3	1300	25	2350 g 290 t
12. Flush Salt Storage Tanks	5	650	96	156	1/2	150	1000	80	
13. Coolant Salt Melt Tank	1	150	42	144	1/4	150	1200	50	
14. Coolant Salt Chemical Treatment Tank	1	50	42	60	1/2	8	1300	100	11,500 g
15. Coolant Salt Drain Tanks	2	750	43.7	864	1/4	200	1100	80	100,000 g 10,000 t

Table 4.3. Heat Transfer Equipment

	Primary Heat Exchangers	Steam Superheaters	Steam Reheaters	Loeffler Boilers	Fuel Salt Drain Tank Condensers
AEC Account Number	221.314	222.32	222.322	222.31	223.312
Design data					
Number of units	8	16	8	4	1
Unit heat rate, Btu/hr	$1,066 \times 10^6$	467×10^6	132×10^6		85×10^6
Geometry	Shell & U-Tube	Shell & U-Tube	Shell & U-Tube	Cyl. Drums	Shell & U-Tube
Number of tubes	2,025	785	766	None	630
Active area, ft ²	6,643	8,905	3,543		1,036
Active length, ft	25	57.8	23.6	100	10
Length of longest tube, ft	28.8	61.8			
Length of shortest tube, ft	23.7	53.8			
Tube OD, in.	0.5	0.75	0.75		0.625
Tube-wall thickness, in.	0.035	0.083	0.065		0.065
Lattice pitch, in.	0.625		1.00		1.5
Tube material	INOR-8	INOR-8	INOR-8		Admiralty
Shell material	INOR-8	INOR-8	INOR-8	Carbon steel	Carbon steel
Shell ID, in.	43.75	31.5	31	72	26
Shell thickness, in.	1.5	0.5	0.5	7	0.25
LMTD, °F	173.7	174.8	187.5		
Shell weight, lb	16,000	11,000	4,500		
Tubing weight, lb	10,000	25,000	9,620		3,800
Design pressure					
Heat transfer coefficient, Btu hr·ft ² ·°F	924	300	119		
Shell-side conditions					
Fluid	Fuel salt no. 2	Int. cool. salt	Int. cool. salt	Steam	Steam
Inlet temperature, °F	1,100	1,100	1,100	240	1,000
Outlet temperature, °F	1,300	950	950	120	636
Flow rate, ft ³ /sec	20.25	13.7	3.84	80,000	3.7×10^6
Pressure, psig	200	300	300	10	2,460
Pressure drop, psi	80	15	40		
Volume, ft ³	61.6	150	64		
Tube-side conditions					
Fluid	Int. cool. salt	Steam	Steam	Water	Water
Inlet temperature, °F	950	670	635	80	545
Outlet temperature, °F	1,100	1,000	1,000	150	636
Flowrate, lb/hr	31	1.28×10^6	0.7×10^6	1.2×10^6	5.2×10^6
Pressure, psig	350	2,490	440	110	2,450
Pressure drop, psi	84	25	20		50

Table 4.4. Pumps and Circulators

	MSCR Fuel Pump	MSCR Coolant Pump	Steam Circulators
Number of units	8	8	4
Type	Centrifugal	Centrifugal	Axial
Fluid pumped	MSCR-2 fuel salt	Constant salt	Steam
Service temperature	1300°F	1100°F	1000°F
Fluid density	190 lb/ft ³	120 lb/ft ³	
Fluid flow per pump	9075 gpm	13,900	5.3×10^6 lb/hr
Suction pressure (17 ft NPSH)	22.5 psia	130 psia	2430 psig
Discharge pressure (150 ft developed head)	220 psia	350 psia	2490 psig
Impeller OD	25 in.	25 in.	
Suction ID	14 in.	14 in.	
Discharge ID	12 in.	12 in.	
Over-all pump OD (Approx.)	50 in.	50 in.	
Over-all pump height-suction opening to pump housing flange face (Approx.)	50 in.	50 in.	
Pump motor rating	1600 hp, 4160 volt	2000 hp, 4160 volt	
Pump motor speed (synchronous)	900 rpm	900 rpm	
Pump motor type	Totally enclosed, 3 phase water cooled	Totally enclosed, 3 phase water cooled	

Table 4.5. Miscellaneous Equipment

Thermal shield	
Dimensions, ft	1.5 × 24 × 24
Material	
Shield	2 in. plate carbon steel
Headers	20 in. × 4 in. carbon steel (1/2 in. wall thickness)
Weight, lb gross (water filled)	250,000
Inlet/outlet pipe	8 in. Sch. 20 carbon steel
Heat removal rate, 10^6 Btu/hr	18
Water flow, gpm	2000
Water temperature/pressure, °F/psig	90–110/15
Shield cooling system	
Heat load, Mwt	37.5
Demineralized water circuit	
Maximum temperature, °F	180
Minimum temperature, °F	125
Flow rate, gpm	4650
Service water conditions	
Maximum temperature, °F	125
Minimum temperature, °F	75
Flow rate, gpm	5120
Cell-air cooling system	
Heat load, Mwt	5
Demineralized water circuit	
Maximum temperature, °F	110
Minimum temperature, °F	95
Flow rate, gpm	2275
Service water conditions	
Maximum temperature, °F	95
Minimum temperature, °F	75
Flow rate, gpm	1700

Table 4.5 (continued)

High level radioactive salt sampler	
Sampler cavity linner containment vessel	
Dimensions	5 ft 4 in. ID × 6 ft high
Material and thickness	304 stainless steel, 1/8 in.
Design temperature/pressure	125°F/±15 psig
Sampler cavity shielding	
Material; thickness	Lead; 1 ft thick all around sides and top
Approximate weight	57 tons
Sampler cavity outer containment vessel	
Dimensions	7 ft 8 in. ID × 8 ft high
Material and thickness	Carbon steel, 1/4 in. thick
Design temperature/pressure	125°F/15 psig
Sampler ducts	
Design pressure	100 psig
Design temperature	200°F
Size	1 1/2 in. Sch. 40 pipe
Material	Inconel
Sampler duct valves	
Design pressure/temperature	100 psig/125°F
Number required	10
Type	1 1/2 in. Vulcan bellows stem double-disc motor-operated gate valve (supplied by Hoke Valve Co.)
Cable drive unit	
Service environment	Drive unit will operate in an inert but radioactive atmosphere at normal temperature. Radiation level will be high only during sampling operation. The cable must be capable of operation at temperatures in the range 100 to 1300°F.

Table 4.5 (continued)

High level radioactive salt
sampler (continued)

Cable drive unit (continued)

Cable size 1/8 in. diam; length sufficient to reach from the sample cavity to the farthest sample point.

UF₄ addition facility

Containment vessel

Dimensions, ft 3 x 10

Design pressure, psig ±15

Material 304 stainless steel

Pellet bin and dispenser

Volume, ft³ 1

Metering chamber

Configuration Coiled tube, 1 in. pipe

Tube length, ft 14

Tube material Stainless steel

Valves

Size (nominal) in. 1

Description Bellows-sealed, 150-lb design, gas-tight, soft-seated

UF₄ addition pipe 1 in. Sch. 40 stainless steel pipe

Dissolver tube

Configuration Perforated, coiled pipe

Size, nominal pipe size (in.) 1

Material INOR-8

Length, ft 4

Other description End blanked off; perforation diameter, 1/8 in.

Shielding

6 in. of lead

Table 4.5 (continued)

Reagent gas disposal system data

Hydrogen supply

Cylinder station capacity, standard cubic ft	3000
Flow rate, scfm	2

Hydrogen fluoride supply

Cylinder station capacity, standard cubic ft	12,000
Flow rate, scfm	8

KOH scrubber for HF disposal

HF flow rate (max), scfm	8
Cooling requirement, Btu/hr	118,000
Cooling water flow rate, gpm	10
KOH solution feed rate, liters/min (max)	1
Flow rate of unreacted hydrogen, scfm	2
Length and diameter, ft	8 and 2.8
Material of construction	Monel
Wall thickness, in.	1/4

KOH supply tank

Dimensions	4 ft diam, 8 ft high
Material	Carbon steel
Chemical feed pump	0-1 liter/min
Mixer	2 hp

Hydrogen burner

Design flow rate, lb-moles H ₂ per hour	1/3
Heat load, B/hr	41,000
Cooling water flow, gpm	4
Design air flow rate, cfm (max)	10
Dimensions	1 ft diam x 4 ft high
Material	Carbon steel

Table 4.5 (continued)

Reagent gas disposal system data
(continued)

Hydrogen burner condenser

Heat load, B/hr	20,000
Cooling water flow, gpm	4
Exit gas flow rate (nitrogen plus unburned oxygen), scfm	9
Design temperature of exit gas, °F	100
Surface area of tubing, ft ²	100
Shell material	Carbon steel
Tubing material	Admiralty
Configuration	Shell-and-tube, single pass, straight tube
Condensate rate, lb H ₂ O per hr	6

Cover gas purification system

Helium dryer

Dessicant used	Molecular sieve
Amount, lb	10
Length/diameter, ft/in.	2.5/4
Pressure rating, psig	300

Container material Carbon steel

Helium heater (electric)

Design temperature gas exit, °F	1200
Helium flow rate, scfm	1.5
Design pressure, psig	300
Heater rating (electric), kw	1

Oxygen removal unit

Design flow rate, scfm	1.5
Container size, length/diameter, in./in. (overall)	26/6 Sch. 40
Active ingredient	Titanium sponge

Table 4.5 (continued)

**Cover gas purification system
(continued)**

Oxygen removal unit (continued)

Design pressure/temperature,
psig/°F 300/1200

Helium cooler

4 in. finned tube with flanges 4 ft long

Inlet/outlet temperature, °F 1200/200

Helium flow rate, scfm 1.5

Treater helium surge tank

Tank volume, ft³ 60

Design pressure/temperature
psig/°F 300/100

Material Carbon steel

Lube oil system

Number of systems 2

Design lube oil flow, gpm 120

Design lube oil temperature,
°F (in/out) 140/120

Design cooling water tempera-
ture, °F (in/out) 75/100

Design cooling water pressure,
psig 25

Design cooling water flow, gpm 45

Number of lube oil pumps 2

Type Rot.

Lube oil pumps head, ft 150

Flow, gpm 300

Motor, hp 20

Reservoir, number 2 1

ID, ft (cylindrical) 5

Height, ft 5

Capacity, gal. 600

Wall thickness, in. 0.25

Table 4.5 (continued)

Lube oil system (continued)

Reservoir, number 2 (continued)

Material	Carbon steel
Weight (full), lb	3000
Cooler, number	2
Type	2 pass shell, 4 pass tube
Tube material	Inconel
Shell material	Carbon steel
Overall heat transfer coefficient, Btu/hr·ft ² ·°F	20
Tube surface area, ft ²	735
Tube size, OD, in.	5/8
Tube wall thickness, in.	0.125
Tube pitch (triangular)	0.938
Shell diameter, ID, in.	18
Shell length, ft	34
Tube design pressure, psig	25
Tube design temperature, °F	100
Shell design pressure, psig	45

Table 4.6. Material Specifications

<u>Properties Assumed for MSCR Graphite</u>		
Items and Units	MSCR	MSRE*
Density, g/cc	1.9	1.9
Thermal conductivity, Btu/hr·ft·°F		
At 68°F and with grain	80	
At 68°F and across grain	45	
At 1200°F, isotropic, after irradiation	15	
Coefficient of thermal expansion, across grain, per °F		
At 68°F		1.7×10^{-6}
At 1200°F, after irradiation	3×10^{-6}	
Maximum allowable strain, in./in.	0.001	
Porosity		
Accessible to salt at 150 psi	0.001	0.005
Accessible to gas	0.01	
Poisson's ratio	0.4	
Young's modulus		
With grain		3×10^6
Across grain	1.25×10^6	1.5×10^6
Helium permeability at 30°C, cm ² /sec		
Diffusivity of xenon at 1200°F, cm ² /sec	10^{-6}	
Specific heat Btu/lb·°F	0.33	

*MSRE values are given for comparison and were mostly taken from reference (12).

Table 4.6 (continued)

Assumed Properties of MSCR Fuel-Salt Mixture at 1200°F

Mixture No.	<u>1</u>	<u>2</u>	<u>3</u>
Composition			
Mole % LiF-BeF ₂ -ThF ₄	71-16-13	68-23-9	66-29-5
Wt % LiF-BeF ₂ -ThF ₄	29-11-60	32-19-49	38-29-33
Liquidus temperature, °F	941	887	860
Molecular weight	66.03	56.2	46.2
Density, lb/ft ³	215.6	190.1	163.0
Viscosity, lb/ft·hr	24.2	21.0	18.9
Thermal conductivity, Btu/hr·ft·°F	2.67	2.91	3.10
Heat capacity, Btu/lb·°F	0.318	0.383	0.449

Assumed Properties of MSCR Intermediate Coolant Salt Mixture at 1062°F*

Composition	
Mole % LiF-BeF ₂	66-34
Wt % LiF-BeF ₂	52-48
Liquidus temperature, °F	851
Molecular weight	33.14
Density, lb/ft ³	120.5
Viscosity, lb/ft·hr	20.0
Thermal conductivity, Btu/hr·ft·°F	3.5
Heat capacity, Btu/lb·°F	0.526

*Reference (12) of the Bibliography.

Properties of INOR-8*

Wt %

Chemical composition	
Nickel, min	66-71 (balance)
Molybdenum	15-18

*Reference (12) of the Bibliography.

Table 4.6 (continued)

<u>Properties of INOR-8 (continued)</u>	<u>Wt % (continued)</u>
Chemical composition (continued)	
Chromium	6-8
Iron, max	5
Manganese, max	1
Silicon, max	1
Carbon	0.04-0.08
Miscellaneous, max	2

Physical Properties at 1200°F

Density, g/cc	8.79
Melting point, °F	2470-2555
Thermal conductivity, Btu/hr·ft·°F at 1200°F	11.7
Young's modulus, psi at 1300°F	25×10^6
Specific heat, Btu/lb·°F at 1200°F	0.1385
Coefficient of thermal expansion, 1/°F at 1200°F	7.8×10^{-6}
Maximum allowable stress, psi at 1200°F	6000
Maximum allowable stress, psi at 1300°F	3500

5. FUEL PROCESSING

5.1 Reprocessing System

Fluorination of spent fuel from the MSCR to recover isotopes of uranium, followed by discard of the carrier salt (containing LiF, BeF₂, ThF₄, and fission product fluorides), was selected as the method of processing for several reasons: (a) The fluorination process is well adapted for future integration with the reactor plant (sharing shielding and maintenance facilities and personnel) with appreciable potential reductions in fuel cycle cost (Sec. 6.9); (b) the necessity for holding the spent fuel for decay of radioactivity is eliminated; (c) no development is required; the plant may be designed and costed on the basis of current technology.

In order to use the next most applicable process, Thorex, it would be necessary to develop special head-end and tail-end steps for converting spent fuel from the fluoride to the nitrate and back again. Also it would be necessary to hold the spent fuel prior to processing for not less than 120 days (to average the equivalent of 90 days of cooling). Further, there is some uncertainty concerning the effect of fluoride ion on the chemistry of the aqueous separations. On the other hand, the thorium could be recovered, and perhaps also the carrier salt could be recovered free from contamination with rare earth isotopes. It would, however, be contaminated with the isotopes Cd, Sr, Ag, Cs, Se, Ba, and Te.

The processing costs for the MSCR fuel have been estimated for both processes.

5.2 Fluoride Volatility Central Plant

A central plant capable of processing about 30 ft³ of fuel salt per day (1 tonne Th/day) was selected for costing. This plant is capable of servicing about 20 reference design MSCR's having a total capability of 20,000 Mwe.

Component design, plant layout, and associated costs for the plant described herein were adapted from a design and cost study of an on-site plant prepared by Carter, Milford, and Stockdale in a prior study (21).

Due allowance for fuel transport to a central location was made, together with other adjustments for difference in capacities, elimination of protactinium recycle, etc.

5.2.1 Process Design

The steps of the proposed fluorination process are indicated in Fig. 5.1. Spent fuel is transferred from the shipping containers to pre-fluorination storage by applying gas pressure or by siphoning. The fuel is then introduced batch-wise into the fluorinators where it is treated with elemental fluorine, possibly diluted with some inert gas, at about 1000°F. The effluent UF_6 is absorbed in beds of NaF at 200°F, is later desorbed at 700°F and collected in cold traps at -45°F. Periodically the cold traps are warmed, and the decontaminated UF_6 is collected in cylinders.

The fluoride volatility process does not provide for recovering thorium or any of the components of the carrier salt. Consequently, after fluorination the $LiF-BeF_2-ThF_4-FP$ melt is drained into interim waste storage, and later transferred to permanent waste storage such as, for example, in a salt mine. The interim storage period has been taken to be 1100 days, a value corresponding to the most favorable economic balance between on-site and permanent storage charges for this particular process.

It will be observed that ^{233}Pa is not recovered in this process. An analysis of Pa recovery versus discard disclosed that additional process equipment and building space requirements made the recovery of Pa uneconomical.

A major problem in the design of vessels which contain irradiated salt is that of heat removal. Volumetric heat release rates are high, and the temperature of the heat source is considerably greater than that of conventional heat sinks (such as cooling water from rivers or wells). In the design evolved, heat is transferred across an air gap into water. The principal heat transfer mechanism is radiation; convection accounts for perhaps 5 to 10 per cent of the transfer. This arrangement, in addition to controlling the heat transfer rate at tolerable levels, provides isolation of the coolant from the molten salt so that a leak of either stream through its containment wall does not contaminate the other stream.

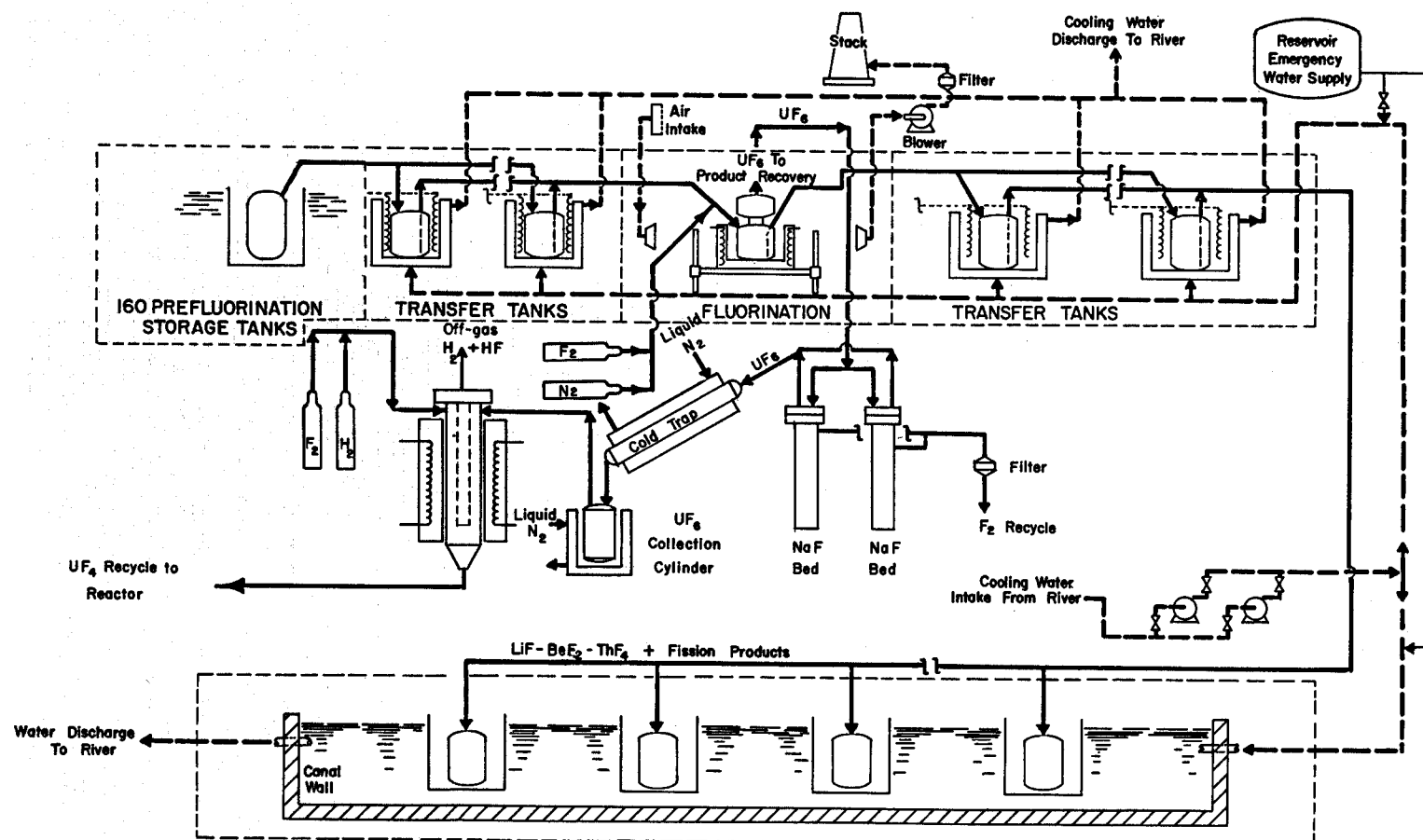


Fig. 5.1. MSCR Fluoride Volatility Fuel Processing Plant.

The fluorinators are cooled by circulating air through the cell. In the case of the prefluorination storage tanks, radiation from storage vessels to a concentric tank in a water bath provides sufficient cooling for 5-day-old fuel salt.

Wherever possible, the equipment was patterned after that used in the ORNL Volatility Pilot Plant described by Milford (66), Carr (18), Cathers et al. (22, 23).

5.2.2 Shipping

Shipment of irradiated fuel is made in a lead shielded carrier shown in Fig. 5.2. The cask is equipped with a water-cooling system which is able to absorb decay heat radiated from the salt container and to dissipate this heat to the atmosphere via finned tube exchangers fastened to the outside of the cask. Heat transfer may be either by boiling the water in the inside jacket followed by condensation in the outside exchanger, or by natural convection.

The shipping container (also used for waste disposal), is designed to hold ~ 10 ft³ salt which is about six days accumulation at the reactor discharge rate of 1.67 ft³/day. For this design it has been assumed that the processing plant is located 500 miles from the reactor site and that shipment will be made by rail. The round trip, including filling and emptying, is anticipated to take 10 days. The average age of spent fuel at shipment is approximately 5 days.

5.2.3 Prefluorination Storage Tanks

One hundred and sixty 30 ft³ tanks receive up to 120 days supply of spent fuel from each of a number of reactor sites. When a 120-day batch is completed, the tanks are removed from their cooling jackets to the transfer area where the material is transferred to 6-ft³ metering transfer tanks. From these tanks the spent fuel can be transferred by gravity or inert gas pressure to the fluorinators.

The cooling jackets for the prefluorination storage tanks are stainless steel tanks 2.2 ft in diameter by 12 ft high immersed in a water bath. Cooling is achieved principally by radiation from the storage tank to the

ORNL-DWG. 65-7911

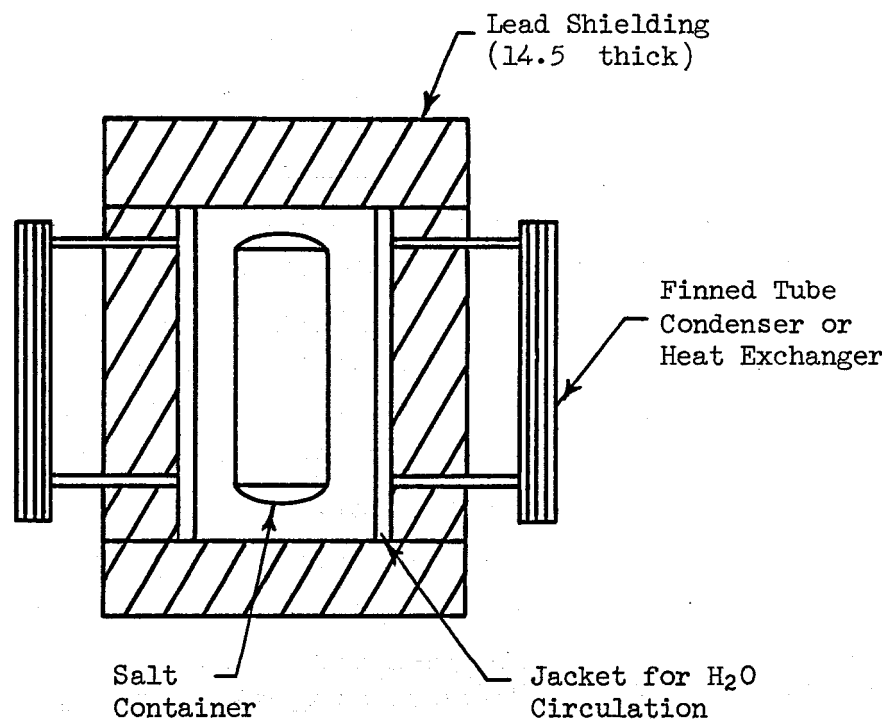


Fig. 5.2. Irradiated Fuel Shipping Cask.

jacket. The transfer tanks are equipped with jackets cooled by circulating water. Electric heaters provide preheating prior to transfer operations, should heating be required.

5.2.4 Fluorinator

The design shown in Fig. 5.3 has been successfully operated in the ORNL Fluoride Volatility Pilot Plant (18). Surmounting the fluorination chamber is a de-entrainment section. The lower chamber is surrounded by an electrically-heated furnace while the upper is heated with electrical strip heaters. Five units are required, each having a capacity of 6 ft³. The corrosion rate is about 1 mil per hour of fluorination time; hence the fluorinator must be inexpensive and accessible for frequent replacement. It was designed to dissipate decay heat and heat of reaction to the atmosphere in the cell through a wall 1/2 in. thick at a temperature of 900°F. The preferred materials of construction are either INOR-8 or Alloy 79-4 (70 per cent Ni, 4 per cent Mo, 17 per cent Fe). L-Nickel has been used for fluorinator construction but is susceptible to intergranular attack.

Spent fuel is fluorinated batchwise at about 1000°F. It takes about 6 hours to volatilize the uranium (99.9+%) from a 6 ft³ batch. In current practice the attack of fluorine on the vessel is severe. The high rate of corrosion is believed to result from the combined action of liquid salt and gaseous fluorine phases. However, several lines of improvement are under investigation. These include the use of the "frozen wall" fluorinator (35) wherein a layer of solid salt is maintained on the vessel wall by proper control of the cooling, and this layer protects the wall. Another approach consists of spraying the molten salt into a relatively cool atmosphere of fluorine. Uranium hexafluoride is formed in and rapidly removed from the microdroplets which then cool and freeze before they strike the wall. Not only are the wall temperatures lower, but there is no liquid phase in contact with the wall.

The fluorides of some fission products, notably Mo, Zr, Nb, Cs, Ru, and Te are volatile and accompany the UF₆. These are separated from the uranium in the CRP trap and NaF absorber described below. It is not expected that the fluoride of Pa will be volatile under conditions specified.

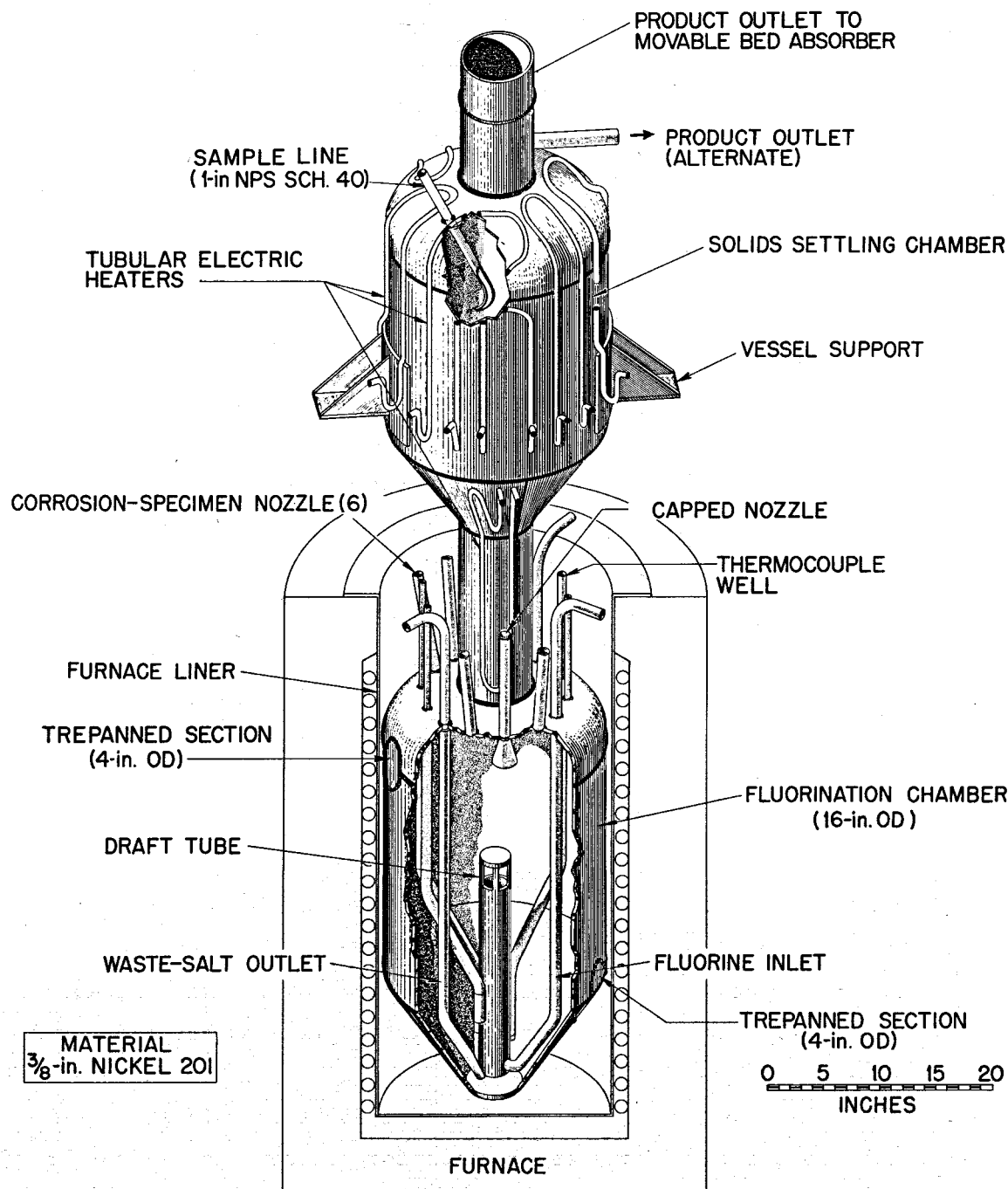


Fig. 5.3. Fluorinator.

Protactinium will remain in the barren salt and be lost to waste. The loss amounts to about 10 g/day in the reference design reactor, and studies have shown that it is not economical to recycle the barren salt to the fluorinators after holding it to allow the Pa to decay. The cost increase of additional fluorinator capacity and interim storage vessels more than offsets the value of the ^{233}U recovered.

5.2.5 CRP Trap and NaF Absorbers

After leaving the fluorinator, UF_6 and accompanying fission product fluorides pass into a two-zoned NaF absorption system. The first, called the complexible radioactive products (CRP) trap is operated at about 400°C and removes fluorides of chromium, zirconium, niobium, cesium, strontium, and rare earths, as well as entrained salt particles. Uranium hexafluoride is not absorbed here, but is absorbed in the second zone operated at 100°C , along with the fluorides of molybdenum and ruthenium, and traces of others. Some ruthenium carries through into the fluorine recirculation system.

Uranium is recovered from the beds by desorption at 400°C . It is collected in cold traps described below.

The stationary bed absorber, shown in Fig. 5.4, contains just over one cubic foot of NaF. Six units are required. Each is mounted in a lightweight, low-heat capacity electric furnace which opens on hinges for removal of the absorber. A cooling-heating tube 2-1/2 inches OD carrying coolant and containing electric heaters extends through the center of the bed. An interior cylindrical baffle forces the process stream to follow a U-shaped path through the bed.

Design limitations arise in the rate at which the bed temperature can be cycled and the bed thickness. The granular bed is a rather effective insulator and must be made in thin sections to facilitate heating and cooling. The absorbers therefore have large length-diameter ratios.

When the bed becomes saturated with fission products, the absorber is removed from the furnace, emptied, and recharged remotely in a 4-5 day cycle.

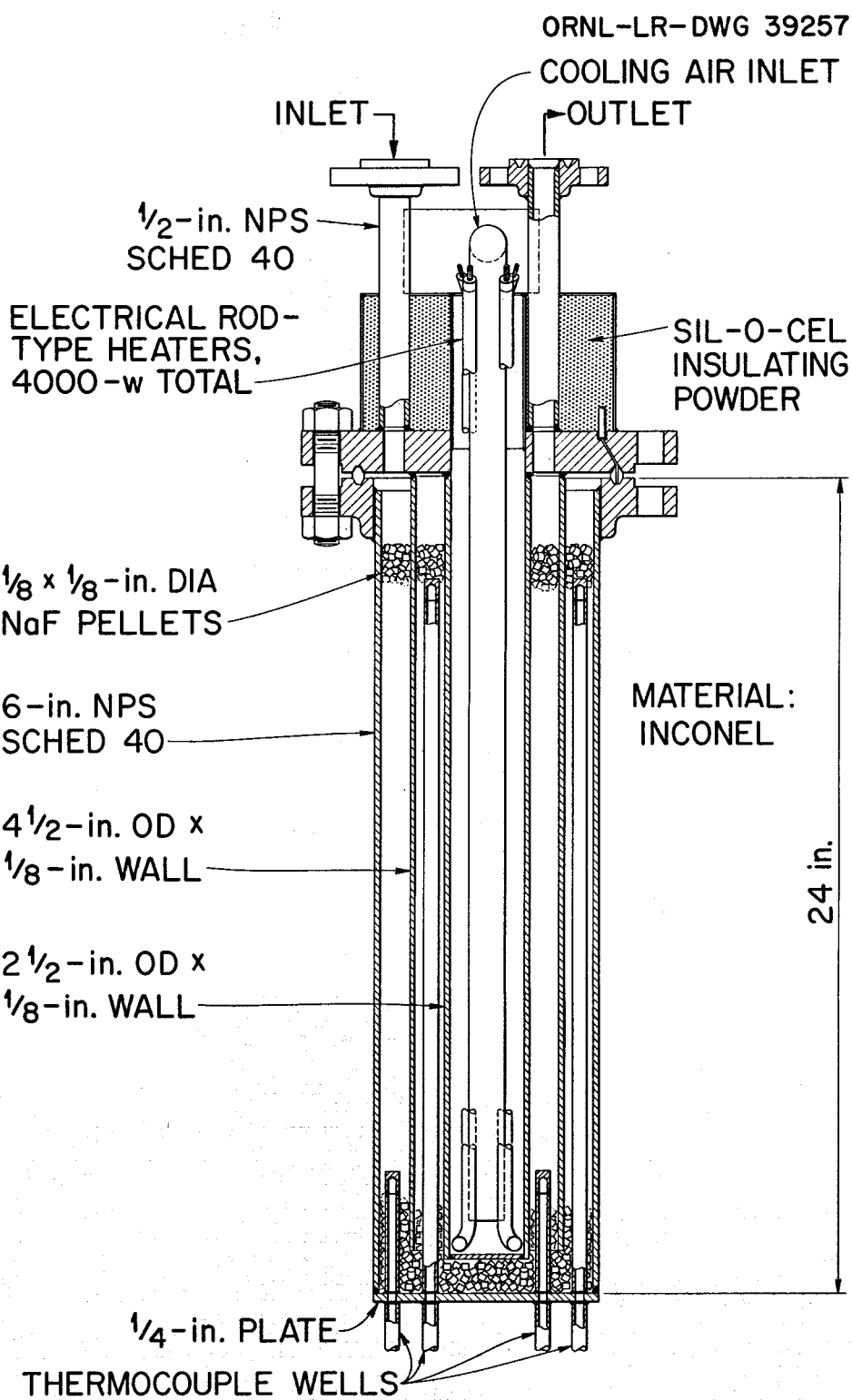


Fig. 5.4. Sodium Fluoride Absorber.

5.2.6 Cold Traps

These are similar to those used in the ORNL Fluoride Volatility Pilot Plant as shown in Fig. 5.5. Two traps are mounted in series. The first is operated at about -40°C and the second at -60°C .

Adequate surface for rapid transfer of heat and collection of solid UF_6 must be provided. The components must have small thermal inertia so that the temperature may be changed quickly. During defrosting, the traps are heated to 90°C at 46 psia to allow UF_6 to melt and drain to collection cylinders.

5.2.7 Reduction Reactor

The reduction of UF_6 to UF_4 is accomplished in a reactor patterned after that described by Murray (70) and consists of a 4-in. diam by 10-ft high column. Uranium hexafluoride and flourine are mixed with excess H_2 in a nozzle at the top of the reaction chamber. The uranium is reduced in the $\text{H}_2\text{-F}_2$ flame, and falls to the bottom of the chamber where it is collected in molten salt of suitable composition. Gaseous materials are discharged through a filter. The reactor has a capacity of 10-15 kg of UF_6 per hour. Losses are very low and typically are less than 0.1 per cent.

5.2.8 Transfer Tanks

Stripped fuel is drained from the fluorinators into transfer tanks (two each) from whence it is distributed to interim waste storage tanks. The transfer tanks have capacities of 60 ft^3 . Decay heat is radiated from the surface of the tank through a 1/2 in. air gap to a water-cooled jacket. While being held in the transfer tanks, the salt is treated with He or other inert gas to remove traces of F_2 or HF that would increase corrosion in the waste storage tanks.

5.2.9 Waste Storage Tanks

Waste salt is stored in stainless steel shipping cylinders 2 ft in diam by 8 ft long. These are placed at the bottom of steel thimbles 2.75 ft in diam and fifteen feet long which dip into a water-filled canal. Heat is dissipated by radiation and convection across the 4-inch

ORNL-LR-DWG 19091

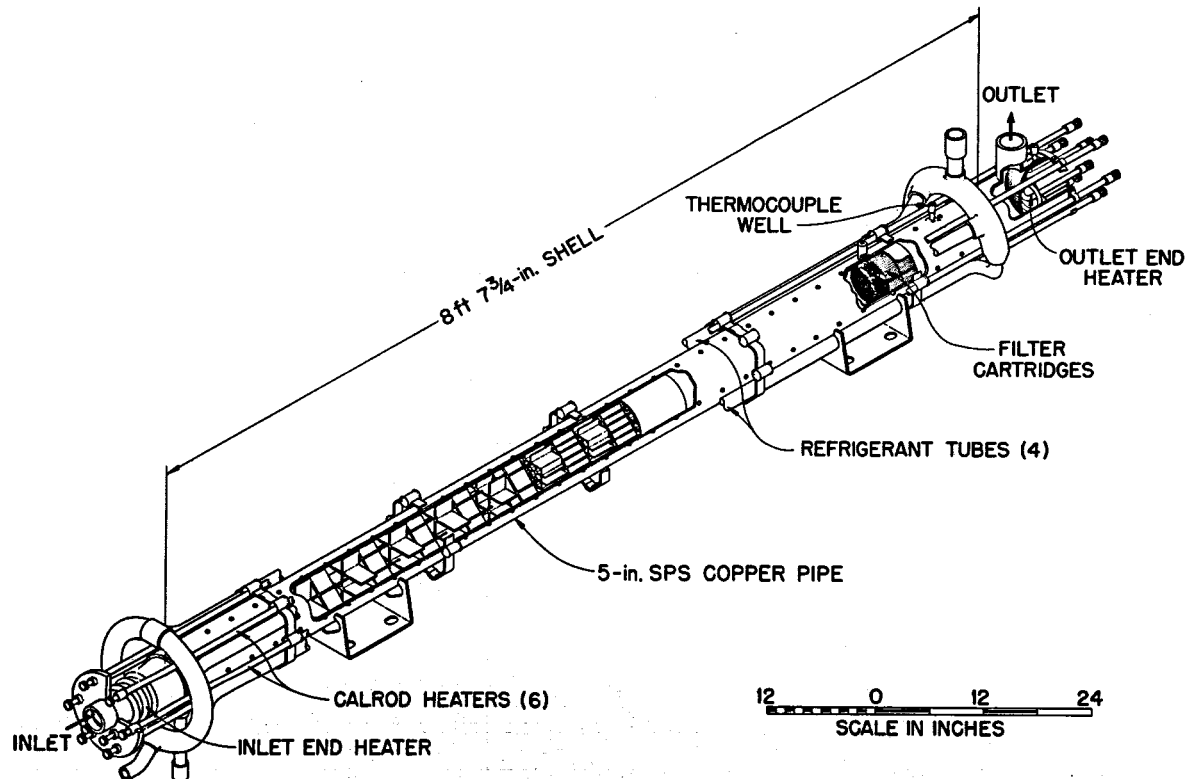
**PRIMARY COLD TRAP**

Fig. 5.5. Primary Cold Traps.

air gap, through the thimble wall and into the water. After cooling, the tanks are shipped to a salt mine for permanent storage.

5.2.10 Freeze Valves

Conventional valves cannot be used with molten salts. Flow stoppage is achieved by freezing a plug of salt in a section of a line with a jet of cooling air. Electric heaters are used to thaw the plug when flow is desired. A freeze valve for the MSRE is shown in Fig. 5.6.

5.2.11 Samplers

The apparatus pictured in Fig. 5.7 is being tested for use with the MSRE (12). Essential features are the hoist and capsule for removing the sample from the vessel; a lead-shielded cubicle with manipulator, heating elements and service piping, and a transport cask for removing the sample from the process area. The sampling cubicle is mounted on the cell biological shield in an accessible area.

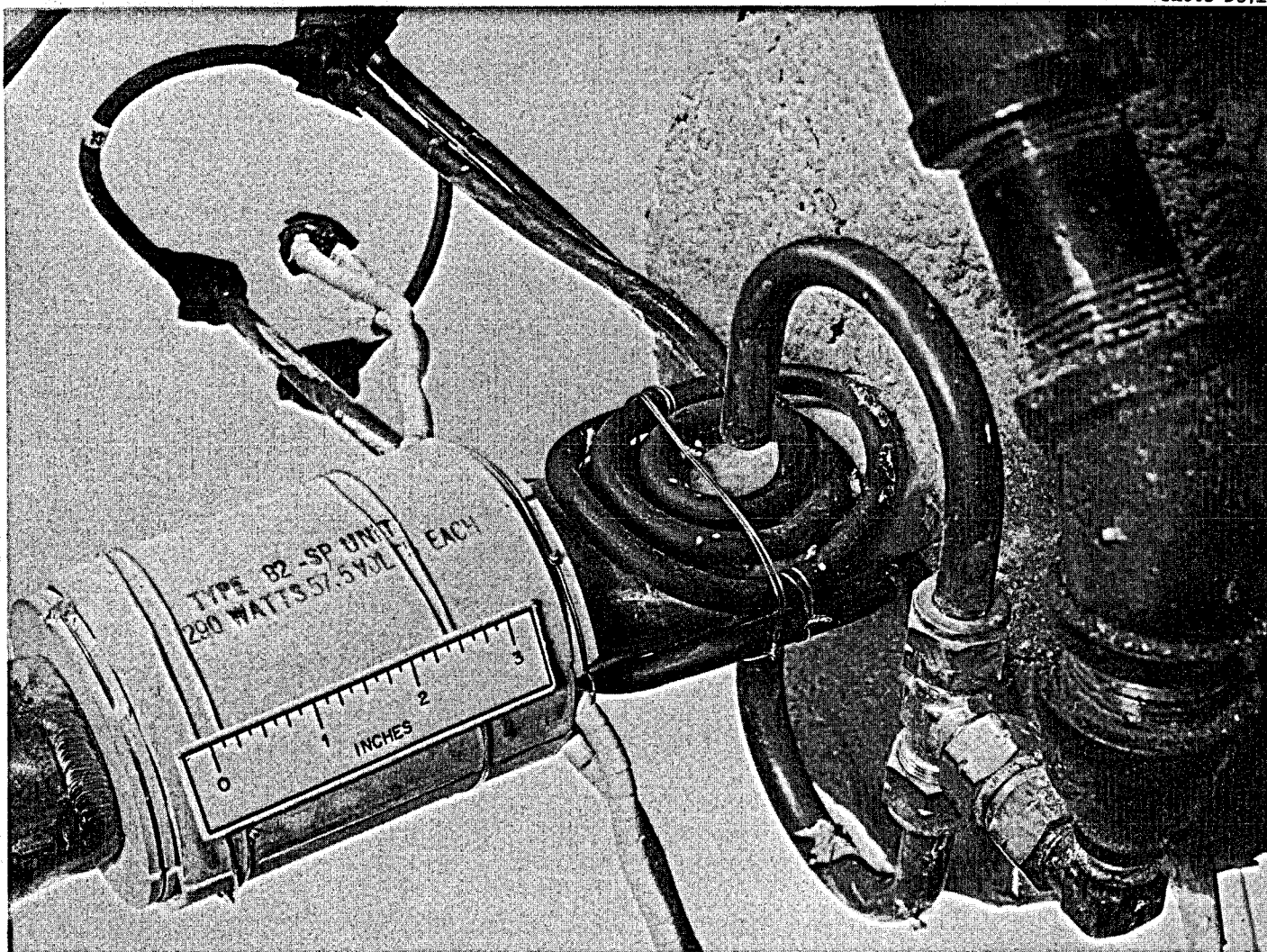
5.2.12 Biological Shield

Calculations were made using the Phoebe program for the IBM 704 computer. In the study by Carter, Milford, and Stockdale (21), on which the present estimate is based, spent fuel was brought to the processing plant immediately after removal from the reactor, and the shield was accordingly made quite thick. In the present instance, the fuel is cooled at the processing plant for not less than 90 days so that the shielding requirements are not as extreme. However, in order that the central plant have more general utility, no reduction in shield thickness was made.

5.2.13 Process Equipment Layout

Process equipment is laid out according to the major process operations: prefluorination storage, fluorination, transfer, NaF absorption, cold traps and product collection, $\text{UF}_6 \rightarrow \text{UF}_4$ reduction, and interim waste storage. Equipment is grouped in cells according to activity level and in an arrangement that minimizes distances between vessels. Three transfers of molten salt are required in the processing sequence.

Photo 36713



103

Fig. 5.6. Freeze Valve.

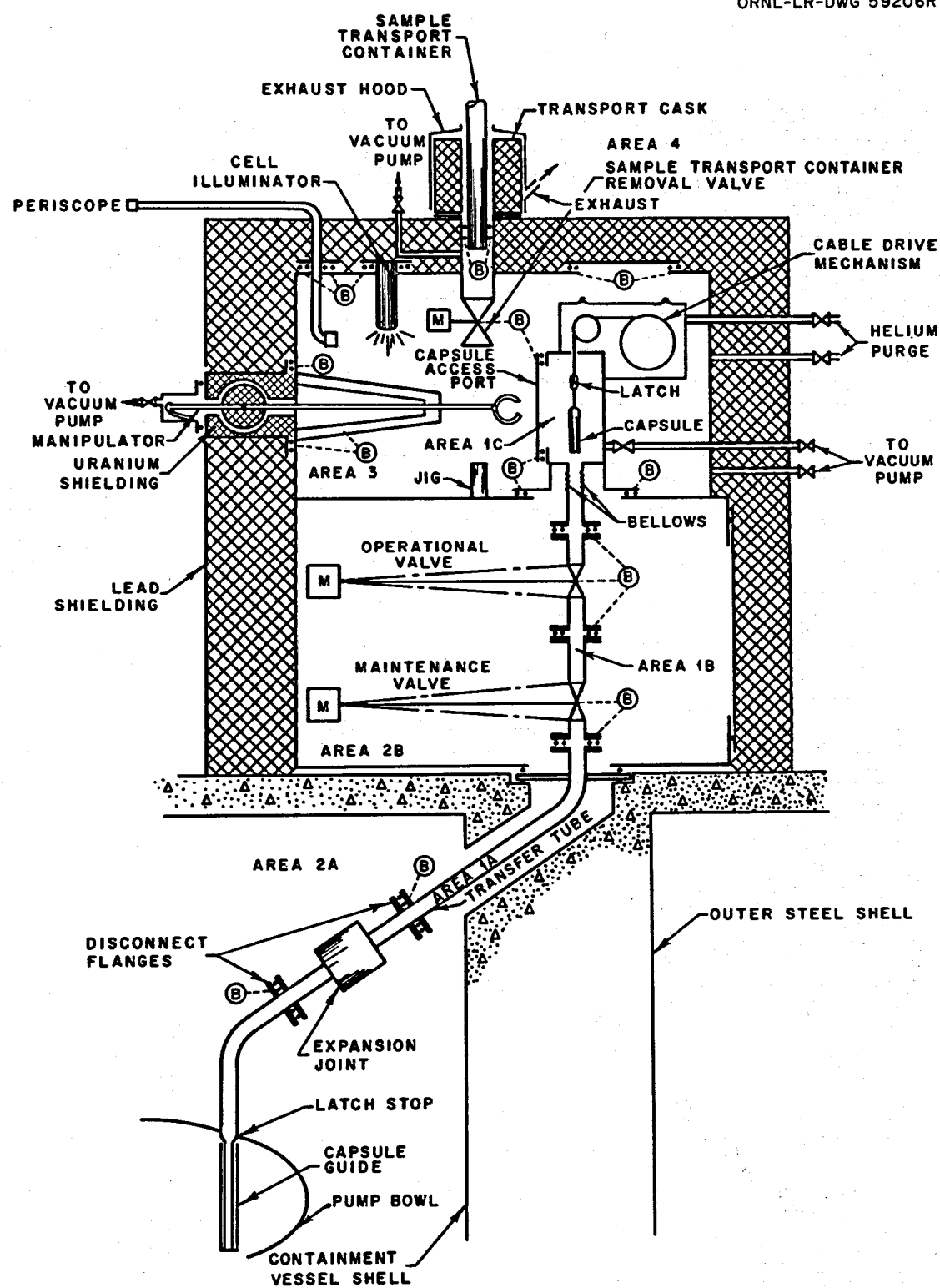


Fig. 5.7. Radioactive Material Sampler.

Interim waste storage vessels are located adjacent to the processing area in a large canal.

To facilitate remote maintenance, vessels are arranged so that all equipment is accessible from above, and all process and service lines can be connected remotely. Over-all building space is dictated by remote maintenance considerations rather than by actual vessel size.

5.2.14 Plant Layout

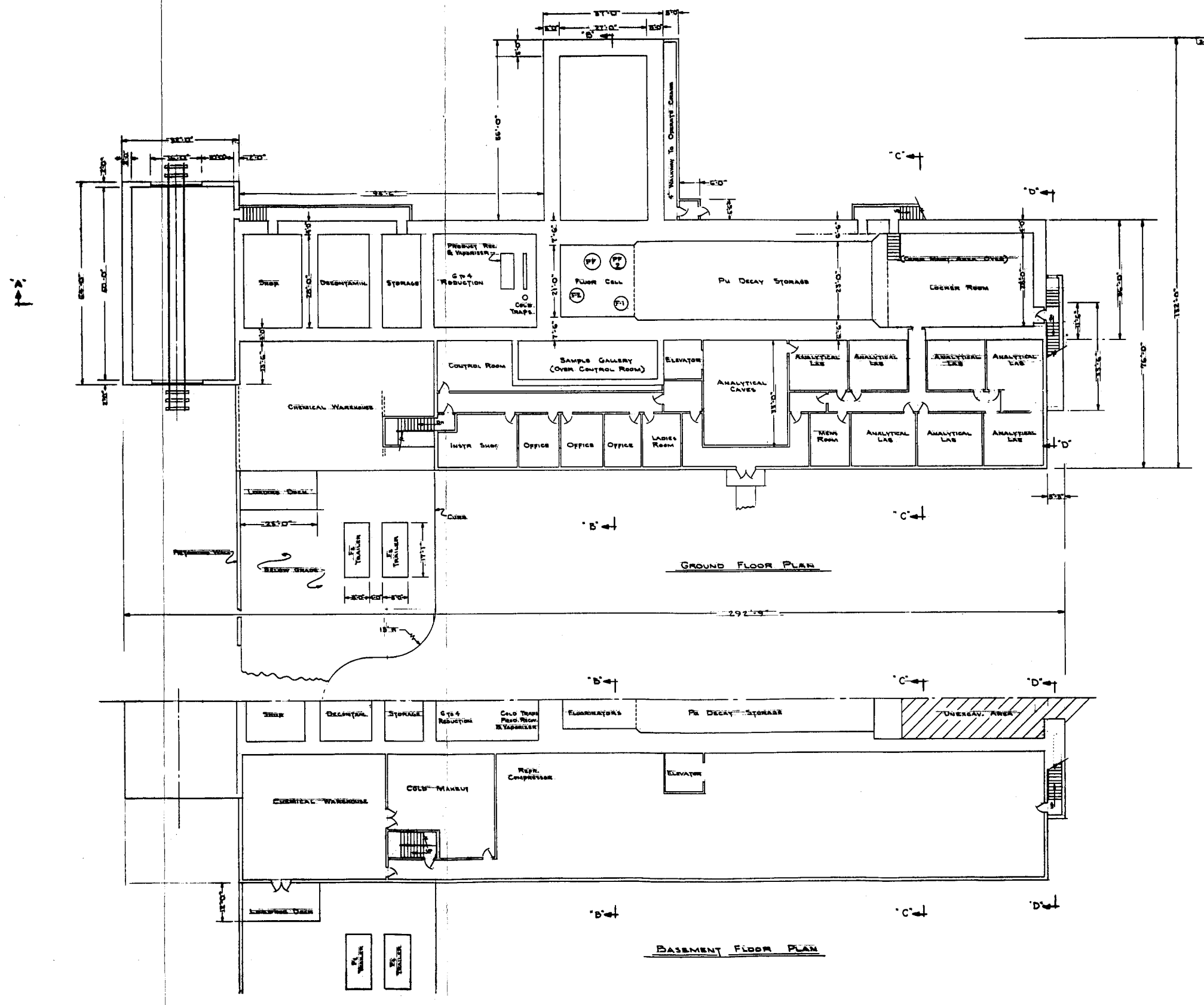
In order to establish uniformity in cost estimation of nuclear power plants, the Atomic Energy Commission has specified certain ground rules (52) covering topography, meteorology, climatology, geology, availability of labor, accounting procedures, fixed charge rates, etc. These ground rules were used in this study.

Advantage was taken of a design study and operating experience with a remotely maintained radioactive chemical plant reported by Farrow (32) to obtain over-all plant arrangements, as shown in Fig. 5.8.

The hypothetical site location is 500 miles from the reactor site. The plant is located on a stream that is navigable by boats having up to 6-ft draft. There is convenient highway and railroad access. The plant is located on level terrain in a grass-covered field. The earth overburden is 8 ft deep with bedrock below.

5.2.15 Capital Cost Estimate

The cost of the fuel processing plant was apportioned among three principal categories: building costs, process equipment costs, and auxiliary process equipment and services costs. The building costs included such items as site preparation, structural materials and labor, permanently installed equipment, and material and labor for service facilities. Process equipment costs were calculated for those tanks, vessels, furnaces, and similar items whose primary function is directly concerned with process operations. Process service facilities are items such as sampling facilities, process piping and process instrumentation which are intimately associated with process operations.



Accounting Procedure. — The accounting procedure set forth in the Guide to Nuclear Power Cost Evaluation (52) was used as a guide in this estimate. This handbook was written as a guide for cost-estimating reactor plants, and the accounting breakdown is not specific for a chemical processing plant. Where necessary the accounting procedures of the handbook were augmented.

Process Equipment. — A large number of process vessels and auxiliary equipment in these plants is similar to equipment previously purchased by ORNL for the fluoride volatility pilot plant for which cost records are available. Extensive use was made of these records in computing material, fabrication and over-all equipment costs. In some cases it was necessary to extrapolate the data to obtain costs for larger vessels. Items that were estimated in this manner include the fluorinators, furnaces, NaF absorbers, and CRP traps. The cost of the UF₆-to-UF₄ reduction unit was based on a unit described by Murray (70). The unit had a larger capacity than was needed for these plants, but it was assumed that the required unit would have about the same over-all cost. Refrigeration equipment and cold traps were estimated from cost data on ORGDP and ORNL equipment.

For vessels and tanks of conventional design, the cost was computed from the cost of material (INOR-8 for most vessels) plus an estimated fabrication charge, both charges being based on the weight of the vessel. A summary of values used in estimating process vessels by weight is given in Table 5.1. Some items of process equipment were of special design and significantly different from any vessels for which cost data were available. For the shells of the prefluorination storage tanks, the high fabrication cost values shown were obtained by comparison with an available shop estimate for a similar vessel.

Auxiliary process items such as process piping, process electrical service, instrumentation, sampling connections and their installation were not considered in sufficient design detail to permit direct estimation. A cost was assigned to these items which was based upon previous experience in design and cost estimation of radiochemical processing plants. In assigning these costs cognizance was taken of the fact that the plant is remotely maintained.

Table 5.1. Vessel, Pipe, and Tubing Costs

	INOR-8 \$/ft	INOR-8 \$/lb	Alloy 79-4	Stainless Steel 304
Metal Cost		3.00	2.66	0.65
Fabrication Cost:				
Prefluorination INOR transfer tanks 3 and 4		3.50	-	-
Fluorinators		-	4.00	-
Transfer vessels		3.50	-	-
Waste storage vessel		-	-	2.50
Waste storage thimbles		-	-	1.85
UF ₄ dissolvers		3.50	-	-
1/2 in. OD x 0.042 wall tube	6.06	26.40	-	-
1 in. IPS, Sch. 40 pipe	30.05	16.04	-	-
1-1/2 in. IPS, Sch. 40 pipe	41.67	13.71	-	-

Buildings. — The building estimate shown in Table 5.2 included the cost of land acquisition, site preparation, concrete, structural steel, painting, heating, ventilation, air conditioning, elevators, cranes, service piping, laboratory and hot cell equipment, etc. The individual costs were calculated using current data for materials and labor, and were based on the drawings prepared.

Process Equipment Capital Cost. — Process equipment capital costs for the two fluoride volatility plants are presented in Table 5.3. These costs are the totals of material, fabrication and installation charges.

Building Capital Cost. — As mentioned above, process equipment and buildings were the only items considered in sufficient design detail to permit direct estimation. The remainder of the capital costs were estimated by extrapolation from previous studies of radiochemical processing plants. The fact that the plant is remotely maintained was an important factor in estimating process instrumentation and electrical and sampling connections. These items are expensive because of counterbalancing, spacing, and accessibility requirements.

Construction overhead fees were taken at 20 per cent of direct materials and labor for all buildings, installed process equipment, piping,

Table 5.2. Fluoride Volatility Processing Building
Costs 30 ft³/day Plant Capacity

	Materials	Labor	Total
Receiving Area			
Excavating and backfill	\$ 38,000	\$ 18,000	\$ 56,000
Concrete, forms, etc.	108,000	133,000	241,000
Structural steel, etc.	58,000	49,000	107,000
Roofing	13,000	16,000	29,000
Services	63,000	39,000	102,000
			\$ 535,000
Processing Cells			
Excavating and backfill	\$184,200	\$ 85,500	\$ 269,700
Concrete, forms, etc.	520,000	639,000	1,159,000
Structural steel, etc.	277,000	235,000	512,000
Crane area roofing, painting, etc.	64,900	75,600	140,500
Crane bay doors	390,000	160,000	550,000
Services	301,000	188,000	489,000
Bldg. movable equipment	865,000	255,000	1,120,000
Viewing windows	40,000	2,000	42,000
			\$4,282,200
Waste Storage			
Excavation and backfill	\$ 95,000	\$ 44,400	\$ 139,400
Concrete, forms, etc.	332,000	496,000	828,000
Structural steel, etc.	400,000	404,000	804,000
Crane area roofing	86,500	100,800	187,300
Painting	44,500	44,500	89,000
Services	565,000	289,000	854,000
Bldg. movable equipment	225,000	30,000	255,000
			\$3,156,700
Operations and Laboratories			
Excavation and backfill	\$ 72,200	\$ 33,400	\$ 105,600
Concrete forms, etc.	82,600	115,100	197,700
Structural steel, etc.	204,700	43,200	247,900
Roofing	8,500	4,300	12,800
Super structure	79,100	27,100	106,200
Misc. structural material	31,900	35,100	67,000
Services	352,000	276,000	628,000
Misc. equipment	300,000	43,500	343,500
			\$1,708,700

Table 5.2. Continued

	Materials	Labor	Total
Outside Utilities			
Cooling tower, motors, pumps, piping		\$ 70,000	
Water reservoir, pumps, piping		300,000	
Fire protection (house & equipment)		35,000	
Yard lighting		5,000	
Boiler house steam heating (4,000 kw at \$75/kw)		300,000	
Air compressor system		10,000	
Steam distribution & con- densate return		3,500	
Cooling water supply & return		40,000	
Water supply connection		1,700	
Process drain lines		3,500	
Sanitary sewer connections		3,700	
Radioactive hot drain connections		12,000	
Cell ventilation connec- tions to stack		9,000	
Off-gas connections to stack		10,000	
Storm sewer system		16,000	
Electrical substation & lines (3000 kw at \$60/kw)		180,000	
Stack (200 ft)		50,000	
Guard house and portals		5,000	
Autos, trucks, crane, bull dozer		50,000	
		\$1,104,400	
Land and Land Improvements			
Land (160 acres at \$100/acre)		16,000	
Leveling & grading		50,000	
Topsoiling and seeding		20,000	
Fencing, (2 miles at \$4/ft)		44,000	
Railroad spur, 100 ft		20,000	
Asphalt roads & parking areas		200,000	
		\$ 350,000	

Table 5.3. Installed Cost of Fluoride Volatility Process
Equipment 30 ft³/day Plant Capacity

	Number	Description	Cost
<u>Receiving</u>			
Cooling jackets for shipping tanks	160	2.75 ID by 15-ft high, carbon steel	\$ 120,000
Instrumentation		Thermocouples, radiation monitors, etc.	480,000
<u>Prefluorination Storage</u>			
Transfer tanks	2	2-ft x 2-ft; INOR-8; 0.375 in. shell, 0.5 in. head	100,000
Furnace	2	2.7 ft x 3 ft; 50 kw	7,000
<u>Fluorination</u>			
Fluorinators	5	1.75 ft d. by 9 ft high; 6 ft ³ salt; Alloy 79-4; 0.5 in. shell, 0.5 in. head	40,000
Furnaces	5	2.7 ft d. x 4 ft h; 75 kw	16,000
Movable bed absorber	5	6 in. d x 4 ft h	25,000
<u>Absorption</u>			
Absorbers with furnaces	30	6 in. sch. 40 pipe, 6.3 ft long	150,000
Cold traps	15	-40°C units, copper	112,500
	15	-75°C units, copper	37,500
NaF chem. trap	5	6 in. sch. 40 pipe x 6 ft; heated	3,000
Vacuum pump	1	50 cfm displacement	3,000
<u>Reduction and Compounding</u>			
Reactor	1	10 kg/day capacity; Inconel	66,150
Dissolver	1	2.7 ft d. x 2.7 ft h; 12 ft ³ salt; INOR-8; 0.5 in. shell	5,500
Heater	1	3.4 ft d. x 3.7 ft h; 71 kw	6,000
Salt make-up tank	2	3.4 ft ³ d. x 6.7 ft h; INOR-8; 40 ft ³ capacity	26,000
Heater	2	4.1 ft d. x 7.7 ft h; 178 kw	34,000

Table 5.3, Continued

	Number	Description	Cost
<u>Transfer Tanks</u>	2	4.5 ft d. x 4.5 ft h; 60 ft ³ of salt; INOR-8 with heaters	\$ 100,000
<u>Waste Storage</u>			
Shipping and storage tanks	As Needed	2 ft ID by 8 ft h; stainless steel 304 L; 10 ft ³ salt; 0.25 in. shell and head	Included with operating expenses
Thimbles	1200	2.75 ft d. x 15 ft h; ordinary steel 304 L; 0.1875 shell	600,000
<u>Miscellaneous Equipment</u>			
Refrigeration unit	2	50,000 Btu/hr at -40°C	10,000
Refrigeration unit	2	8,000 Btu/hr at -75°C	10,000
HF disposal unit	1	2.8 ft d. x 5.3 ft h	500
F ₂ supply system	5	Tank and trailer	35,000
Total Process Equipment			\$1,987,150

instrumentation, electrical and other direct charges. This rate is higher than current charges for this type of construction and estimates. Architect engineering and inspection fees were taken as 15 per cent of all charges including construction overhead.

A summary of the capital cost estimate is presented in Table 5.4.

Table 5.4. Summary of Capital Cost Estimate for Molten-Salt Reactor-Fuel Fluoride Volatility Processing Plant

Capacity - 30 ft³ of Salt/Day

Receiving Area	\$ 535,000
Processing Cells	4,282,200
Waste Storage	3,156,700
Operations and Laboratories	1,708,700
Outside Utilities	1,104,400
Land and Improvements	350,000
Process Equipment	1,987,150
Process Piping	320,000
Process Instrumentation	205,000
Process Electrical Connections	39,000
Sampling Connections	30,000
 Total, Installed Equipment and Buildings	\$13,718,150
 General Construction Overhead at 20% subtotal	2,743,660
Architectural Engineer, etc., at 15% subtotal	2,469,294
Contingency at 20% subtotal	3,786,250
Interest During Construction, 9.3% of subtotal	2,112,728
 Total	\$24,830,082

5.2.16 Operating and Maintenance Cost Estimates

The manpower requirements were estimated consistently with the procedures outlined in the Guide (52); the results are listed in Table 5.5. Materials, utilities, maintenance materials, etc. were estimated by consideration of the process steps involved; the estimates are listed in Table 5.6 together with a summary of the labor cost. The total operating cost was estimated to be \$4,040,850 annually.

5.2.17 MSCR Irradiated Fuel Shipping Cost

The shipping cask must accommodate a molten-salt shipping cylinder having a volume of 10 ft³. The cost was estimated from the weight which was determined by the shielding requirements. A unit cost of \$1.00/lb fabricated was allowed, including charges for an INOR liner and a condensing-water radiator. Three casks were allowed so that one might be at the reactor site, a second at the processing plant, and a third in transit. Results are listed in Table 5.7.

Table 5.5. Operating Manpower Estimates for
30 ft³/day - Fluoride Volatility Plants

	No.	Cost (\$/year)
Management		
Manager	1	18,000
Assistant manager	1	15,000
Secretary	2	10,000
	4	43,000
Production		
Superintendent	1	12,000
Shift supervisor	4	30,000
Operator	12	66,000
Helper	12	60,000
Secretary	2	9,600
	31	177,600
Maintenance		
Superintendent	1	10,000
Mechanical engineer	2	16,000
Mechanic	12	69,600
Machinist	3	18,000
Instrument man	8	46,400
Clerk	1	4,350
Storeroom keeper	2	8,700
	29	173,050
Laboratory		
Supervisor	1	8,000
Chemist	6	39,000
Technician	10	52,000
Helper	6	28,800
	23	127,800
Health Physics		
Supervisor	1	8,000
Monitor	4	20,800
Clerk	1	4,000
Records keeper	1	3,600
	7	36,400

Table 5.5. Continued

	No.	Cost (\$/year)
Accountability		
Engineer	1	7,000
Clerk	1	4,000
	2	11,000
Engineering		
Mechanical engineer	2	16,000
Chemical engineer	4	36,000
Draftsman	3	15,900
Secretary	1	4,500
	10	72,400
General Office		
Manager	1	5,000
Accountant	1	4,800
Payroll clerk	2	8,000
Purchasing agent	1	4,800
Secretary	2	8,000
	7	30,600
Miscellaneous		
Guard	8	32,000
Fireman	4	16,000
Receptionist	1	4,000
Laundry worker	3	10,800
Nurse	1	4,800
Janitor	3	10,800
	20	78,400
Total	133	750,250

Table 5.6. Fluoride Volatility Plant Direct Annual Operating Cost

Shipping - Storage Tanks (50 at \$2,500)	\$ 125,000
Chemical Consumption	
Fluorine (at \$2.00/lb)	120,000
KOH (at \$0.10/lb)	16,600
Hydrogen (at \$2.00/lb)	4,500
NaF (at \$0.15/lb)	300
Nitrogen (at \$0.05/ft ³)	3,400
HF (at \$0.20/lb)	6,100
Graphite (at \$0.15/lb)	1,100
Miscellaneous	5,300
	<hr/>
	157,300
Utilities	
Electricity (at \$0.01/kw hr)	362,000
Water (at \$0.015/1000 gal)	5,700
Heating (based on steam at \$0.25/1000 lbs)	8,500
	<hr/>
	376,200
Labor^a	
Operating	406,400
Laboratory	127,800
Maintenance	173,050
Supervision	43,000
Overhead (at 20% of above)	150,000
	<hr/>
	900,250
Maintenance Materials	
Site	10,000
Cell structures and buildings ^b	76,000
Service and utilities	78,800
Process equipment ^c	243,300
	<hr/>
Total Direct Operating Cost	482,100
	<hr/>
	\$2,040,850

^aSummarized from Table 5.5.

^bBuilding services excluded.

^cIncludes process equipment, process instrumentation and sampling.

Table 5.7. MSCR Irradiated Fuel Shipping Cask Data and Shipping Cost*

Cask weight	100,000 lbs
Cost of cask	\$100,000
Number of casks	3
Salt volume in shipment	10 ft ³
Age of salt at shipment	20 days
Days salt accumulation in shipment	6 days
Round trip distance	1000 miles
Round trip time	10 days
Method of shipment	Rail
Number of shipments per full power year	50
Freight rate	\$2.40/100 lbs- 1000 miles
Unit shipping cost	\$330/ft ³ salt

*Data and cost adapted from Reference 20.

5.2.18 MSCR Unit Processing Cost

The various bases and contributions to the unit processing cost are collected in Table 5.8 for the fluoride volatility central plant processing of MSCR fuel. For the reference design fuel containing 32 kg of thorium per ft³, the unit cost was \$36.90 per kg of thorium.

Although the cost was expressed in terms of \$/kg of Th, it should be remembered that only isotopes of uranium are recovered. Stripped salt, containing valuable thorium, lithium-7, and beryllium, as well as fission products, is discarded. Additional or alternate processing would be required to recover any of these components.

Table 5.8. Unit Processing Costs, Central Fluoride Volatility Processing Plant for MSCR Fuel

Capacity of plant	30 ft ³ /day
Reference design fuel	32 kg Th/ft ³
Annual charges:	
Capital (\$24.8 million at 15%)	\$3.7 million
Operation and maintenance	\$2.0 million
Daily charge (80% plant factor)	\$19,500/day
Batch size	188 ft ³ or 6000 kg Th
Processing time	6.3 days
Turn-around time	2 days
Processing plant cost	\$26.60/kg Th
Shipping cost	\$10.30/kg Th
Total processing cost	\$36.90/kg Th

5.3 Thorex Central Plant

The reference plant described in the Guide (52) is a central facility capable of processing 1000 kg Th/day with thorium discard or 600 kg Th/day with thorium recovery. The plant was designed specifically for thorium metal or thorium oxide fuels; however, since other types of thorium fuels were not specifically excluded, it was assumed that the plant would also accept a fluoride-salt fuel. It was further assumed that the fluoride fuel would be processed at the same base charge as the metal or oxide fuel. This assumption amounted to assigning the same charge to a fluoride head-end treatment as to dissolution and feed preparation steps for the other fuels. The tail-end treatment for the conversion of Thorex nitrate product to fluoride feed material was assigned a cost that was thought to be representative of the processing steps.

5.3.1 Head-End Treatment

The head-end treatment shown schematically in Fig. 5.9 has not been demonstrated. However, the chemical principles have been established (40) by laboratory investigations of the stability of fluoride salt fuels.

It is known (40) that the oxides of uranium, thorium and beryllium are very stable compounds having the indicated order of stability



and that oxygen or oxygen-bearing compounds must be eliminated from fluoride salt fuels to insure their stability. In the proposed head-end treatment, the draw-off from the reactor at 500 - 550°C would be contacted in a spray with steam or high temperature water ($\sim 200^\circ\text{C}$) to precipitate the oxides of uranium, beryllium, thorium, protactinium and some of the fission products. It is believed that rare earth oxides can be precipitated in this manner. Lithium fluoride is a very stable compound and would probably not enter into reaction with water. It should remain in the system as LiF and be frozen into small crystalline particles.

The hydrolysis would form large quantities of HF which in aqueous media is rather corrosive. Therefore the selection of materials of construction for the precipitator will be a problem. Disposal of HF can be accomplished by dilution with large volumes of air and dispersion from a stack or by neutralization with an inexpensive base. Some cleanup of the HF stream will be required because of volatile fission products. Reuse of this HF in the subsequent hydrofluorination step (see Fig. 5.8) may not be feasible because of water vapor in the gas.

The second step in the head-end treatment is dissolution of all the hydrolyzed components that are soluble in nitric acid. The oxides of uranium, thorium, protactinium and rare earth products should dissolve quite readily. Since lithium fluoride and beryllium oxide are quite insoluble in aqueous media, negligible amounts of these compounds should be dissolved. Also, it is almost certain that some of the fission products will be insoluble and remain with the lithium and beryllium. Dissolution should proceed smoothly because it has been shown by Pitt (73) that the particle sizes produced when a molten salt is sprayed into water are in the micron and submicron range.

ORNL-LR-DWG 71093

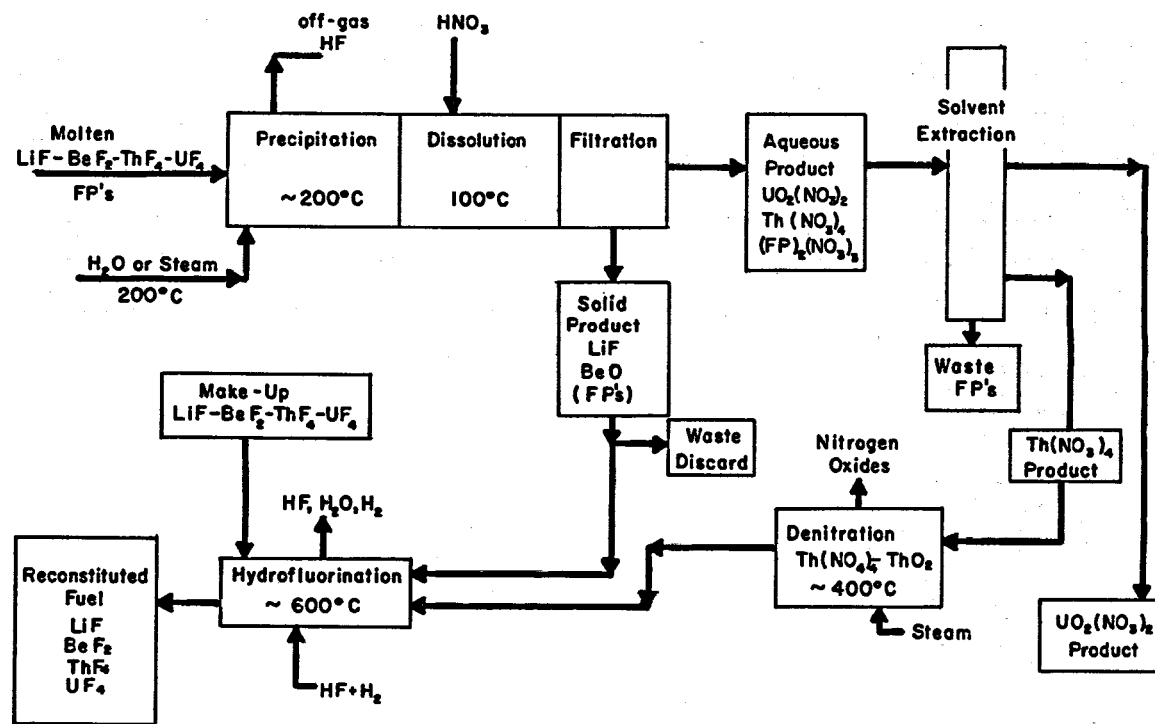


Fig. 5.9. Proposed Aqueous Processing for MSCR.

Dissolution is followed by solid-liquid separation either by filtration or centrifugation. Aqueous nitrate solutions are fed into a feed adjustment step preceding solvent extraction by Thorex and the insoluble material is routed to hydrofluorination. At this point a portion of the solids can be discarded as a purge of fission products that remain in the precipitate.

5.3.2 Solvent Extraction

Decontamination of thorium and uranium can be accomplished by well-established Thorex procedures. Aqueous nitrate solutions are evaporated until about 0.15 N acid deficient and fed to an extraction column. In the extraction column both thorium and uranium are extracted into an organic phase (tributyl phosphate) leaving the bulk of the fission products in the aqueous phase, with decontamination factors up to 10^5 .

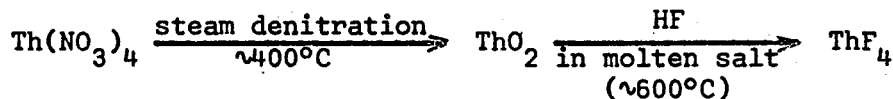
Waste from the first extraction cycle contains all of the protactinium that was in the feed stream. However, the amount is insufficient to warrant recycling the waste after an additional decay period. In the interim between discharge from the reactor and chemical processing, the fuel ages about 120 days so that only about 15% of the protactinium remains undecayed. The waste is given permanent storage in large underground tanks.

In a fuel recycle system such as the MSCR it is not necessary to de-contaminate further by the use of additional extraction cycles. The presence of ^{232}U and ^{228}Th will make recycle fuel too radioactive for direct handling, regardless. After extraction, therefore, it is sufficient to partition uranium and thorium in a stripping column by the proper adjustment of organic and aqueous flow rates. In this operation, thorium is stripped from the organic phase into an aqueous phase; uranium remains in the organic phase. A subsequent stripping operation returns the uranium to the aqueous phase. The produce streams are respectively $\text{Th}(\text{NO}_3)_4$ and $\text{UO}_2(\text{NO}_3)_2$.

5.3.3 Tail-End Treatment

Fuel reconstitution begins with acceptance of the nitrate products from the solvent extraction plant. It is necessary to convert the nitrates

to the fluorides. In the case of thorium this is accomplished by preparing the oxide in a denitration process followed by hydrofluorination in a molten salt mixture. The steps are as follows:



Steam denitration is an established procedure in the sol-gel process (33) for preparing highly fired, dense ThO_2 or $\text{ThO}_2 - \text{UO}_2$ fuel. In this case the aqueous nitrate solution from the Thorex process would be evaporated to crystallize $\text{Th}(\text{NO}_3)_4$; the crystals in turn would be contacted with superheated steam for the actual denitration. Final preparation of the fluoride has to be accomplished in a second high temperature operation in molten fluoride salts. Thorium oxide is quite intractable to attack by hydrogen fluoride under most conditions; however, in the presence of molten fluorides the reaction will occur. The presence of other high valence compounds, e.g., other thorium or uranium fluorides, in the melt abets the dissolution.

The conversion of uranyl nitrate to the tetrafluoride is not as straightforward as that of thorium because of the required valence change. In the Excer process developed at ORNL, uranyl nitrate from the last Thorex stripping column can be fed directly onto a cation exchange resin (Dowex 50 W) which absorbs the uranyl ion. After loading, the resin is eluted with aqueous hydrofluoric acid to produce UO_2F_2 , which is reduced in an electrolytic cell. The aqueous solution is allowed to flow into a mercury cathode in which $\text{UF}_4 \cdot 0.75 \text{H}_2\text{O}$ precipitates from the aqueous phase. The precipitate is separated by centrifugation or filtration and dried. Water of hydration is not tenaciously held, and moderate drying conditions are sufficient to expel it.

A second method of converting $\text{UO}_2(\text{NO}_3)_3$ to UF_4 is to reduce U(VI) to U(IV) in the presence of fluoride at 500 - 600°C. In this tail-end treatment the two nitrate solutions of thorium and uranium are mixed and co-denitrated using superheated steam to yield ThO_2 and UO_3 . The mixed oxides are converted to the fluorides in a 500 - 600°C molten fluoride salt bath

by contacting with a gaseous mixture of $H_2 + HF$. Uranium is reduced by the hydrogen and hydrogen fluoride to the tetravalent form and dissolves as UF_4 ; thorium is metathesized to ThF_4 which also dissolves in the melt.

The processing cycle is completed when the uranium fluoride is mixed with fluorides of thorium, lithium, and beryllium oxide plus make-up feed and hydrofluorinated. Beryllium recycled as BeO dissolves as BeF_2 when hydrofluorinated in molten fluoride solutions.

5.3.4 Processing Costs

The unit processing costs were computed according to the prescription given in Guide to Nuclear Power Cost Evaluation, Vol. 4, Section 460. The escalated daily charge for operation of the Thorex plant was taken as \$17,500 in late 1962. Since the thorium was recycled, the capacity was 600 kg/day. As described in a previous section, the daily increments of fuel withdrawn from the reactor were accumulated for 120 days and combined into a single processing batch. If the withdrawal rate exceeded $1.25 \text{ ft}^3/\text{day}$ (40 kg Th/day), the batch size exceeded 4800 kg of Th and required eight days or longer to process. For this range of process times, the "turn-around-time" is specified to be eight days in the Guide. Thus the total processing time is $120r/600 + 8$ days (where r is the withdrawal rate in kg Th/day) and the total amount processed is $120r$ kg of Th. The cost for operating the Thorex plant is thus

$$\begin{aligned} \text{Separation Cost} &= \frac{17,500 \left[\frac{120r}{600} + 8 \right]}{120r} \\ &= (29.2 + 1167/r) \text{ \$/kg Th} \end{aligned}$$

The cost of reducing solid fuel elements into a form suitable for processing (aqueous solution of uranyl and thorium nitrates) is included in the daily operating cost (104). It seems likely that the cost of converting the MSCR fuel by the method proposed in Sec. 5.2 would be less costly than the reduction of solid fuel elements by Darex or Zircex. However, an investment of \$500,000 for MSCR fuel head-end treatment was allowed, based

on estimates extracted from reference 20. This resulted in a head-end treatment charge of \$0.53/kg Th processed.

The cost of converting recovered thorium nitrate to ThF_4 was not given in the Guide. However, the cost of converting low enrichment uranium to UF_6 was only \$5.60/kg. Since the proposed thorium conversion process is simpler and shorter than the uranium process, it seemed adequate and conservative to assign a cost of \$5.00/kg Th for the conversion of ThF_4 .

Summing these charges, one has

$$\text{Processing Plant Cost} = (34.7 + 1167/r) \text{ \$/kg}$$

where r = kg Th/day removed from the reactor.

Shipping costs are presented in Section 465 of the Guide (52), and include freight, handling, cask rental, and property insurance. The cost is \$16/kg of uranium (or thorium) for spent fuel elements.

MSCR fuel must be packaged before shipment. In the scheme proposed, the daily productions of 1.67 ft^3 /day are accumulated in 35 ft^3 batches in the spent fuel facility (Sec. 4.8.10) which contains 5 tanks each having a capacity of 35 ft^3 and provided with sufficient cooling to remove afterheat from freshly irradiated fuel. A 10 ft^3 batch is drained into an INOR "bottle" (cylinder) one foot in diameter and 13 feet long. This is inserted into an individual shipping cask and transported to the Thorex plant. If the bottles cost as much as \$10,000 apiece, but are re-usable for at least 10 years, they will add to the shipping cost only \$1.74/kg Th at the lowest rate of processing (40 kg/day).

The charge for shipping decontaminated thorium back to the plant is represented to be \$1.00/kg in the Guide.

Since the processing plant operating charge was all levied against the thorium, the only charges on the uranium are shipping at \$17/kg per round trip and reconversion, for which operation the Handbook gives \$32/kg for converting the nitrate of highly enriched ^{235}U to UF_6 . Although the cost of conversion to UF_4 should be less, the given cost was assumed. The total charge for the uranium was thus \$49/kg, and was charged against all isotopes of uranium, including ^{238}U and the precursor, ^{233}Pa .

5.4 Comparison of Processing Cost Estimates

For the purposes of comparison, the results of three other processing cost studies are cited. The first, by Carter (20), dealt with a central Fluoride Volatility plant designed especially for processing MSCR fuel at a rate of 31.5 ft³/day (1000 kg Th/day). The estimates were based on the same design study (21) used to prepare the estimates reported in Sec. 5.2. The scaling, however, was performed on the plant as a whole, rather than with individual items, and the scaling factor was 0.31. The estimated capital cost was \$31.5 million, and the annual operating expense was \$3.0 million. This study is referred to below as the "CMS" study.

The second study, also by Carter (20), dealt with a central Thorex facility adapted to process fluoride fuels (1000 kg Th/day) and was based on a detailed analysis of the head-end and tail-end processes (described in the previous section) as well as the Thorex separation process, and was based on an unpublished design and cost study performed by Carter, Harrington, and Stockdale at ORNL in which flow sheets, equipment specifications, plant arrangement drawings, building drawings, etc. were prepared and the items were costed. For brevity, this study is referred to below as the "CHS" study. It is, essentially, an independent estimate of the facility assumed in the Guide to Nuclear Power Cost Evaluation (52), adapted for fluoride fuels. The estimated capital cost, scaled to a capacity of 1000 kg Th/day, was \$36.5 million, and the annual operating expense was \$3.6 million.

The third study, performed by W. H. Farrow, Jr. (32), dealt with several radiochemical separation plants for several different solid fuels and clads and with both direct and remote maintenance. The purex process, which is similar to Thorex, was employed for the separations. The most applicable case was that of a remotely maintained plant capable of treating one tonne per day of natural uranium. Although the process was described in considerable detail, a cost breakdown was not given by Farrow. The capital cost was \$43 million, and the annual direct operating cost was \$3.7 million. One might reasonably assume that a Thorex plant of the same capacity would have approximately the same costs, and that the head and tail-end treatments for fluoride fuels would be no more expensive, and perhaps less, than those of the solid fuels.

It is seen that the estimates of the total cost, including shipping, vary by a factor of two, ranging from \$37 to \$75/kg of thorium processed. It seems plausible that processing MSCR fuel in a central Fluoride Volatility facility will cost less than \$50/kg, and possibly less than \$40, and that processing in a Thorex plant will cost less than \$70, and possibly less than \$50 per kg of thorium.

Table 5.9. Comparison of Estimates of Processing Costs for the MSCR Reference Design^a

	This Work	CMS	AEC	CHS	Farrow
Type of Plant	Fl. Vol.	Fl. Vol.	Thorex	Thorex	(Purex)
Location	Central	Central	Central	Central	Central
Capacity, kg Th/day	1000	1000	600	1000	(1000) ^b
Batch Size, kg Th	6000	6000	6000	6000	6000
Turn-Around-Time, Days	2	2	8	2	(2) ^c
Capital Cost, \$10 ⁶	25.2	31.2	-	36.5	43
Annual Operating & maintenance Cost, \$10 ⁶	2.0	3.0	-	3.6	3.7
Process Plant Cost, ^d \$/kg Th	26.6	34.5	56.5	40.5	46.4
Shipping Cost, \$/kg Th	10.3 ^f	10.3 ^f	18.7	10.3 ^f	(20) ^c
Processing Cost, \$/kg Th	36.9	44.8	75.2 ^e	50.8	(66.4) ^c

^aSpent fuel is withdrawn from the reactor ($1.67 \text{ ft}^3/\text{day}$; 53.3 kg Th/day) and shipped to a central processing plant in 10 ft^3 batches. These are accumulated in 6000 kg Th batches, cooled for an average of 90 days, and processed in six days (10 days in AEC plant).

^bPurex plant capacity of one tonne of natural uranium per day assumed equivalent to one tonne thorium per day.

^cThese items were not estimated by Farrow; values chosen were thought to be consistent with his general treatment.

^dFixed charges were 14.46%, except for AEC plant where daily operating charge (escalated to 1962) was given in reference 52.

^eTurn-around-time was 8 days. With a more realistic time of 2 days, and shipping costs of \$10.30/kg Th, the total costs would be only about \$50, which is comparable to the other estimates listed, except Farrow's.

^fTable 5.7.

6. FUEL CYCLE ANALYSIS

6.1 Analysis of Nuclear System

The nuclear calculations for the MSCR were performed by means of the MERC-1 program for the IBM-7090. This program, described by Kerlin et al., in Appendix D, uses the multigroup neutron diffusion code Modric and the isotope code ERC-10 as chain links.

6.1.1 Computer Programs

Modric. — This program was employed in a 34-group version using the group energies and cross sections of the various elements given in reference 54. The cross sections were adopted for the most part from Nestor's tabulation (72), with some minor modifications described below. Maxwell-Boltzman averaged thermal cross sections and resonance integrals of important materials are listed in Table 6.1. Thermal spectrum hardening was ignored.

Although the treatment of downscattering in Modric provides for the transfer of neutrons from any group into any of the ten next lower groups, the required scattering matrices were not available when the MSCR calculations were begun. Subsequently, the matrices were computed taking into account fast fissions and inelastic scattering in thorium and the fact that the elastic scattering lethargy decrements were in some ranges larger than the group widths. A single calculation was made to determine the importance of treating the downscattering in this more precise manner. The effect was found to be insignificant.

ERC-10. — The basic isotope equation in ERC-10 computes the concentration that is in equilibrium with the sources (make-up, recycle, transmutation, decay, fission) and the sinks (transmutation, decay, waste, sales, recycle). One isotope (usually ^{233}U or ^{235}U) may be selected to satisfy a criticality equation; the feed rate or sales rate required to maintain the critical concentration is then computed.

Three isotopes, ^{234}U , ^{236}U , and ^{238}U , approach equilibrium with periods long compared to the assumed fuel life (30 years). The equilibrium

Table 6.1. Cross Sections and Resonance Integrals Used in
MSCR Multigroup Neutron Calculations
(Values in barns per atom)

Material	Thermal Cross Section ^a		Resonance Integrals ^b	
	Fission ($v\sigma_f$)	Absorption (σ_a)	Fission ($v\sigma_f$)	Absorption (σ_a)
^{232}Th		3.77	8.286×10^{-1}	9.684×10
^{233}Pa		1.8943×10		8.67221×10^2
^{233}U	6.54×10^2	3.40×10	2.01972×10^3	9.60119×10^2
^{234}U		5.54×10	1.0602×10	6.89453×10^2
^{235}U	6.29×10^2	3.05×10^2	7.54945×10^2	4.66792×10^2
^{236}U		2.10	5.487	2.87528×10^2
^{237}Np		1.07×10^2	1.0983×10	5.70047×10^2
^{238}U		1.36	3.225	2.77241×10^2
^6Li		4.720×10^2		4.58811×10^2
^7Li		1.66×10^{-2}		1.5774×10^{-2}
^9Be		5.048×10^{-3}		4.748×10^{-3}
^{19}F		4.5×10^{-3}		1.975×10^{-3}
^{12}C		5.048×10^{-3}		1.897×10^{-1}
INOR-8		2.874		6.004
^{135}Xe		1.60×10^6		4.5756×10^4

^aMaxwell-Boltzman averaged at 1200°F.

^bCut-off at 0.437 ev.; infinite dilution values.

concentrations of these were not computed; instead, first approximations of their time-mean concentrations (starting with a reactor initially inventoried with ^{235}U 95% enriched) were computed as described in Appendix H.

The transient behavior of all other isotopes, including ^{233}Pa , ^{233}U , and fission products, was ignored in the optimization studies. The approximations involved in this approach are examined in Appendix H.

MERC-1. — Input (54) consists of specifications of the geometry and dimensions of the reactor regions, initial guesses at the composition, information on power, fuel volume, processing modes and rates, composition of make-up materials, unit values, and processing costs. The output consists

of nuclear data (breeding ratio, mean eta, neutron balance, etc.), processing data (feed and production rates), and a fuel cycle cost (inventory, make-up processing, etc.). An examination of these data discloses the principal items of cost and suggests changes in specifications which might reduce these. In some cases, the effect of changing an input parameter is not readily predictable; e.g., increasing the concentration of thorium in the fuel stream usually increases the conversion ratio and so reduces the ^{235}U feed requirements but on the other hand increases the fissile inventory. In cases such as this, the input parameters are varied systematically in a "factored" set of calculations yielding the maximum information from a minimum number of cases. The fuel cycle cost is thus optimized with respect to several variables simultaneously. (See Section 6.4.1.)

6.1.2 Reactor Physics Model

The reactor was computed as a homogeneous mixture in equivalent spherical geometry (i.e., the input diameter was 1.09 times the diameter of the cylindrical core). Thus the heterogeneity of the core, which is appreciable, was ignored. But this treatment is conservative in that the resonance escape is underestimated, resulting in a pessimistic estimate of the mean eta of the system. In regard to the estimated captures in thorium, these can always be matched at some neighboring concentration. Aside from a minor effect on the spectrum of neutrons, the chief error introduced is a slight underestimate of the thorium inventory. But this is not important, for the inventory charges contribute only a small portion of the total fuel costs (less than 5%).

The equivalent spherical core comprised three zones; an inner zone consisting of a homogeneous mixture of fuel salt and graphite, a spherical annulus about one inch thick filled with fuel salt, and a spherical reactor vessel one inch thick. The mean, effective temperature of the fuel was assumed to be 1200°F , and this temperature was also assigned to the graphite, which, however, may run two or three hundred degrees warmer.

6.1.3 Cross Section Data

Thorium-232. — Saturation of resonances (self-shielding) was found to be important in five of the neutron energy groups. The effective cross

sections of thorium in these groups were calculated by means of a correlation developed by J. W. Miller (Appendix B) and based on the theoretical analysis of effective resonance integrals made by L. Dresner (29).

Protactinium-233. — A 2200 m/s cross section of 39 barns, as recommended by Eastwood and Werner (30), was assigned. A resonance integral of 900 barns was adopted. This was distributed as shown in Appendix A.

Uranium-233. — A value of 2.29 was adopted for eta at thermal energies, based on the recent measurements of Gwin and Magnuson (43). For energies above thermal, Nestor's estimates (72) were used, as tabulated in Appendix A. Resonance saturation effects were ignored.

Beryllium. — The ($n,2n$) reaction of energetic neutrons in ^9Be was ignored. It is of small importance in this graphite moderated reactor, and is moreover offset by the disadvantageous (n,α) reaction which uses up a neutron and leads to the formation of ^6Li .

Fission Products. — These, excepting xenon and samarium, were handled collectively in the Modric calculation and individually in the ERC calculation, as described below. An "effective" concentration of an "aggregate" fission product was computed from ERC results and used in the multigroup calculation in conjunction with an arbitrary set of group cross sections composed of a hypothetical standard absorber having a thermal cross section of one barn and an epithermal cross section corresponding to a $1/v$ variation above thermal.

Thermal cross sections and resonance integrals for fission products were mostly taken from the compilation of Garrison and Roos (37), supplemented by estimates from Bloemeke (9), Nephew (71), and Pattenden (90). The data used, including fission yields and decay constants, are tabulated in Appendix E.

6.2 Analysis of Thermal and Mechanical System

The analysis included consideration of fluid flow in and mechanical arrangement of the reactor and equipment associated with the extraction of heat from the fuel stream, as they affect fuel cycle costs.

6.2.1 Maximum Fuel Temperature

It is believed that the rate of corrosion of INOR will be very small and that the heat exchangers will have a very long lifetime if the temperature of the fuel solution does not exceed 1300°F (12). The maximum allowable temperature may be higher; if so, future generations of molten-salt reactors will be able to achieve higher specific powers and higher thermal efficiencies.

6.2.2 Minimum Fuel Temperature

For this, 1100°F was selected. Earlier work (3) had shown this to be a reasonable value, and calculations summarized in Table 6.2 confirmed its optimal quality for the MSCR. Perturbations of the affected capital costs were calculated in Table 6.2, and it was concluded that the optimum temperature is very near 1100°F (see also Sec. 3.1.12).

6.2.3 Velocity

Erosion does not appear to be a problem in salt-INOR systems, nor does there appear to be any dependence of the corrosion rate on velocity. Rather, the velocity appears to be limited by considerations of pumping power and stresses induced by pressure gradients. Pressure drop across the heat exchangers is limited by the rapid increase in cost of INOR shells with increasing wall thickness. Likewise, maximum allowable pressure drop across the reactor core is determined by limitations on strength and thickness of the reactor vessel and internal support members. Velocities, pressures, and wall thicknesses at various points in the fuel circuit of the reference design are listed in Table 6.3.

The pumping power required per heat exchanger loop was calculated to be about 1500 horsepower; with a margin of 500 horsepower for pump and motor inefficiencies and unforeseen losses. This pumping power requirement results in a pumping cost (with electric power at 4 mills/kwhr) of 0.004 mills/kwhre.

Table 6.2. MSCR Minimum Fuel Temperature Optimization*

	<u>Case 1</u>	<u>Case 2</u>	<u>Case 3</u>
Minimum fuel temp., °F	1050	1100	1150
Fuel stream temp. rise, °F	250	200	150
Fuel salt flow rate, lb/hr $\times 10^{-6}$	89	111	148
Heat exchanger log-mean temp. difference, °F	144	174	200
Heat exchanger area, ft ²	64,000 (+\$477*)	53,000	46,000 (-\$306)
Heat exchanger pressure drop, psi			
Fuel side	62	80	123
Coolant side	101	84	73
Heat exchanger volume, ft ³			
Fuel side	696 (+\$3,025)	575	504 (-\$1,775)
Coolant side	584 (+\$125)	488	424 (-\$83)
Fuel circuit piping			
Pressure drop, psi	133	150	195
Pipe volume, ft ³	255 (-\$1,625)	320	410 (+\$2,250)
Pipe weight, lbs.	15,400 (-\$31)	18,500	21,300 (+\$28)
Pumps			
Fuel circuit, hp	9,100 (-\$736)	12,800	22,200 (+\$1,872)
Coolant circuit, hp	17,300 (+\$256)	16,000	15,200 (-\$160)
Net capital cost increment \$million	\$+1.49	Reference Condition	\$+1.83

*Capital cost increments with respect to reference condition (1100°F) associated with each item are given in parenthesis in \$thousands. In this calculation, reactor outlet temperature, configuration, heat exchanger cross section, fuel velocity in piping were held constant, as was flow rate of coolant salt and its temperature extremes. The power of the reactor was constant, and the thermal efficiency was not affected.

Table 6.3. Characteristics of Fuel Circuit of 1000-Mwe Molten Salt Converter Reference Design Reactor

Location	Velocity (ft/sec)	Pressure (psia)	Minimum Wall Thickness (inches)
Pump discharge	35	190	0.406
Top of heat exchanger	-	185	-
Heat exchanger tubing	8*	-	0.035
Bottom of heat exchanger	35	95	0.250
Bottom of reactor	-	80	-
Fuel channels in core	4.3 - 7.4	-	-
Top of reactor (Pump suction)	20	22.5	0.312

*Shell-side

6.2.4 Fuel Volume

Contributions to the volume of the fuel system are listed in Table 4.1 for the reference design. The volume of fuel in the external system depends on the power level and various limitations such as those on salt temperature, pressure, velocity, thermal stress in and minimum thickness of heat exchanger tubing, etc. The reference system was designed with considerable conservatism. The fuel volume could be reduced appreciably with an increase in specific power; pumping power costs and capital investment in pumps would increase. Cost of heat exchangers might also increase. The design of the system should be optimized with respect to the sum of all the costs affected; but this lay outside the scope of the present study.

The power density in the external portion of the fuel system of the reference design is approximately $2.8 \text{ Mwt}/\text{ft}^3$. This is very much smaller than the $7.6 \text{ Mwt}/\text{ft}^3$ used in a prior study of a molten salt breeder (3) which was based on a study by Spiewak and Parsly (99), who estimated a specific power of $4.9 \text{ Mwt}/\text{ft}^3$ for a first generation plant and $7.6 \text{ Mwt}/\text{ft}^3$ for subsequent plants.

Since only about one fourth of the total is contributed by the fuel in the active core, the total fuel volume is not very sensitive to changes in fuel volume fraction in the core. The total volume is rather more sensitive to changes in core diameter. The volume of neutron-active fuel increases as the cube of the core diameter (height equal to diameter), while volume in the radial annulus and in top and bottom plenums increases as the square. About 40% of the total volume is affected.

In a fully optimized system, the fuel volume might plausibly be 2000 ft³, and perhaps be as low as 1800 ft³, provided some of the holdup in end-plenums, etc. can be eliminated.

6.3 Analysis of Chemical System

The composition of the fuel stream as a function of its chemical interaction with the reactor environment and with the processing plant is considered. Behavior of xenon-135 is important and is discussed in detail in Section 6.8. Stagnation of fuel in crevices between moderator elements may be important; however, it does not seem possible at this time to evaluate the effect except to say that parasitic captures of neutrons in fission products immobilized in such places will take place. This uncertainty was lumped with that associated with corrosion products as discussed below.

So far as the composition of the fuel stream is concerned, the chemical effects of the two proposed processing methods (Thorex vs fluoride volatility) are the same. The recycled uranium is radioactive and must be handled at least semi-remotely whether the thorium is recycled or not. Both methods result in recycle feed containing only negligible amounts of nuclear poisons (other than isotopes of uranium) and both return ²³³Pa removed from the reactor as ²³³U with losses that depend only on the holding time prior to chemical treatment.

6.3.1 Thorium-232

Thorium may be recycled if Thorex processing is used; however, according to the Guide, the capacity of a multi-purpose processing plant would be

reduced by 40% (52). (One could design the plant to handle the thorium without loss of capacity, however, and recover the thorium at no extra cost.) It turns out that this reduction in capacity almost exactly offsets the value of the thorium saved. With the fluoride volatility processing, thorium is not recovered except by means of an additional step presently not available.

6.3.2 Protactinium-233

With mean residence times of the order of 1000 days, protactinium for the most part decays while still in the circulating fuel system. However, the process stream carries 60-80 grams per day out of the reactor system. In the proposed reference design processing scheme (Section 5.2), the processing stream is accumulated for 120 days and then held as a batch for an additional 30 days, giving a total hold-up time of 150 days and an average decay time of 90 days. At the time of processing, 85% of the ^{233}Pa in the mixed batch will have decayed to ^{233}U , so that the maximum loss of ^{233}Pa will be only 9 to 12 grams per day.

6.3.3 Uranium-233

The loss per pass through the processing plant was assumed to be 0.3%.

In the reference design reactor, the product stream from the process plant was recycled to the reactor; however, the economics of sale of the product stream was also examined.

6.3.4 Uranium-234

Natural uranium is 99.27 weight per cent ^{238}U , 0.72 per cent ^{235}U , and 0.0055 per cent ^{234}U . If there were no enrichment in ^{234}U relative to ^{235}U , a diffusion plant product containing 95 weight per cent ^{235}U would also contain 0.726 per cent ^{234}U , with the balance being ^{238}U . In order to allow for some enrichment, the composition of the feed was taken to be 95 per cent ^{235}U , 1 per cent ^{234}U , and 4 per cent ^{238}U . As with ^{233}U , the processing losses were 0.3 per cent/pass.

Initially the reactor contains little ^{234}U . The approach to equilibrium is slow, and, as seen in Appendix H, the average concentration over

a period of thirty years is only 65 per cent of the equilibrium concentration. The average value, rather than the equilibrium value, was therefore used in the nuclear calculations.

6.3.5 Uranium-235

An enrichment of 95% was selected for the make-up. Losses in processing were assumed to be 0.3% per pass.

6.3.6 Uranium-236

The concentration of this isotope also approaches equilibrium slowly with respect to a fuel lifetime of 30 years. A concentration averaged over the 30-year life was used. Losses in processing were assumed to be 0.3%.

6.3.7 Neptunium-237

This was assumed to be removed completely in the processing plant.

6.3.8 Uranium-238

For reasons given above, the fuel make-up stream was assumed to contain 4% ^{238}U by weight. Losses in the process plant were assumed to be 0.3%. The 30-year average concentration was used in the nuclear calculations instead of the equilibrium concentration.

6.3.9 Neptunium-239 and Plutonium Isotopes

Only small amounts of these will be formed, and they are lost in the waste. Accordingly, their formation in the fuel stream was ignored and no breeding credit was taken for absorptions in ^{238}U .

6.3.10 Salt

The fuel carrier in the reference design consisted of 68 mole per cent LiF, 23 per cent BeF_2 , and 9 per cent ThF_4 . Lithium in the make-up salt was 99.995% ^7Li . Captures in ^7Li , Be, and F were lumped under an equivalent isotope "Carrier-1." The mean reactor concentration of ^6Li and neutron captures therein were computed separately. Lithium and beryllium in the process stream are lost to the waste, and no value was assigned to

the waste. The make-up rate was made equal to the discard rate for ^{7}Li and Be; the ^{6}Li feed rate was proportioned to the ^{7}Li make-up rate.

6.3.11 Xenon-135 and Related Isotopes

In the reference design reactor, it was assumed the graphite has a diffusion coefficient no greater than $10^{-6} \text{ cm}^2/\text{sec}$ ($D = 10^{-5} \text{ cm}^2/\text{sec}$ for MSRE graphite), a porosity no greater than 0.01, and that 10 per cent of the fuel stream is recirculated to the dome of the expansion chamber and the pump bowls. Here Xe is desorbed and swept away in a stream of helium gas with an efficiency of 100 per cent per pass. With these assumptions, the loss in breeding ratio due to absorptions in ^{135}Xe is 0.017 as shown in Appendix G, where the losses corresponding to other assumptions are also given.

6.3.12 Noble Metal Fission Products

It was assumed that this group of isotopes, comprising Mo, Rh, Ru, Pd, and In, "plate out" on INOR surfaces in the fuel circuit with an efficiency of 1.0 per cent per pass.

6.3.13 Other Fission Products

These are removed 100 per cent in the Fluoride Volatility process, and only negligible amounts will be present in the recycle stream from a Thorex plant.

6.3.14 Corrosion Products

Data are meager from which the concentration of corrosion products in the circulating fuel stream could be estimated. In an in-pile loop operated for 15,000 hours, the concentrations of iron, nickel, and chromium appeared to fluctuate about equilibrium values (84, p. 79). On the basis of these data one might expect the fuel to contain 50 ppm of nickel, 500 ppm of chromium, and about 250 ppm of iron. In the reference design reactor., these concentrations would result in a poison fraction (loss in breeding ratio) of 0.006 units. A poison fraction of 0.008 units was arbitrarily assigned to corrosion products in the calculations, making some

allowance for fission products immobilized in cracks and crevices in the moderator, etc.

6.4 Fuel Cycle Optimization

The designer has little control over some of the independent variables that affect the fuel cycle cost. For instance, the maximum allowable fuel temperature is fixed by necessity of limiting corrosion rates. For some variables the fuel cost may decrease monotonically as the variable tends toward an extreme value, but other costs may increase. For example, decreasing the external volume of fuel salt decreases inventory charges but increases pumping costs. A plausible and conservative external volume was selected for the reference design optimization; however, effect on fuel cycle cost of decreasing the external volume is easily estimated.

After the values of such fixed or limiting variables were established, there remained several which required optimization simultaneously with respect to the fuel costs. These variables were designated the "key" variables.

The key independent variables were found to be the diameter (D) of the core, the volume fraction (F) of fuel in the core, the concentration (M) of thorium in the fuel salt, and the processing rate (R). The second and third combine to fix an important subsidiary variable, the C/Th atom ratio (an indication of the degree of moderation of the system). Fixing all four and then satisfying the criticality equation together with the equilibrium isotope equation results in fixing the Th/U ratio, breeding ratio, fuel cost, etc.

Exploratory calculations showed that the fuel cycle cost is a rather sensitive function of the C/Th ratio, but is insensitive to the diameter of the core in the range from 15 to 20 feet. Relative breeding ratios and fuel cycle costs for a series of calculations are shown in Table 6.4.

On the basis of these results, the 20-foot core having a fuel volume fraction of 10 per cent and using a fuel salt containing 9 mole per cent ThF_4 was selected for further study. The optimum processing rate for this

Table 6.4. Conversion Ratios and Fuel Cycle Costs 1000 Mwe
Molten Salt Reference Design Reactor Processing at Rate
of Two Cubic Feet per Day

Case	Core Diam ft.	Vol. Frac. Fuel	Mole % ThF ₄	C/Th	Th/U	Conv. Ratio	FCC m/kwhr
1	15	0.18	13	107	10.6	0.91	1.09
2	17.7	0.18	13	107	12.4	0.96	1.02
3	20	0.18	13	107	13.5	0.99	1.04
4	15	0.10	9	293	21.0	0.84	0.73
5	17.7	0.10	9	293	23.1	0.87	0.69
6*	20	0.10	9	293	24.0	0.90	0.70
7	15	0.107	5	468	20.0	0.68	0.82
8	17.7	0.107	5	468	21.7	0.72	0.78
9	20	0.107	5	468	22.9	0.74	0.77

*Reference case, preferred over Case 5 because of lower power density, lower velocities, etc.

combination of key variables was then determined from results listed in Table 6.5.

The numbers given in Table 6.5 are plotted in Fig. 6.1. The fuel cost has a minimum somewhat below 0.7 mills/kwhre at conversion ratios lying between 0.85 and 0.9. Slight changes in cost assumptions, etc. could shift the location of this minimum over a wide range.

To the left of the cost minimum, loss of neutrons to fission products increases burnup costs more rapidly than processing costs decline; to the right the processing losses outweigh the gain in conversion. The extreme in the conversion ratio results from the fact that processing losses increase linearly with processing rate whereas loss of neutrons to fission products decreases only inversely.

The processing costs used in computing Table 6.5 were those associated with a central Fluoride Volatility Plant (Sec. 5.2) but followed, where applicable, the prescription given in the Guide (52). The "turn-around" time was 2 days for all of the cases listed.

ORNL-DWG. 65-7912

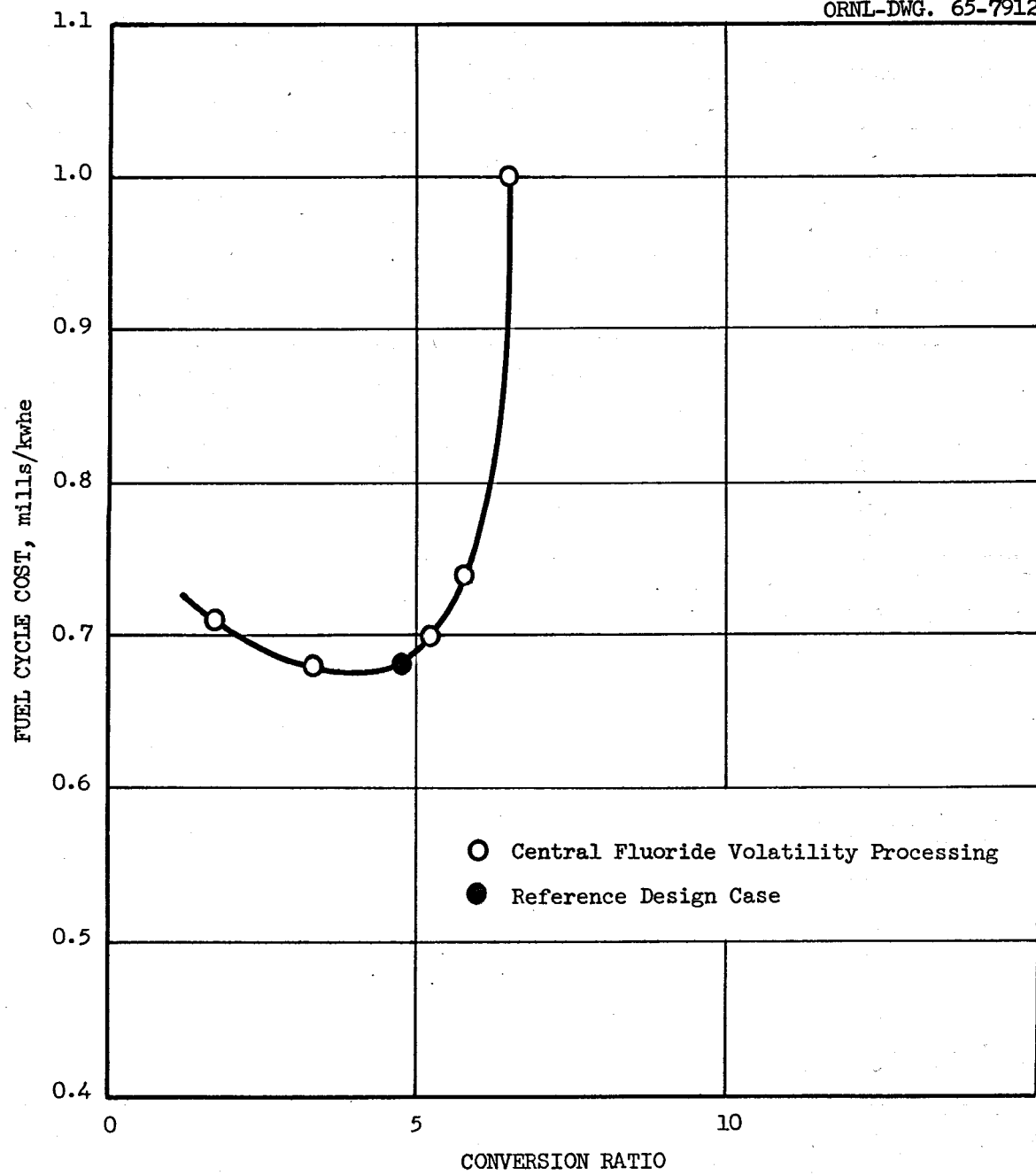


Fig. 6.1. MSCR Fuel Cycle Cost Versus Conversion Ratio.

Table 6.5. Processing Variables

Case	Cycle Time days	Volume Rate ft ³ /day	Weight Rate kg Th/day	Conv. Ratio	Fuel Cycle Cost mills/kwhre
1	3000	0.83	27	0.835	0.71
2	2000	1.25	40	0.868	0.68
3*	1500	1.67	53	0.895	0.68
4	1250	2.00	64	0.904	0.70
5	1000	2.50	80	0.917	0.74
6	500	5.0	160	0.930	1.01
7	250	10.0	320	0.908	1.64

*Reference Design Case

6.5 Reference Design Reactor

The MSCR is capable of producing power at a fuel cycle cost, including salt charges, of 0.7 mills/kwhre at a conversion ratio of 0.9.

The most important uncertainties in this calculation arise in connection with (a) the behavior of xenon in the core, (b) costs estimated for the Fluoride Volatility processing plant, (c) validity of the base charges assigned to the materials and (d) cost of packaging the spent fuel for shipment. The influence of xenon behavior is examined in Sec. 6.6, and the cost assumptions in Sec. 6.7. If the losses to xenon assumed for the reference design case are attainable (and it should be possible to achieve the assumed performance by improving the graphite and the sparging process), then all the uncertainty resides in the processing cost. Since processing costs are only about 0.08 mills/kwhre (Table 6.10), even a large error would not significantly influence the total fuel cycle cost.

Uncertainties in regard to technical feasibility arise in connection with compatibility and stability of the graphite moderator (Sec. 4.2.2), of the reactor vessel and its internal structure (Sec. 4.2.2). Also, the hazards associated with the proposed methods of control (Sec. 4.2.3) have not been evaluated.

6.5.1 Specifications

Case 3 was selected for the reference design before the complete curve was generated; its fuel cost is not significantly greater than the minimum. The reactor characteristics and operating data for the reference design are given in Section 4, nuclear data in Table 6.6.

Table 6.6. Nuclear Characteristics of 1000 Mwe
Molten Salt Converter Reactor

Case No.	3
Carbon/thorium atom ratio	~300
Thorium/fissile uranium atom ratio	~27
Fraction of fissions in thermal neutron group	0.82
Fraction of fissions in ^{235}U	0.15
Fraction of fissions in ^{233}U	0.85
Ratio of total fissions to fissions in ^{233}U and ^{235}U	1.0018
Mean eta of ^{233}U	2.253
Mean eta of ^{235}U	1.979
Mean eta of all fissions*	2.219
Effective resonance integral of ^{232}Th	66 barns
Thermal cross section of ^{233}Pa	39 barns
Effective resonance integral of ^{233}Pa	900 barns
Average power density in core	14.1 kw/liter
Ratio peak-to-radial average power density	2.1
Maximum graphite exposure rate, nvt/yr	
Neutron energy >0.1 Mev	5.0×10^{21}
Neutron energy >1.0 Mev	1.8×10^{21}
Average thermal flux	3.7×10^{13}
Average fast flux	4.2×10^{13}
Fissions per ^{235}U atom added	9.2
Fissions per fissile atom processed	1.5
Exposure, Mwd/tonne of thorium	47,000
Specific power, Mwt/kg fissile	0.9

*Neutrons produced from all sources per absorption in ^{233}U and ^{235}U .

6.5.2 Neutron Economy

From Table 6.7, it is seen that fissions in ^{232}Th contribute very little to neutron production. The fast fission cross sections of thorium are appreciably less than those of ^{238}U ; moreover, the fast flux in the MSCR is not particularly high (Table 6.6). Also, the thorium is rather dilute compared to concentrations customarily proposed for blankets.

The nuclear loss resulting from absorptions in Pa is appreciable but not serious. It could be reduced by reducing further the volume fraction of fuel in the core, but this is already about as low (0.1) as seems technically feasible; a further decrease would probably add more to the fuel cost in terms of increased inventory charges (since concentration of thorium and uranium in the fuel stream would increase, while the external volume would remain the same) than would be saved in terms of fuel replacement costs. Increasing the external volume in order to dilute the Pa would not be economical for the same reason.

The nuclear loss to Pa could be reduced by removing the Pa rapidly from the circulating stream and holding it until it decays to ^{233}U . In order to be effective, such a process would have to treat the entire fuel stream for Pa removal in a period not greater than ten days (mean life of Pa is about 40 days). Thus an extremely simple and efficient process is required, as for example, the passage of the fuel stream through beds where Pa is selectively absorbed and retained until ^{233}U is formed, which then desorbs in the presence of large amounts of uranium in solution. No such process is presently known, although some work has been reported (19 p. 117, 74) on the precipitation of protactinium oxide from molten salt solutions containing up to 2000 ppm of uranium by contacting the melt with BeO , ThO_2 , or UO_2 . Development of such a process might reduce the losses to Pa appreciably and add ~0.01 units to the conversion ratio.

For reasons indicated in Sec. 6.1, the concentration of ^{234}U used in the equilibrium calculation was averaged over a period of 30 years. Although the reactor was assumed to be initially fueled with enriched uranium containing 1.0% ^{234}U and to be supplied with make-up fuel of the same composition, ninety-nine per cent of the ^{234}U is formed by transmutation of ^{233}U . It disappears from the reactor by transmutation to ^{235}U and loss in

Table 6.7. Neutron Economy^a in the 1000 Mwe Molten Salt Converter Reference Design Reactor

Item	Captures	Fissions	Absorptions
^{232}Th	0.8535	0.0011	0.8546
^{233}Pa	0.0084	0.0000	0.0084
$^{233}\text{U}^{\text{c}}$	0.0888	0.7488	0.8376
^{234}U	0.0572	0.0002	0.0574
^{235}U	0.0301	0.1323	0.1624
^{236}U	0.0184	0.0001	0.0185
^{237}Np	0.0074	--	0.0074
^{238}U	0.0029	0.0000	0.0029
Carrier salt	0.0387	--	0.0387
Graphite	0.0564	--	0.0564
^{135}Xe	0.0170 ^c	--	0.0170 ^c
Other fission products	0.0867	--	0.0867
Corrosion products	0.0082	--	0.0082
Delayed neutrons	0.0046	--	0.0046
Leakage	0.0513	--	0.0513
Neutron yield ^a			2.2121
Processing losses ^b			0.005
Net conversion ratio ^d			0.90

^aNeutrons per neutron absorbed in ^{233}U and ^{235}U .

^bProcessing loss of 0.3%/pass for ^{233}U and ^{235}U , and undecayed ^{233}Pa .

^cLoss corresponding to graphite having gas porosity of 1% and diffusion coefficient of 10^{-6} compared to current graphite properties of 10% and 10^{-5} .

^dExcluding captures in ^{238}U and correcting for fissions of thorium.

the processing cycle (0.3% per pass). Since ^{235}U is inferior with respect to ^{233}U as a nuclear fuel, it is advantageous to keep the concentration of ^{234}U as low as possible. However, the designer has little control over this, inasmuch as the only means of removing it is to sell spent fuel to the AEC, and this, as shown in Sec. 6.8.3, is not advantageous.

The concentration of ^{236}U used was also averaged over a period of thirty years, starting with a clean reactor containing no ^{236}U . In this case, the only source is capture of neutrons in ^{235}U ; the sinks are transmutation to ^{237}U (which decays promptly to ^{237}Np) and losses (0.3% per pass) in the processing cycle. The only effective control the designer has over ^{236}U is by varying the conversion ratio thus varying the amount of ^{235}U fed to the system, and by sale of spent fuel.

It is assumed that ^{237}Np was removed 100 per cent per pass through the processing cycle. Parasitic captures are appreciable (0.0074 units on the conversion ratio); however, special processing for this reason does not appear to be worthwhile, although it might be for other reasons.

Parasitic captures in carrier salt resulted in a conversion loss of 0.039 units. Of this, captures in ^6Li contributed 0.014 units. The grade of salt used (99.995% ^7Li) appears to be about the best available at attractive prices. On the other hand, use of inferior grades would not result in lower fuel costs.

The best way to control losses to ^6Li is to recycle carrier salt from processing instead of discarding it as was assumed in the reference design. The possibilities are examined in Sec. 6.8, where it is shown that about 0.01 units might plausibly be saved on the conversion ratio, and about 0.08 mills in replacement costs.

The fuel cost was optimized with respect to parasitic captures in moderator and neutron leakage simultaneously as described in Sec. 6.4. Losses to graphite might be decreased by decreasing the C/Th ratio, but the gain would be more than offset by losses in eta of ^{233}U and increased leakage. Leakage decreases slowly with increasing diameter, but fuel cost is insensitive, as shown in Table 6.4. Efforts to reduce the leakage by use of a graphite reflector were not successful (Appendix M), largely because of the necessary presence of a fuel annulus at least one inch thick.

at the periphery of the core as a result of tolerance allowance for differential thermal expansion.

The estimate of the loss of neutrons to xenon (0.017 units on C.R.) was based on an assumed diffusion coefficient of 10^{-6} cm²/sec., a porosity accessible to gas of 1.0 per cent, and a sparging rate of 10 per cent (16 ft³/sec) of the circulating fuel stream with 100 per cent removal of xenon per pass (Sec. 6.8.2). The prospects are good for the development of grades of graphite that would reduce the losses to xenon in the MSCR to no more than 0.005 units on the conversion ratio.

Captures in samarium (¹⁴⁹Sm and ¹⁵¹Sm) result in a loss of 0.013 units in conversion ratio. This loss is independent of the processing rate except at very short cycle times of the order of days. Thus, there is not much prospect of reducing this loss except by the application of some simple, rapid process similar to that suggested for ²³³Pa above.

Captures in other fission products can be controlled by varying the processing rate. The savings from greater fuel conversion must be balanced against increased processing cost. For the particular price structure and nuclear properties assumed, the optimum rate of processing is ~1.7 ft³/day (53 kg of Th/day). The corresponding loss in conversion ratio due to captures in other fission products is 0.074 units. In this calculation, it was assumed that xenon is sparged as described above, noble metals are reduced by chromium in metal structures to the zero valence state and "plated out," and all other fission products are removed by passage through the processing cycle which, at the costs estimated in Sec. 5.1, optimized at a cycle time of ~1500 days.

If the processing cost schedule (Sec. 3.2 and 5.1) were to change in the direction of lower costs, the optimum processing rate would increase, and the fission product captures could be decreased. Although improvements and economies in the Fluoride Volatility process are to be expected, the remote operations and maintenance costs of this process are likely to remain high; therefore the process eventually used should be as simple as possible. The solution may lie in the direction of distillation or fractional crystallization (80, p. 80), or perhaps extraction with liquid metals.

The estimated loss in conversion ratio to corrosion products was 0.006 units; a loss of 0.008 units was allowed in the calculations (Sec. 6.3). Since the concentration of corrosion products (Fe, Ni, and Cr) in the melt appears to reach an equilibrium in times that are short compared to the processing cycle time, it seems unlikely that the processing will have much influence on the concentrations of corrosion products, and the associated loss of neutrons seems unavoidable.

6.5.3 Inventories and Processing Rates

It may be inferred from Table 6.8, Column 1, that the specific power of the MSCR is 0.35 Mwe/kg fissile, which is comparable with many of the advanced systems currently being put forward. The exposure (about 40,000 Mwdt/tonne of thorium) is of the same order as that of "competitive" reactors.

Table 6.8. Inventories of Nuclear Materials - 1000 Mwe Molten Salt Converter Reference Design Reactor

Material	Inventories, kg		
	Reactor Plant	Processing	Total
232Th	80,000	6500	86,500
233Pa	95.5	7.8	103
233U	2110	172	2,282
234U	484	39.6	524
235U	420	45*	465
236U	682	56	738
237Np	49	5	54
238U	109	11	120
Salt	109,000	8,900	117,900
Fission products	4,400	360	4,760
Corrosion products	82	7	89

*Including 10.6 kg in reserve to keep reactor in operation for 30 days after unscheduled interruption of recycle from processing plant.

The processing rates given in Table 6.9 are the amounts removed daily from the circulating fuel stream. These daily increments are accumulated for 116 days to form a processing batch. The average fission product activity in the material as processed corresponds to an effective holding time of about 90 days (based on the Way-Wigner correlation as reported in reference 55, p. 81). Thus, a process batch contains 6500 kg of thorium; this is processed at the rate of 1000 kg/day for uranium recovery, taking ~7 days to process and two days for "turn-around."

Table 6.9. Process and Make-up Rates - 1000 Mwe
Molten Salt Converter Reference Design Reactor

Material	Rate, kg/day	
	To Processing	Make-up
^{232}Th	53.3	3.56
^{233}Pa	0.064	
^{233}U	1.400	
^{234}U	0.322	0.003
^{235}U	0.280	0.324
^{236}U	0.463	
^{237}Np	0.033	
^{238}U	0.073	
Salt	72.7	72.7
Fission products	2.94	
Corrosion products	0.055	

6.5.4 Fuel Cycle Cost

The fuel cycle cost for the reference design reactor, which is near optimum on the bases chosen, comes to 0.68 mills/kwhre. A breakdown is given in Table 6.10.

Inventory of fissile materials costs about 1/4 mills/kwhre, when optimized with respect to the processing rate. It could possibly be reduced at a given processing rate by improving the graphite to reduce xenon poisoning and by reducing the volume of fuel in the external heat transfer circuit at the expense of greater pumping power costs.

Table 6.10. Fuel Cycle Cost - 1000 Mwe Molten Salt Converter
Reference Design Reactor with Salt Discard

Material	Charges,* mills/kwhre			
	Inventory	Replacement	Processing	Total
^{232}Th	0.03	0.04		
^{233}Pa	0.01			
^{233}U	0.18			
^{235}U	0.04	0.16	{ 0.08 }	
Total	0.26	0.20	0.08	0.54
Salt costs	0.06	0.08		0.14
Total charges				0.68

*Cost bases are given in Sec. 3

Replacement costs for fissile material are most sensitive to conversion ratio. Increasing this from 0.90, as in the reference design reactor, to 0.95 would cut the cost in half. The increase in conversion ratio might be achieved by means discussed in Sec. 6.7.3.

The inventory charge for salt is strictly a function of the fuel salt volume. The replacement cost depends on the processing rate, and was optimized. A major improvement here would consist of adding equipment in the processing plant for recovering lithium and beryllium.

The fuel cycle cost of 0.68 mills/kwhre estimated for the MSCR is conservatively based on the scale-up of proven technology (including the processing) with the following minor exceptions:

1. Technology of reactor vessel design.
2. Graphite technology.
3. Xenon sparging technology

These, however, are considered within the reach of current technology, i.e., no developmental break-throughs are required.

Although difficult problems in gamma heating may be encountered in the design of the reactor vessel and its internal members, it appears that these can be solved. The problem in relation to graphite is to produce

pieces of the size required that are chemically compatible with fuel salt and have porosity and permeability suitably low with respect to xenon absorption (Sec. 6.8.2).

6.6 Parameter Studies

In this section, the effect on the fuel cycle cost of various assumptions concerning the processing cost, and of several modes of processing are considered.

6.6.1 Processing Cost as Parameter

The fuel cycle cost reported in Sec. 6.7 (Table 6.10) was based on the assumed use of a central Fluoride Volatility facility requiring approximately \$20 million in capital investment and having an annual operating expense of \$2 million (Table 5.7). In Sec. 5.4, this estimate was compared with other current estimates for similar plants and for Thorex plants of comparable capacity. In this section, the processing plant capital investment and the operating cost are considered as parameters, without regard to the kind of plant. The effect on the fuel cycle cost of the MSCR at various processing rates of varying processing costs for a plant having a nominal capacity of 1000 kg Th/day ($30 \text{ ft}^3/\text{day}$ of reference design salt) was calculated. In all cases, the output of the reactor was accumulated until a processing batch of about 6000 kg of Th was collected; this was then shipped to the processing plant and processed at a rate of 1000 kg Th/day. The turn-around time was assumed to be 2 days.

The results of the calculation are presented in Fig. 6.2. The curves corresponding to daily charges of \$20,000 to \$60,000. It is seen that, in the conversion ratio range from 0.8 to 0.9, the fuel cycle cost is not very sensitive to the processing cost; in the reference design, the fuel cycle cost does not exceed 0.85 mills/kwhre at a daily charge of \$40 thousand, and only slightly exceeds 1.0 mills/kwhre for a charge of \$60 thousand. At \$40 thousand, the minimum fuel cycle cost is less than 0.8 mills/kwhre at a conversion ratio of about 0.85, and the cost remains below 1.0 mills/kwhre for conversion ratios up to about 0.92.

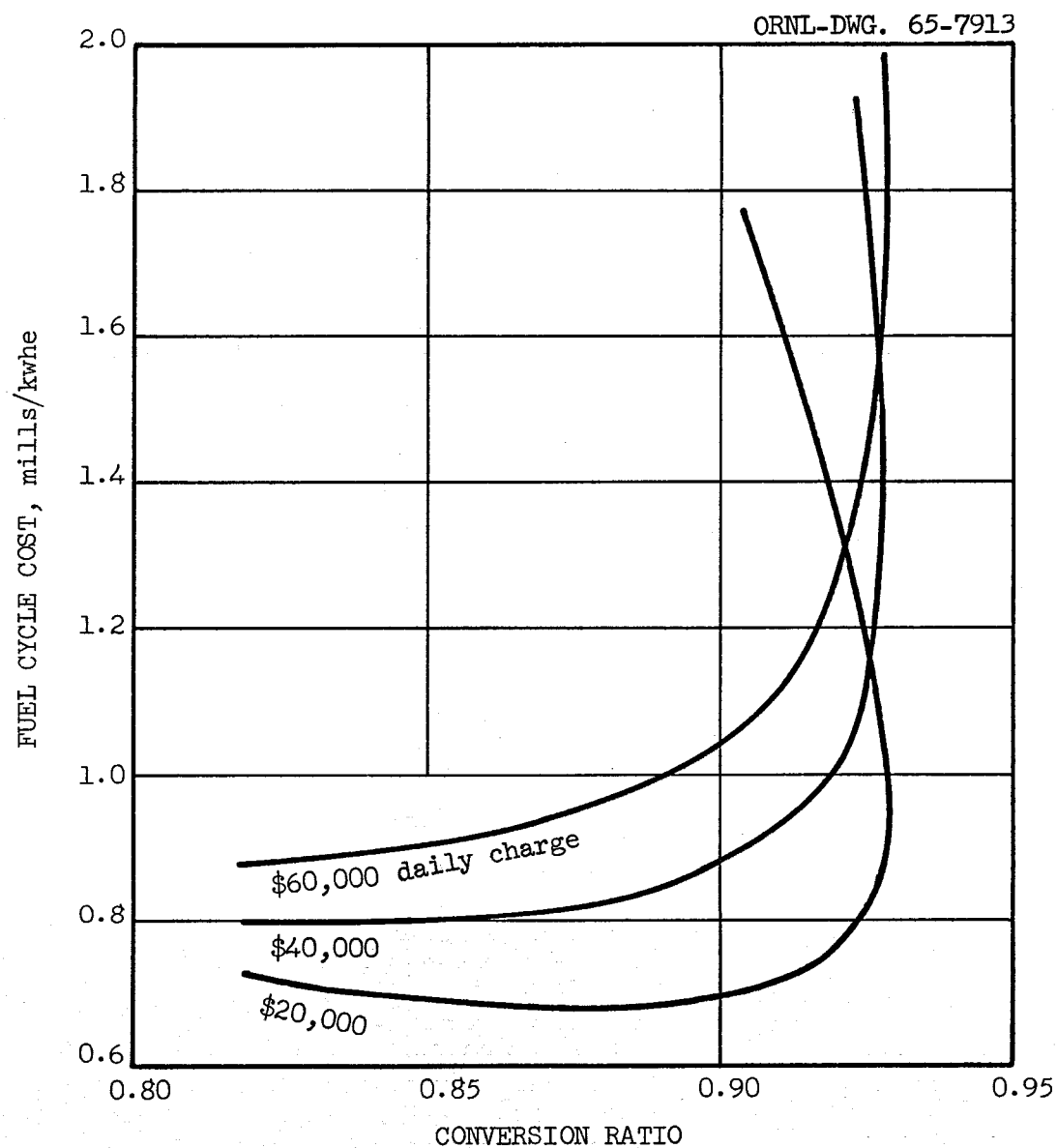


Fig. 6.2. MSCR Processing Cost Versus Conversion Ratio.

It was concluded that, on any reasonable cost basis, the optimum fuel cycle cost for the MSCR will not exceed 0.8 mills/kwhre, and that conversion ratios up to 0.92 can be obtained at fuel cycle costs not exceeding 1.0 mills/kwhre.

6.6.2 Effect of Xenon Removal

The solubility of xenon in LiF-BeF₂ is very low (107); in the reference design reactor the equilibrium pressure is about 0.06 atmospheres. Xenon thus tends to leave the salt at any phase boundary. It can be removed rapidly by spraying a portion of the circulating stream into a space filled with helium or by subsurface sparging. It may form microbubbles clinging to the surface of the graphite moderator, and it will tend to diffuse into pores in the graphite, including pores inaccessible to the salt. Xenon is also removed from the system by decay to ¹³⁵Cs and by reaction with neutrons to form ¹³⁶Xe, which is stable and has a low neutron capture cross section.

Xenon poisoning in the MSCR was calculated by the method of Watson and Evans (107), as shown in Appendix G. The important physical properties are the porosity, e , of the graphite (fraction of graphite volume accessible to xenon) and the diffusivity of xenon, D (cm^2/sec). The key variables are the diameter of the graphite logs, the fuel circulation rate, and the sparging fraction, r , (fraction of circulating stream sparged or sprayed to remove xenon). In the reference design, the logs are six inches in diameter, and the circulation rate is $160 \text{ ft}^3/\text{sec}$.

In the reference design reactor, a gas-accessible porosity of 0.01 and a diffusion coefficient of 10^{-6} with a sparging fraction of 0.1 ($16 \text{ ft}^3/\text{sec}$), would result in a tolerable xenon poison fraction of 0.017 neutrons per neutron absorbed by fissile atoms. These physical property values are an order of magnitude smaller than those of currently available graphite where $e = 0.1$ and $D = 10^{-5}$; however, the assumed values are both presently attainable in small pieces of graphite (107) and the control of xenon poisoning in the MSCR appears to lie within the reach of developing technology.

The conversion ratio increases and the fuel cycle cost decreases with decreasing xenon poisoning. Table 6.11 compares the calculated results for

Table 6.11. Effect of Graphite Properties and Sparge Rate
on Performance of 1000 Mwe Molten Salt Converter Reactor

Case	Xe P.F.	Conversion Ratio	Fuel Cycle Cost mills/kwhre
a	0.054	0.84	0.79
b	0.045	(0.86)*	(0.77)*
c	0.017	0.90	0.68
d	0.001	0.92	0.66

*Interpolated

three cases: (a) "Worst" case, with a very porous graphite (say AGOT) and with no sparging; (b) available graphite with $eD = 10^{-6}$ and $r = 0.1$; (c) Reference Design Reactor with $eD = 10^{-8}$ and $r = 0.1$; (d) "impermeable" graphite with $eD = 0$ and $r = 0.1$.

It is seen that while available graphite (Case b) is not significantly better than the "worst" graphite (Case a), nevertheless, the fuel cycle cost is only 0.1 mill/kwhre higher than for "impermeable" graphite (Case d). It is concluded that the fuel cost is not very sensitive to xenon poisoning, that it will be less than 0.8 mills/kwhre, with available graphite, and that with modest improvements over available graphite (to e of 0.01 and D of 10^{-6}), the fuel cost will be not more than 0.7 mills/kwhre.

6.6.3 Effect of Product Sale Without Recycle

At least two benefits accrue from the sale of recovered fissile isotopes (as UF_6) to the AEC: (a) Make-up fuel (^{235}U) would then be non-radioactive and could be compounded with fresh salt in a directly maintained and operated facility; (b) the reactor would tend to be purged of ^{236}U . The second benefit is really illusory, inasmuch as the ^{236}U produced will eventually capture a neutron in some reactor somewhere, and therefore reduces the value of the recovered isotopes by an appropriate amount.

On the other hand, a penalty is incurred in that ^{233}U , a superior fuel in thermal reactors, is also lost from the system. As seen in Table 6.12, the penalties outweigh the advantages considerably.

Table 6.12. Effect of Sale of Spent Fuel on MSCR Performance

Case	A	B
Spent fuel is . . .	Recycled	Sold
Absorptions in ^{236}U	0.0185	0.0105
Mean Eta	2.21	2.11
Conversion Ratio	0.90	0.82
Fuel Cycle Cost, mills/kwhre		
Inventory Charges	0.32	0.36
Replacement Charges	0.28	1.38
Processing Charges	0.08	0.08
Production Credit	--	0.53
Net Fuel Cost, mills/kwhre	0.68	1.29

6.7 Alternative Design and Cost Bases

6.7.1 Thorex Processing Cost Estimates

The preferred method of processing MSCR fuel is by fluorination (Sec. 5.2), mainly because the processing can conveniently be integrated with the reactor and thus achieve very low fuel cycle costs. However, for one reason or another, it may be desirable to process the spent fuel from the first MSCR installations in a central Thorex facility. Accordingly, the facility specified in the Guide to Nuclear Power Cost Evaluation (52, 104) was modified appropriately as described in Sec. 5.3 to handle MSCR fuel. An allowance of \$500,000 additional capital cost for the head-end treatment was made. Costs were calculated on the bases given in the Guide. The turn-around time was eight days and the shipping charge was \$17/kg for round trip. The assumed loss of fissile material was 1.3 per cent/pass.

The fuel cycle costs for the reference design reactor (Tables 6.6 through 6.10) were recomputed using a cost schedule estimated from the Guide (52), as shown in Table 6.13, where they are compared to corresponding results for central Fluoride Volatility processing (Sec. 5.2).

Table 6.13. Effect of Processing Method
on Fuel Cycle Cost

	Central Thorex	Central Fluoride Volatility
Processing cost, \$/kg Th	75.2	44.8
Processing losses, per cent/pass	1.3	0.3
Conversion Ratio	0.89	0.90
Fuel cycle cost, mills/kwh		
Inventory charges	0.33	0.32
Replacement charges	0.24	0.28
Processing charges	0.17	0.08
Total, mills/kwh	0.74	0.68

Thus, even though processed through the AEC reference plant, the costs of which appear to be conservatively high, the fuel cycle cost for the reference design MSCR will not exceed 0.75 mills/kwh.

6.7.2 Reactor-Integrated Fluoride Volatility Processing

Several advantages can be realized by integrating the processing with reactor operations. The principal saving results from sharing reactor shielding and remote maintenance equipment. Savings in laboratory facilities and personnel are also important. Shipping costs and associated receiving facilities are eliminated.

A 30 ft³/day central fluoride volatility plant requires a capital outlay of about \$25 million and would need to service fifteen to twenty 1000 Mwe MSCR's in order to achieve the unit processing costs estimated in Section 5.2. An integrated plant requires a much smaller investment and the unit processing cost will be, of course, independent of the number of reactors in use.

An integrated facility should be designed for continuous flow processing, at least in the fluorinator and the UF₆ reduction reactor, in order that the equipment and the volume of fuel-salt held up might both be small.

6.7.3 Reactor-Integrated Precipitation Process

At a processing rate of 1.7 ft³/day, the concentration of rare earth fluorides in the fuel salt will be approximately 0.5 mole per cent, which is perhaps slightly in excess of the solubility limit at the minimum fuel temperature of 1100°F. This suggests that it may be possible to remove rare earths fission products from the MSCR fuel stream by fractional crystallization — an extremely attractive possibility, for such a process could conveniently be carried out in the reactor cell and closely integrated with the reactor system. The steps involved are exceedingly simple, involving only the transfer of liquids and heat, and is therefore inherently safe and economical.

The fission product neutron poisoning estimated for the reference design can be approximately matched by charging every day five cubic feet of fuel salt containing 0.5 mole per cent rare earth thorides to a crystallizer. The salt is cooled to 900°F, which is 13°F above the temperature at which solid solutions containing Th or U separate. At this temperature, the solubility of the rare earth fluorides is 0.2 mole per cent or less, judging from the data of Ward et al., (108, 106). Thus about 60 per cent of the rare earths will precipitate or "freeze" on the walls of the crystallizer. The total mass of the solids will be only 6-8 kg. After the fuel salt is returned to the reactor system, the fission products are dissolved in flush salt

The process described should effectively remove rare earths from the fuel salt. It will not remove alkali metals, alkaline earths, and miscellaneous other metals. These will accumulate in the fuel, but their ingrowth can be partially compensated by operating the freeze-process at a slightly more rapid rate and maintaining the rare earth concentration at say 0.45 mole per cent or by discarding barren fuel-salt in a 1500 day cycle.

6.8 Evolution of a Self-Sustaining MSCR

Although the MSCR concept may not have the capability of evolving into a breeder reactor (see Sec. 7.1) having a doubling time less than 25 years,

the possibility exists, however, that it could, without increase in power costs, achieve a net conversion ratio slightly greater than unity, and thus become self-sustaining and independent of outside supplies of fissile isotopes. Conditions under which this might be achieved are listed and discussed below.

6.8.1 Reduction of Leakage

With the advent of separated ^{92}Mo , it becomes feasible to surround the core of the MSCR with a thin blanket of high-density thorium salt (25% ThF_4 , 75% LiF). This salt, having a liquidus temperature below 1100°F , could be circulated slowly through 6-inch diameter molybdenum tubes replacing the outer two layers of graphite moderator logs, and replacing 1-ft end sections of the central logs. The isotope ^{92}Mo is a magic nuclide, having a 2200 m/s cross section of 6 millibarns. The epithermal cross section is currently being measured at ORNL, and preliminary results indicate that the resonance integral is also very small. Thus, structural molybdenum should capture only a negligible fraction of neutrons.

It would be necessary to remove the bred ^{233}U rapidly from the fertile stream for two reasons: (a) fissions in the fertile stream would tend to increase the leakage, (b) fission products in the fertile stream would capture neutrons. If the fertile stream were processed rapidly by fluorination, the concentration of ^{233}U could be kept very low, fissions would be suppressed, the inventory charge for ^{233}U would be largely avoided. The fertile stream carrier salt could be recycled without further treatment. The rapidity of the processing, however, implies the use of an on-site, reactor-integrated facility such as that described in Sec. 6.9.2.

By this means perhaps half the leakage neutrons could be saved, adding about 0.025 units to the conversion ratio.

6.8.2 Reduction of Xenon Captures

In the reference design, graphite properties an order of magnitude better than those characteristic of current graphites were assumed, resulting in a loss in conversion ratio due to captures in ^{135}Xe absorbed in the graphite of only 0.017 units. By further improvements (e.g., by spraying a thin coating of ^{92}Mo on the moderator logs and carburizing to prevent xenon

from penetrating the moderator) perhaps another 0.01 units on the conversion ratio could be saved.

6.8.3 Reduction of Fission Product Poisoning

Somewhat over 0.085 units were lost from the conversion ratio as a result of captures in fission products in the reference design (Table 6.7). The processing cost in a central Fluoride Volatility facility was about 0.08 mills/kwhr. If an on-site, reactor-integrated Fluoride Volatility and HF-Solution facility were used (Sec. 2.2.14), the rate of removal of rare earths could be increased perhaps by a factor of 10. Solubles (Cs, Ba, etc.) could be purged by discarding salt in a 1500 day cycle, as in the reference design. If this were done, the loss of conversion ratio to fission products could be reduced to about 0.010 units.

6.8.4 Improvement of Mean Eta and Reduction of ^{236}U Captures

Other than by varying the C/Th ratio, the designer has no direct control over these. Nevertheless, the above improvements in neutron economy have an effect on the conversion ratio that is greater than their cumulative sum, for ^{233}U is superior to ^{235}U in respect to neutron production, and moreover yields a fertile isotope (^{234}U) upon capture of a neutron. An increase in relative concentration of ^{233}U by any means increases the number of neutrons available for breeding, and reduction of ^{235}U feed rate results in a decrease in ^{236}U concentration.

The above listed improvements should result in an increase in eta of 0.01 units and a reduction of captures in ^{236}U by 0.01 units, at least.

6.8.5 Ultimate Breeding Potential of MSCR

The conversion ratio in the reference design is about 0.90. With the improvements listed above, conversions slightly in excess of 1.0 may be achieved, as shown in Table 6.14.

Thus, the MSCR may be capable of evolving stepwise into an economical, self-sustaining breeder reactor with fuel cycle costs probably in the range of 0.7 - 1.0 mills/kwhre.

It should be emphasized that the limiting conversion ratio estimated for the MSCR does not apply to molten salt breeder reactors. It has been

Table 6.14. Ultimate Breeding Potential of Molten Salt Converter Concept

Conversion ratio in reference design	0.90
Savings due to:	
Reduction in leakage	0.025
Reduction in xenon captures	0.010
Reduction of fission product captures	0.075
Improvement in eta and reduction of captures in ^{236}U	0.020
Ultimate conversion ratio	1.03

shown (3) that two-region, two-fluid, thermal reactors optimized with respect to breeding are capable of achieving doubling times of 25 years or less. (See also Sec. 1.7.) In addition, the advent of structural ^{92}Mo makes possible, in principle, the design of two-region, two-fluid, fast molten-salt reactors which may have doubling times as short as ten years, which will not need to use separated ^6Li in the carrier salt, and which therefore may be processed economically by fluorination only.

7. MSCR CAPITAL INVESTMENT, FIXED CHARGES, AND OPERATING EXPENSE

7.1 Introduction

The equipment, auxiliaries, and auxiliary services described in Sec. 4 were costed for ORNL by Sargent and Lundy Engineers of Chicago, Illinois (95, 96). Equipment arrangement drawings sufficient for piping take-offs and building cost estimates were made. Details of these studies are given in the referenced reports.

7.2 Summary of MSCR Capital Investment

In Table 7.1 are listed the principal items of cost in the MSCR reference design. A detailed breakdown is given in Appendix N. The account numbers correspond, where applicable, to the AEC systems of accounts given in The Guide to Nuclear Power Cost Evaluation (52).

Table 7.1. 1000 Mwe Molten Salt Converter
Reactor Capital Investment

Fission energy release rate, Mwt	2500 Mwt
Net station power	1038 Mwe
Gross station power	1083 Mwe
Station efficiency	41.5%
Heat rate	8220 Btu/kwhr
Plant factor	0.8
Total capital investment	\$143/kwe

Direct Construction Costs

21 Structures and Improvements

211 Improvements to site	\$ 501,500
212 Buildings	5,465,450
218 Stacks	31,000
Reactor Container	(Included in 212)
Total Account 21	(5,997,950)

Table 7.1. Continued

22	Reactor Plant	
221	Reactor equipment	\$ 8,823,300
222	Heat transfer system	23,609,700
223	Fuel fabrication and handling system	1,517,200
224	Fuel processing system waste disposal	(Not included)
225	Low-level radioactive waste disposal	361,150
226	Instrumentation and controls	1,100,000
227	Feed water supply	4,939,500
228	Steam, condensate, and water piping	7,925,000
229	Other reactor equipment	3,048,500
	Total Account 22	(51,324,350)
23	Energy Conversion System	
231	Turbo-generator unit	21,495,000
232	Circulating water system	1,644,200
233	Condensers and auxiliaries	3,104,900
234	Central lubrication system	36,000
235	Turbine plant instruments & controls	426,000
236	Turbine plant piping	(Included in 228)
237	Auxiliary equipment for generators	137,000
238	Other equipment	(Included in 228)
	Total Account 23	26,843,700
24	Accessory Electrical Equipment	
241	Switchgear	637,400
242	Switchboards	286,000
243	Protection equipment	131,600
244	Electrical structures	213,200
245	Conduit	210,200
246	Power and control wiring	2,281,900
247	Station service equipment	615,000
	Total Account 24	4,375,300
25	Miscellaneous Plant Equipment	
251	Cranes and hoists	195,000
252	Air compressors and vacuum pumps	64,900
253	Other	540,000
	Total Account 25	799,900
	Total Direct Construction Cost	89,341,200
	<u>Indirect Construction Costs</u>	
	Construction overhead (20% of direct labor)	2,333,300
	General and administration (2.5% of direct costs)	5,775,500
	Subtotal	(97,450,000)

Table 7.1. Continued

Miscellaneous costs (1.2% of subtotal)	\$ 974,500
Subtotal	(98,424,500)
Engineering Design and Inspection	
Architect-engineers (11.1% of subtotal)	10,925,000
Subtotal	(109,349,500)
Nuclear engineers (3.8% of subtotal)	4,155,300
Start-up expense (35% annual O&M expense)	746,900
Land and land rights	360,000
Subtotal	(114,611,700)
Contingency (10% of subtotal)	11,461,200
Subtotal	(126,072,900)
Interest during construction (9.4% of subtotal)	11,850,900
Total Indirect Construction Costs	48,582,600
<u>Total Construction Costs</u>	137,923,800
<u>Intermediate Coolant-Salt Inventory*</u>	10,951,800
<u>TOTAL MSCR CAPITAL INVESTMENT</u>	\$ 148,875,600

*Including interest during startup

7.3 MSCR Fixed Charges

The fixed charges were computed in accordance with the instructions in The Guide to Nuclear Power Cost Evaluation, Vol. 5, Production Costs, page 510-2 (52), for an investor-owned public utility, and are shown in Tables 7.2 and 7.3.

Table 7.2. Nation-Wide Approximated Fixed Charge Rates

	Percent Per Year	
	Depreciating	Non-Depreciating
Profit on investment	6.75	6.75
Depreciation (30-yr sinking fund)	1.11	--
Interim replacements	0.35	--
Property insurance	0.40	0.40
Federal income taxes	3.40	3.40
State and local taxes	2.45	2.45
Total	14.46	13.00

Table 7.3. 1000 Mwe Molten Salt Converter
Reactor Fixed Charges

Item	Investment	Rate %/yr	Annual Expense \$/yr	Power Cost Mills/kwhre
Depreciating capital	137,600,000	14.46	19,950,000	2.74
Non-depreciating capital				
Land, etc.	360,000	13.0		
Coolant	10,950,000	13.0	1,530,000	0.21
Working capital	450,000	13.0		
Nuclear insurance	----		340,000	0.05
Annual fixed charges			21,820,000	3.0

7.4 MSCR Operating and Maintenance Cost Estimate

The MSCR is a single reactor, single turbine plant, and, although its power generation capacity is high, its manpower requirements are relatively low because of the single unit operation. Plant personnel totals 101 with a cost of \$872,000 per year. Materials cost \$220,000. Maintenance, including provision for periodic equipment overhaul, special services provided by off-site personnel and organizations, totals \$800,000. With an allowance of 14 percent for central office expense, the total cost is \$2,154,000 or 0.30 m/kwh. The Guide to Nuclear Power Cost Evaluation (52) criteria were followed where applicable in determining plant organization.

7.4.1 Labor and Materials

The manpower requirements of the 1000-Mwe MSCR plant are shown in Table 7.4 for operations and general supervision. Routine operation of the plant may require fewer people, particularly on the technical staff. Review of reactor plant personnel requirements developed by Sargent and Lundy (94), and Kaiser Engineers (51) for 300 Mwe (net) plants are compared in Table 7.4 for single unit systems.

In practice, the actual distribution of manpower may shift, but the total labor cost should remain approximately as shown. For example, one storekeeper may be insufficient, in which case an engineering assistant or maintenance mechanic helper might be replaced by a stores clerk.

In general, the turbine room operation includes, in addition to the turbo-generator proper, (a) water supply and disposal systems, e.g., sanitary service, treated and circulating water systems, (b) boiler feed systems which include boiler feed pumps, steam circulators, and Loeffler boilers, and (c) the turbine auxiliaries, e.g., lubricating oil systems, liquid and gas coolant systems, and instrument and compressed air systems. The reactor operation includes (a) salt charging systems, (b) salt withdrawal systems, (c) salt shipping facilities, (d) liquid and gaseous waste disposal systems, and (e) pressurized gas supply and treatment systems. These facilities are staffed on a semi-automated basis; for fully automated operation, the manpower requirements would be less.

Table 7.4. Personnel Requirement Estimates

	Sargent & Lundy 150 Mw - 350 Mw	Kaiser 300 Mw	AEC Guide 300 Mw(PWR)	MSCR 1000 Mw
Plant Management, Office & Stores	9	4	4	7
Operating Dept.	47	32-39	36	49
Technical Staff	26	6	6	16
Maintenance Dept.	13	20	13	29
Total	95	62-69	59	101

7.4.2. Operation and Maintenance Cost

The estimate of \$2,154,000 shown in Table 7.5 does not take into account any unforeseen difficulties and expenses that may be encountered in the MSCR. It may well be that requirements for personnel and equipment for maintaining a radioactive molten salt system are greater than estimated - possibly by as much as a factor of three. This cannot be accurately determined until maintenance procedures have been more clearly defined and the reactor plant designed in greater detail than was possible in the present study.

Based on 1038 Mwe net and a plant factor of 0.8, the contribution to the power cost is 0.3 mills/kwhre.

Table 7.5. 1000 Mwe MSCR Annual Operating
and Maintenance Expense

<u>Wages & Salaries</u>	Salary or Wage Rate	Personnel Required	Annual Expense
Plant Management			
Station Supt.	\$ 15,000/yr	1	\$ 15,000
Ass't Supt.	12,000/yr	2	24,000
Clerk-Steno	2.50/hr	1	5,200
Clerk-Typist	2.31/hr	2	9,600
Clerk-Steno	2.50/hr	1	5,200
		7	59,000

Table 7.5. Continued

	Salary or Wage Rate	Personnel Required	Annual Expense
Technical Staff			
Supv. Eng. (L)*	\$ 11,000/yr	1	\$ 11,000
Nuclear Eng. (L)	9,600/yr	1	9,600
Engineer	8,400/yr	3	25,200
Health Physics Supv.	8,400/yr	1	8,400
Eng. Ass't.	6,000/yr	3	18,000
Lab Technician	2.85/hr	5	29,700
Radiation Protection	3.25/hr	<u>2</u>	<u>13,500</u>
		16	115,400
Operating Staff			
Shift Supt. (L)	10,800/yr	5	54,000
Senior Control Oper. (L)	3.75/hr	6	46,800
Control Oper. (L)	3.65/hr	4	30,400
Turbine Oper.	3.50/hr	10	72,800
Equipment Attendant	3.00/hr	8	50,000
Special Operator (L)	3.50/hr	9	65,500
Janitor	2.25/hr	2	9,400
Watchman	2.25/hr	<u>5</u>	<u>23,400</u>
		49	352,300
Maintenance Staff			
Maintenance Supt.	10,800/yr	1	10,800
Foreman	7,500/yr	3	22,500
Instrument Mechanic	3.25/hr	6	40,600
Electrician	3.25/hr	5	33,800
Pipe Fitter-Welder	3.25/hr	2	13,500
Machinist	3.25/hr	2	13,500
Mechanic	3.25/hr	8	54,100
Helper	2.65/hr	<u>2</u>	<u>11,100</u>
		29	200,000
Total Labor		101	725,700
Fringe Benefits at 20%			<u>145,300</u>
Total Wages & Salaries			872,000
Materials for Routine Operations			
Oil Supply			84,000
Gas Supply			4,000
Treated Water			2,000
Coolant Salt Make-Up			40,000
Office Supplies			15,000
Laboratory Supplies & Chem.			5,000

*(L) Denotes licensed reactor operator.

Table 7.5. Continued

	Salary or Wage Rate	Personnel Required	Annual Expense
Miscellaneous (e.g., radiation protection, clothing & equip.			\$ 50,000
Consulting Services			<u>10,000</u>
Subtotal			210,000
Contingency			<u>10,000</u>
Total Materials			220,000
<u>Maintenance</u>			
Turbine & turbine auxiliaries routine maintenance materials			150,000
Reactor & reactor auxiliaries routine maintenance materials			300,000
Turbine 3-yr overhaul (prorata)			50,000
Turbine system auxiliaries overhaul			50,000
Reactor system overhaul			100,000
Reactor auxiliaries overhaul			<u>50,000</u>
Subtotal			700,000
Contingency			<u>100,000</u>
Total Maintenance			800,000
Central Office, General & Admin. Expenses at 14 Percent			<u>262,000</u>
Grand Total Operating & Maintenance Expense			\$2,154,000

8. RESULTS AND CONCLUSIONS

The cost of electric power is commonly resolved into three components: The fuel cost, the fixed charges, and operation and maintenance expense.

8.1 Fuel Cost

As shown in Sec. 6, the fuel cycle cost in the MSCR ranges from 2 mills/kwhr (electrical) down to 0.7 depending on the conversion ratio desired and the method and/or cost of processing assumed. For present purposes, the minimum cost associated with the reference design reactor summarized in Table 6.6 was selected as representative. This reactor is "near-term" and predicated on the scale-up of current technology with the exception of the moderator graphite, which was an order of magnitude better than currently available graphite in respect to porosity and permeability. The fuel cycle cost, using Fluoride Volatility processing in a central plant with discard of carrier salt and contained thorium and recycle of isotopes of uranium, was reported in Sec. 6.7.1.

Table 8.1 1000 Mwe Molten Salt Converter
Reactor Fuel Cycle Cost

Item	Mills/kwhr	
Inventories		
Fertile	0.03	-
Fissile	0.23	-
Salt	0.06	0.32
Replacement		
Fertile	0.04	-
Fissile (95% ^{235}U)	0.16	-
Salt	0.08	0.28
Reprocessing		<u>0.08</u>
Total, mills/kwhr	<u>0.68</u>	

8.2 Fixed Charges

The capital investment for the 1000 Mwe (1038 Mwe net) station was estimated by Sargent and Lundy, Engineers from information supplied by ORNL, as reported in Sec. 7, and summarized in Table 7.1. The investment comprised \$137,564,000 for depreciating capital items, and \$11,311,800 for non-depreciating items (coolant salt and land). Fuel salt fixed charges are included in fuel cycle cost.

Working capital was estimated according to the prescription given in the Guide (52), and is shown in Table 8.2.

Table 8.2. 1000 Mwe MSCR Working Capital

1. 2.7% of annual operating labor and fuel costs:	\$ 200,000
2. 25% of annual maintenance and materials:	<u>250,000</u>
Total Working Capital	\$ 450,000

Similarly, the nuclear hazard insurance premium was estimated by prescription at \$340,000 per year. The fixed charges are collected in Table 8.3.

Table 8.3. 1000 Mwe Molten Salt Converter
Reactor Fixed Charges

Item	Investment	Rate %/yr	Annual Expense \$/yr	Power Cost Mills/kwhr
Depreciating capital	137,600,000	14.46	19,950,000	2.74
Non-depreciating capital	11,760,000	13.0	1,530,000	0.21
Nuclear insurance			340,000	0.05
Annual fixed charges			21,820,000	3.0

8.3 Operation and Maintenance Expense

This expense was estimated in Sec. 7.2 and amounted to \$2,154,000 per year, of which \$1,020,000 was for maintenance and materials and the rest was for labor, supervision, and management. At 1038 Mwe net, the contribution to the power cost is 0.3 mills/kwhr (electrical).

8.4 Cost of Power

The three components of the power cost are assembled in Table 8.4.

Table 8.4. Cost of Power in a 1000 Mwe Molten Salt Converter Reactor

Item	Mills/Kwhr
Fuel cycle cost	0.7
Fixed charges	3.0
Operation and maintenance	<u>0.3</u>
Cost of power, mills/Kwhr	4.0

In regard to the fuel cycle cost, it was shown in Sec. 6.8 that this would not exceed 1.0 mill/kwhr even though the fuel were processed in a 1.0 tonne/day Thorex plant costing up to \$60 thousand per day to operate. Such a general purpose plant could provide processing of fuel from thorium reactors having a total power capability of about 20,000 Mwe at an exposure of 50,000 Mwd/tonne.

The energy conversion system, accessory electrical equipment, and miscellaneous plant equipment (Items 23, 24, and 25 in Table 7.1) are conventional items, and the estimation of their cost appears to be relatively unambiguous. Items 21 and 22 are perhaps subject to considerable uncertainty. But their total is only about \$57 million, whereas the contingency item is \$11 million. However, the possibility exists that Item 21 was

grossly underestimated, or that the effect of radiation shielding requirements on building costs was underestimated. Supposing Item 21 to be \$18 million (factor of 3), and allowing another \$5 million for the reactor plant (10%), the investment comes to \$166/kw, and the fixed charges to 3.5 mills/kwhr, as an upper limit.

Provision for labor in Sec. 7.2 seems adequate. Materials and supplies accounted for about half the operation and maintenance costs; if this were doubled, the contribution to the cost of power would be about 0.5 mills/kwhr.

Collecting these probable upper limits on the cost of power in the MSCR, the sum is 5.0 mills/kwhr.

8.5 Breeding Potential of the MSCR

The nuclear capability of the reference design MSCR is summarized in Fig. 8.1. With central Fluoride Volatility processing, the minimum fuel cycle cost is about 0.7 mill/kwhr and the conversion ratio about 0.9 at a processing cycle time of 1500 days. Increasing the rate increases the conversion ratio to perhaps as high as 0.93, but the fuel cost rises steeply.

The use of an on-site reactor-integrated (inside the reactor cell) Fluoride Volatility facility would increase the fuel cost by only 0.1 mill/kwhr in the 1000 Mwe station.

The use of an on-site reactor-integrated precipitation process for removing rare earths might reduce the fuel cost below 0.5 mills/kwhr.

By taking advantage of potential improvements in neutron economy (but retaining the essential features of the MSCR) an upper limit on the conversion ratio of 1.03 was estimated. This was interpreted to mean that the MSCR is capable of evolving into a self-sustaining reactor requiring only thorium feed. Outside source of fissile isotopes would not be needed.

This limitation does not apply to two-region breeders, which were shown previously to be capable of doubling times as short as 25 years (1).

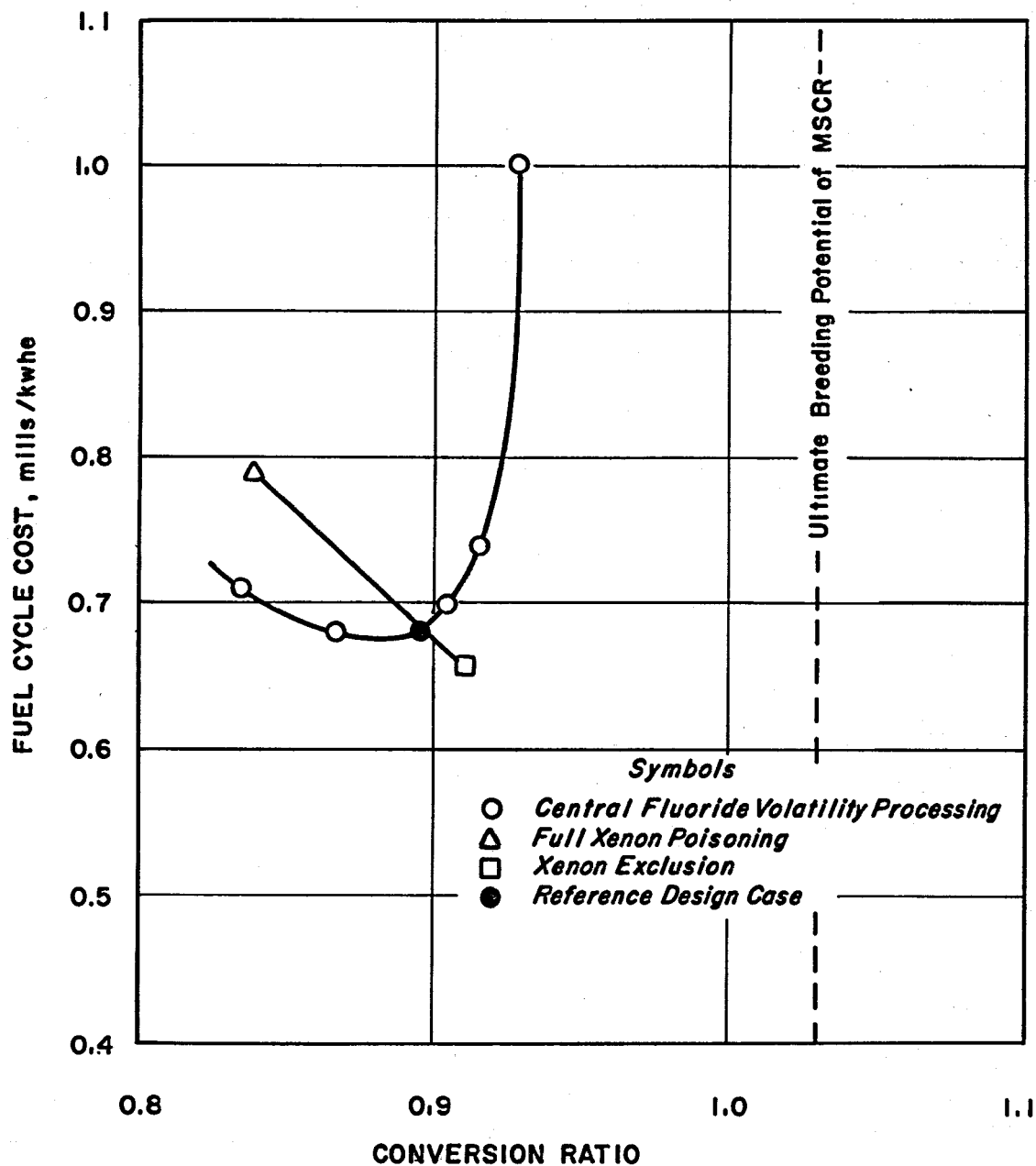


Fig. 8.1. Nuclear Capability of 1000 Mwe Molten Salt Converter Reactor.

8.6 Conclusions

The 1000 Mwe MSCR requires a capital investment of \$143/kwhr. The fixed charges are 3.0 mills/kwhr, the fuel cost is 0.7 mills/kwhr, the maintenance and operation expense of 0.3 mills/kwhr, and the net power cost is 4.0 mills/kwhr.

Substitution of sodium for LiF-BeF₂ as the intermediate coolant and replacement of the Loeffler boiler-superheater complex with a more conventional sodium-heated boiler would reduce the capital investment to about \$125/kwhr. Development of alternative methods of processing (e.g., precipitation of rare earth fluorides) provides potential for reducing fuel cycle cost. An examination of the neutron economy indicates that the MSCR should be capable of evolving into a self-sustaining breeder reactor (BR ~1.0) not dependent on outside sources of fissile isotopes.

8.7 Recommendations

The comprehensive program of research and development for molten salt reactors in progress at ORNL is concerned at present with the construction and operation of the MSRE. This MSCR evaluation has disclosed certain additional areas of study, research, and development important to the realization of the nuclear and economic potential of molten salt reactors. These areas are listed below, together with specific examples in each area.

8.7.1 Title 1 Design Study of MSCR

This should be performed for two plant capacities (100 and 1000 Mwe) in order to detect unrecognized development problems and to verify the economic predictions made in this report. The study preferably should be conducted by an organization outside the Laboratory, but with close liaison and cooperation in special studies (e.g., nuclear design, reactor-integrated chemical processing). A study of 100 Mwe installation is desirable to bridge the gap between the MSRE (10 Mwt) and a full-scale prototype.

8.7.2 Conceptual Design Studies of Advanced Breeder Reactors

Prior studies have established the nuclear potential of a thermal molten salt-thorium breeder. However, this concept should be re-examined and developed in greater detail in the light of the technology accumulated in recent years. In addition, the potential of fast molten-salt breeders, including those breeding plutonium, or possibly both plutonium and ^{233}U , should be evaluated. A number of concepts have been proposed, and it is not clear, at present, which of these offers the greatest ultimate potential coupled with the least difficulty of development.

8.7.3 Fundamental Studies of Alternative Chemical Processes

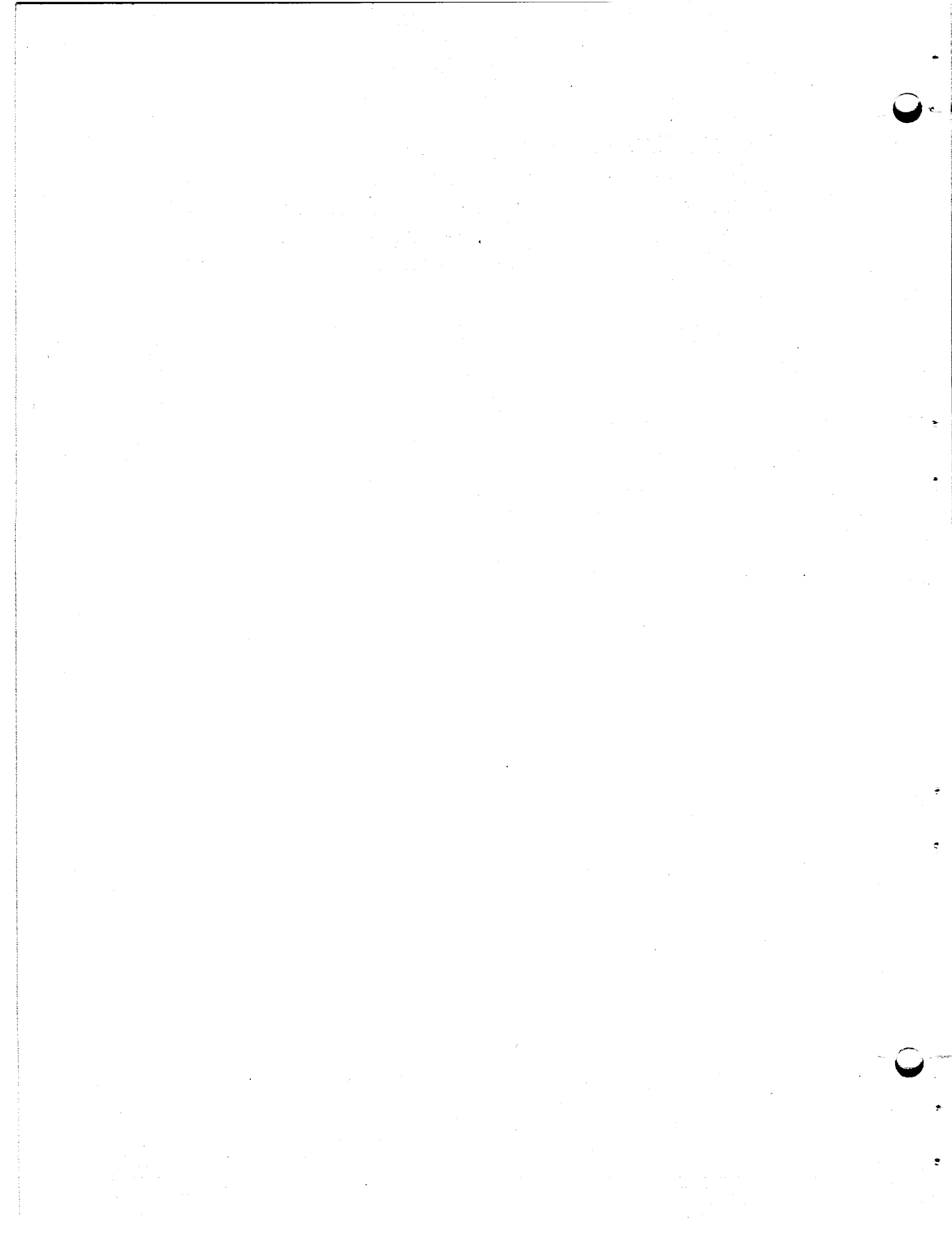
While the fluoride volatility process is suitable for the recovery of isotopes of uranium from short-cooled fuel, its use alone does entail the discard of the carrier salt to rid the system fission products. This fact limits the processing rate and conversion ratio in thermal reactors using valuable isotopes of lithium and beryllium, although fast reactors using fluorides of sodium and potassium, etc., are not so limited. For the thermal reactors at least, an alternative process is needed in which separation of valuable components (thorium, uranium, lithium, beryllium) from fission product isotopes is effected by transfer between fluid phases, e.g., by extraction of molten salt fuel with a liquid metal. Driving forces for the transfer can be provided by the use of active metals and easily reduced fluorides or perhaps by the application of electric potentials.

8.7.4 Engineering Laboratory Study of Precipitation Processing

This process, which has great potential for reducing the fuel cycle cost in the MSCR and which, by necessity, must be integrated with the operation of the reactor and placed within the reactor cell, could make the introduction of MSCR power reactor plants independent of the availability of central processing facilities for molten salts. This is an enormous advantage for the initial installations, particularly if these are widely scattered in remote locations. Also, the competitive position of the smaller installations (100 Mwe) would be improved.

8.7.5 Pilot Plant Study of HF Dissolution Process

This process, though not essential to the realization of the economic potential of the MSCR would, if developed, make possible the evolution of the MSCR into a self-sustaining system, and would constitute a large step in the development of two-region, two-fluid breeders.

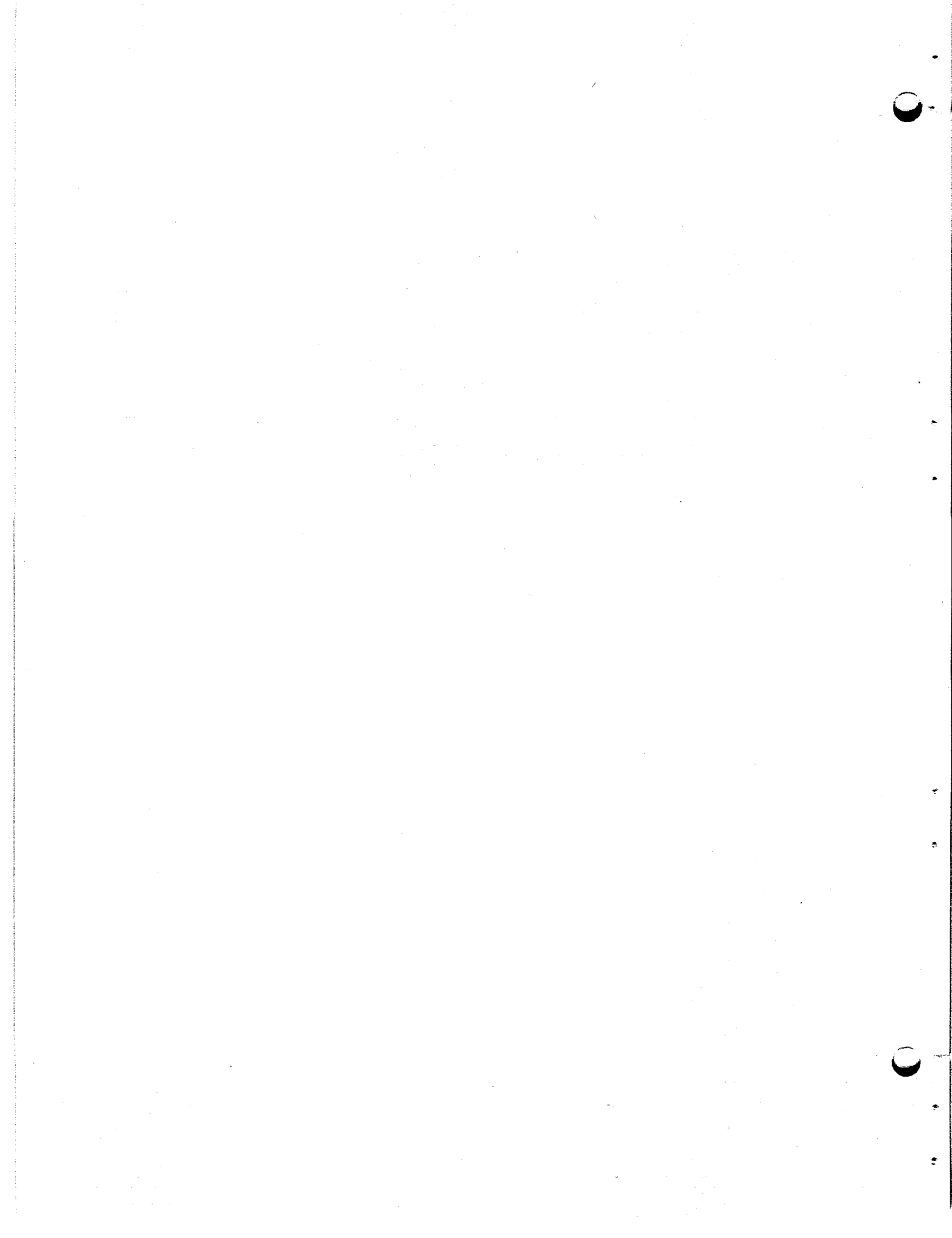


APPENDICES

Introduction

In this portion of the report are collected reference materials, preliminary studies, and detailed discussions that support the assumptions used or conclusions drawn in the main body of the report.

Literature references in the Appendices do not refer to the Bibliography which follows, but to separate lists of references given at the end of each sub-appendix.



Appendix A

MULTIGROUP CROSS SECTIONS FOR
MSCR CALCULATIONS

C. W. Nestor

Table A.1. Group Structure

Group	Δu	u	Energy (ev)
1	0.91629	0.916	$4 \times 10^6 \rightarrow 10^7$
2	0.69315	1.609	$2 \times 10^6 \rightarrow 4 \times 10^6$
3	0.69315	2.302	$1 \rightarrow 2 \times 10^6$
4	0.20400	3.506	$3 \times 10^5 \rightarrow 10^6$
5	1.09860	4.605	$1 \times 10^5 \rightarrow 3 \times 10^5$
6	1.20400	5.808	$3 \times 10^4 \rightarrow 1 \times 10^5$
7	1.09860	6.907	$1 \times 10^4 \rightarrow 3 \times 10^4$
8	1.20400	8.111	$3 \times 10^3 \rightarrow 1 \times 10^4$
9	1.09860	9.210	$1 \times 10^3 \rightarrow 3 \times 10^3$
10	0.91629	10.126	$400 \rightarrow 10^3$
11	0.98083	11.107	$150 \rightarrow 400$
12	0.40547	11.512	$100 \rightarrow 150$
13	0.10536	11.617	$90 \rightarrow 100$
14	0.11778	11.735	$80 \rightarrow 90$
15	0.20764	11.942	$65 \rightarrow 80$
16	0.26236	12.204	$50 \rightarrow 65$
17	0.10536	12.309	$45 \rightarrow 50$
18	0.19574	12.505	$37 \rightarrow 45$
19	0.11441	12.619	$33 \rightarrow 37$
20	0.09531	12.714	$30 \rightarrow 33$
21	0.18232	12.896	$25 \rightarrow 30$
22	0.22314	13.119	$20 \rightarrow 25$
23	0.16252	13.282	$17 \rightarrow 20$
24	0.23052	13.572	$13.5 \rightarrow 17$
25	0.30010	13.813	$10 \rightarrow 13.5$
26	0.28768	14.101	$7.5 \rightarrow 10$
27	0.31015	14.411	$5.5 \rightarrow 7.5$
28	0.31845	14.729	$4 \rightarrow 5.5$
29	0.47000	15.199	$2.5 \rightarrow 4$
30	0.57982	15.779	$1.4 \rightarrow 2.5$
31	0.55962	16.339	$0.8 \rightarrow 1.4$
32	0.28768	16.627	$0.6 \rightarrow 0.8$
33 Ep. Thermal	0.31705	16.944	$0.437 \rightarrow 0.6$
34 Thermal Group	(1200°F)		0.07940

Table A.2. Lithium-6

Group	$\xi\sigma_T$	$\bar{\sigma}_a$	$\bar{v}\sigma_f$	$3\bar{\sigma}_{tr}$
1	6.16×10^{-1}	6.74×10^{-2}	0	5.04
2	4.19×10^{-1}	1.618×10^{-1}	0	4.76
3	4.36×10^{-1}	2.530×10^{-1}	0	3.78
4	2.02×10^{-1}	7.142×10^{-1}	0	7.59
5	4.99×10^{-1}	1.463×10^{-1}	0	1.22×10
6	4.96×10^{-1}	7.680×10^{-1}	0	4.55
7	7.38×10^{-1}	1.163	0	5.92
8	1.11	2.057	0	9.87
9	1.75	3.650	0	1.67×10
10	2.62	6.020	0	2.64×10
11	4.04	9.689	0	4.07×10
12	4.81	1.359×10	0	5.55×10
13	5.05	1.542×10	0	6.24×10
14	5.32	1.631×10	0	6.56×10
15	5.83	1.770×10	0	7.07×10
16	6.52	1.991×10	0	7.88×10
17	6.85	2.181×10	0	8.56×10
18	7.48	2.353×10	0	9.18×10
19	7.92	2.542×10	0	9.85×10
20	8.28	2.678×10	0	1.01×10^2
21	8.91	2.872×10	0	1.10×10^2
22	9.93	3.179×10	0	1.21×10^2
23	1.07×10	3.500×10	0	1.32×10^2
24	1.20×10	3.863×10	0	1.44×10^2
25	1.38×10	4.413×10	0	1.63×10^2
26	1.57×10	5.110×10	0	1.87×10^2
27	1.81×10	5.940×10	0	2.14×10^2
28	2.12×10	6.950×10	0	2.47×10^2
29	2.69×10	8.470×10	0	2.97×10^2
30	4.35×10	1.100×10^2	0	3.78×10^2
31	5.61×10	1.470×10^2	0	4.90×10^2
32	6.39×10	1.810×10^2	0	5.94×10^2
33	7.49×10	2.21×10^2	0	6.70×10^2
34	7.49×10	4.720×10^2	0	1.42×10^3

Table A.3. Lithium-7

Group	$\xi\sigma_T$	$\bar{\sigma}_a$	$\overline{v\sigma}_f$	$3\bar{\sigma}_{tr}$
1	4.45×10^{-1}	2.11×10^{-6}	0	4.915
2	4.06×10^{-1}	3.17×10^{-6}	0	3.502
3	3.28×10^{-1}	5.76×10^{-6}	0	3.451
4	3.28×10^{-1}	7.37×10^{-6}	0	4.947
5	7.86×10^{-1}	1.34×10^{-5}	0	6.286
6	2.75×10^{-1}	2.66×10^{-5}	0	2.850
7	2.75×10^{-1}	4.08×10^{-5}	0	2.850
8	2.75×10^{-1}	7.31×10^{-5}	0	2.850
9	2.75×10^{-1}	1.31×10^{-4}	0	2.850
10	2.75×10^{-1}	2.03×10^{-4}	0	2.850
11	2.75×10^{-1}	3.44×10^{-4}	0	2.850
12	2.75×10^{-1}	4.57×10^{-4}	0	2.850
13	2.75×10^{-1}	5.75×10^{-4}	0	2.850
14	2.75×10^{-1}	5.75×10^{-4}	0	2.850
15	2.75×10^{-1}	5.75×10^{-4}	0	2.850
16	2.75×10^{-1}	7.31×10^{-4}	0	2.850
17	2.75×10^{-1}	7.73×10^{-4}	0	2.850
18	2.75×10^{-1}	7.73×10^{-4}	0	2.850
19	2.75×10^{-1}	8.73×10^{-4}	0	2.850
20	2.75×10^{-1}	1.11×10^{-3}	0	2.850
21	2.75×10^{-1}	1.11×10^{-3}	0	2.850
22	2.75×10^{-1}	1.11×10^{-3}	0	2.850
23	2.75×10^{-1}	1.11×10^{-3}	0	2.850
24	2.75×10^{-1}	1.30×10^{-3}	0	2.850
25	2.75×10^{-1}	1.50×10^{-3}	0	2.850
26	2.75×10^{-1}	2.00×10^{-3}	0	2.850
27	2.75×10^{-1}	2.00×10^{-3}	0	2.850
28	2.75×10^{-1}	2.55×10^{-3}	0	2.850
29	2.75×10^{-1}	3.36×10^{-3}	0	2.850
30	2.75×10^{-1}	3.36×10^{-3}	0	2.850
31	2.75×10^{-1}	5.12×10^{-3}	0	2.850
32	2.75×10^{-1}	6.17×10^{-3}	0	2.850
33	2.75×10^{-1}	7.24×10^{-3}	0	2.850
34	2.75×10^{-1}	1.66×10^{-2}	0	2.850

Table A.4. Beryllium-9

Group	$\xi\sigma_T$	$\bar{\sigma}_a$	$\bar{v}\sigma_f$	$3\bar{\sigma}_{tr}$
1	0.4608	6.3425×10^{-7}	0	5.2490
2	0.3240	9.4485×10^{-7}	0	6.6160
3	0.6813	1.3362×10^{-6}	0	6.6919
4	0.8700	2.1688×10^{-6}	0	1.0649×10
5	1.1913	3.8471×10^{-6}	0	1.3588×10
6	1.2122	6.8585×10^{-6}	0	1.6068×10
7	1.2122	1.2165×10^{-5}	0	1.6112×10
8	1.2122	2.1688×10^{-5}	0	1.6112×10
9	1.2122	2.8471×10^{-5}	0	1.6112×10
10	1.2122	6.3425×10^{-5}	0	1.6112×10
11	1.2122	1.0204×10^{-4}	0	1.6112×10
12	1.2122	1.4312×10^{-4}	0	1.6112×10
13	1.2122	1.6236×10^{-4}	0	1.6112×10
14	1.2122	1.7167×10^{-4}	0	1.6112×10
15	1.2122	1.8628×10^{-4}	0	1.6112×10
16	1.2122	2.0956×10^{-4}	0	1.6112×10
17	1.2122	2.2960×10^{-4}	0	1.6112×10
18	1.2122	2.4762×10^{-4}	0	1.6112×10
19	1.2122	2.6752×10^{-4}	0	1.6112×10
20	1.2122	2.8190×10^{-4}	0	1.6112×10
21	1.2122	3.0224×10^{-4}	0	1.6112×10
22	1.2122	3.3454×10^{-4}	0	1.6112×10
23	1.2122	3.6832×10^{-4}	0	1.6112×10
24	1.2122	4.0646×10^{-4}	0	1.6112×10
25	1.2122	4.6430×10^{-4}	0	1.6112×10
26	1.2122	5.3775×10^{-4}	0	1.6112×10
27	1.2122	6.2450×10^{-4}	0	1.6112×10
28	1.2122	7.3085×10^{-4}	0	1.6112×10
29	1.2122	8.1920×10^{-4}	0	1.6112×10
30	1.2122	1.1601×10^{-3}	0	1.6112×10
31	1.2122	1.5142×10^{-3}	0	1.6112×10
32	1.2122	1.9013×10^{-3}	0	1.6112×10
33	1.24	2.15×10^{-3}	0	1.611×10
34	1.24	5.048×10^{-3}	0	1.611×10

Table A.5. Carbon-12

Group	$\xi\sigma_T$	$\bar{\sigma}_a$	$\bar{\sigma}_f$	$3\bar{\sigma}_{tr}$
1	0.303676	2.1565×10^{-7}	0	3.7354
2	0.2686	3.213	0	5.4204
3	0.4108	4.544	0	0.0604
4	0.6241	7.380	0	9.2352
5	0.694568	1.308×10^{-6}	0	1.19114×10
6	0.74181	2.332×10^{-6}	0	1.28686×10
7	0.7584	4.187×10^{-6}	0	1.35370×10
8	0.7584	7.375×10^{-6}	0	1.35936×10
9	0.7584	1.308×10^{-5}	0	1.35936×10
10	0.7584	2.157	0	1.35936×10
11	0.7584	3.470	0	1.35936×10
12	0.7584	4.866	0	1.35936×10
13	0.7584	5.520	0	1.35936×10
14	0.7584	5.830	0	1.35936×10
15	0.7584	6.335	0	1.35936×10
16	0.7584	7.125	0	1.35936×10
17	0.7584	7.805	0	1.35936×10
18	0.7584	8.420	0	1.35936×10
19	0.7584	9.095	0	1.35936×10
20	0.7584	9.585	0	1.35936×10
21	0.7584	1.028×10^{-4}	0	1.35936×10
22	0.7584	1.138	0	1.35936×10
23	0.7584	1.253	0	1.35936×10
24	0.7584	1.382	0	1.35936×10
25	0.7584	1.579	0	1.35936×10
26	0.7584	1.829	0	1.35936×10
27	0.7584	2.124	0	1.35936×10
28	0.7584	2.485	0	1.35936×10
29	0.7584	3.030	0	1.35936×10
30	0.7584	3.944	0	1.35936×10
31	0.7584	5.245	0	1.35936×10
32	0.7584	6.465	0	1.35936×10
33	7.585×10^{-1}	1.85×10^{-3}	0	1.359×10
34	7.585×10^{-1}	5.048×10^{-3}	0	1.359×10

Table A.6. Fluorine-19

Group	$\xi\sigma_T$	$\bar{\sigma}_a$	$\bar{v\sigma}_f$	$3\bar{\sigma}_{tr}$
1	1.62×10^{-1}	2.00×10^{-1}	0	5.40
2	2.00×10^{-1}	0	0	7.50
3	3.45×10^{-1}	0	0	9.60
4	3.50×10^{-1}	1.00×10^{-3}	0	1.35×10
5	7.70×10^{-1}	1.00×10^{-3}	0	2.40×10
6	2.55×10^{-1}	3.00×10^{-3}	0	1.50×10
7	4.35×10^{-1}	0	0	1.35×10
8	3.70×10^{-1}	0	0	1.11×10
9	3.70×10^{-1}	0	0	1.11×10
10	3.70×10^{-1}	0	0	1.11×10
11	3.70×10^{-1}	0	0	1.11×10
12	3.70×10^{-1}	0	0	1.11×10
13	3.50×10^{-1}	0	0	1.05×10
14	3.50×10^{-1}	0	0	1.05×10
15	3.50×10^{-1}	0	0	1.05×10
16	3.50×10^{-1}	0	0	1.05×10
17	3.50×10^{-1}	0	0	1.05×10
18	3.50×10^{-1}	0	0	1.05×10
19	3.50×10^{-1}	0	0	1.05×10
20	3.50×10^{-1}	0	0	1.05×10
21	3.50×10^{-1}	0	0	1.05×10
22	3.50×10^{-1}	0	0	1.05×10
23	3.50×10^{-1}	0	0	1.05×10
24	3.50×10^{-1}	0	0	1.05×10
25	3.50×10^{-1}	0	0	1.05×10
26	3.50×10^{-1}	0	0	1.05×10
27	3.50×10^{-1}	0	0	1.05×10
28	3.50×10^{-1}	0	0	1.05×10
29	3.50×10^{-1}	0	0	1.05×10
30	3.50×10^{-1}	0	0	1.05×10
31	3.50×10^{-1}	0	0	1.05×10
32	3.50×10^{-1}	0	0	1.05×10
33	3.59×10^{-1}	1.80×10^{-3}	0	1.05×10
34	3.59×10^{-1}	4.5×10^{-3}	0	1.05×10

Table A.7. INOR-8

Group	$\xi\sigma_T$	$\bar{\sigma}_a$	$\bar{\sigma}_f$	$3\bar{\sigma}_{tr}$
1	5.98×10^{-1}	1.868×10^{-1}	0	10.347
2	5.89×10^{-1}	1.904×10^{-1}	0	10.693
3	6.98×10^{-1}	1.936×10^{-1}	0	10.521
4	1.010	1.972×10^{-1}	0	10.760
5	2.375	2.006×10^{-1}	0	13.270
6	3.158	2.031×10^{-1}	0	14.48
7	3.165	2.057×10^{-1}	0	20.793
8	3.175	2.096×10^{-1}	0	42.011
9	3.010	2.264×10^{-1}	0	48.153
10	2.939	2.544×10^{-1}	0	54.372
11	2.930	3.531×10^{-1}	0	59.116
12	2.941	5.778×10^{-1}	0	57.442
13	2.967	1.159	0	56.977
14	2.967	1.159	0	57.488
15	2.967	1.159	0	57.58
16	2.967	1.159	0	57.62
17	2.967	1.160	0	58.23
18	2.967	1.161	0	57.30
19	2.977	9.800×10^{-1}	0	56.00
20	3.018	2.009×10^{-1}	0	57.070
21	3.018	2.016×10^{-1}	0	56.140
22	3.018	2.027×10^{-1}	0	57.349
23	3.018	2.043×10^{-1}	0	58.698
24	2.995	2.092×10^{-1}	0	57.628
25	2.978	2.291×10^{-1}	0	58.698
26	3.077	2.652×10^{-1}	0	58.837
27	3.077	3.038×10^{-1}	0	58.930
28	3.156	3.554×10^{-1}	0	59.116
29	3.270	4.215×10^{-1}	0	58.279
30	3.270	5.099×10^{-1}	0	58.279
31	3.141	6.740×10^{-1}	0	57.349
32	3.152	8.809×10^{-1}	0	57.74
33	3.285	1.258	0	58.695
34	3.285	2.874	0	58.693

Table A.8. Xenon-135

Group	$\xi\sigma_T$	$\bar{\sigma}_a$	$\bar{\nu\sigma}_f$	$3\bar{\sigma}_{tr}$
1	0	7.43×10^{-2}	0	0
2	0	3.908×10^{-1}	0	0
3	0	7.242×10^{-1}	0	0
4	0	9.843×10^{-1}	0	0
5	0	9.546×10^{-1}	0	0
6	0	3.960×10^{-1}	0	0
7	0	1.515×10	0	0
8	0	3.045×10	0	0
9	0	5.133×10	0	0
10	0	8.580×10	0	0
11	0	1.047×10^2	0	0
12	0	1.870×10^2	0	0
13	0	2.198×10^2	0	0
14	0	2.198×10^2	0	0
15	0	2.198×10^2	0	0
16	0	3.050×10^2	0	0
17	0	3.282×10^2	0	0
18	0	3.282×10^2	0	0
19	0	4.222×10^2	0	0
20	0	8.254×10^2	0	0
21	0	8.254×10^2	0	0
22	0	8.254×10^2	0	0
23	0	8.254×10^2	0	0
24	0	7.035×10^2	0	0
25	0	6.781×10^2	0	0
26	0	2.439×10^3	0	0
27	0	2.439×10^3	0	0
28	0	8.561×10^3	0	0
29	0	1.720×10^4	0	0
30	0	1.720×10^4	0	0
31	0	2.100×10^4	0	0
32	0	5.697×10^4	0	0
33	0	4.20×10^4	0	0
34	0	1.60×10^6	0	0

Table A.9. Samarium-149

Group	$\xi\sigma_T$	$\bar{\sigma}_a$	$\bar{\nu\sigma}_f$	$\bar{3\sigma}_{tr}$
1	0	3.000×10^{-1}	0	0
2	0	3.000×10^{-1}	0	0
3	0	3.262×10^{-1}	0	0
4	0	3.600×10^{-1}	0	0
5	0	1.027	0	0
6	0	1.570	0	0
7	0	1.570	0	0
8	0	2.240	0	0
9	0	1.641×10	0	0
10	0	4.857×10	0	0
11	0	4.857×10	0	0
12	0	8.829×10	0	0
13	0	1.911×10^2	0	0
14	0	1.911×10^2	0	0
15	0	1.911×10^2	0	0
16	0	1.756×10^2	0	0
17	0	1.714×10^2	0	0
18	0	1.714×10^2	0	0
19	0	1.586×10^2	0	0
20	0	1.037×10^2	0	0
21	0	1.037×10^2	0	0
22	0	1.037×10^2	0	0
23	0	1.037×10^2	0	0
24	0	1.463×10^2	0	0
25	0	1.887×10^2	0	0
26	0	5.991×10^2	0	0
27	0	5.991×10^2	0	0
28	0	5.991×10^2	0	0
29	0	1.000×10^2	0	0
30	0	1.000×10^2	0	0
31	0	1.391×10^3	0	0
32	0	4.774×10^3	0	0
33	0	7.95×10^2	0	0
34	0	4.20×10^4	0	0

Table A.10. Samarium-151

Group	$\xi\sigma_T$	$\bar{\sigma}_a$	$\bar{v}\sigma_f$	$3\bar{\sigma}_{tr}$
0-26	0	0	0	0
27	0	5.50×10^2	0	0
28	0	0	0	0
29	0	1.30×10^2	0	0
30	0	7.20×10^2	0	0
31	0	2.28×10^3	0	0
32	0	7.25×10^2	0	0
33	0	9.80×10^2	0	0
34	0	4.91×10^3	0	0

Table A.11. Thorium-232 (Infinite Dilution)*

Group	$\xi\sigma_T$	$\bar{\sigma}_a$	$\bar{v}\sigma_f$	$3\bar{\sigma}_{tr}$
1	6.100×10^{-2}	0.2408	5.642×10^{-1}	1.883×10
2	5.669×10^{-2}	0.1684	3.190×10^{-1}	1.998×10
3	5.841×10^{-2}	0.1450	1.306×10^{-1}	1.966×10
4	8.160×10^{-2}	0.1622	0	2.366×10
5	1.039×10^{-1}	0.2708	0	3.132×10
6	1.119×10^{-1}	0.4627	0	3.718×10
7	1.130×10^{-1}	0.5680	0	3.739×10
8	1.156×10^{-1}	0.7958	0	3.739×10
9	1.168×10^{-1}	1.029	0	3.739×10
10	1.180×10^{-1}	1.168	0	3.739×10
11	1.339×10^{-1}	7.234	0	4.658×10
12	1.824×10^{-1}	20.802	0	6.349×10
13	1.202×10^{-1}	1.481	0	3.739×10
14	1.204×10^{-1}	1.502	0	3.739×10
15	2.301×10^{-1}	82.755	0	8.040×10
16	1.728×10^{-1}	16.568	0	6.014×10
17	1.213×10^{-1}	1.615	0	3.739×10
18	1.217×10^{-1}	1.646	0	3.739×10
19	1.219×10^{-1}	1.678	0	3.739×10
20	1.221×10^{-1}	1.701	0	3.739×10
21	1.224×10^{-1}	1.731	0	3.739×10
22	5.117×10^{-1}	198.0	0	1.781×10
23	1.232×10^{-1}	1.819	0	3.739×10
24	1.236×10^{-1}	1.864	0	3.739×10
25	1.242×10^{-1}	1.927	0	3.739×10

*Groups 11, 12, 15, 16, 22 computed in Appendix B.

Table A.11 (continued)

Group	$\xi\sigma_T$	$\bar{\sigma}_a$	$\overline{v\sigma}_f$	$3\bar{\sigma}_{tr}$
26	1.249×10^{-1}	2.000	0	3.739×10
27	1.256×10^{-1}	2.076	0	3.739×10
28	1.263×10^{-1}	2.160	0	3.739×10
29	1.274×10^{-1}	2.269	0	3.739×10
30	1.290×10^{-1}	2.424	0	3.739×10
31	1.305×10^{-1}	2.604	0	3.739×10
32	1.314×10^{-1}	2.745	0	3.739×10
33	1.324×10^{-1}	2.848	0	4.591×10
34	1.324×10^{-1}	3.77	0	4.87×10

Table A.12. Protactinium-233

Group	$\xi\sigma_T$	$\bar{\sigma}_a$	$\overline{v\sigma}_f$	$3\bar{\sigma}_{tr}$
1	4.285×10^{-2}	0.002403	0	1.496×10
2	4.286×10^{-2}	0.00358	0	1.496×10
3	8.569×10^{-2}	0.00506	0	1.496×10
4	8.577×10^{-2}	0.00822	0	2.991×10
5	8.589×10^{-2}	0.01457	0	2.991×10
6	8.613×10^{-2}	0.02599	0	2.991×10
7	8.652×10^{-2}	0.4609	0	2.991×10
8	8.728×10^{-2}	0.08218	0	2.991×10
9	8.851×10^{-2}	0.1457	0	2.991×10
10	9.020×10^{-2}	0.2403	0	2.991×10
11	9.312×10^{-2}	0.3866	0	2.991×10
12	9.480×10^{-2}	0.5422	0	2.991×10
13	9.530×10^{-2}	0.6151	0	2.991×10
14	9.589×10^{-2}	0.6502	0	2.991×10
15	9.702×10^{-2}	0.7059	0	2.991×10
16	9.862×10^{-2}	0.7939	0	2.991×10
17	9.932×10^{-2}	0.8697	0	2.991×10
18	1.007×10^{-1}	1.1608	0	2.991×10
19	1.016×10^{-1}	1.0130	0	2.991×10
20	1.024×10^{-1}	1.0680	0	2.991×10
21	1.040×10^{-1}	1.145	0	2.991×10
22	1.062×10^{-1}	1.267	0	2.991×10
23	1.079×10^{-1}	1.396	0	2.991×10
24	1.106×10^{-1}	1.540	0	2.991×10
25	1.147×10^{-1}	1.759	0	2.991×10
26	1.192×10^{-1}	2.037	0	2.991×10
27	1.248×10^{-1}	2.366	0	2.991×10

Table A.12 (continued)

Group	$\xi\sigma_T$	$\bar{\sigma}_a$	$\overline{v\sigma}_f$	$3\bar{\sigma}_{tr}$
28	1.316×10^{-1}	2.769	0	2.991×10
29	1.438×10^{-1}	3.376	0	2.991×10
30	1.630×10^{-1}	737.0	0	2.991×10
31	1.885×10^{-1}	764.0	0	2.991×10
32	2.044×10^{-1}	7.204	0	2.991×10
33	2.25×10^{-2}	8.374	0	7.486×10
34	2.25×10^{-1}	18.943	0	1.32×10^2

Table A.13. Uranium-233

Group	$\xi\sigma_T$	$\bar{\sigma}_a$	$\overline{v\sigma}_f$	$3\bar{\sigma}_{tr}$	$\bar{\eta}$	\bar{v}
1	7.400×10^{-2}	1.940	6.570	1.230×10	3.39	3.39
2	7.110×10^{-2}	1.810	5.190	1.442	2.87	2.87
3	6.950×10^{-2}	1.950	5.240	1.191	2.69	2.69
4	9.320×10^{-2}	2.160	5.430	1.461	2.51	2.51
5	1.140×10^{-1}	2.610	6.180	2.271	2.37	2.50
6	1.263×10^{-1}	3.560	8.120	2.930	2.28	2.50
7	1.371×10^{-1}	5.864	1.319×10	2.991	2.25	2.50
8	2.366×10^{-1}	1.698×10	3.801×10	2.390	2.24	2.50
9	1.838×10^{-1}	1.008×10	2.268×10	3.739	2.25	2.50
10	2.427×10^{-1}	1.411×10	3.175×10	3.739	2.25	2.50
11	3.309×10^{-1}	2.131×10	4.795×10	3.739	2.25	2.50
12	4.451×10^{-1}	3.832×10	8.622×10	3.739	2.25	2.50
13	4.324×10^{-1}	5.031×10	1.132×10^2	3.739	2.25	2.50
14	3.673×10^{-1}	4.089×10	9.201×10	3.739	2.25	2.50
15	5.273×10^{-1}	4.352×10	9.799×10	3.739	2.25	2.50
16	3.253×10^{-1}	4.614×10	1.038×10^2	3.739	2.25	2.50
17	2.351×10^{-1}	3.679×10	8.277×10	3.739	2.25	2.50
18	6.391×10^{-1}	3.923×10	8.828×10	3.739	2.25	2.50
19	6.420×10^{-1}	7.249×10	1.631×10^2	3.739	2.25	2.50
20	5.564×10^{-1}	6.879×10	1.548×10^2	3.739	2.25	2.50
21	7.434×10^{-1}	6.837×10	1.480×10^2	3.739	2.16	2.50
22	5.650×10^{-1}	1.525×10^2	3.30×10^2	3.739	2.16	2.50
23	7.289×10^{-1}	2.148×10^2	4.65×10^2	3.739	2.16	2.50
24	1.019×10^{-1}	1.158×10^2	2.51×10^2	3.739	2.17	2.50
25	2.284×10^{-1}	2.059×10^2	4.46×10^2	3.739	2.17	2.50
26	1.050×10^{-1}	5.000×10	1.14×10^2	1.80×10^2	2.28	2.50
27	6.010×10^{-1}	1.900×10^2	3.73×10^2	6.00	2.07	2.50
28	6.350×10^{-1}	8.38×10	1.83×10^2	2.80	2.18	2.50
29	6.010×10^{-1}	9.26×10	1.90×10^2	3.00	2.05	2.50
30	8.750×10^{-1}	5.29×10^2	1.01×10^3	1.50×10^3	1.91	2.50

Table A.13 (continued)

Group	$\xi\sigma_T$	$\bar{\sigma}_a$	$\overline{v\sigma}_f$	$3\bar{\sigma}_{tr}$	$\bar{\eta}$	\bar{v}
31	2.740	1.79×10^2	3.990×10^2	5.40×10^2	2.23	2.50
32	1.430	1.405×10^2	3.217×10^2	3.739×10	2.29	2.50
33	1.545	1.27×10^2	2.9×10^2	5.40×10^2	2.29	2.50
34	1.545	3.40×10	6.54×10^2	8.47×10^2	2.29	2.50

Table A.14. Uranium-234

Group	$\xi\sigma_T$	$\bar{\sigma}_a$	$\overline{v\sigma}_f$	$3\bar{\sigma}_{tr}$
1	7.298×10^{-2}	1.556	3.875	1.754×10
2	6.865×10^{-2}	1.529	3.800	2.019×10
3	6.718×10^{-2}	1.353	3.350	1.990×10
4	8.020×10^{-2}	0.673	1.630	2.347×10
5	1.007×10^{-1}	0.083	0.121	3.176×10
6	1.122	0.067	0	3.709×10
7	1.188	0.118	0	4.011×10
8	1.167	2.104	0	4.104×10
9	1.234	0.373	0	4.187×10
10	1.258	0.615	0	4.187×10
11	1.044	9.054	0	3.290×10
12	1.068	2.077×10	0	3.290×10
13	1.075	5.957×10	0	3.290×10
14	1.083	5.486	0	3.290×10
15	1.099	1.833×10	0	3.290×10
16	1.122	2.109×10	0	3.290×10
17	1.132	7.901×10	0	3.290×10
18	1.152	2.402	0	3.290×10
19	1.165	2.595	0	3.290×10
20	1.176	2.690×10^2	0	3.290×10
21	1.199	2.932	0	3.290×10
22	1.229	3.245	0	3.290×10
23	1.254	3.573	0	3.290×10
24	1.293	3.943	0	3.290×10
25	1.350	4.504	0	3.290×10
26	1.244	5.216	0	2.692×10
27	1.324	6.509×10^2	0	2.692×10
28	1.420	1.158×10^3	0	2.692×10
29	1.593	8.645	0	2.692×10
30	1.871	1.125×10	0	2.692×10
31	2.228	1.496×10	0	2.692×10
32	2.454	1.844×10	0	2.692×10
33	2.749×10^{-1}	2.144×10	0	9.104×10
34	2.749×10^{-1}	5.54×10	0	2.20×10^2

Table A.15. Uranium-235

Group	$\xi\sigma_T$	$\bar{\sigma}_a$	$\bar{\nu\sigma}_f$	$3\bar{\sigma}_{tr}$	$\bar{\eta}$
1	6.62×10^{-2}	2.80	3.547	1.23×10	3.31
2	6.11×10^{-2}	2.80	2.195	1.44×10	2.76
3	5.71×10^{-2}	2.80	3.185	1.19×10	2.50
4	7.73×10^{-2}	2.80	3.124	1.46×10	2.26
5	1.00×10^{-1}	2.80	3.852	2.27×10	2.09
6	1.14×10^{-1}	2.80	5.36	2.92×10	1.92
7	1.23×10^{-1}	4.173	8.143	2.99×10	1.76
8	2.03×10^{-1}	7.44	1.14×10	3.74×10	1.54
9	2.46×10^{-1}	1.36×10	1.74×10	3.74×10	1.28
10	2.38×10^{-1}	1.97×10	2.92×10	3.74×10	1.48
11	3.44×10^{-1}	2.66×10	4.44×10	3.74×10	1.67
12	2.86×10^{-1}	2.78×10	5.63×10	3.74×10	2.02
13	3.82×10^{-1}	2.78×10	4.73×10	3.74×10	1.70
14	3.24×10^{-1}	3.76×10	7.08×10	3.74×10	1.88
15	3.44×10^{-1}	2.85×10	6.95×10	3.74×10	2.43
16	6.79×10^{-1}	5.12×10	1.09×10^2	3.74×10	2.14
17	5.94×10^{-1}	5.40×10	9.14×10	3.74×10	1.69
18	4.04×10^{-1}	4.52×10	9.42×10	3.74×10	2.08
19	3.82×10^{-1}	1.58×10^2	2.00×10^2	3.74×10	1.27
20	2.12×10^{-1}	5.97×10	1.04×10^2	3.74×10	1.75
21	5.40×10^{-1}	4.91×10	8.99×10	3.74×10	1.83
22	3.99×10^{-1}	1.01×10^2	1.29×10^2	3.74×10	1.28
23	4.42×10^{-1}	1.47×10^2	2.07×10^2	3.74×10	1.41
24	4.03×10^{-1}	6.19×10	8.46×10	3.74×10	1.37
25	2.80×10^{-1}	1.28×10^2	1.31×10^2	3.74×10	1.03
26	1.81×10^{-1}	1.14×10^2	2.38×10^2	3.74×10	2.09
27	2.39×10^{-1}	7.02×10	7.60×10	3.74×10	1.08
28	2.29×10^{-1}	2.95×10	2.40×10	3.74×10	0.81
29	2.97×10^{-1}	4.21×10	7.53×10	3.74×10	1.79
30	3.27×10^{-1}	3.39×10	4.09×10	3.74×10	1.21
31	6.45×10^{-1}	7.20×10	1.42×10^2	3.74×10	1.98
32	7.89×10^{-1}	7.17×10	1.45×10^2	3.74×10	2.03
33	1.12	9.22×10	1.99×10^2	3.25×10^2	2.16
34	1.12	3.05×10^2	6.29×10^2	9.62×10^2	2.06

Table A.16. Uranium-236

Group	$\xi\sigma_T$	$\bar{\sigma}_a$	$\bar{\nu\sigma}_f$	$3\bar{\sigma}_{tr}$
1	6.759×10^{-2}	1.196	2.965	1.754×10
2	6.167×10^{-2}	9.344×10^{-1}	2.242	2.019×10
3	5.992×10^{-2}	8.993×10^{-1}	1.592	1.990×10
4	7.831×10^{-2}	3.88×10^{-2}	9.325×10^{-2}	2.347×10
5	9.924×10^{-2}	2.69×10^{-3}	0	3.176×10
6	1.106×10^{-1}	4.80×10^{-3}	0	3.709×10
7	1.166×10^{-1}	8.50×10^{-3}	0	4.011×10
8	1.136×10^{-1}	1.52×10^{-2}	0	4.104×10
9	1.186×10^{-1}	2.69×10^{-2}	0	4.187×10
10	1.188×10^{-1}	4.44×10^{-2}	0	4.187×10
11	9.371×10^{-2}	7.14×10^{-2}	0	3.290×10
12	9.388×10^{-2}	1.944×10	0	3.290×10
13	9.394×10^{-2}	1.136×10^{-1}	0	3.290×10
14	9.400×10^{-2}	8.035×10	0	3.290×10
15	9.411×10^{-2}	1.304×10^{-1}	0	3.290×10
16	9.427×10^{-2}	1.467×10^{-1}	0	3.290×10
17	9.434×10^{-2}	9.507×10	0	3.290×10
18	9.449×10^{-2}	7.022×10	0	3.290×10
19	9.458×10^{-2}	7.142×10	0	3.290×10
20	9.466×10^{-2}	1.405×10	0	3.290×10
21	9.482×10^{-2}	7.452	0	3.290×10
22	9.504×10^{-2}	2.342×10^{-2}	0	3.290×10
23	9.522×10^{-2}	2.578×10^{-1}	0	3.290×10
24	9.550×10^{-2}	2.845×10^{-1}	0	3.290×10
25	9.591×10^{-2}	3.250×10^{-1}	0	3.290×10
26	7.946×10^{-2}	3.764×10^{-1}	0	2.692×10
27	8.004×10^{-2}	3.712×10^2	0	2.692×10
28	8.073×10^{-2}	3.616×10^2	0	2.692×10
29	8.196×10^{-2}	6.238×10^{-1}	0	2.692×10
30	8.395×10^{-2}	8.120×10^{-1}	0	2.692×10
31	7.710×10^{-2}	1.079	0	2.692×10
32	7.726×10^{-2}	1.331	0	2.692×10
33	9.85×10^{-2}	1.54	0	3.45×10
34	9.85×10^{-2}	2.10	0	3.05×10

Table A.17. Neptunium-237

Group	$\xi\sigma_T$	$\bar{\sigma}_a$	$\bar{v\sigma}_f$	$3\bar{\sigma}_{tr}$
1	0	1.970	5.110	6.000
2	0	1.450	3.780	4.350
3	0	1.340	3.480	4.020
4	0	0.382	0.994	1.100
5	0	0.025	0.065	0.075
6-28	0	0	0	0
29	0	8.52×10	0	2.85×10^2
30	0	2.08×10^2	0	6.50×10^2
31	0	1.72×10^2	0	5.40×10^2
32	0	3.74×10^2	0	1.50×10^2
33	0	6.35×10^2	0	0
34	0	1.07×10^2	0	0

Table A.18. Uranium-238

Group	$\xi\sigma_T$	$\bar{\sigma}_a$	$\bar{v\sigma}_f$	$3\bar{\sigma}_{tr}$
1	6.37×10^{-2}	7.74×10^{-1}	1.92	1.75×10
2	5.95×10^{-2}	6.04×10^{-1}	1.45	2.02×10
3	5.78×10^{-2}	3.48×10^{-1}	6.64×10^{-1}	1.99×10
4	7.88×10^{-2}	1.34×10^{-1}	0	2.35×10
5	1.01×10^{-1}	1.98×10^{-1}	0	3.18×10
6	1.13×10^{-1}	3.37×10^{-1}	0	3.71×10
7	1.21×10^{-1}	5.23×10^{-1}	0	4.01×10
8	1.22×10^{-1}	7.79×10^{-1}	0	4.10×10
9	1.27×10^{-1}	1.19	0	4.19×10
10	1.28×10^{-1}	2.30	0	4.19×10
11	1.03×10^{-1}	8.51	0	3.29×10
12	1.03×10^{-1}	2.61×10	0	3.29×10
13	1.03×10^{-1}	1.44	0	3.29×10
14	1.03×10^{-1}	1.16×10	0	3.29×10
15	1.03×10^{-1}	4.92×10	0	3.29×10
16	1.03×10^{-1}	1.26	0	3.29×10
17	1.03×10^{-1}	1.26	0	3.29×10
18	1.03×10^{-1}	1.26	0	3.29×10
19	1.03×10^{-1}	3.85×10^2	0	3.29×10
20	1.03×10^{-1}	1.26	0	3.29×10
21	1.03×10^{-1}	1.27	0	3.29×10
22	1.03×10^{-1}	2.76×10^2	0	3.29×10
23	1.03×10^{-1}	1.27	0	3.29×10
24	1.03×10^{-1}	1.28	0	3.29×10
25	1.03×10^{-1}	1.46	0	3.29×10

Table A.18 (continued)

Group	$\xi\sigma_T$	$\bar{\sigma}_a$	$\sqrt{\nu}\sigma_f$	$3\bar{\sigma}_{tr}$
26	8.62×10^{-2}	1.28	0	2.69×10
27	8.62×10^{-2}	4.14×10^2	0	2.69×10
28	8.63×10^{-2}	1.29	0	2.69×10
29	8.63×10^{-2}	1.30	0	2.69×10
30	8.64×10^{-2}	1.31	0	2.69×10
31	8.65×10^{-2}	1.32	0	2.69×10
32	8.65×10^{-2}	1.32	0	2.69×10
33	7.98×10^{-2}	6.01×10^{-1}	0	2.85×10
34	7.98×10^{-2}	1.36	0	3.47×10

Appendix B

EFFECTIVE THORIUM RESONANCE INTEGRALS

J. W. Miller*

Introduction

The "effective" resonance integral to lethargy u_m of a particular isotope in a mixture of isotopes is defined by the equation

$$I(\text{eff}) = \int_0^{u_m} (\sigma_{a0})_{\text{eff}} du .$$

The value of $(\sigma_{a0})_{\text{eff}}$ is a complex function of a number of variables. A most important item is the scattering power of the medium, measured by σ_p , macroscopic scattering cross section per thorium atom,

$$\sigma_p = \sum_n N_n \sigma_s^n / N_{\text{th}} .$$

The greater the scattering power, the greater the probability that a neutron will be slowed through a resonance without absorption. The thermal motion of absorber nuclei, on the other hand, increases the probability of absorption due to Doppler broadening of the resonances. This effect is small at 20°C, the standard temperature for reporting measured values, but increases at higher temperatures. Dresner has developed a method for computing the temperature effect for resolved resonances.¹

Group averaged cross sections for thorium are related to the effective resonance integral and were calculated by means of the equation

$$\overline{\sigma_i^a} = \frac{1}{\Delta u_i} \int_{u_i}^{u_i + \Delta u_i} (\sigma_{a0})_{\text{eff}} du ,$$

where i is the group number.

*Adapted from ORNL-CF 61-1-26.

Analysis

By assuming a Maxwell-Boltzmann speed distribution for the moderating medium and the Breit-Wigner formula for a single resonance, Dresner² has arrived at the following equation for the resonance integral, I_{eff} , for a single absorption resonance:

$$I_{\text{eff}} = \frac{\pi}{2} \frac{\sigma_0 \Gamma \gamma}{E_0} \frac{2\beta}{\pi} J(\xi, k),$$

where

$$\sigma_0 = \frac{4\pi \chi^2 \Gamma n}{\Gamma},$$

$$\beta = \frac{\sigma_p}{\sigma_0},$$

$$\xi = \frac{\Gamma}{\Delta},$$

$$\Delta = \left(\frac{4\mu E K T}{M} \right)^{1/2},$$

$$k = \frac{\ln \beta + 5 \ln 10}{\ln 2}.$$

Other terms are defined in the nomenclature.

The function $J(\xi, k)$ is tabulated in ref. 1. The tabulated results have been plotted as the family of curves in Fig. B.1.

The reduced mass of the neutron μ is equal to neutron mass (~ 1.0) multiplied by $M/(M+1)$, where M is the mass of the absorbing atoms. Since the mass of thorium is 232, μ was taken as unity for these calculations.

Table B.1 lists the resonance parameters for each of the 13 resolved thorium resonances (2). These parameters were used in the equation for I_{eff} for computing the resonance integral for each resonance. (Since these calculations were performed, additional thorium resonances have been resolved, and improved parameter values for previously resolved resonances have been obtained. The effect of these new values has not been evaluated.) The total resonance integral for each energy group is then obtained by adding together the separate integrals for each resonance. Table B.1 also

ORNL-LR-DWG. 54604

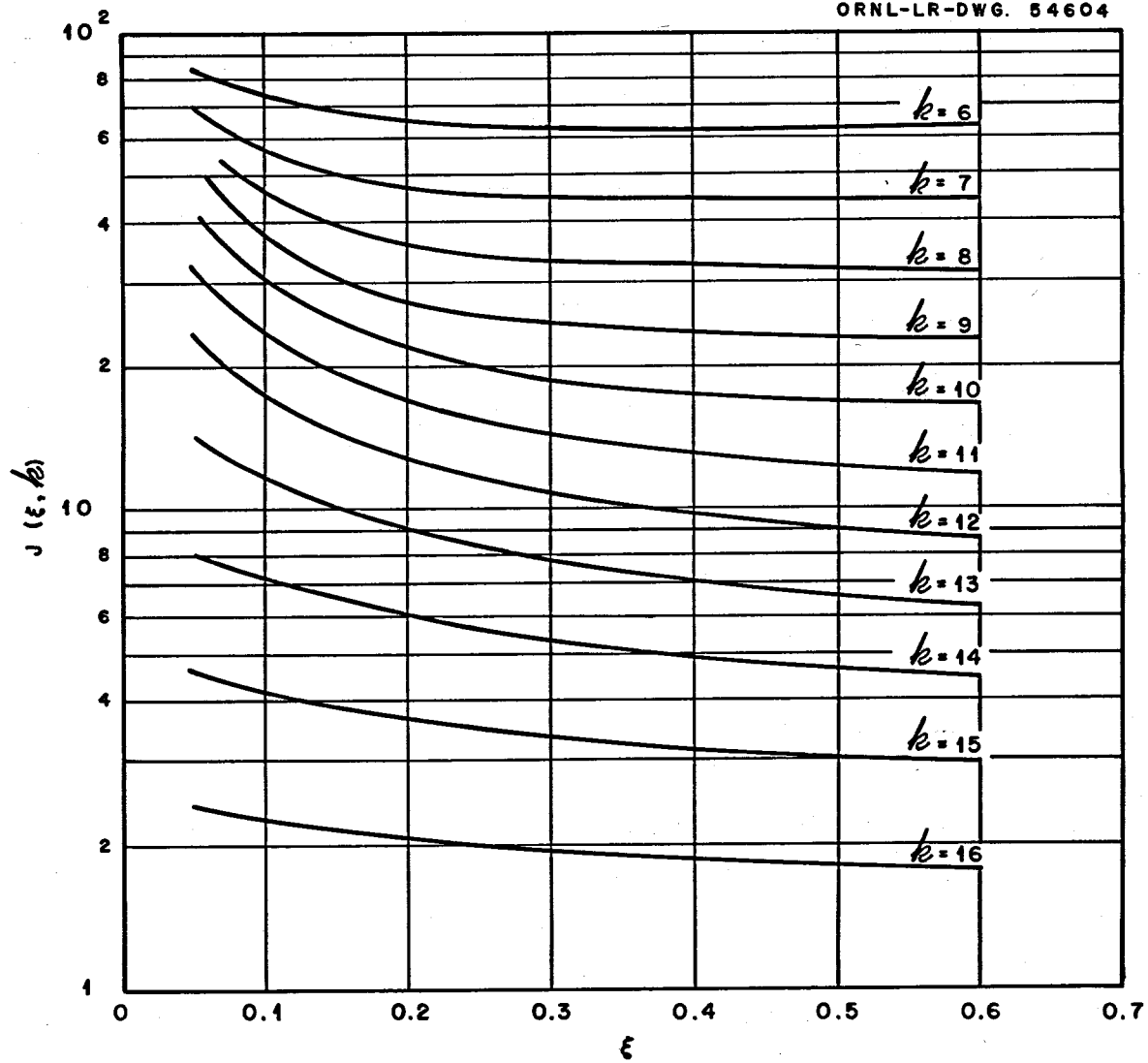
Fig. B.1. $J(\xi, k)$ Versus ξ for $k = 6.16$.

Table B.1. Resonance Parameters of Thorium-232

GNU Group No.	Δu	E_0 (ev)	Γ_n (ev)	Γ_γ (ev)	Infinite Dilution Resonance Integral	
11	0.98083	235	0.0017	0.034	7.10	
		234	0.027	0.034		
		212	0.0012	0.034		
		201	0.016	0.034		
		195	0.022	0.034		
		172	0.067	0.034		
12	0.40547	130	0.009	0.034	8.4	
		122	0.023	0.034		
		114	0.013	0.034		
15	0.20763	69.7	0.039	0.043	17.2	
16	0.26236	59.6	0.0046	0.021	4.4	
22	0.22314	23.6	0.004	0.039	44.2	
		21.9	0.0022	0.034		
Unresolved Resonances - Group 1 through Group 10					5.3	
Nonresonance Contribution - Groups 13, 14, 17-21, and 23-33					10.3	
Total - Cut-off at 0.0795 ev					96.9	

lists the lethargy width for each group. The group-averaged cross section is simply the group total resonance integral divided by the group lethargy width.

The infinite-dilution resonance integral (I_∞) for a particular resonance may be obtained from

$$I_\infty = - \frac{\pi}{2} \sigma_0 \frac{\Gamma_\gamma}{E_0} .$$

Sample Calculation

Example: Compute the effective resonance integral (I_{eff}) for the thorium resonance at 23.6 ev with a carbon-to-thorium ratio of 200 and an absorber temperature of 649°C. The nonresonance scattering cross section, σ_s^C , of carbon is 4.8 barns, and the thorium nonresonance scattering cross section, σ_s^{Th} , is 12.5 barns.

$$1. \quad \sigma_p = \sigma_s^{\text{Th}} + \left(\frac{N_c}{N_{\text{Th}}} \right) \sigma_s^C$$

$$= 972.5 \text{ barns} .$$

$$2. \quad \pi^2 = \left(\frac{2.86 \times 10^{-9}}{2 \pi \sqrt{E}} \right)^2$$

$$= 0.877 \times 10^{-20} \text{ cm}^2 .$$

$$3. \quad \sigma_o = 4\pi\pi^2 \frac{\Gamma_n}{\Gamma}$$

$$= 10,250 \text{ barns} .$$

$$4. \quad \beta = \frac{\sigma_p}{\sigma_o}$$

$$= 0.0949 .$$

$$5. \quad \Delta = \left(\frac{4\mu E K T}{M} \right)^{1/2}$$

$$= 0.1797 .$$

$$6. \quad \xi = \frac{\Gamma}{\Delta}$$

$$= 0.2393 .$$

$$7. \quad k = \frac{\ln \beta + 5 \ln 10}{\ln 2}$$

$$= 13.2$$

$$8. \quad J(\xi, k) = J(0.2393, 13.2)$$

$$= 7.6 \text{ (from Fig. B.1).}$$

$$9. \quad I_{\text{eff}} = \frac{\pi \sigma_0 \Gamma_\gamma}{2 E_0} \frac{2 \beta}{\pi} J(\xi, k)$$

$$= 12.2 \text{ barns.}$$

The infinite-dilution resonance integral (I_∞) obtained is 26.6 barns for the case considered.

Results

The MERC-1 program used in the MSCR study is a 34-group diffusion-theory code. The group structure is such that the resolved resonances of thorium fall into five groups: 11, 12, 15, 16, and 22. The group-averaged absorption cross section for each of these five groups as a function of σ_p at 649°C is plotted in Fig. B-2. The total resolved resonance integral is plotted in Fig. B-3 for three reactor temperatures.

Symbols

Γ_γ = Radiative capture width (ev)

Γ_n = Neutron width (ev)

Γ = Total width (ev)

$\pi = \frac{\text{Wavelength of the neutron}}{2}$ (cm)

E_0 = Resonance energy (ev)

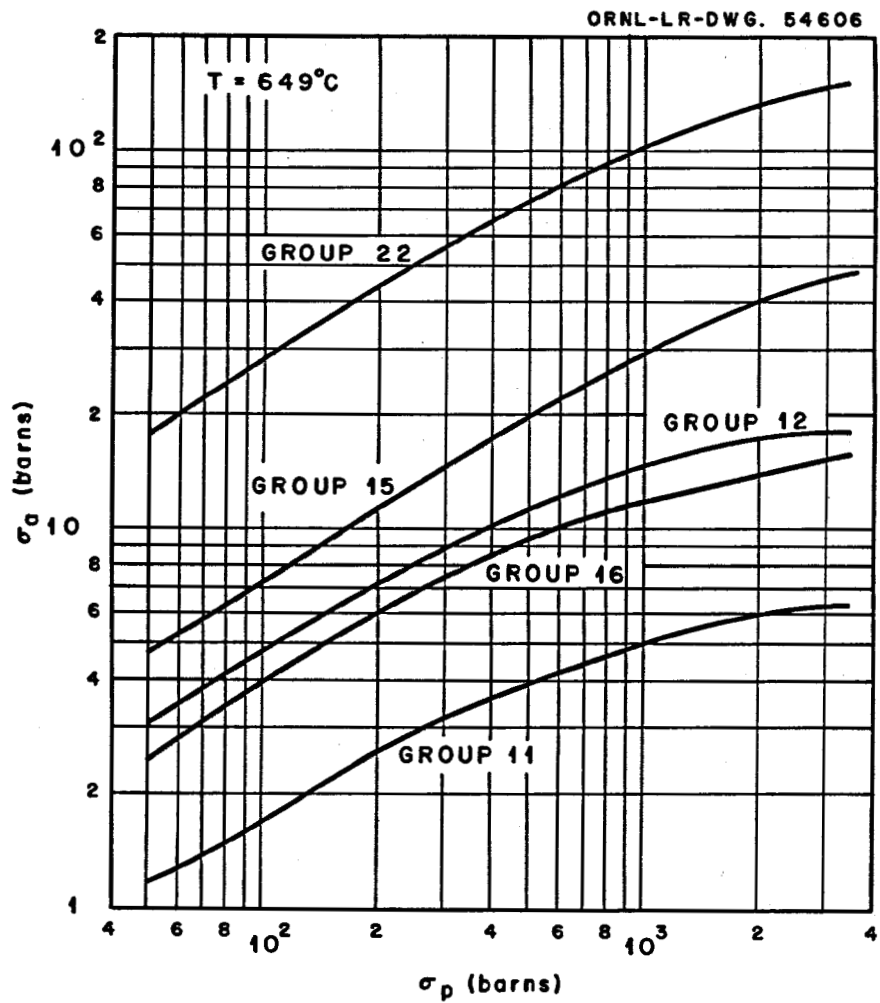


Fig. B.2. Group Averaged Absorption Cross Section Versus σ_p 649°C.

ORNL-LR-DWG. 54608

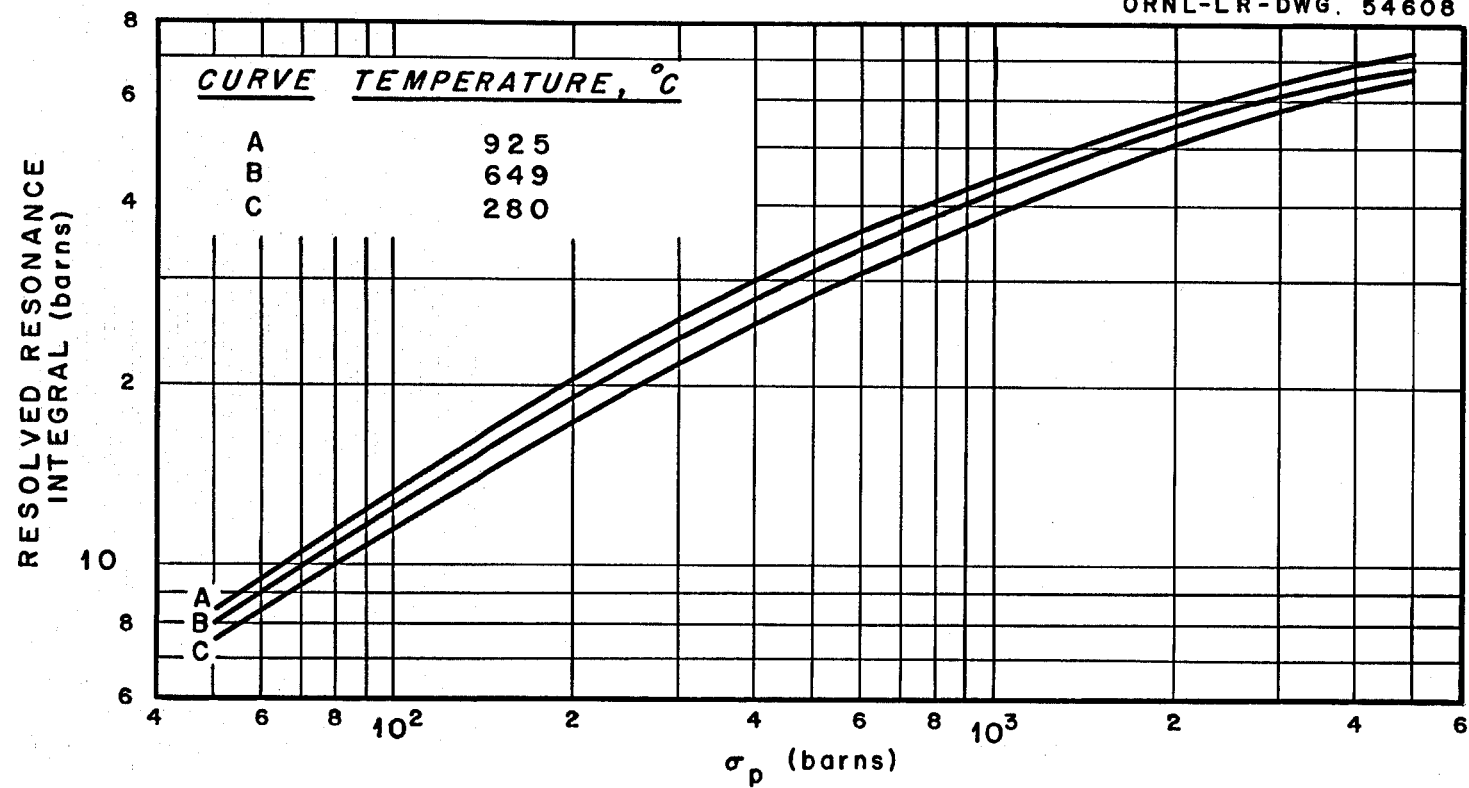


Fig. B.3. Total Resolved Resonance Integral Versus σ_p for Moderator Temperatures of 280°C, 649°C, and 925°C.

σ_p = Nonresonance scattering cross section (macroscopic scattering cross section per thorium atom density)
E = Relative energy in the center-of-mass-system
M = Mass of absorbing nucleus (amu)
KT = Absorber temperature in energy units (ev)
 μ = Reduced mass of neutrons (amu)

References

1. Lawrence Dresner, Tables for Computing Effective Resonance Integrals Including Doppler Broadening of Nuclear Resonances, USAEC Report ORNL-CF 55-9-74, Oak Ridge National Laboratory, September 19, 1955.
2. D. J. Hughes and R. B. Schwartz, Neutron Cross Sections, USAEC Report BNL-325, Brookhaven National Laboratory, July 1, 1958.

Appendix C

ENERGY DEPENDENCE OF ETA OF $^{233}\text{U}^*$

C. W. Nestor

Summary

A parameter of great interest in nuclear calculations of a thorium reactor is η , the number of neutrons produced per neutron absorbed. Experimental information on the energy dependence of η in the range of 0 to 10 ev as measured at the MTR was used to calculate group averaged fission cross sections, using absorption cross sections calculated from the recent total cross section data^{1,2} and the scattering cross section as calculated by Vogt.¹ The η values used in preparation of the cross sections was normalized to a 2200 m/sec value of 2.29.³

In the energy range of 0 to 0.8 ev, η was assumed to be constant at 2.29. In the range of 0.8 ev to 10 ev, as mentioned, group averaged values of $\bar{\eta}\sigma_f = \bar{\eta}\sigma_a$ were calculated by numerical evaluation of the integrals

$$\bar{\eta} = \frac{\int \eta(E) \sigma_a(E) \frac{dE}{E}}{\int \sigma_a(E) \frac{dE}{E}}$$

$$\bar{\sigma}_a = \frac{1}{\Delta u} \int \sigma_a(E) \frac{dE}{E}$$

where Δu denotes the lethargy width of the group.

In the range of 10 ev to 30 ev η was estimated to be 2.17; the data of Gaerttner and Yeater⁴ indicate an average η in this range of about 0.95 times the 2200 m/sec value.

*Adapted from ORNL-CF 61-6-87 (Rev).

From 30 ev to 30 kev, η was assumed to be 2.25; this is the value reported by Spivak⁵ et al., at 30 kev.

From 20 kev to 900 kev, measurements of η are available;⁵ fission cross sections are reported in BNL-325 for the range 30 kev to 10 Mev. The total cross section in this range was taken to be equal to that of ^{235}U , as suggested by J. A. Harvey.¹ The value of v was assumed to be linear in energy with a 2200 m/sec value of 2.50 (ref. 3) and a slope of 0.127 per Mev.⁶ A plot of the experimental η and the group averaged values from 0.01 ev to 1 kev is shown in Fig. C.1. Group values are also listed in Table A.1 of Appendix A.

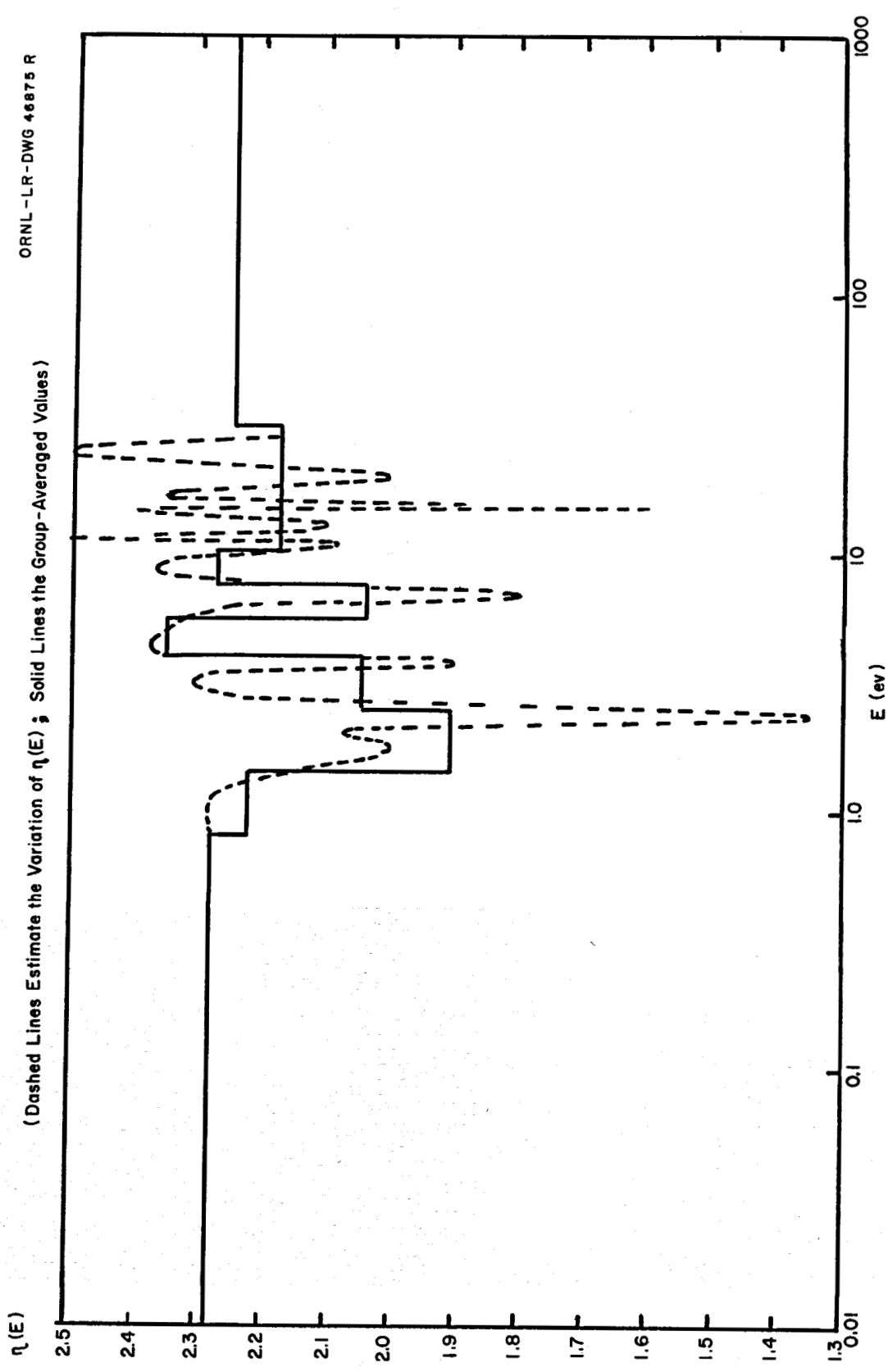


Fig. C.1. Group Values of $\gamma_23(e)$ Used in MSCR Study.

References

1. J. A. Harvey, ORNL, personal communication to C. W. Nestor, ORNL, March 1960.
2. M. S. Moore, MTR Nuclear Physics Group, personal communication to C. W. Nestor, ORNL, March 1960.
3. J. E. Evans, reported at the Argonne National Laboratory Conference on the Physics of Breeding, October 1959.
4. E. R. Gaerttner and M. L. Yeater, Reports to the AEC Nuclear Cross Section Advisory Group, USAEC Report Wash-194, USAEC, February 1958.
5. P. E. Spivak et al., Measurement of Eta for ^{233}U , ^{235}U , and ^{239}Pu with Epithermal Neutrons, J. Nucl. Energy, 4:70 (January 1957).
6. G. N. Smirenkin et al., J. Nucl. Energy, 9:155 (1955).

Appendix D

THE MERC-1 EQUILIBRIUM REACTOR CODE

T. W. Kerlin

Introduction

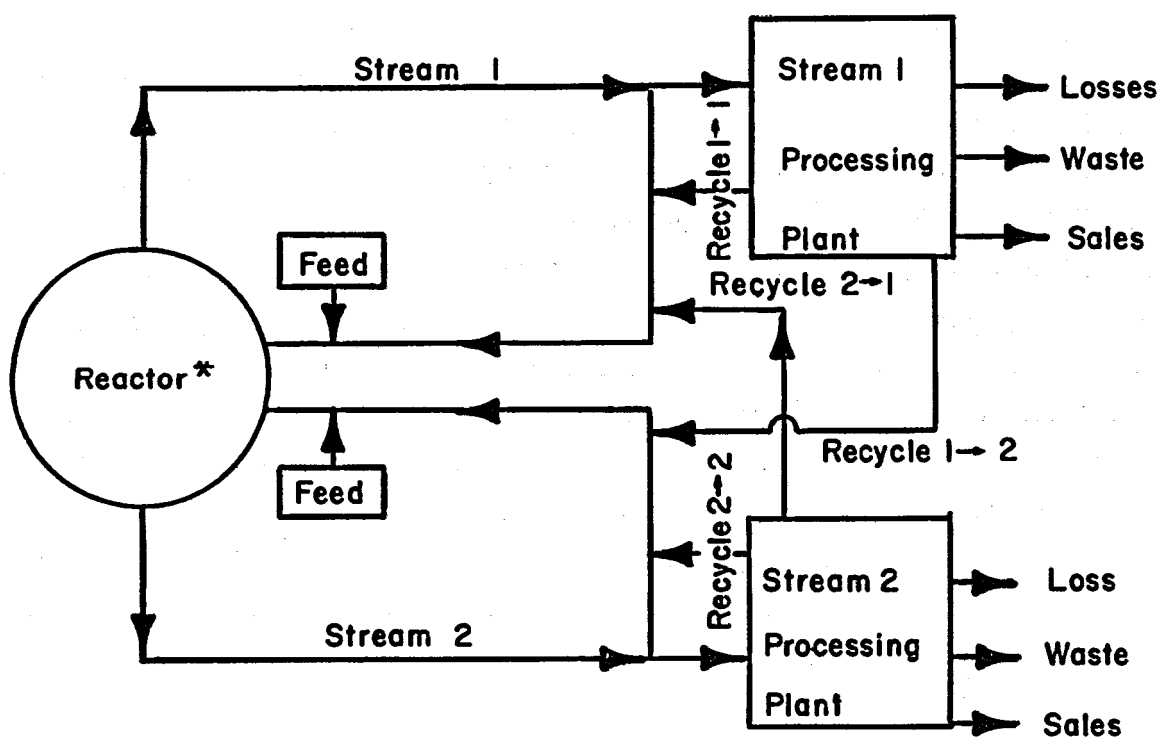
The MERC-1 code automatically calculates the composition of a fluid-fuel reactor so that equilibrium and criticality conditions are simultaneously satisfied. MERC-1 uses the MODRIC¹ multigroup-diffusion-theory code and the ERC-10 equilibrium reactor code as chain links. These codes were previously used separately at ORNL in iterative calculations to determine equilibrium reactor compositions. MODRIC was developed by the Central Data Processing Group at the Oak Ridge Gaseous Diffusion Plant as a replacement for GNU.² The ERC-10 code was prepared as a later version of ERC-5.³ The MERC-1 code automatically transmits necessary data from one chain link to the other until sufficient iterations have been performed to cause criticality and equilibrium requirements to be satisfied simultaneously. The output consists of equilibrium concentrations, a neutron balance, and fuel-cycle costs.

The system which is considered in the MERC-1 analysis is shown in Fig. D.1. A complete specification of data required for controlling the flow and losses in each stream is included in the MERC-1 input. Note in Fig. D.1 that material is removed from the reactor system by losses, waste, and sale as well as by nuclear transformation (decay and neutron absorption), and that fresh material is fed to the system. Therefore, the calculated equilibrium concentrations are in equilibrium with respect to the feed and discharge rates as well as with respect to nuclear transformation rates.

Theory

MODRIC is a typical neutron-diffusion-theory code. It allows 50 neutron energy groups with downscattering from a group to any of the

ORNL-LR-DWG 76824



*The reactor may have as many as two active regions, and each region may contain either or both of the fluid streams

Fig. D.1. The Reactor System.

following ten groups. It will perform concentration searches on specified elements. The output consists of criticality search converged concentrations, group macroscopic cross sections, normalized nuclear events (absorptions, fission, leakage, etc.) by region and group, absorptions and fissions by material and region, group flux distributions, and fission density distributions.

ERC-10 requires extensive input. Rewriting of large quantities of input is avoided by using basic input decks which include information applicable to a number of cases. To specify a new case, it is necessary only to specify changes in the basic input deck. For instance, one might prepare a basic input deck for a particular reactor with a given power level. A set of cases with different power levels would need only the basic input deck and the new power level as input.

Basically, ERC solves two equations. They are:

$$v_j \frac{dN_{ij}}{dt} = Q_{ij}^f + R_{ij} + F_{ij} + T_{ij} + D_{ij} - N_{ij} (t_{ij} + d_{ij} + q_{ij} - r_{ij}) = 0 , \quad (1)$$

or if the material must be fed to maintain criticality

$$\left(N_{ij}^{s-1} - N_{ij}^s \right) v_i \sum_k C_{ijk}^f = \sum_{ijk}^{s-1} N_{ij}^{s-1} C_{ijk}^a - \sum_{ijk}^{s-1} N_{ij}^{s-1} C_{ijk}^f v_i . \quad (2)$$

Equation (2) is just the conservation requirement, saying that enough fissile material must be added (or removed) in iteration s to overcome the neutron production deficiency (or excess) in iteration (s-1). These are inner iterations in ERC. The terms are defined as:

v_j = volume of stream j, cm^3 ,

N_{ij} = atoms of material i per barn cm of stream j,

t = time, sec,

- Q_{ij} = feed rate of material i into stream j, atoms/sec,
 R_{ij} = rate of growth of material i in stream j due to recycle from
 other streams, atoms/sec,
 F_{ij} = rate of growth of fission fragment i in stream j, atoms/sec,
 T_{ij} = rate of growth of material i in stream j due to neutron ab-
 sorptions in other materials, atoms/sec,
 D_{ij} = rate of growth of material i in stream j due to radioactive
 decay of other materials, atoms/sec,
 t_{ij} = rate coefficient for loss of material i in stream j because
 of neutron capture, atoms per sec per atom/barn cm,
 d_{ij} = rate coefficient for loss of material i in stream j because
 of radioactive decay, atoms per sec per atom/barn cm,
 q_{ij} = rate coefficient for loss of material i in stream j because
 of processing removal, atoms per sec per atom/barn cm,
 r_{ij} = rate coefficient for growth of material i in stream j because
 of recycle from stream j, atoms per sec per atom/barn cm,
 v_i = neutrons produced per fission in material i,
 C_{ijk}^f = reaction rate coefficient, number of fissions in material i
 per atom/barn cm in stream j in region k per fission neutron
 born in reactor,
 C_{ijk}^a = reaction rate coefficient, number of absorptions in material
 i per atom/barn cm in stream j in region k per fission neutron
 born in reactor.

Superscripts:

- i = material,
- j = stream,
- k = region.

The use of stream and region indexes allows reactors with two streams in the same region to be analyzed.

The equilibrium concentration calculations in ERC use reaction rate coefficients (C_{ijk}^f) obtained from an earlier MODRIC calculation. However, the initial concentrations used in the MODRIC calculation will not, in general, agree with the equilibrium concentrations computed by ERC. This new set of concentrations will alter the neutron spectrum and flux level, thereby changing the reaction rate coefficients. Therefore, it is necessary to repeat the MODRIC criticality calculation with the latest value for the estimated concentrations to get new reaction rate coefficients.

This process is repeated until the MODRIC and ERC concentrations are equal. The flow of information in the code is shown in Fig. D.2.

The reaction rate coefficients (C_{ijk}) used in ERC are spectrum-averaged cross sections which are available directly from MODRIC. The MODRIC calculation gives A_{ik} and $v_{iF_{ik}}$, the absorptions and neutron productions in material i in region k , normalized to 1.0 total neutron produced. The distribution of nuclear events between two streams in a region is accomplished by introducing the stream volume fractions, f_{jk} , in this manner:

$$A_{ijk} = A_{ik} \cdot \left(\frac{\text{atoms of } i \text{ in stream } j \text{ in region } k}{\text{atoms of } i \text{ in region } k} \right),$$

$$v_{iF_{ijk}} = v_{iF_{ik}} \cdot \left(\frac{\text{atoms of } i \text{ in stream } j \text{ in region } k}{\text{atoms of } i \text{ in region } k} \right).$$

The multiplying factor in each term is

$$\left(\frac{\text{atoms of } i \text{ in stream } j \text{ in region } k}{\text{atoms of } i \text{ in region } k} \right) = \frac{N_{ij} f_{jk}}{\sum_j N_{ij} f_{jk}},$$

where the units on these factors are

$$N_{ij} = \frac{\text{atoms of } i \text{ in stream } j}{\text{barn cm of stream } j},$$

$$f_{jk} = \frac{\text{cm}^3 \text{ of stream } j \text{ in region } k}{\text{cm}^3 \text{ of region } k}.$$

The material, stream, and region dependent absorption and production terms are automatically transferred from the MODRIC link to the ERC link of the MERC-1 calculation. ERC obtains the reaction rate coefficients (intensive quantities) from the absorption and production terms (extensive quantities) by dividing by N_{ij} , the stream concentration

$$C_{ijk} = \frac{A_{ijk}}{N_{ij}},$$

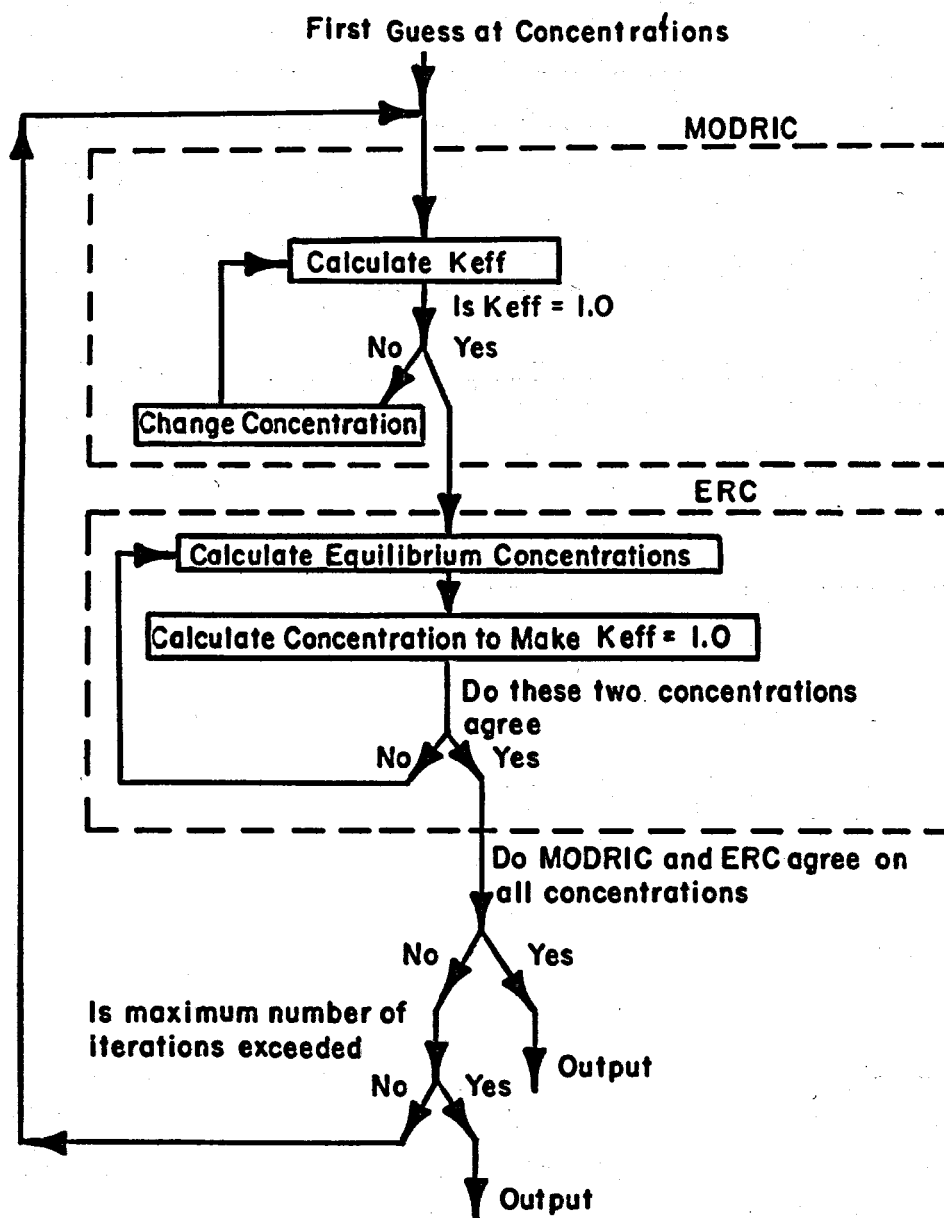


Fig. D.2. The MERC Flow Diagram.

$$v_i C_{ijk} = \frac{v_i F_{ijk}}{N_{ij}}.$$

The absolute reaction rate coefficient \bar{C}_{ijk} is obtained in the ERC calculation using the total neutron production rate as determined by the reactor power

$$\bar{C}_{ijk}^a = C_{ijk}^a \times 3.1 \times 10^{16} P \bar{v} \times 10^{-24},$$

where

3.1×10^{16} = number of fissions per sec per megawatt,

P = power level in megawatts,

\bar{v} = average number of neutrons produced per fission

$$= \frac{\sum_{ijk} N_{ij} C_{ijk}^f v_i}{\sum_{ijk} N_{ij} C_{ijk}^f}.$$

A similar argument applies for the fission reaction rate.

The restriction to fluid-fuel reactors occurs because the ERC calculation requires that the reactor discharge composition be equal to the mean reactor composition. This restriction is satisfied in fluid-fuel reactors but not in solid-fuel reactors where the discharge has experienced a much greater exposure than the mean.

In ERC-10, effective, one-group cross sections of individual fission products were calculated by reference to a standard absorber exposed to the MSCR spectrum of neutrons as generated by the multigroup program Modric. The thermal cross section and the resonance integral can be used in a two-group model to calculate relative one-group cross sections. Thus, set

$$\bar{\sigma} \bar{\phi} = \sigma_e \phi_e + \sigma_t \phi_t$$

where the bar denotes effective, one-group values, "e" denotes "epithermal," and "t" denotes "thermal." Rearranging and taking a ratio of the cross

section of the i^{th} material to that of a standard material, denoted by the subscript "s,"

$$\frac{\bar{\sigma}_i}{\bar{\sigma}_s} = \frac{\left(\sigma_t + \frac{\phi_e}{\phi_t} \sigma_e \right)_i}{\left(\sigma_t + \frac{\phi_e}{\phi_t} \sigma_e \right)_s}$$

The epithermal cross section is defined in terms of the resonance integral by the relation

$$\sigma_e = \frac{\int_0^{u_e} \sigma du}{\int_0^{u_e} du} = \frac{RI}{u_e}$$

where u_e is the lethargy at the lower energy bound of the epithermal group.

The ratio $\frac{\phi_e}{\phi_t}$ is obtained by equating the slowing down current from the epithermal group to neutrons absorbed or leaking in the thermal group.

$$\Sigma_{r,e} \phi_e = (\Sigma_{a,t} + D_t B^2) \phi_t$$

where $\Sigma_{r,e}$ is the "removal" cross section.

$$\text{Let } \Sigma_{r,e} \approx \xi \Sigma_{T,e} / u_e$$

where T denotes "total." Ignoring leakage gives

$$\frac{\phi_e}{\phi_t} = \frac{\Sigma_{a,t} u_R}{\Sigma_{t,e}}$$

Combining these results gives

$$\bar{\sigma}_i = \bar{\sigma}_s \frac{\left[\sigma_{t,e} + K(RI)_i \right]}{\left[\sigma_{t,s} + K(RI)_s \right]}$$

where

$$K = \frac{\sum_{a,t}}{\xi \sum_T} .$$

The spectral index, K, is computed by Modric from input data. The reference element was the standard absorber referred to above. The product of the reference element cross section and the effective flux integrated over the core is computed from Modric output by dividing the fraction of neutrons as absorbed by the reference element by its atomic density, N_s . This product is the desired number for use in the ERC calculations; the working equation becomes

$$\bar{\sigma}_i \bar{\phi} V = \frac{A}{N_s} \frac{\left[\sigma_{t,i} + K(RI)_i \right]}{\left[\sigma_{t,s} + K(RI)_s \right]} .$$

The thermal cross sections σ_t are computed from the 2200 m/s cross sections by multiplying by a factor that averages them over a Maxwell-Boltzman spectrum around the reactor temperature. This factor was computed for a $1/v$ energy dependence of the cross section and applied uniformly to all fission product isotopes, except noble gases.

In all, 115 fission product isotopes were so treated, linked by transmutation and decay into chains. Provision was made in ERC-11 to remove each at a rate determined by its chemical or physical properties in relation to the processing method. For instance, xenon is removed rapidly by transpiration in an expansion chamber, whereas rare earths are removed only by discard of the fuel salt with a period measured in hundreds of days.

Xenon was treated separately in the Modric calculation, not only to determine accurately its effective cross section in the MSCR neutron spectrum but also to permit special treatment of its exceptional behavior. It may be possible to remove xenon rapidly from the fuel solution by circulating a portion of the salt through the dome of the expansion tank mounted over the core (Sec. 4.2.2) provided the xenon does not diffuse rapidly into the moderator graphite. Provision was made in ERC-11 to calculate the extreme cases (complete absorption in graphite vs. zero absorption) as well as intermediate situations where removal competes with absorption.

Samarium was also treated separately because of its importance.

The fission product calculation is thought to result in a reasonably good approximation of the poisoning in reactors where the fission products are exposed to neutrons for a long time. The ingrowth of second and higher generation isotopes by transmutation and decay is treated in detail. The transient period following start-up of a clean reactor with an initial loading of ^{235}U is ignored, and all concentrations are calculated at their maximum, equilibrium values. Hence, the poisoning is overestimated somewhat, thus providing a margin of safety in respect to assignment of the cross sections and resonance integrals.

The fission-product reaction rate coefficient is obtained by reference to a specified standard absorber:

$$C^{\text{FP}} = C^R \frac{\sigma^{\text{FP}}}{\sigma^R}, \quad (3)$$

where

C^{FP} = fission-product reaction rate coefficient,

C^R = reference material reaction rate coefficient,

σ^{FP} = effective fission-product absorption cross section,

σ^R = effective reference material absorption cross section.

The effective cross section ratio is obtained from a two-group formulation:

$$\frac{\sigma^{\text{FP}}}{\sigma^R} = \frac{(\sigma_1 \phi_1/\phi_2 + \sigma_2)^{\text{FP}}}{(\sigma_1 \phi_1/\phi_2 + \sigma_2)^R}, \quad (4)$$

where

σ_1 = fast absorption cross section

$$= \frac{\int_0^{u_{\text{th}}} \sigma_a(u) du}{u_{\text{th}}} = \frac{(RI)_a}{u_{\text{th}}},$$

$\bar{\sigma}_2$ = absorption cross section averaged over the thermal flux,

ϕ_1 = fast flux,

ϕ_2 = average thermal flux.

For a two-group treatment, all neutrons removed from the fast group must either be absorbed or leak from the reactor while thermal:

$$\sum_{R_1} \phi_1 = \sum_{a_2} \phi_2 + DB^2 \phi_2 .$$

Ignoring leakage,

$$\frac{\phi_1}{\phi_2} = \frac{\sum_{a_2}}{\sum_{R_1}} . \quad (5)$$

Also,

$$\sigma_2 = f \sigma_a^{2200} \quad (6)$$

where

f = thermal spectrum factor = $\sqrt{\left(\frac{\pi}{4}\right)\left(\frac{298}{T+273}\right)}$ for a Maxwell-Boltzmann distribution,

σ_a^{2200} = 2200 m/s absorption cross section.

Substituting Eqs. (4), (5), and (6) into Eq. (3) gives

$$C^{FP} = C^R \left\{ \frac{\left[K(RI) + \sigma_a^{2200} \right]^{FP}}{\alpha} \right\} \quad (7)$$

where

$$K = \frac{\sum_{a_2}}{\sum_{R_1} f \Delta u} ,$$

$$\alpha = \left[K(RI) + \sigma_a^{2200} \right]^R .$$

K is calculated as follows:

$$K = WS ,$$

$W = \frac{1}{f \Delta u} =$ input to linkage section of input,

$S = \sum_{a_2} / \sum_{R_1} =$ value automatically calculated by MODRIC.

The value of α must be specified if fission product option 1 is specified on card BN=5. This value should be calculated using an estimated value for K. If fission product option 2 is specified on card BN-5, α is calculated by the code using the latest value of K. The required values of σ_a^{2200} and RI for a special reference material are built into the code for fission product option 2. The nuclear constants for a l/v absorber with a 2200 m/s cross section of 1.0 barns are built into the code. Therefore, to use fission product option 2, the reference element must correspond to an artificial element in MODRIC which has cross sections for a l/v absorber with $\sigma_a^{2200} = 1.0$.

References

1. J. Replogle, MODRIC - A One-Dimensional Neutron Diffusion Code, USAEC Report K-1520, Oak Ridge Gaseous Diffusion Plant, September 1962.
2. C. L. Davis, J. M. Bookston, and B. E. Smith, GNU-II, A Multigroup One-Dimensional Diffusion Program for the IBM-704, GMR-101, General Motors, November 12, 1957.
3. L. G. Alexander, ERC-5 Program for Computing the Equilibrium States of Two-Region Thorium Breeder Reactors, USAEC Report ORNL CF-60-10-87, Oak Ridge National Laboratory, October 1960.

Appendix E

FISSION PRODUCT NUCLEAR DATA^a

L. G. Alexander

Number	Isotope	Fission Yield ^b		β , Decay λ , sec ⁻¹	Cross Section σ , barns	Resonance Integral RI, barns
		²³³ U	²³⁵ U			
26	⁸² Se	0.007	0.0028		2.1	1.4
27	⁸¹ Br	0.0045	0.0014		3.3	60
28	⁸² Kr				45	45
29	⁸³ Kr	0.012	0.00544		205	201
30	⁸⁴ Kr	0.019	0.010		0.16	5.5
31	⁸⁵ Kr	0.006	0.00293	0.214×10^{-8}	7	29
32	⁸⁶ Kr	0.032	0.0202		0.06	0.04
33	⁸⁵ Rb	0.019	0.010		0.91	0.67
34	⁸⁷ Rb	0.040	0.249		0.13	0.21
35	⁸⁶ Sr				1.3	(0.6) ^c
36	⁸⁷ Sr					
37	⁸⁸ Sr	0.050	0.0357		0.0055	0.06
38	⁸⁹ Y	0.065	0.0479		1.31	0.78
39	⁹⁰ Y	0.065	0.0577	0.298×10^{-5}	1	1.8
40	⁹¹ Zr	0.065	0.0584		1.2	9
41	⁹² Zr	0.067	0.0603		0.15	0.55
42	⁹³ Zr	0.070	0.0645		1.1	28
43	⁹⁴ Zr	0.068	0.0640		0.076	0.2
44	⁹⁵ Zr	0.057	0.0633		0.053	0.07
45	⁹⁵ Nb			0.229×10^{-6}		
46	⁹⁵ Mo	0.062	0.0627		13.9	109
47	⁹⁶ Mo				1.2	34
48	⁹⁷ Mo	0.053	0.0609		2.2	16
49	⁹⁸ Mo	0.052	0.0578		0.51	5.6
50	¹⁰⁰ Mo	0.044	0.0630		0.3	6.2
51	⁹⁹ Te	0.048	0.0606		22.2	140
52	¹⁰⁰ Ru				1.7	7
53	¹⁰¹ Ru	0.030	0.050		5	77
54	¹⁰² Ru	0.024	0.041		1.44	11
55	¹⁰⁴ Ru	0.0097	0.018		0.7	8
56	¹⁰³ Rh	0.016	0.030		184	1030
57	¹⁰⁴ Pd				6	19
58	¹⁰⁵ Pd	0.005	0.009		11	76
59	¹⁰⁶ Pd	0.0028	0.0038		6	12
60	¹⁰⁷ Pd	0.0015	0.0019		10	40
61	¹⁰⁸ Pd	0.0006	0.0007		10.7	169
62	¹¹⁰ Pd	0.0003	0.00024		0.28	10

^aCompiled from Appendix E list of references.^bAtoms per fission.^cValues in parentheses estimated by comparison with similar nuclides.

Fission Product Nuclear Data (continued)

Number	Isotope	Fission Yield		β , Decay λ , sec ⁻¹	Cross Section gr, barns	Resonance Integral RI, barns
		²³³ U	²³⁵ U			
63	¹⁰⁹ Ag	0.0004	0.0003		91	1420
64	¹¹¹ Cd	0.00025	0.00019		2	52
65	¹¹² Cd	0.0002	0.0001		1	13
66	¹¹³ Cd	0.0002	0.0001		59,500	652
67	¹¹⁴ Cd	0.0002	0.0001		1.2	15
68	¹¹⁵ In	0.0002	0.0001		228	3300
69	¹¹⁶ Sn				0.006	
70	¹²⁵ Te				1.56	(0.8)
71	¹²⁶ Te	0.0024	0.0005		0.8	12
72	¹²⁸ Te	0.010	0.0037		0.3	2
73	¹²⁷ I	0.0039	0.0013		6.2	154
74	¹²⁹ I	0.02	0.009		27	39
75	¹²⁸ Xe				5	45
76	¹²⁹ Xe				45	302
77	¹³⁰ Xe				5	45
78	¹³¹ Xe	0.037	0.0293		120	806
79	¹³² Xe	0.051	0.0438		0.2	1.8
80	¹³³ Xe			0.152 × 10 ⁻⁵	190	1270
81	¹³⁴ Xe	0.066	0.0806		0.2	0.6
82	¹³⁵ Xe ^d	0.067 ^d	0.0641 ^d	0.211 × 10 ⁻⁴	3.344 × 10	0.6512 × 10
83	¹³⁶ Xe	0.069	0.0646	0.296 × 10 ⁻³	0.15	0.1
84	¹³³ Cs	0.062	0.0659		28	420
85	¹³⁴ Cs			0.110 × 10 ⁻⁷	137	1400
86	¹³⁵ Cs	0.067 ^e	0.0641		8.7	62.0
87	¹³⁶ Cs			0.617 × 10 ⁻⁶		
88	¹³⁷ Cs	0.072	0.0615	0.666 × 10 ⁻⁹	0.11	0.3
89	¹³⁸ Cs			0.362 × 10 ⁻³	8.7	62
90	¹³⁴ Ba				2	(1)
91	¹³⁶ Ba				0.4	(0.2)
92	¹³⁷ Ba				4.9	(2.5)
93	¹³⁸ Ba	0.068	0.0574		0.68	0.3
94	¹³⁹ La	0.064	0.0655		8.9	11.0
95	¹⁴⁰ Ce	0.061	0.0644		0.66	0.5
96	¹⁴¹ Ce			0.251 × 10 ⁻⁶		
97	¹⁴² Ce	0.057	0.0595		0.94	1.3
98	¹⁴³ Ce			0.601 × 10 ⁻⁵	6	(3)
99	¹⁴¹ Pr	0.059	0.064		11.5	23.5
100	¹⁴² Pr				18.0	(9.0)
101	¹⁴³ Pr				89	(0.45 × 10)
102	¹⁴⁴ Pr			0.660 × 10 ⁻³		
103	¹⁴³ Nd	0.052	0.0598		308	130
104	¹⁴⁴ Nd	0.041	0.0567		5	12
105	¹⁴⁵ Nd	0.030	0.0395		67	245
106	¹⁴⁶ Nd	0.023	0.0307		10	25
107	¹⁴⁷ Nd			0.710 × 10 ⁻⁶	180	2510

^dIncludes indirect yield from ¹³⁵I.

^eIncluded in Xe yields.

Fission Product Nuclear Data (continued)

Number	Isotope	Fission Yield		β , Decay λ , sec ⁻¹	Cross Section g σ , barns	Resonance Integral RI, barns
		^{233}U	^{235}U			
108	^{148}Nd	0.012	0.0170		3.4	48
109	^{149}Nd			0.963×10^{-4}		
110	^{150}Nd	0.0048	0.0067		1.5	14
111	^{151}Nd			0.700×10^{-5}		
112	^{147}Pm	0.017	0.0238	0.846×10^{-8}	180	2510
113	^{148}Pm			0.151×10^{-5}	27,000	
114	^{147}Sm				87	690
115	^{148}Sm				9	50
116	^{149}Sm	0.0062	0.0113		87,770	2440
117	^{150}Sm				85	460
118	^{151}Sm	0.0026	0.0045	0.301×10^{-9}	10,260	3565
119	^{152}Sm	0.0017	0.00285		194	2500
120	^{153}Sm			0.410×10^{-5}		
121	^{154}Sm	0.00037	0.00077		5	25
122	^{153}Eu	0.00095	0.0015		382	1380
123	^{154}Eu			0.137×10^{-8}	1500	750
124	^{155}Eu			0.129×10^{-7}	8490	4245
125	^{156}Eu			0.521×10^{-6}		
126	^{154}Gd					
127	^{155}Gd	0.00015	0.0003		58,000	1630
128	^{156}Gd	0.00005	0.00013		4	44
129	^{157}Gd	0.5×10^{-4}	0.78×10^{-4}		0.24×10^6	740
130	^{158}Gd	0.1×10^{-4}	0.2×10^{-4}		3.9	29
131	^{155}Gd			0.107×10^{-4}		
132	^{159}Tb	0.5×10^{-5}	0.1×10^{-4}		46	420
133	^{89}Sr			0.148×10^{-6}	130	(65)
134	^{90}Zr				1.5	0.7
135	^{135}I	(f)	(f)	0.289×10^{-4}		
136	^{135}Ba				5.6	(3)
137	^{151}Eu				8400	(4200)
138	^{152}Eu				5500	(2750)
139	^{160}Tb				525	(262)
140	^{130}Te	0.027	0.020		0.5	2.6
TOTAL		2.02285	2.06485			

^fYield of ^{135}I combined with that of ^{135}Xe .

References

1. J. O. Blomeke and M. F. Todd, Uranium-235 Fission-Product Production As a Function of the Thermal Neutron Flux, Irradiation Time, and Decay Time. II: Summations of Individual Chains, Elements, and the Rare-Gas and Rare-Earth Groups, USAEC Report ORNL-2127, Pt. II, Vols. 1, 2, and 3, Oak Ridge National Laboratory, November 1958.
2. J. D. Garrison and B. W. Roos, Fission Product Capture Cross Sections, Nucl. Sci. Eng., 12: 115 (January 1962).
3. E. A. Nepheu, Thermal and Resonance Absorption Cross Section of the ^{233}U , ^{235}U , and ^{239}Pu Fission Products, USAEC Report ORNL-2869, Oak Ridge National Laboratory, March 1960.
4. J. J. Pattenden, Fission Product Poisoning Data, USAEC Report ORNL 2778, Oak Ridge National Laboratory, October 1959.
5. C. R. Greenhow and E. C. Hensen, Thermal and Resonance Fission-Product Poisoning for ^{235}U System, USAEC Report KAPL-2172, Knolls Atomic Power Laboratory, October 1961.
6. N. F. Wikner and S. Jaye, Energy-Dependent and Spectrum-Averaged Thermal Cross Sections for the Heavy Elements and Fission Products for Various Temperatures and C: ^{235}U Atom Ratios, USAEC Report GA-2113, General Atomic, June 1961.
7. R. L. Ferguson and G. D. O'Kelley, A Survey and Evaluation of ^{233}U Fission Yield Data, USAEC Report ORNL CF-62-3-71, Oak Ridge National Laboratory, March 1962.
8. E. C. Hensen, A Critical Examination of the Uncertainties in Predicted Gross Fission Product Poisoning, USAEC Report KAPL-M-ECH-8, Knolls Atomic Power Laboratory, March 1962.
9. E. C. Hensen and C. R. Greenhow, An Improved Generalized Analysis of Fission Product Poisoning and Thermal and Resonance Fission Fragment Cross Sections, USAEC Report KAPL-M-ECH-7, Knolls Atomic Power Laboratory, September 1960.
10. C. H. Wescott, Effective Cross Section Values for Well-Moderated Thermal Reactor Spectra, Canadian Report CRRP-787 (Rev. August 1958); AECL-670.
11. J. O. Blomeke, Nuclear Properties of ^{235}U Fission Products, USAEC Report ORNL-1783, Oak Ridge National Laboratory, April 1957.

Appendix F

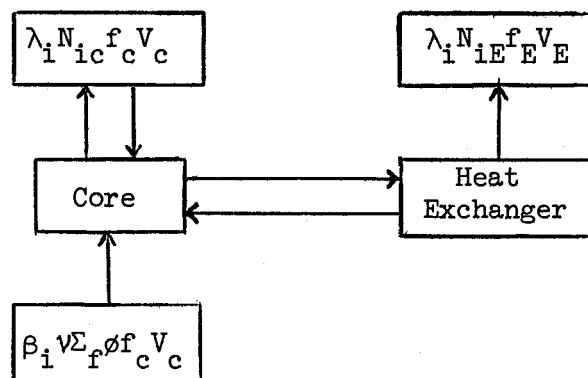
TREATMENT OF DELAYED NEUTRONS

T. W. Kerlin

Summary

Circulating fuel reactors lose neutrons because some of the delayed neutrons are emitted outside of the core. These losses depend on core residence time, external loop residence time, and decay characteristics of the precursors.

A symbolic representation of the system is



where

λ_{ij} = decay constant of the i^{th} precursor from fissionable material j ,

β_{ij} = number of i^{th} precursors formed per fission neutron from fissionable material j ,

N_{ijc} = atoms of i^{th} precursor per unit volume of fuel stream in the core resulting from fissions in material j ,

N_{ije} = atoms of i^{th} precursor per unit volume of fuel stream in the external loops resulting from fissions in material j ,

f_c = volume fraction of fuel in the core,

f_E = volume fraction of fuel in the external loops,

V_c = core volume,

V_E = external loop volume,

$\nu \sum_j f_j \phi f_c V_c$ = rate of production of fission neutrons in the core from fissionable material j.

The precursor concentrations are described by these equations:

$$\frac{dN_{ijc}}{dt_c} = \beta_{ij} \nu \sum_j f_j \phi - \lambda N_{ijc}, \quad (1)$$

$$\frac{dN_{ije}}{dt_E} = -\lambda N_{ije}, \quad (2)$$

where

t_c = time in the core,

t_E = time in the external loops.

The boundary conditions are:

$$N_{ijc}(T_c) = N_{ije}(0), \quad (3)$$

$$N_{ije}(0) = N_{ije}(T_E), \quad (4)$$

where

T_c = time for the fuel stream to pass through the core,

T_E = time for the fuel stream to pass through the external loops.

The solution to Eqs. (1) and (2) are:

$$N_{ijc} = \frac{\beta_{ij} \nu \sum_j f_j \phi}{\lambda_{ij}} \left(1 - e^{-\lambda_{ij} T_c} \right) + N_{ijc}(0) e^{-\lambda_{ij} T_c}, \quad (5)$$

$$N_{ijE} = N_{ijE}(0) e^{-\lambda_{ij} t_E}. \quad (6)$$

Note that the precursor production rate is assumed constant for the fuel stream during its stay in the core. This idealized case would exist only for uniform power density along the fuel stream or for core residence times which are short compared to the half-life of the precursor.

The boundary conditions become

$$\frac{\beta_{ij} v_j \sum f_j \phi}{\lambda_{ij}} \left(1 - e^{-\lambda_{ij} T_c} \right) + N_{ijc}(0) e^{-\lambda_{ij} T_c} = N_{ijE}(0), \quad (7)$$

$$N_{ijc}(0) = N_{ijE}(0) e^{-\lambda_{ij} T_E}. \quad (8)$$

Eliminating $N_{ijc}(0)$ in Eqs. (7) and (8) and substituting the result in Eq. (6) gives

$$N_{ijE} = \frac{\beta_{ij} v_j \sum f_j \phi}{\lambda_{ij}} \frac{\left(1 - e^{-\lambda_{ij} T_c} \right) e^{-\lambda_{ij} t_E}}{\left[1 - e^{-\lambda_{ij} (T_c + T_E)} \right]}. \quad (9)$$

The rate of decay of precursors in the external loops is

$$f_E V_E \frac{N_{ijE}}{T_E} = \frac{\beta_{ij} v_j \sum f_j \phi f_E V_E \left(1 - e^{-\lambda_{ij} T_c} \right) \left(1 - e^{-\lambda_{ij} T_E} \right)}{\lambda_{ij} T_E \left[1 - e^{-\lambda_{ij} (T_c + T_E)} \right]}. \quad (10)$$

The total rate of precursor decay (at equilibrium) is $\beta_{ij} v_j \sum f_j \phi f_c V_c$. Thus the fraction of the delayed neutrons which appear in external loops is

$$\frac{\frac{N_{ijE} f_E V_E}{T_E}}{\beta_{ij} v_j \sum f_j \phi f_c V_c} = \frac{f_E V_E \left(1 - e^{-\lambda_{ij} T_c} \right) \left(1 - e^{-\lambda_{ij} T_E} \right)}{f_c V_c \lambda_{ij} T_E \left[1 - e^{-\lambda_{ij} (T_c + T_E)} \right]}. \quad (11)$$

Since $\frac{f_E V_E}{f_c V_c} = \frac{T_E}{T_c}$, Eq. (11) becomes

$$\frac{\beta_{ijE}}{\beta_{ij}} = \frac{\left(1 - e^{-\lambda_{ij} T_c}\right) \left(1 - e^{-\lambda_{ij} T_E}\right)}{\lambda_{ij} T_c \left[1 - e^{-\lambda_{ij} (T_c + T_E)}\right]} . \quad (12)$$

For using these results in an equilibrium reactor code such as ERC-5¹ the term $v_j \sum f_j \phi$ may be replaced by a neutron production rate given by

$$N_j C_j^f v_j ,$$

where

C_j^f = reaction rate coefficient for fissions in material j.

Using this in Eq. (12) gives the following result for the number of neutrons lost in the external loops per neutron produced:

$$\text{losses} = \sum_j N_j C_j^f v_j \sum_i \frac{\beta_{ij} \left(1 - e^{-\lambda_{ij} T_c}\right) \left(1 - e^{-\lambda_{ij} T_E}\right)}{\lambda_{ij} T_c \left[1 - e^{-\lambda_{ij} (T_c + T_E)}\right]} . \quad (13)$$

The necessary constants for ^{232}Th , ^{233}U , ^{235}U , ^{238}U , and ^{239}Pu are:²

Group	$\lambda_i (\text{sec}^{-1})$	^{232}Th	^{233}U	^{235}U	^{238}U	^{239}Pu
1	0.0128	0.00085	0.00020	0.0003	0.00015	0.0001
2	0.0315	0.0035	0.00075	0.0018	0.0017	0.0006
3	0.125	0.0045	0.00105	0.0022	0.0028	0.00045
4	0.325	0.0120	0.00075	0.0023	0.0071	0.00085
5	1.55	0.0045	0.00025	0.0007	0.0042	0.0003
6	4.5	0.0009	—	0.0002	0.0015	—
		0.02625	0.0030	0.0075	0.01745	0.0023

References

1. L. G. Alexander, ERC-5 Program for Computing the Equilibrium States of Two-Region, Thorium Breeder Reactors, ORNL-CF-60-10-87 (October 20, 1960).
2. A. M. Weinberg and E. P. Wigner, The Physical Theory of Neutron Chain Reactors, p. 136, The University of Chicago Press, Chicago, 1958.

Appendix G

TREATMENT OF XENON ABSORPTION IN GRAPHITE

L. G. Alexander

Introduction

Some ^{135}Xe is formed directly during fission; however, the major part (>90%) is formed by the decay of ^{135}I which has a half-life of 6.7 hours. The iodine remains in solution as the iodide ion (I^-). Thus, at equilibrium, the rate of formation of xenon in the fuel is proportional to the sum of the direct fission yields of xenon and iodine, here taken to be 0.066 atoms per fission.

All of the xenon is released in the fuel salt, and since the half-life for the decay of ^{135}I is long compared to the time required for the fuel to make one complete trip around the fuel circuit (about 15 seconds), the rate of release of ^{135}Xe is nearly uniform throughout the fuel volume, being augmented somewhat in the core by the direct fission yield. For purposes of this study, the concentration of xenon in the salt was assumed to be uniform.

The solubility of noble gases in molten salts is low (1), especially in mixtures of LiF-BeF_2 . A concentration of only 2×10^{15} atoms of xenon per cc of salt at 1200°F is in equilibrium with a partial pressure of xenon in the gas phase of one atmosphere. In the reference design case, the equilibrium pressure is about 0.06 atmosphere.

Xenon thus tends to leave the salt at any phase boundary. It may form microbubbles clinging to the surface of the graphite moderator. It will tend to diffuse into the pores of the graphite. It can be removed rapidly by spraying a portion of the circulating stream into a space filled with helium or by subsurface sparging with helium.

Xenon is also removed from the system by decay to ^{135}CS and by reaction with neutrons to form ^{136}Xe , which is stable and has a low neutron capture cross section.

Analysis

Watson and Evans¹ have analyzed the equilibrium xenon poisoning resulting from the interaction of all these modes of production and removal, obtaining an equation which may be rendered in the form

$$\text{Xe P.F.} = \frac{\bar{\eta}Y}{\bar{v}} \left[\frac{\phi_c \alpha \left(\frac{V_{fc}}{V_f} \right) + \frac{\phi_c}{\phi_c \alpha + \lambda n_f} \dot{n}_d}{\phi_c \alpha \left(\frac{V_{fc}}{V_f} \right) + \frac{\dot{n}_s}{n_f} + \frac{\dot{n}_d}{n_f}} \right] \quad (1)$$

where

P.F. = Poison Fraction, or number of neutrons absorbed by xenon per neutron absorbed in fissile isotopes,

$\bar{\eta}$ = neutron productions, number of neutrons produced from all sources per neutron absorbed in fissile isotopes (2.21 in reference design),

Y = sum of fission yields of ^{135}Xe and ^{135}I , taken as 0.066 atoms per fission,

\bar{v} = neutron yield, or number of neutrons produced from fission per fission (2.50 in reference design),

ϕ_c = mean effective flux in reactor core (neut-cm/cm³ sec),

α = effective ^{135}Xe neutron capture cross section Captures neut-cm Atom Xe, cc

V_{fc} = volume of fuel stream in core (600 ft³),

V_f = volume of fuel stream (2500 ft³),

λ = decay constant for ^{135}Xe , $2.09 \times 10^{-5}/\text{sec}$,

\dot{n}_d = rate of diffusion of xenon into graphite, atoms/sec,

\dot{n}_s = rate of removal of xenon by sparging, atoms/sec,

n_f = number of atoms of xenon dissolved in fuel salt.

The product $\phi_c \alpha$ is readily evaluated by reference to a multigroup calculation. Thus

$$\phi_c \alpha N_c V_c = F v A$$

where

N_c = concentration of xenon atoms in the core, atoms/cc,

V_c = volume of core, cc,

F = fission rate in core, fissions/sec,

A = fraction of all neutrons captured in ^{135}Xe .

The fission rate is readily calculated from the power, using the conversion: 3.1×10^{16} fissions/Mw-sec. Solving for the product

$$\phi_c \alpha = \frac{3.1 \times 10^{16} P v}{V_c} \left(\frac{A}{N_c} \right) . \quad (2)$$

The ratio A/N_c is, at low concentrations, independent of N_c and may be determined by means of a multigroup neutron calculation. In the reference reactor it has a value of 2.22×10^{-16} .

By insertion of numerical values, it is found that $\phi_c \alpha$ equals $2.54 \times 10^{-4} \frac{\text{Captures/cc}}{\text{atom Xe sec}}$.

The ratio \dot{n}_s/n_f is equal to the volumetric rate of sparging divided by the volume of the fuel stream. Let Q be the fuel stream rate of flow through the core ($160 \text{ ft}^3/\text{sec}$) and r be the fraction of this diverted through a sparge or spray chamber. Then

$$\dot{n}_s/n_f = rQ/V_f .$$

For the term \dot{n}_d , Watson and Evans give a relation which may be rendered

$$n_d = N_g^* A_g \left[e D (\phi_c \alpha + \lambda) \right]^{1/2} \quad (3)$$

where

N_g^* = gas-phase xenon concentration that is in equilibrium with xenon dissolved in the salt, atoms/cc,

A_g = area of interface between salt and moderator graphite, (For 810 g logs 8 in. diam \times 20 ft long, $A_g = 31.5 \times 10^6 \text{ cm}^2$),

e = porosity of graphite or fraction of graphite volume accessible to xenon,

D = coefficient of diffusion of xenon in graphite, cm^2/sec .

The value of N_g^* is related by Henry's law to the concentration in the salt.

$$N_f = N_g^* KRT \quad (4)$$

where

N_f = concentration of xenon in the salt, atoms/cc,

K = Henry's law constant for xenon in salt, 3.2×10^{-9}

$\frac{\text{moles Xe}}{\text{cc of salt, atom}}$,

R = gas constant, 82 cc-atom/mole °K,

T = absolute temperature, 922°K,

Values of K for xenon dissolved in various salts at various temperatures are given by Watson and Evans.¹ For MSCR salt at 1200°F, K is about 3.2×10^{-9} moles Xe/cc salt-atom. Noting that $n_f = N_f V_f$, one has, from Eq. (3),

$$\frac{n_d}{n_f} = \frac{A_g [e D (\phi_c \alpha + \lambda)]^{1/2}}{KRTV_f} \quad (5)$$

Substituting these results and numerical values into Eq. (1) yields

$$\text{Xe P.F.} = 0.0584 \left[\frac{1 + 42.6 \times 10^4 (e D)^{1/2}}{1.32 + 1000r + 46.0 \times 10^4 (e D)^{1/2}} \right]$$

Values of the poison fraction calculated by means of this equation for various values of r and the product $e D$ are displayed below in Table G.1.

Table G.1. Xenon Poison Fraction in MSCR

r	Poison Fraction			
	$e D^a = \infty$	$e D^a = 10^{-6}$	$e D^a = 10^{-8}$	$e D^a = 0$
0.1	0.054	0.0445	0.0173	0.0006
0.01	0.054	0.053	0.0445	0.0052
0.001	0.054	0.054	0.053	0.0251

^aIn cm²/sec.

Reference

1. G. M. Watson and R. B. Evans III, Xenon Diffusion in Graphite: Effects of Xenon Absorption in Molten Salt Reactors Containing Graphite, USAEC Report ORNL CF-61-2-59, Oak Ridge National Laboratory, February 1961.

Appendix H

THE EQUILIBRIUM STATE AS A BASIS FOR ECONOMIC
EVALUATION OF THORIUM REACTORS

T. W. Kerlin

Introduction

The equilibrium condition is currently being used as the basis for fluid-fuel reactor economic evaluation and for new computer code development. Because of this increasing application of calculations based on the equilibrium state, it is advisable to clearly define equilibrium and to assess the validity of evaluations based on the equilibrium condition. These problems were considered in this study for thorium-fueled reactors, fueled initially with ^{235}U , and particularly for the molten-salt converter reactor (MSCR).

The equilibrium condition is defined as that condition in which the reactor composition is time independent because of a balance between nuclide production rates and loss rates. It is important to note that these are the total production and loss rates (including feed, recycle, discharge, processing losses, etc.) and are not restricted to nuclear transformation rates. The mathematical formulation of the equilibrium state is obtained by setting the time derivative of the nuclide concentration equal to zero:

$$\frac{dN_i}{dt} = Q_i^f + R_i + F_i + T_i + D_i - N(t_i + d_i + q_i) = 0 , \quad (1)$$

where

N_i = nuclide concentration of i^{th} nuclide,

t = time,

Q_i^f = feed rate,

R_i = recycle rate,

F_i = fission fragment formation rate,

T_i = growth rate due to neutron capture in other materials,

D_i = growth rate due to radioactive decay in other materials,

t_i = loss rate due to neutron capture in i^{th} nuclide,

d_i = loss rate due to radioactive decay of i^{th} nuclide,

q_i = processing loss rate.

Equation (1) should be valid for reactor evaluation if the nuclide concentration is near equilibrium (90-95%) over a large fraction (90-95%) of the reactor's operating life.

Estimates of the saturation behavior of the nuclides of interest in thorium-fueled reactors were made using the methods discussed below.

Methods

The time-dependent behavior of the nuclide concentrations in a thorium-fueled reactor, fueled initially with ^{235}U , was calculated by solving Eq. (1) without the restriction that $dN_i/dt = 0$. The treatment for the individual isotopes along with special assumption for each case is given below:

1. Fission Products

Assume that fission products are produced at a constant rate, S , and are removed by neutron capture, radioactive decay, and processing. This leads to

$$\frac{dN_i}{dt} = S_i - N_i \left(t_i + d_i + \frac{1}{\tau} \right), \quad (2)$$

where

τ = time to process a complete reactor volume.

Solving Eq. (2) gives

$$N_i(t) = \frac{s_i}{t_i + d_i + \frac{1}{\tau}} \left[1 - e^{-\left(t_i + d_i + \frac{1}{\tau}\right)t} \right]. \quad (3)$$

The fractional saturation is

$$\frac{N_i(t)}{N_i(\infty)} = 1 - e^{-\left(t_i + d_i + \frac{1}{\tau}\right)t}. \quad (4)$$

A lower limit on the fractional saturation at any time may be obtained by setting $t_i = d_i = 0$. This gives

$$\frac{N_i(t)}{N_i(\infty)} = 1 - e^{-\frac{1}{\tau}}. \quad (5)$$

2. Uranium-233

Neglecting processing losses and captures in ^{233}Pa , the concentration of ^{233}U is given by

$$\frac{dN^{23}}{dt} = N^{02} \sigma_c^{02} \phi - N^{23} \sigma_a^{23} \phi, \quad (6)$$

where

N^{23} = concentration of ^{233}U ,

N^{02} = concentration of ^{232}Th (assumed invariant),

σ_c^{02} = effective capture cross section of ^{232}Th ,

ϕ = neutron flux (defined below),

σ_a^{23} = effective absorption cross section of ^{233}U .

The neutron flux is given by

$$V \sum_f \phi = P \times 3.1 \times 10^{10}, \quad (7)$$

$$\phi = \frac{P}{VN_f} \frac{3.1 \times 10^{10}}{\bar{\sigma}_f}, \quad (8)$$

where

P = reactor power (watts),

V = fuel volume (cc),

N_f = concentration of fuel (atoms/cc),

$\bar{\sigma}_f$ = effective fission cross section (average over all fissile nuclides).

The term, VN_f , is the total number of fissile atoms. Taking the average atomic weight of the fissile nuclides as 235 gives

$$VN_f = W \times 2.563 \times 10^{21}, \quad (9)$$

where

W = mass of fissile material (grams).

Substituting Eq. (9) into Eq. (8) gives

$$\phi = \left(\frac{P}{W} \right) \times \frac{1.21 \times 10^{-11}}{\bar{\sigma}_f} \quad (10)$$

Solving Eq. (6) and using Eq. (10) gives

$$\frac{N^{23}(t)}{N^{23}(\infty)} = 1 - e^{- \frac{P}{W} \times \frac{\sigma_a^{23}}{\sigma_f} \times 3.816 \times 10^{-4} T}, \quad (11)$$

where

T = time (years).

The term, P/W , is the specific power of the fuel in units of watts/g. The ratio, σ_a^{23}/σ_f , is about 1.2 for the molten-salt converter reactor (MSCR).

3. Uranium-234

The concentration of ^{234}U is given by

$$\frac{dN^{24}}{dt} = N^{23} \sigma_c^{23} \phi - N^{24} \sigma_a^{24} \phi, \quad (12)$$

where

N^{24} = concentration of ^{234}U ,

σ_c^{23} = capture cross section of ^{233}U ,

σ_a^{24} = absorption cross section of ^{234}U .

Solving Eqs. (6), (10), and (12) simultaneously gives

$$\frac{N^{24}(t)}{N^{24}(\infty)} = \frac{1 - e^{-\frac{P}{W} \times \frac{\sigma_a^{24}}{\sigma_f} \times 3.816 \times 10^{-4} T}}{1 - \frac{e^{-\frac{P}{W} \frac{\sigma_a^{23}}{\sigma_f} \times 3.816 \times 10^{-4} T} - e^{-\frac{P}{W} \frac{\sigma_a^{24}}{\sigma_f} \times 3.816 \times 10^{-4} T}}{\frac{\sigma_a^{23}}{\sigma_a^{24}}}}. \quad (13)$$

The ratio, σ_a^{24}/σ_f , is about 0.4 for the MSCR.

4. Uranium-235

The concentration of ^{235}U at any time is that required by the criticality condition. For these estimates, it is assumed that the fissile inventory is constant. This gives

$$N^{25}(t) = N^{25}(\infty) + N^{23}(\infty) - N^{23}(t),$$

$$\frac{N^{25}(t)}{N^{25}(\infty)} = 1 + \frac{N^{23}(\infty)}{N^{25}(\infty)} \left(1 - \frac{N^{23}(t)}{N^{23}(\infty)} \right). \quad (14)$$

If $\sigma_a^{23} = \sigma_a^{25}$, as is approximately the case in the MSCR, then

$$\frac{N^{23}(\infty)}{N^{25}(\infty)} = \frac{CR}{1 - CR}, \quad (15)$$

where

CR = conversion ratio (assumed constant).

Using Eqs. (11) and (15) in Eq. (14) gives

$$\frac{N^{25}(t)}{N^{25}(\infty)} = 1 + \frac{CR}{1 - CR} e^{-\frac{P}{W} \frac{\sigma_a^{23}}{\sigma_f} \times 3.816 \times 10^{-4} T}. \quad (16)$$

The assumptions of constant fissile inventory and constant conversion ratio are very crude, but will suffice for the qualitative evaluation desired in this study.

5. Uranium-236

The concentration of ^{236}U is given by

$$\frac{dN^{26}}{dt} = N^{25} \sigma_c^{25} \phi - N^{26} \sigma_a^{26} \phi, \quad (17)$$

where

N^{26} = concentration of ^{236}U ,

σ_c^{25} = capture cross section of ^{235}U ,

σ_a^{26} = absorption cross section of ^{236}U .

Solving Eq. (17) and using Eqs. (10) and (16) gives

$$\frac{N^{26}(t)}{N^{26}(\infty)} = 1 - e^{-\frac{P}{W} \frac{\sigma_a^{26}}{\sigma_f} \times 3.816 \times 10^{-4} T} + \frac{CR}{1 - CR} \left[\frac{e^{-\frac{P}{W} \frac{\sigma_a^{23}}{\sigma_f} \times 3.816 \times 10^{-4} T} - e^{-\frac{P}{W} \frac{\sigma_a^{26}}{\sigma_f} \times 3.816 \times 10^{-4} T}}{1 - \frac{\sigma_a^{23}}{\sigma_a^{26}}} \right]. \quad (18)$$

The ratio, σ_a^{26}/σ_f , is about 0.1 for the MSCR.

6. Uranium-238

The ^{238}U appears only in the feed along with ^{235}U

$$\frac{dN^{28}}{dt} = (\text{feed rate}) \left(\frac{N^{28}}{N^{25}} \right)_{\text{feed}} - N^{28} \sigma_a^{28} \phi, \quad (19)$$

where

N^{28} = concentration of ^{238}U ,

σ_a^{28} = absorption cross section of ^{238}U .

The ^{235}U feed rate is equal to the nuclear transmutation rate

$$\text{feed rate} = N^{25}(t) \sigma_a^{25} \phi = N^{25}(\infty) + N^{23}(\infty) - N^{23}(t) \sigma_a^{25} \phi, \quad (20)$$

Solving Eq. (20) gives

$$\frac{N^{28}(t)}{N^{28}(\infty)} = 1 - e^{-\frac{P \sigma_a^{28}}{W \sigma_f} \times 3.816 \times 10^{-4} T} \left[\frac{1}{1 - \frac{1}{1 - CR} \left(\frac{\sigma_a^{28}}{\sigma_a^{25}} \right)} \right]$$

$$= 1 - \frac{1}{1 - CR \left(\frac{\sigma_a^{23}}{\sigma_a^{28} - 1} \right)} - \left(\frac{1 - CR}{CR} \right) \frac{-\frac{P \sigma_a^{23}}{W \sigma_f} \times 3.816 \times 10^{-4} T}{\left(\frac{\sigma_a^{23}}{\sigma_a^{28}} - 1 \right)}. \quad (21)$$

The ratio, σ_a^{28}/σ_f , is about 0.1 for the MSCR.

Results and Conclusions

The results are shown in Figs. H.1 through H.6. They are discussed individually below:

1. Fission Products

Figure H.1 shows the saturation behavior of a material removed only by processing. In actual operation, the approach to saturation would be faster because of nuclear transformations. It is clear from Fig. 1 that the fission product nuclides which saturate slowly with respect to their nuclear reaction rates are at equilibrium (90% or greater) for 90% of a 30-year reactor life for processing times of less than 500 days. A 1000-day processing time (typical for the MSCR) gives equilibrium (90% or greater) for only 80% of the time. Therefore, the equilibrium treatment is doubtful for fission-product nuclides with low cross sections or long half lives. However, these effects are small.

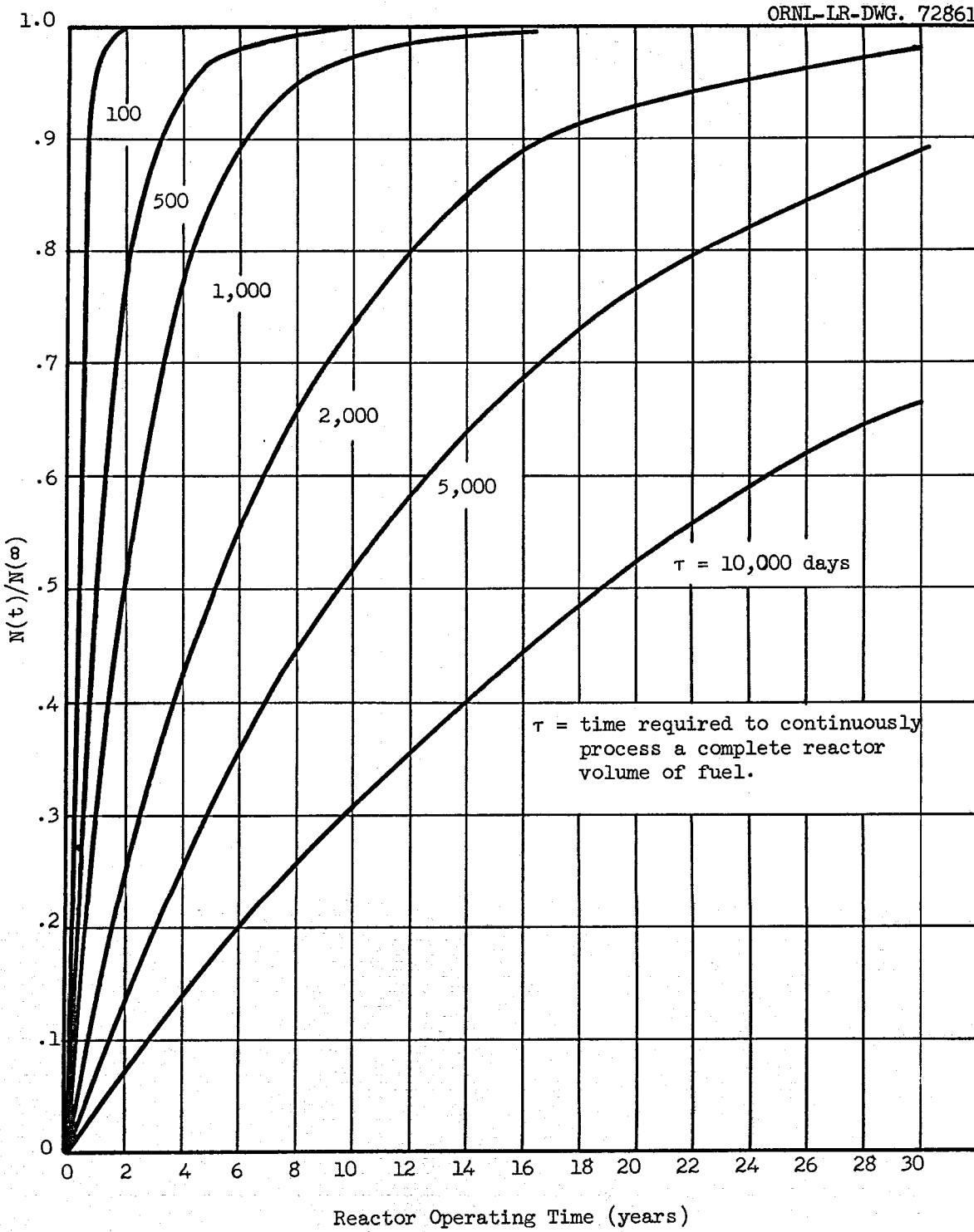
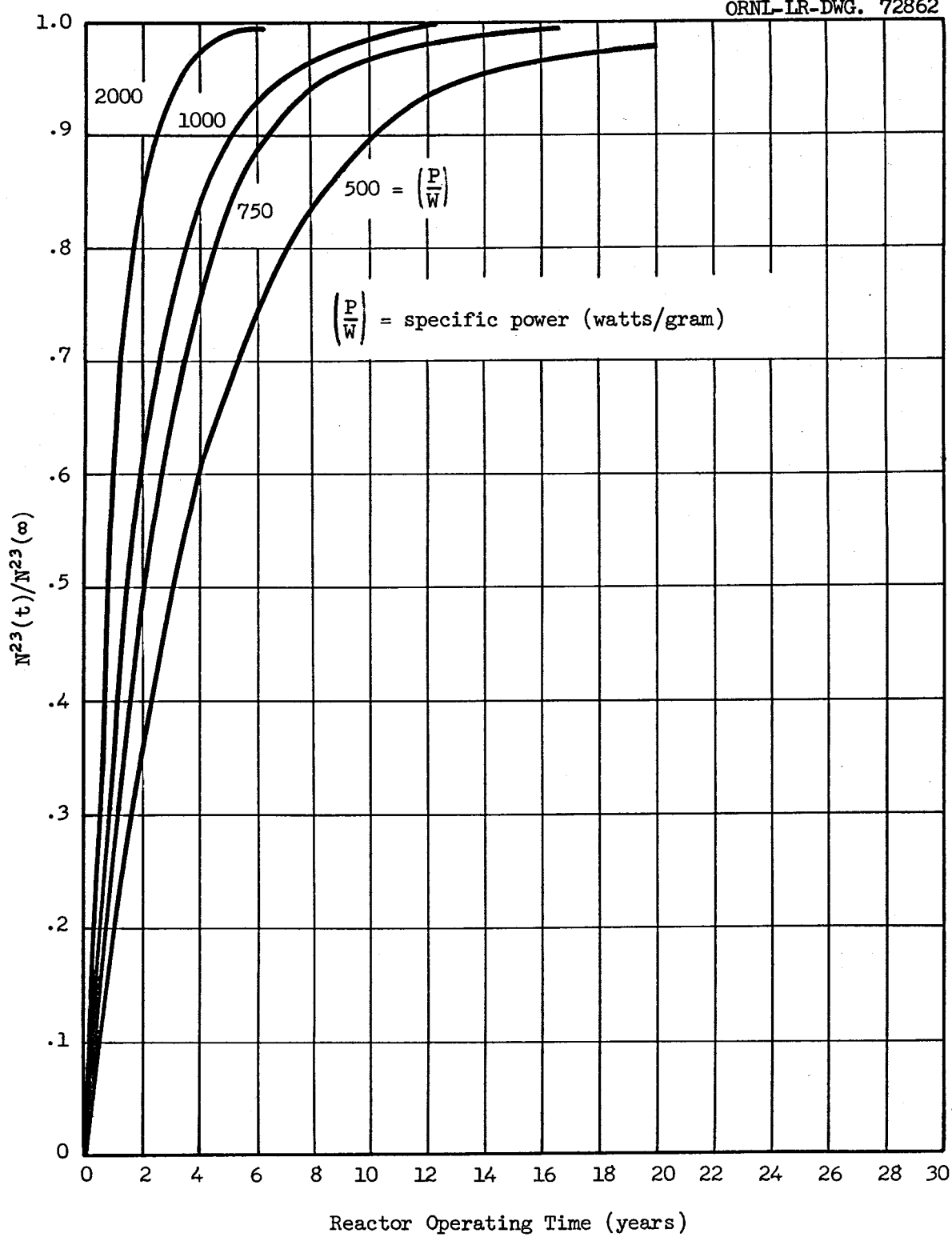
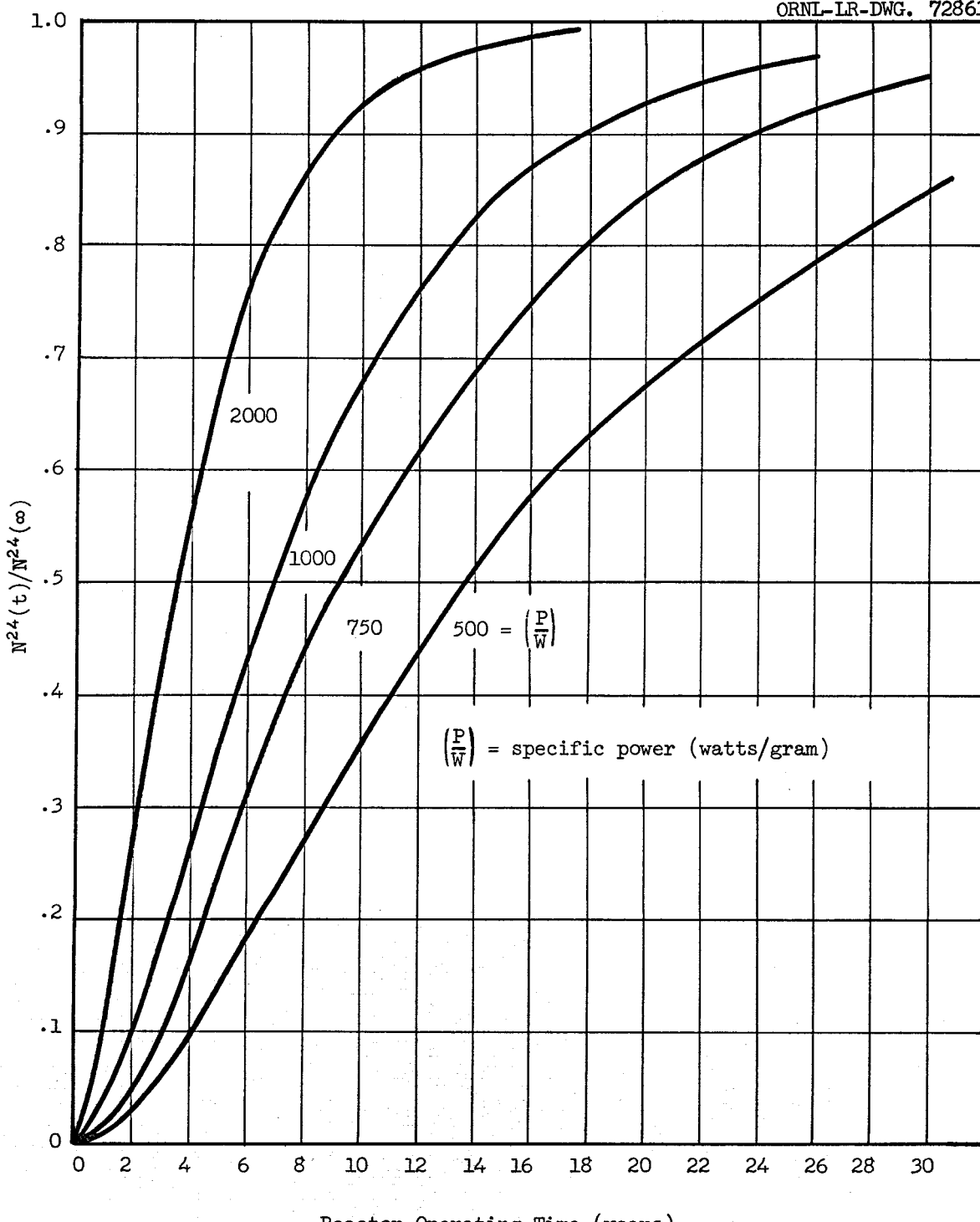


Fig. H.1. Fission Product Saturation.

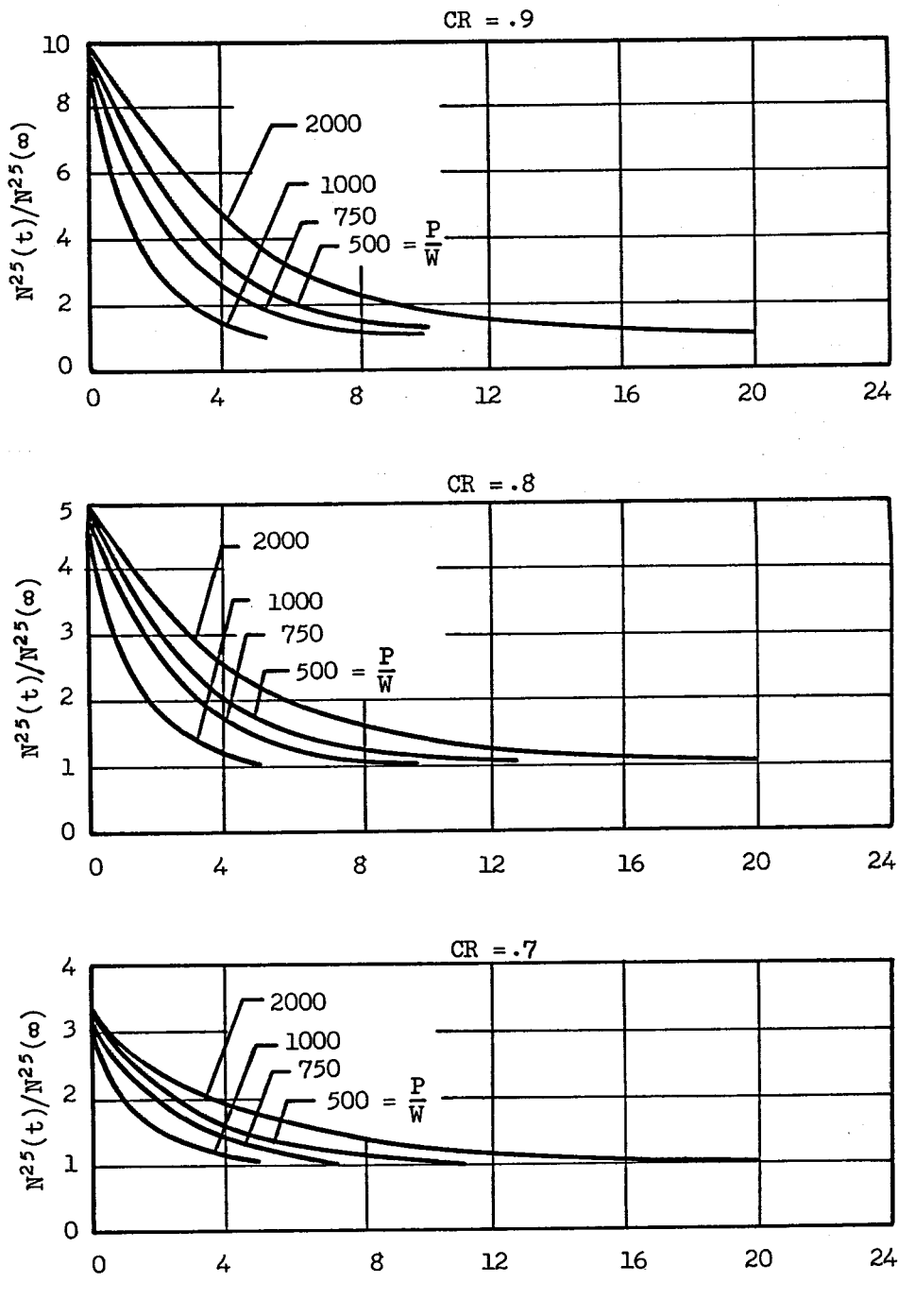
Fig. H.2. ^{233}U Saturation.



Reactor Operating Time (years)

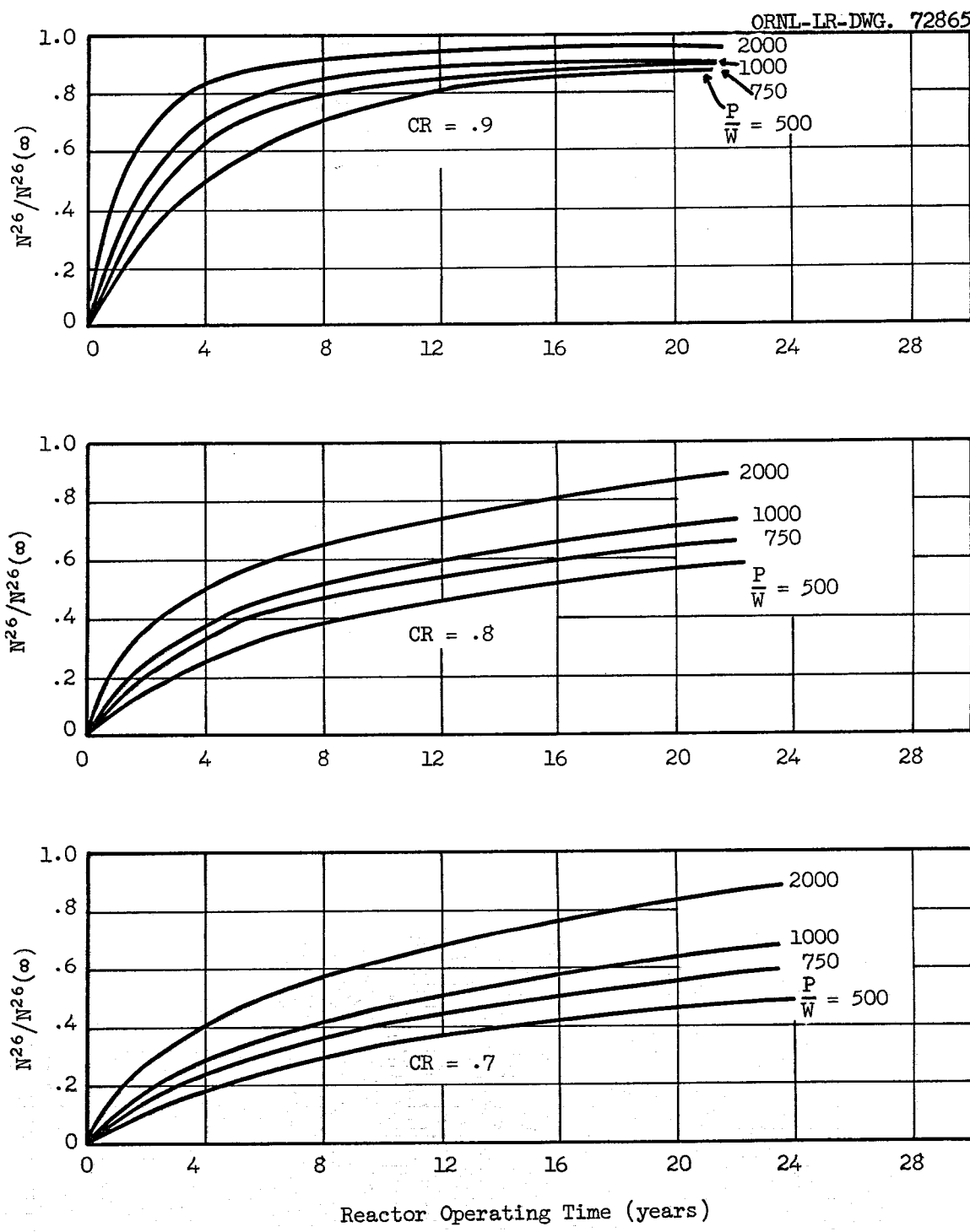
Fig. H.3. ^{234}U Saturation.

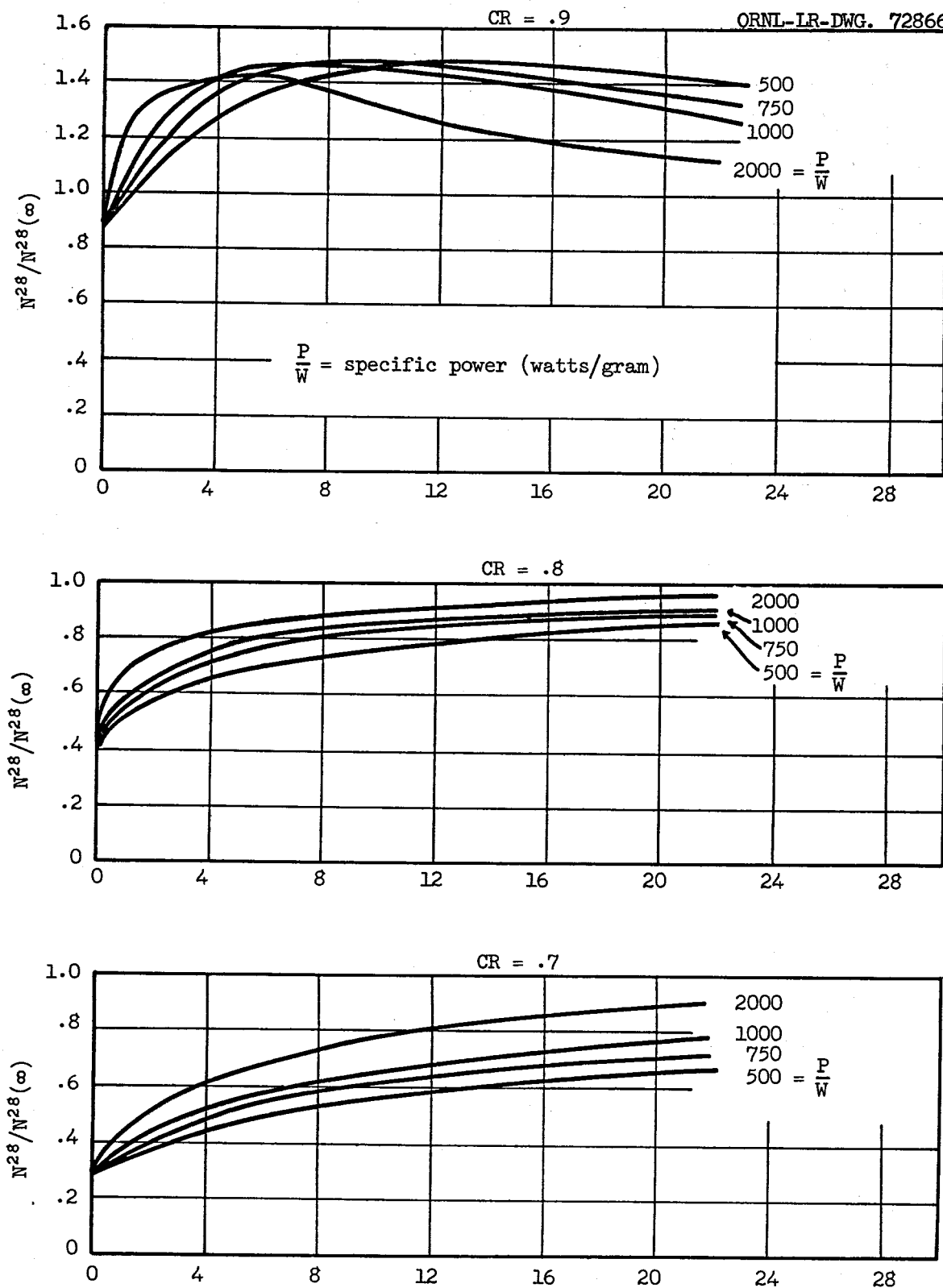
ORNL-LR-DWG. 72864

 $\left(\frac{P}{W}\right)$ = specific power (watts/gram)


Reactor Operating Time (years)

Fig. H.4. ^{235}U Saturation.

Fig. H.5. ^{236}U Saturation.

Fig. H.6. ^{238}U Saturation.

2. Uranium-233

Figure H.2 shows the saturation behavior of ^{233}U . The curves show that equilibrium (90% or greater) exists for 90% of the reactor life only if the specific power is greater than about 1800 w/gram. A specific power of 750 w/gram (typical for the MSCR) insures equilibrium (90% or greater) for 80% of the 30-year reactor life.

3. Uranium-234

Figure H.3 shows that ^{234}U saturates very slowly for all practical values of specific power. A specific power of 750 w/gram (typical for the MSCR) gives an average concentration over the 30-year reactor life only 65% of the equilibrium value.

4. Uranium-235

Figure 4 shows the saturation behavior of ^{235}U . For a conversion ratio of 0.8 and a specific power of 750 w/gram (typical MSCR conditions), the ^{235}U concentration is within 10% of the equilibrium concentration for 65% of the reactor operating life.

5. Uranium-236

Figure 5 shows that the approach to equilibrium is quite slow for ^{236}U . For a conversion ratio of 0.8 and a specific power of 750 w/gram (typical MSCR conditions), the ^{236}U concentration never reaches 90% of the equilibrium concentration.

6. Uranium-238

Figure H.6 shows the approach to saturation for ^{238}U . For a conversion ratio of 0.8 and a specific power of 750 w/gram (typical MSCR conditions), equilibrium (90% or greater) is insured for 20% of a 30-year reactor operating lifetime.

The results for the six materials considered in this study are shown in Table H.1 for MSCR conditions.

Consideration of the methods used to obtain the results in Table H.1 does not indicate high accuracy. However, the results should be qualitatively

Table H.1. Percentage of MSCR Lifetime Having Nuclide Concentrations Within 10% of Equilibrium

Nuclide	MSCR Lifetime Having Nuclide Concentration Within 10% of Equilibrium (%)
Fission Products (1000-day processing)	80
^{233}U	80
^{234}U	20
^{235}U	65
^{236}U	0
^{238}U	20

correct; and they should create some concern over the validity of the equilibrium state as a suitable condition for reactor economic evaluation. Table H.2 shows the expected direction of the error introduced by assuming the equilibrium condition for the nuclides considered. It is apparent from Table H.2 that it is not possible to predict whether equilibrium calculations are intrinsically optimistic or conservative from these results. Also, since the relative magnitude of the competing effects depends on reactor type, the characteristics of the particular reactor must enter into an assessment of the direction and magnitude of the error associated with the equilibrium assumption.

The magnitude of the effect of these factors on reactor economic evaluations is not known. However, an extensive study should be made to examine these problems. Reactor evaluations based on the equilibrium condition are so convenient, economical, and unambiguous that they should be used if possible.

Table H.2. Effect of the Equilibrium Assumption
on Calculated Reactor Performance

Material	Effect on Calculated Performance
Fission Products	Conservative (overestimate)
^{233}U	Optimistic (overestimate)
^{234}U	Conservative* (overestimate)
^{235}U	Optimistic (underestimate)
^{236}U	Conservative* (overestimate)
^{238}U	Conservative* (overestimate)

*These conclusions are based on an equilibrium calculation with no corrections. These materials are actually calculated using adjustment factors which average the concentrations over the life of the reactor. The direction of the expected error under this assumption is not known.

Appendix I

ESTIMATES OF PHYSICAL PROPERTIES OF LITHIUM-BERYLLIUM
MSCR FUEL AND COOLANT SALTS

R. Van Winkle

Introduction

Estimated physical properties of three fuel salt mixtures at 1200°F and one coolant salt at 1062°F for use in heat transfer and pressure drop calculations of the MSCR study are listed below in Table I.1.

Table I.1. MSCR Salt Properties

Mixture	MSCR No. 1	MSCR No. 2	MSCR No. 3	Coolant
Temperature, °F	1200	1200	1200	1062
Composition mole % LiF-BeF ₂ -ThF ₄	71-16-13	68-23-9	66-29-5	66-34-0
Liquidus Temp, °F	941	887	860	851
Mol. Wt.	66.03	56.2	46.2	33.14
Density, lb/ft ³	215.6	190.1	163.0	120.5
Density, g/cc	3.454	3.045	2.610	1.931
Viscosity, lb/hr-ft	24.2	21	18.9	20.0
Thermal Conductivity Btu/hr-ft-°F	2.67	2.91	3.10	3.5
Heat Capacity, Btu/lb-°F	0.318	0.383	0.449	0.526

The bases for these estimates, some temperature-dependent relationships and atom number densities are given for cases of interest.

Viscosity

Experimental values of the viscosity of several different compositions of the mixture LiF-BeF₂-UF₄-ThF₄ (and some estimated values) are listed in Table I.2 at temperatures of 600°, 700° and 800°C. These are plotted in Fig. I.1 which also includes plots of what appear to be reasonable estimates of the viscosity of MSCR Salts 2 and 3. The estimates on these two salts depend on the fact that their compositions lie between those of Mixture 75 and Mixture 133 (which is the same as MSCR No. 1); hence, their viscosity curves may be expected to lie between the curves of the two known mixtures. Viscosities and temperature-dependent viscosity equations of MSRE fuel and coolant salts are listed in Tables I.3 and I.4 for comparison.

The viscosity equation for Mixture 133 (MSCR No. 1) is (1):

$$\eta = 0.0526 \exp(4838/T ^\circ K) \text{ centipoise}$$

Table I.2. Some Physical Properties of Various
Lithium-Beryllium Molten Fluoride Salts

Mixture Number	Composition, m/o LiF-BeF ₂ -UF ₄ -ThF ₄				Viscosity, cp			Heat Capacity ⁽²⁾ at 700°C	Mol. Wt.
					600	700	800°C		
74	69	31	0	0	7.5 7.25	4.9 4.54	3.45(5) 3.10(6)	0.67*(5)	32.4
75	67	30.5	2.5	0	8.4*	5.5*	3.8*(5)	0.57*(5)	39.5
111	71	16	1	12	13.0	7.1	4.8(5)	0.37*(5)	66.02
112	50	50	0	0	22.2 22.5	10.7 11.6	5.95(5) 6.03(6)	0.65*(5)	36.5
131	60	36	4	0	13.0	7.96	5.30(6)	--	44.96
132	57	43	0	0	13.4	7.38	4.50(6)	--	35.03
133	71	16	0	13	13.4	7.55	4.76(1)	0.306(1)	66.03

*Estimated values (all others listed are experimental).
Numbers in parenthesis are references.

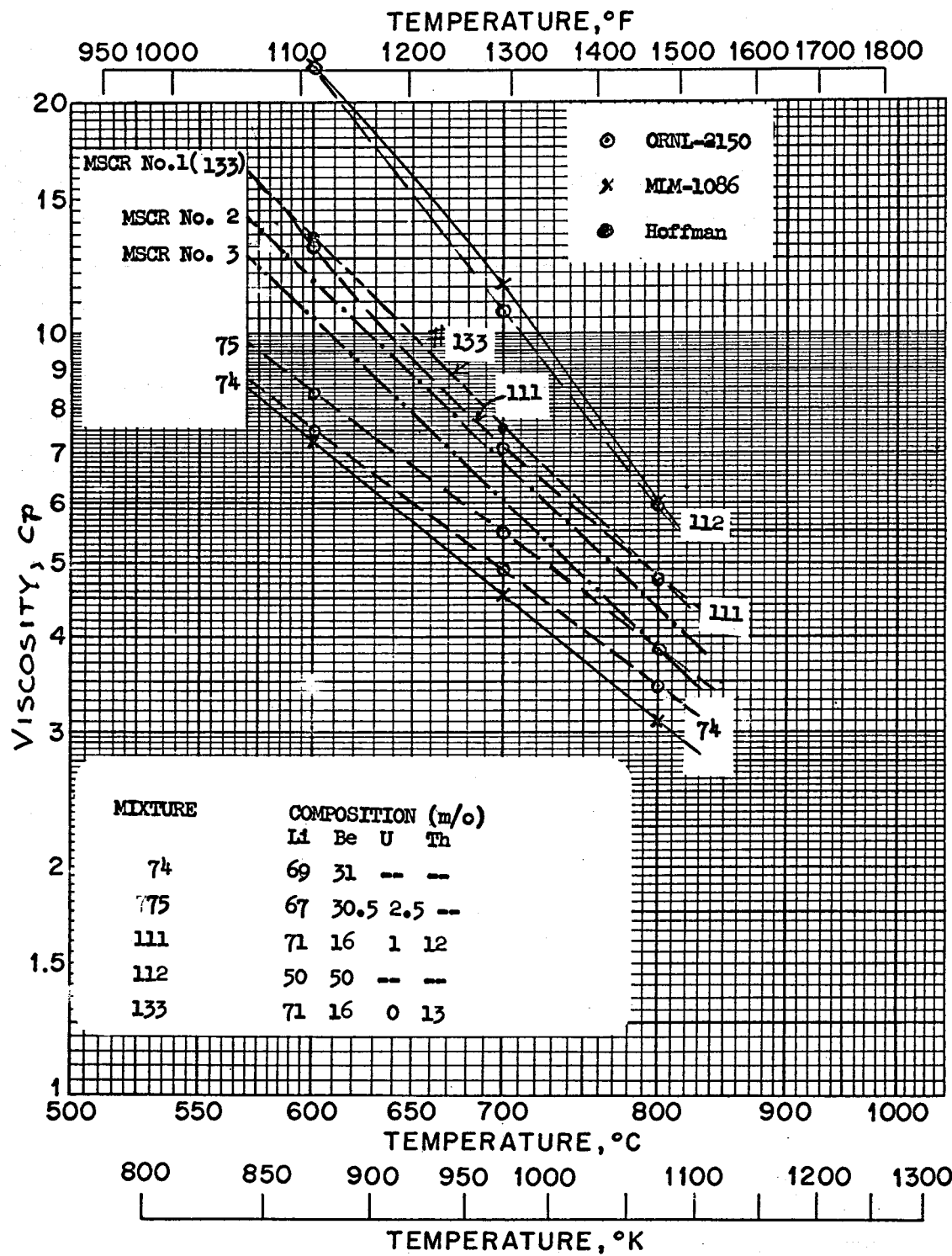


Fig. I.1. MSCR Salt Viscosity.

Table I.3. Composition and Properties of
Fuel Salt for MSRE

I. Chemical Composition	Mole Percent
LiF	70
BeF ₂	23
ZrF ₄	5
ThF ₄	1
UF ₄	1
II. Molecular wt	43.59
III. Physical Properties	
Density (above liquidus) lb/ft ³	$177.8 - (1.94 \times 10^{-2})t$
t in °F	
@ 1200°F	154.5
Liquidus, °F	842
Heat capacity, Btu/lb-°F	
Solid 212 - 806°F	$0.132 + (4.033 \times 10^{-4})t$
Liquid 887 - 1472°F	$0.575 - (9.99 \times 10^{-5})t$
@ 1200°F	0.455
Heat of fusion (@ 842°F), Btu/lb	138.6
Viscosity, centipoise, T in °F	$0.1534 e^{6476/T}$
Range: 1122-1472°F	
@ 1200°F	7.64
Thermal conductivity, Btu/hr-ft-°F	$2.74 + (5.516 \times 10^{-4})t - (1.37 \times 10^{-7})t^2$
t in °F	
@ 1200°F	3.21

Table I.4. Composition and Properties of
Coolant Salt for MSRE

I. Chemical Composition	Mole Percent
LiF	66
BeF ₂	34
II. Molecular Weight	33.14

Table I.4. Continued

III. Physical Properties (at normal ave operating Temperature, (1062°F)	
Density, lb/ft ³	120.5
Viscosity, lb/ft-hr	20.0
Specific heat, Btu/lb-°F	
Solid (122 - 680°F)	0.210 + (4.71 × 10 ⁻⁴)t
Liquid (896 - 1508°F)	0.174 + (3.31 × 10 ⁻⁴)t
@ 1062°F	0.526
Thermal conductivity, Btu-ft/ft ² -hr-°F	3.5
Liquidus temperature, °F	851

Heat Capacity

The temperature-dependent equation for heat capacity of Mixture 133 is (1):

$$C_p = 0.473 - 0.000238 T \text{ cal/g-}^{\circ}\text{C} \quad (T = ^{\circ}\text{C})$$

Values of heat capacity of MSCR Salts 2 and 3 at a given temperature may be estimated by interpolating between published values of other salts of different molecular weights, since heat capacity of molten salts probably varies inversely with molecular weight. Published values of heat capacity at 700°C of some known salts are shown in Fig. I.2, which contains a plot of heat capacity as a function of molecular weight.

Heat capacity relationships for MSRE fuel and coolant salts are shown in Tables I.3 and I.4.

Thermal Conductivity

Like heat capacity, thermal conductivity can be expected to vary inversely with molecular weight. An estimate of the thermal conductivities of the MSCR fuel salts has been made by extrapolating the published

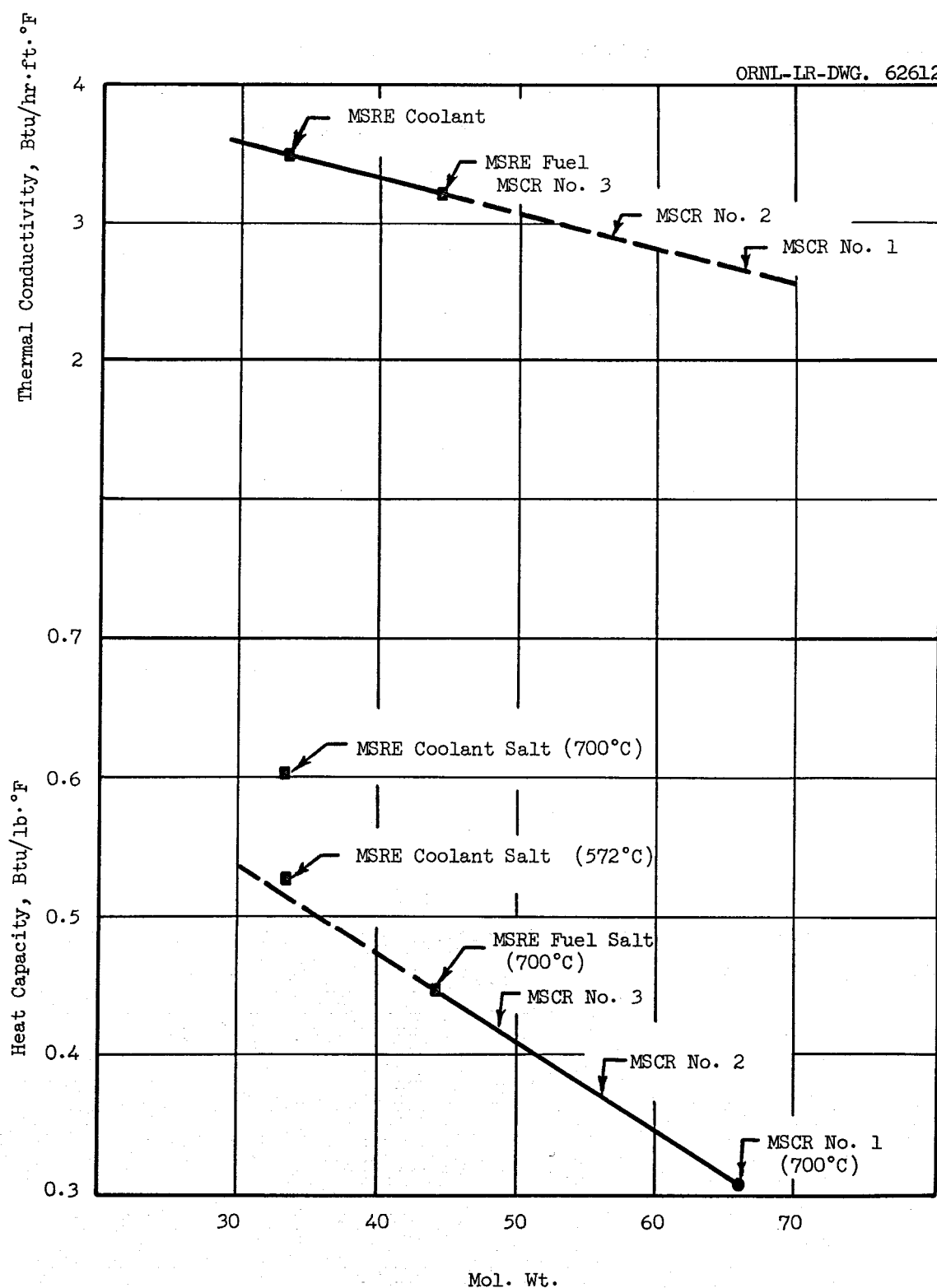


Fig. I.2. MSCR Salt Thermal Conductivity and Heat Capacity.

values of the lower molecular weight MSRE salts to the higher weights of the MSCR salts. This extrapolation is shown in Fig. I.2. However, the published values may not have much precision or accuracy (1).

Density

Temperature dependent relationships for calculating the densities of the three MSCR salts are (2):

$$\rho_{\text{MSCR No. 1}} = 3.934 - 7.4 \times 10^{-4}T \quad \text{g/cm}^3 \quad (T = ^\circ\text{C})$$

$$\rho_{\text{MSCR No. 2}} = 3.480 - 6.7 \times 10^{-4}T$$

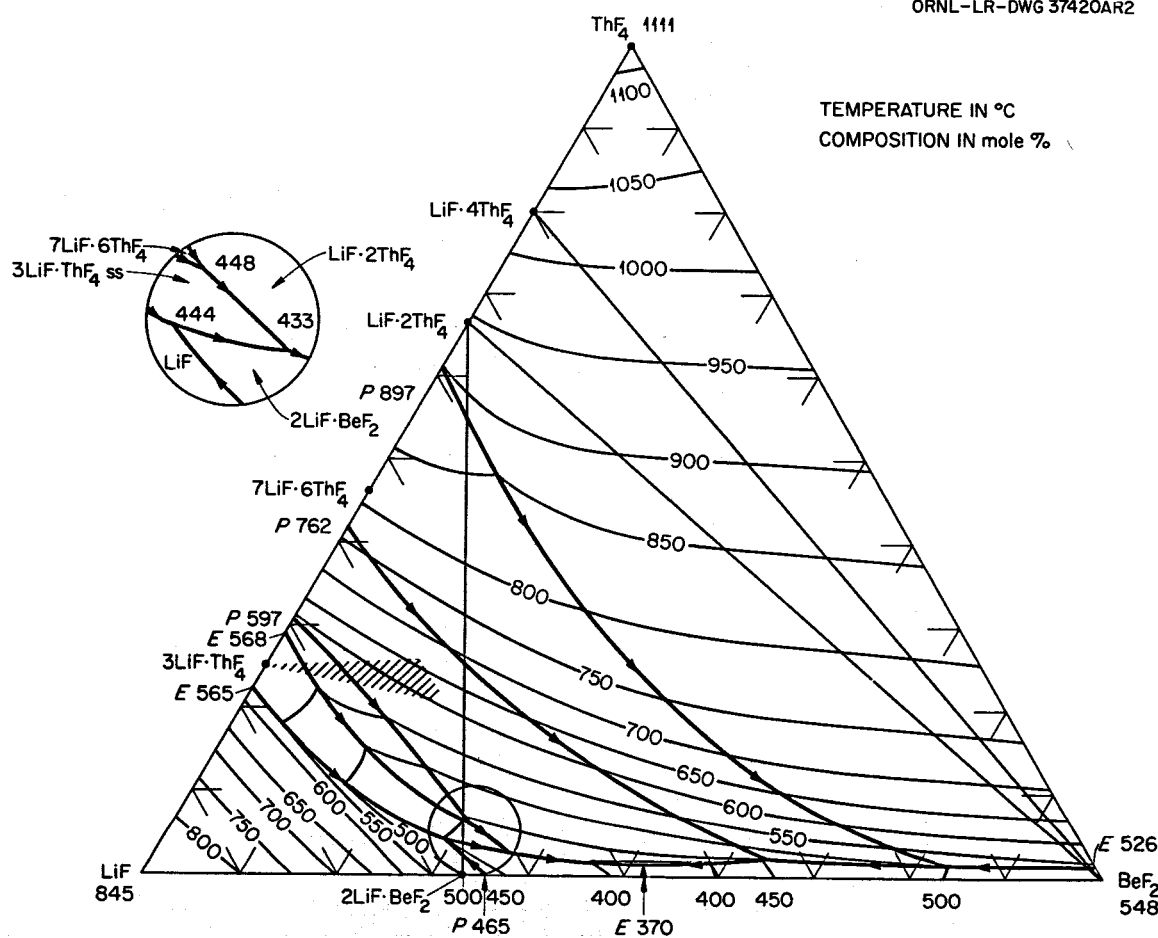
$$\rho_{\text{MSCR No. 3}} = 2.993 - 5.9 \times 10^{-4}T$$

The basis for these estimates is the same as given in reference (3), page 123 with an added term for the ionic volume of thorium equal to $2.82 - 2.94 \times 10^{-3}T$.

Liquidus Temperature

Figure I.3 (from reference 4) was used to obtain the liquidus temperature for the MSCR salts. Mixture 133 (MSCR No. 1) has a liquidus temperature of 505°C (p. 58, ref. 4).

ORNL-LR-DWG 37420AR2

Fig. I.3. The System LiF-BeF₂-ThF₄.

References

1. Private communication from H. W. Hoffman.
2. Private communication from S. Cantor.
3. Oak Ridge National Laboratory, MSRP Semiann. Progr. Rept. August 1, 1960 to February 28, 1961, USAEC Report ORNL 3122.
4. C. F. Weaver et al., Phase Equilibria in Molten Salt Breeder Reactor Fuels. I. The System LiF-BeF₂-UF₄-ThF₄, USAEC Report ORNL-2896, Oak Ridge National Laboratory, December 27, 1960.
5. S. I. Cohen, W. D. Powers, and N. D. Greene, A Physical Property Summary for ANP Fluoride Mixtures, USAEC Report ORNL-2150, Oak Ridge National Laboratory, August 23, 1956. (Declassified 11/24/59.)
6. B. C. Blanke et al., Density and Viscosity of Fused Mixtures of Lithium, Beryllium, and Uranium Fluorides, USAEC Report MLM-1086, Monsanto Research Corporation, March 23, 1959.

W. L. Breazeale, Revisions to MSRE Design Data Sheets - Issue No. 4, MSR-61-100, August 15, 1961.

Appendix J

FUEL AND CARRIER SALT COST BASES

W. L. Carter

Introduction

A survey was conducted among suppliers of ThF_4 , ThO_2 , LiF , BeF_2 , ZrF_4 and NaF to determine current market prices. The data are evaluated and a recommended set of values to be used in molten salt converter and breeder reactor calculations is presented. The cost data are needed in calculating fuel cycle costs.

The following values are recommended for use in molten salt reactor calculations:

ThF_4	\$ 6.50 per pound
BeF_2	7.00 per pound
LiF	14.70 per pound
ZrF_4	4.00 per pound

One of the purposes of the study of thorium breeder and converter reactors is to furnish comparative fuel cycle cost data on the various systems as well as nuclear performance data. The market survey was conducted to obtain current and reliable price information on several chemical compounds which will be needed in rather large inventory and for which the consumption rate may be significant. The inquiries were concerned primarily with molten salt reactor materials, namely, thorium fluoride, lithium fluoride, beryllium fluoride, zirconium fluoride and sodium fluoride; in addition, prices were obtained for thorium oxide.

Several manufacturers of these chemicals were contacted, and a summary of their price schedules is given in Tables J.1 through J.6. Since it is appropriate to associate a date with a market quotation, it may be noted that these data were obtained during the period November 1961 - January 1962. There is one exception: the comparative figures quoted from document Y-1312 were published in December 1959.

Table J.1. Cost Data for Thorium Fluoride

Vendor or Source of Information	Cost			
	\$/lb ThF ₄ ^a	\$/lb ThF ₄	\$/kg Th ^a	\$/kg Th
Quantity	GCD ^b	Y-1312 ^c	GCD	Y-1312
Initial order of 127,000 kg ThF ₄	6.00 ^d	6.50	17.52 ^d	18.98
Replacement rate of 37,100 kg ThF ₄ /yr	(d)		(d)	
Initial order of 1,271,000 kg ThF ₄	6.00 ^d		17.52 ^d	
Replacement rate of 371,000 kg ThF ₄ /yr	(d)		(d)	

^aNo assay given for the material.^bGCD - General Chemical Division, Allied Chemical Corporation, P.O. Box 70, Morristown, New Jersey. This vendor says price is only a rough estimate.^cR. G. Orrison, Thorium Metal Processes, Y-1312 (December 18, 1959). This price is not based on the indicated quantity.^dNo distinction made in price because of quantity or rate.

Table J.2. Cost and Composition Data for Thorium Oxide

Vendor or Source of Information	Cost Data					
	Cost					
	\$/lb ThO ₂	\$/lb ThO ₂	\$/lb ThO ₂	\$/kg Th	\$/kg Th	\$/kg Th
Material Designation	AP ^a	AP	Y-1312 ^b	AP	AP	Y-1312
Material Form	Code 111 Powder	Code 112 Powder	Not stated	Code 111 Powder	Code 112 Powder	Not stated
Cost quoted for						
Initial order of 127,000 kg ThO ₂	7.00	7.50	5.75-8.50	17.52	18.78	14.39-21.28
Replacement rate of 37,100 kg ThO ₂ /yr	7.00	7.50		17.52	18.78	
Initial order of 1,270,000 kg ThO ₂	7.00	7.50		17.52	18.78	
Replacement rate of 371,000 kg ThO ₂ /yr	7.00	7.50		17.52	18.78	
Composition Data						
Typical Analysis (ppm unless indicated)						
Vendor or Source of Information	AP		AP		Y-1312	
Element or Compound						
ThO ₂	99% min		99% min		Not given	

^aAP - American Potash and Chemical Corporation, 99 Park Avenue, New York 16, New York.

^bR. G. Orrison, Thorium Metal Processes, Y-1312 (December 18, 1959). This price is not based on the indicated quantity.

Table J.2 (continued)

Vendor or Source of Information Element or Compound (continued)	Composition Data		
	AP	AP	Y-1312
Rare earth oxide	50	30	
Sulfate, SO ₃	100	50	
Phosphate, P ₂ O ₅	50	10	
Fe	50	6	
CaO	100	10	
MgO	100	1	
Na + K + Li	2000	1	
Silica, SiO ₂	500	5	
Boron, B		0.1	
Uranium, U		10	
Loss on ignition	5000	5000	
Sm	10	1-2	
Eu	1	0.2	
Gd	10	1	
Dy	5	1	

264

Table J.3. Cost Data^a for Lithium Fluoride

Quantity	Cost ^b	
	\$/lb LiF	\$/kg Li
Initial order of 16,000 kg Li	(c)	(c)
Replacement rate of 5,100 kg Li/yr	(c)	(c)

^aThe sources of information are Atomic Energy Commission-Oak Ridge Operations, Oak Ridge Gaseous Diffusion Plant, and Union Carbide Company - Y-12 Plant.

^bThe price is for (c) at. % ⁷Li and includes a basic charge for the material produced as the monohydrate ($\text{LiOH}\cdot\text{H}_2\text{O}$) plus a conversion cost for $\text{LiOH}\cdot\text{H}_2\text{O} \rightarrow \text{LiF}$ plus a feed cost plus an AEC overhead cost.

^cClassified information.

Table J.4. Cost and Composition Data for Beryllium Fluoride

Vendor Quantity ^c	Cost Data			
	Cost			
	\$/lb BeF ₂ BBCo ^a	\$/lb BeF ₂ BCorp ^b	\$/kg Be BBCo	\$/kg Be BCorp
Initial order of 23,800 kg BeF ₂	6.66	7.25	76.52	83.29
Replacement rate of 6,950 kg BeF ₂ /yr	6.00	7.25	68.93	83.29
Initial order of 238,000 kg BeF ₂	6.48	6.95	74.45	79.85
Replacement rate of 69,500 kg BeF ₂ /yr	6.00	6.95	68.93	79.85

Element or Compound	Composition Data	
	Manufacturing Specifications	Typical Analysis of Manufactured Material ^d
BeF ₂	99.5 ± 0.5 wt %	99.5 wt % min
H ₂ O	0.1 - 0.5 wt %	0.06 wt%
Fe	400 ppm max	25 ppm
Ni	100 ppm max	20 ppm
Cr	100 ppm max	<1 ppm
Al	200 ppm max	90 ppm
S	500 ppm max	750 ppm

^aBrush Beryllium Company, 5209 Euclid Avenue, Cleveland 3, Ohio.

^bThe Beryllium Corporation, Reading, Pennsylvania.

^cShipped as 1 × 1 × 1-inch lumps.

^dThe analysis given is for BBCo material; no analysis was given for BCorp material.

Table J.5. Cost and Component Data for Zirconium Fluoride

Vendor	Cost Data		Cost	
	\$/lb ZrF ₄		\$/kg Zr	
	TAD ^a	GCD ^b	TAD	GCD
Quantity				
Initial order of 55,100 kg ZrF ₄	4.00	4.50	16.13	18.15
Replacement rate of 16,100 kg ZrF ₄ /yr	4.00	(c)	16.13	
Initial order of 551,000 kg ZrF ₄	3.55	(c)	14.32	
Replacement rate of 161,000 kg ZrF ₄ /yr	3.55	(c)	14.32	
Composition Data				
Typical Assay (wt %)				
Vendor			TAD	
			GCD	
Element or Compound				
ZrF ₄	Not given		98.5+	
Chlorides	0.007		0.003	
S	0.003		0.01	
Hf	0.01		0.03	
Fe	0.03		0.003	
Ni				

^aTAD - Titanium Alloy Manufacturing Division, National Lead Co., 111 Broadway, New York 6, New York. No assay was given; however, the bid was for Hf-free material.

^bGCD - General Chemical Division, Allied Chemical Corp., P.O. Box 70, Morristown, New Jersey. This vendor says the price is approximate.

^cNo cost distinction is made for quantity or rate.

Table J.6. Cost and Composition Data^a for Sodium Fluoride

	Cost Data	
	\$/lb NaF	Cost ^b \$/kg Na
Shipping Containers		
100 lb multiwall paper bags	0.135	0.542
375 lb leverpak fiber drums	0.139	0.558
Composition Data		
Elements		
Na	Major constituent	
Ca	0.05-0.5	
Al	0.03-0.3	
Si	0.01-0.1	
Fe, Mg	0.0005-0.005 each	
Cu	Trace, <0.0001	
Sc	Not detected, <0.1	
K, Ba	Not detected, <0.01 each	
B, Mo	Not detected, <0.001 each	
Ti, Mn, Co, Ni, V	Not detected, <0.0005 each	
Cr, Ag	Not detected, <0.0001 each	

^aAll information is from the Blockson Chemical Company, P.O. Box 1407, Joliet, Illinois.

^bFor an initial order of 75,800-758,000 kg NaF and a replacement rate of 22,100-221,000 kg NaF/yr.

Bases for Establishing Prices

It was assumed that prices would be established for a large molten salt, power-producing system. Two conditions were visualized: (a) A 1000 Mwe (2500 Mwt) station and (b) ten of these 1000 Mwe stations in simultaneous operation. These conditions established the initial inventory requirements. The consumption rates were calculated by assuming that the fuel salt would be discarded after removal of fissile material on a 1000-day cycle. It was assumed that thorium and carrier salt could not be decontaminated and recovered.

Vendors were asked to quote prices on the basis of producing materials in the quantities desired by existing methods and according to current specifications. It was not considered appropriate to ask a vendor in an information-seeking survey such as this to do much research into manufacturing procedures and schedules if his operations would be significantly affected by these additional quantities. Consequently, no rigid specifications were affixed to these chemicals other than the obvious one that all materials should have extremely low concentrations of high neutron cross section materials.

General Comments on Price QuotationsThorium Fluoride

Only one manufacturer was interested in making a quotation for ThF_4 , and it was admitted that this was a rough approximation. The price compared favorably with the value quoted by Orrison (1) in a previous market survey.

Zirconium Fluoride

Vendors were asked to quote on hafnium-free ZrF_4 . The quantities requested are apparently quite large compared with available production.

Beryllium Fluoride

The suppliers indicate that there would be no problem in supplying the quantities requested. Beryllium fluoride is an intermediate compound in the production of beryllium metal. Although the vendors state that the prices quoted are tentative, they are probably rather accurate.

Sodium Fluoride

This chemical is available in large supply. The quoted prices should be quite firm. Sodium fluoride is so inexpensive that its use in a reactor contributes negligibly to the fuel cycle cost.

Thorium Oxide

Thorium oxide is available in large supply; the quoted prices are perhaps rather firm. The quotes compare favorably with the values given by Orrison (1).

Lithium Fluoride

Lithium fluoride occupies a singular position in the molten salt fuel system particularly with regard to availability and price. Since the lithium content must have a high ^{7}Li assay, the only source of material is from AEC production facilities. AEC-ORO, Y-12 and ORGDP personnel (2) were instrumental in developing a classified price schedule for high isotopic purity ^{7}Li in quantities to meet the requirements of a large molten salt power installation.

Lithium is produced as $\text{LiOH}\cdot\text{H}_2\text{O}$ for which a reasonably accurate price can be computed. However, an uncertainty exists in the charge for converting the hydroxide to an anhydrous fluoride product since this operation has not been attempted except in small-scale batches; this charge was estimated. A schedule of basic charges was recommended (3,4) for computing the price of lithium fluoride in 99.995 at. % ^{7}Li :

\$/kg Li*

$\text{LiOH}\cdot\text{H}_2\text{O}$	=
$\text{LiOH}\cdot\text{H}_2\text{O} - \text{LiF conversion}$	=
Cascade feed cost (4)	=
Base cost	=
Plus 15% AEC overhead (4)	=

The values have not been released by the Atomic Energy Commission as an official price for high purity ^7Li ; they are confidential information for internal use only.

The official price was \$120/kg of Li metal as the fluoride in November 1959 (5) for a grade containing 99.99% of ^7Li . This price was adopted for material containing 99.995% ^7Li produced in large quantities.

Recommended Values for Molten Salt Fuel

Based on the values given in Tables J.1, J.3, J.4, and J.5, the following prices are recommended for use in molten salt reactor fuel cycle calculations. These prices were chosen more or less arbitrarily from the accumulated data since there was no reason to have more credence in one value than another.

<u>Element</u>	<u>\$/lb of fluoride compound</u>	<u>\$/kg of metal (as fluoride)</u>
Thorium	6.50	19.00
Beryllium	7.00	80.42
Lithium	14.70	120.00
Zirconium	4.00	16.13

*This information is classified.

References

1. R. G. Orrison, Thorium Metal Processes, Y-1312 (December 18, 1959).
2. Personal communications with E. E. Keller, AEC-ORO, Neal Dow, UCC-Y-12 Plant, and Murray Hanig, UCC-ORGDP.
3. Letter from R. G. Jordan (Y-12) to C. A. Keller (AEC-ORO), No. Y-AO-2314, January 10, 1962.
4. Personal communication with E. L. Keller, AEC-ORO (January 18, 1962).
5. Nucleonics, 17(11): 31 (November 1959).

Appendix K

MSCR POWER LIMITATION RESULTING FROM
MODERATOR THERMAL STRESS

R. H. Chapman

Summary

In order to achieve the maximum performance from the MSCR, it is necessary to operate at a power level corresponding to some limiting condition. The limiting condition may be arbitrarily imposed upon the system or it may be an inherent feature in the design. In certain conceivable situations thermal stress in the graphite moderator may limit the power output of a single reactor core. It is therefore of interest to estimate the maximum power output as a function of core diameter for the case where thermal stress is the limiting condition.

It is assumed for the purpose of this memorandum that the reactor core is a cylinder of $L/D = 1.0$. Honeycomb shaped fuel channels are formed by the proper spacing of hexagonal graphite moderator prisms. For the purpose of estimating the thermal stress, it is also assumed that the hexagonal prisms can be approximated by a right circular cylinder of a diameter equal to the distance across the flats of the hex. It is noted from the geometry of the hexagonal unit cell that the fuel volume fraction, f_v , the fuel channel thickness, t_c , and the distance across flats, d_c , are interrelated. Figure K.1 shows the relationship for the region of interest. The size of the unit cell is obtained by adding the channel thickness to the distance across flats of the moderator prisms.

Assuming uniform heat generation, the maximum thermal stress (at the surface) is given¹ for a solid cylinder as

$$\sigma_t = \frac{1}{2} \frac{\alpha E}{1-\nu} \frac{q'''}{4k} r_o^2 \quad (1)$$

where

σ_t = tangential thermal stress, psi,

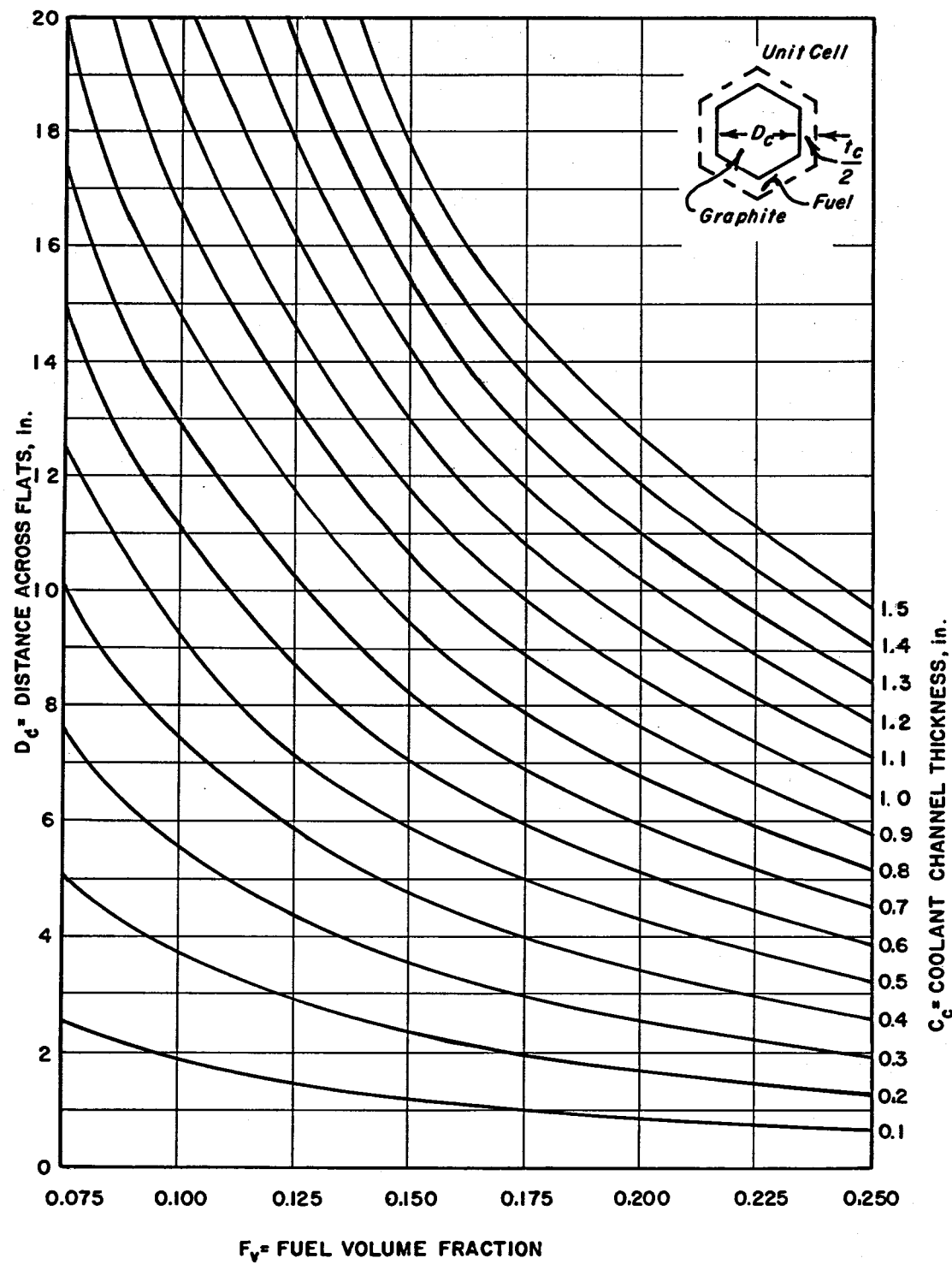


Fig. K.1. Hexagonal Unit Cell Relationship.

α = coefficient of thermal expansion, $\frac{\text{in.}}{\text{in. } ^\circ\text{F}}$,

E = modulus of elasticity, psi,

ν = Poisson's ratio,

q''' = volumetric heat source, $\frac{\text{BTU}}{\text{hr ft}^3}$,

r_o = radius of cylinder, ft,

k = thermal conductivity, $\frac{\text{BTU}}{\text{hr ft } ^\circ\text{F}}$.

It is assumed that the uniform volumetric heat generation term can be related to the core heat production rate by

$$q''' = \frac{f_p Q_c}{V_M} \left(\frac{P_{\max}}{\bar{P}} \right) C_1 \quad (2)$$

where

f_p = fraction of total heat which is produced in moderator,

Q_c = core heat production rate, Mwt,

V_M = volume moderator in core, ft^3 ,

C_1 = conversion factor = $3.413 \times 10^6 \frac{\text{BTU}}{\text{hr - Mw}}$,

$\frac{P_{\max}}{\bar{P}}$ = ratio of peak-to-average core power density.

The core moderator volume is given for $L/D_c = 1.0$ as

$$V_M = (1 - f_v) \frac{\pi D_c^3}{4} \quad (3)$$

Substituting Eq. (2) and (3) into (1) and rearranging, the following expression is obtained:

$$\frac{Q_c}{1 - f_v} = \frac{2\pi k}{C_1} \frac{1 - \nu}{\alpha E} \sigma_t \left(\frac{\bar{P}}{P_{max}} \right) \frac{D_c^3}{f_p r_o^2} \quad (4)$$

Assuming values for the various properties of graphite, i.e., σ_t , α , E , ν , and k , and representative values for the fraction of total heat generated in the graphite and for the peak-to-average power density ratio, a family of curves of heat production versus diameter may be plotted wherein r_o is the parameter.

Choosing an allowable stress value of graphite is a somewhat arbitrary operation. Experience has shown in the production of AGOT graphite for the EGCR (16 in. \times 16 in. \times 20 ft long columns) that the mechanical properties vary widely between different blocks of the material, vary across the cross-section of the large blocks, and depend on the orientation relative to the direction of extrusion.² Fracture strain is probably a better criteria for failure than stress, since it has been shown to be fairly constant at about 0.1 to 0.2%. Tests have also shown that strength is not temperature dependent at least up to 1100°F. Since the ratio of stress to modulus of elasticity appears in Eq. (4), the value of the fracture strain can be substituted and thus side-step the issue of fraction stress. A value of 0.1% is assumed as a failure criterion.

For Poisson's ratio a value of 0.4 is recommended, and for the thermal coefficient of expansion, a value of 2.7×10^{-6} in./in. °F is used.³ A value of 15 BTU/hr·ft·°F is used for the thermal conductivity at 1200°F.⁴ A value of 2.5 is assumed for the ratio of peak-to-average power density to account for the maximum thermal stress condition. This is about the value computed for the MSRE.⁵ A value of 0.05 is assumed for the fraction of total heat produced in the moderator, essentially the same as for the MSRE.

Multiplying the heat rate by the overall net thermodynamic efficiency, one obtains the net power output. An assumed value of 40% efficiency is used. With these assumptions Eq. (4) becomes

$$\frac{P}{1 - f_v} = 0.0196 \frac{D_c^3}{r_o^2}, \text{ Mwe (net)} . \quad (5)$$

Figure K.2 is a plot of Eq. (5) for the range of interest. Also shown in the figure are 500 and 1000 Mwe condition for fuel volume fractions of 0.10, 0.15, and 0.20. With the figure, and for a given set of conditions one is able to estimate quickly the maximum graphite size permitted by thermal stress considerations. For example, if it is desired to provide 1000 Mwe with single core of 20 ft diam and 10 vol. % fuel, it is seen from the figure that the largest graphite moderator prism is limited to about 9 in. across flats.

It should be pointed out that the data used in constructing the figure are subject to considerable uncertainty. Design data for large sections of graphite such as likely to be used in the MSCR are, of course, unavailable at this time. However, it is believed that the results obtained from the figure will be conservative.

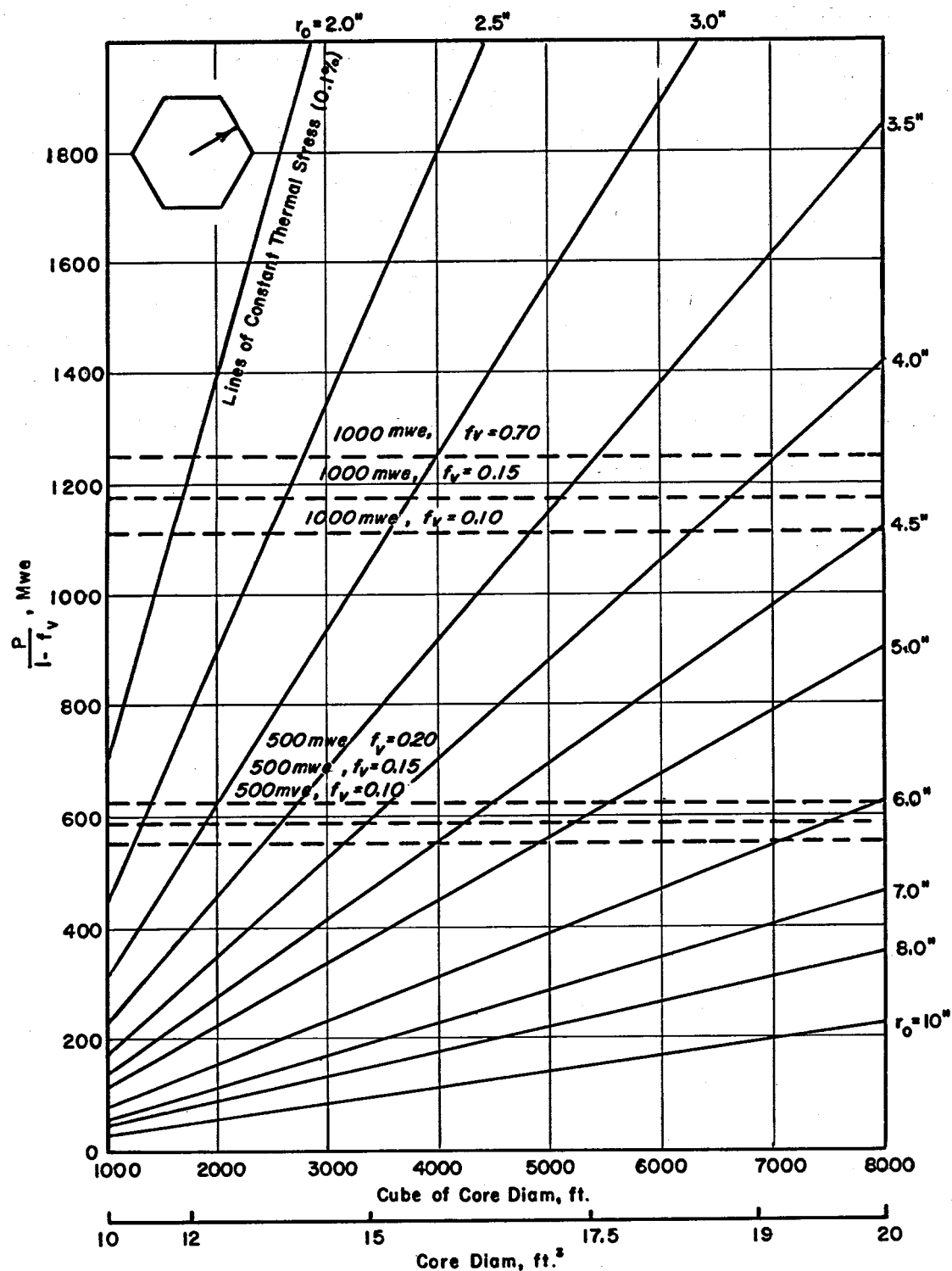


Fig. K.2. Thermal Stress Power Limitation.

References

1. Ralph Hankel, Stress Temperature Distributions, Nucleonics, Vol. 18, No. 11, pp. 168-169 (November 1960).
2. B. L. Greenstreet, Oak Ridge National Laboratory, personal communication.
3. S. E. Moore, Oak Ridge National Laboratory, personal communication.
4. L. G. Alexander et al., Thorium Breeder Reactor Evaluation, Part 1 - Fuel Yield and Fuel Cycle Costs in Five Thermal Breeders - Appendices, ORNL-CF-61-3-9, Appendices, p. 33 (May 24, 1961).
5. C. W. Nestor, MSRE Preliminary Physics Report, ORNL-CF-61-4-62 (April 9, 1961).

Appendix L

VOLUMES OF FUEL SALT AND INTERMEDIATE COOLANT SALT FOR
1000 Mwe MOLTEN SALT CONVERTER REACTOR

D. B. Janney

Introduction

The volumes of the salt streams (including heels in dump tanks, etc.) were calculated for the reference design described in Sec. 4.

Fuel Salt Volume

Table L.1. Volume of MSCR Fuel Salt

A. Reactor	1360 ft ³
B. Piping	320 ft ³
C. Pumps	130 ft ³
D. Primary Heat Exchangers	575 ft ³
E. Dump Tanks, Control Tanks	<u>115 ft³</u>
TOTAL	2500 ft ³

These volumes were calculated as follows:

A. Reactor

Core (L = 20 ft, D = 20 ft)

$$0.785 (20)^3 \times 10\% = 630 \text{ ft}^3$$

Annulus (L = 20 ft, t = 1 in.)

$$\frac{\pi}{12} (20)^2 = 105 \text{ ft}^3$$

Top Plenum (h = 13 in., D = 20 ft,
incl. core hold-down grid* of
 $h_g = 4$ in., t = 1 in.)

*See Fig. 4.8.

$$\left[0.785 (20)^2 \cdot \frac{13}{12}\right] - \left[\frac{0.785 (20)^2}{6 \times 5.2} \times 24 \left(\frac{1}{2}\right) 4\right] = 340 - 48 = 290 \text{ ft}^3$$

Bottom Plenum ($h = 11$ in., $D = 20$ ft,
incl. core support grid* of $h_g = 3$ in.,
 $t = 1$ in.)

$$\left[0.785 (20)^2 \times \frac{11}{12}\right] - \left[\frac{0.785 (20)^2}{6 \times 5.2} \times 24 \left(\frac{1}{2}\right) 3\right] = 288 - 36 = 250 \text{ ft}^3$$

Dome ($L = 6$, $D = 6$)

$$0.785 (6)^3 \times \frac{1}{2} (\text{liq. vol.}) = \underline{\underline{85 \text{ ft}^3}}$$

REACTOR TOTAL $\underline{\underline{1360 \text{ ft}^3}}$

B. Piping

Pump Suction (6 ft, 14 in. Sch. 20)

$$6 \times \frac{140.5}{144} \times 8 = \underline{\underline{50 \text{ ft}^3}}$$

Pump Discharge (20 ft, 12 in. Sch. 40)

$$20 \times \frac{111.9}{144} \times 8 = \underline{\underline{125 \text{ ft}^3}}$$

Reactor Inlet (25 ft, 10 in. Sch. 20)

$$25 \times \frac{82.5}{144} \times 8 = \underline{\underline{115 \text{ ft}^3}}$$

Misc. Piping (Estimate)

$$\underline{\underline{30 \text{ ft}^3}}$$

PIPING TOTAL

$$\underline{\underline{320 \text{ ft}^3}}$$

C. Pump Bowl (8)

(Equiv. ann. 1 ft, equiv. depth 1 1/2 ft)

$$\pi \times 1(3 \frac{1}{2}) \times 1 \frac{1}{2} \times 8 = \underline{\underline{130 \text{ ft}^3}}$$

D. Primary Heat Exchanger (8)

(Shell ID 43.75 in., shell length
13 1/2 ft)

$$\left[\frac{0.785 (43.75)^2}{144} - \frac{0.785 (0.5)^2 4050}{144} \right] 13.5 \times 8$$

$$+ \left[0.667 \times \pi \left(\frac{21}{12} \right)^3 \left(1 - \frac{5.5}{10.4} \right) \right] 8 = 530 + 45 = 575 \text{ ft}^3$$

Coolant Salt Volume

Table L.2. Volume of Coolant Salt

A. Superheaters	2425 ft ³
B. Reheaters	485 ft ³
C. Primary Heat Exchangers	510 ft ³
D. Piping	2710 ft ³
E. Pumps	100 ft ³
F. Flush Salt	<u>2385 ft³</u>
TOTAL	8615 ft ³

These volumes were calculated as follows:

A. Superheaters (16)

(Shell ID 31.5 in., U-shell length 58 ft,
0.5 in. tube bundle annulus)

$$\left(0.0029 \text{ ft}^3 \frac{\text{salt vol.}}{\text{ft tube}} \times 785 \times 58 \times 16 \right)$$

$$+ \left[\frac{\pi \times 0.5 (31)}{144} \times 58 \times 16 \right] = 2112 + 313 = 2425 \text{ ft}^3$$

B. Reheaters (8)

(Shell, ID 31 in., U-shell length 23.6 ft,
0.5 in. to be bundle annulus)

$$\left[0.0029 \text{ ft}^3 \frac{\text{salt vol.}}{\text{ft tube}} \times 766 \times 23.6 \times 8 \right]$$

$$+ \left[\frac{\pi \times 0.5 (30.5) \times 23.6 \times 8}{144} \right] = 424 + 61 = 485 \text{ ft}^3$$

C. Primary Heat Exchangers (8)

(Tube ID 0.43 in., tube length 25 ft,
2025 tubes)

$$\left[\frac{0.785 (0.43)^2}{144} \times 25 \times 2025 \times 8 \right] + 100 \text{ (H-X heads)}$$

$$= 410 + 100 = 510 \text{ ft}^3$$

D. Piping (avg. lengths)

Primary H-X outlet (155 ft,
14 in. Sch. 20)

$$155 \frac{140.5}{144} \times 8 = 1250 \text{ ft}^3$$

Primary H-X inlet (125 ft,
14 in. Sch. 20)

$$125 \frac{140.5}{144} \times 8 = 970 \text{ ft}^3$$

Superheater inlet/outlet
(5 ft, 8 in. Sch. 20)

$$5 \frac{51.8}{144} \times 32 = 60 \text{ ft}^3$$

Reheater inlet/outlet (5 ft,
5 in. Sch. 40)

$$5 \frac{20}{144} \times 16 = 10 \text{ ft}^3$$

Pump Suction (70 ft, 12 in.
Sch. 20)

$$70 \frac{118}{144} \times 8 = 460 \text{ ft}^3$$

PIPING TOTAL

2710 ft^3

E. Pumps (System pressurizing and
salt sampling volume only)

100 ft^3

F. Flush Salt (Amount required
equal to reactor system
volume)

2385 ft^3

Appendix M

EVALUATION OF A GRAPHITE REFLECTOR FOR THE
MOLTEN SALT CONVERTER REACTOR

T. W. Kerlin

Introduction

Nuclear calculations on large molten salt converter reactors (MSCR) indicate that the neutron leakage is large enough (2 to 4% of the neutrons produced) to warrant consideration of a graphite reflector. A reactor was chosen from a set presently under study to evaluate the desirability of a reflector. This reactor, which current results indicate is near the optimum with respect to fuel cycle costs, has the characteristics given in Table M.1.

Table M.1. Typical Characteristics of MSCR

Diameter of core, ft	17.7
Height of core, ft	17.7
Carbon-to-thorium ratio	293
Fuel salt composition	68LiF-23BeF ₂ -5ThF ₄
Fuel salt volume fraction	0.10
Fuel processing rate, ft ³ /day	2

The core consists of a graphite matrix inside a 2-in.-thick INOR-8 vessel. Because of the different coefficients of thermal expansion, the vessel will move away from the graphite when the reactor is at power, creating an annulus. Since no adequate metal-to-graphite seal is available, this annulus will contain fuel salt.

The designer may choose to place a reflector between the core and the annulus by merely increasing the size of the graphite region and omitting fuel channels in the outer portion. The designer also might choose to pin graphite blocks to the inside of the vessel so that the reflector moves with the vessel, creating an annulus between the core and the reflector.

A third possibility is a combination of the above two methods, creating an annulus between two reflector regions.

Calculations were made to determine the relative characteristics of the MSCR with (a) no reflector, (b) a 15-in. reflector outside the annulus, (c) a 7.5-in. graphite region between the core and annulus and a 7.5-in. graphite region outside the annulus. The core composition was determined by an iterative procedure to achieve equilibrium with respect to a 2 ft³/day fuel processing rate.

Results

The results are summarized in Table M.2. Here the materials cost is the sum of the inventory and replacement costs. The leakage includes all neutrons which escape from the system, are captured in the vessel, or are captured in the reflector.

Table M.2. Materials Cost and Nuclear Characteristics
of MSCR as a Function of Reflector Condition

Case	Reflector	Materials Cost (mills/kwhr) ^a	Conversion Ratio	Leakage %
1	None	0.783	0.828	2.62
2	Outside annulus	0.740	0.849	1.90
3	Between core and annulus	0.805	0.812	3.16
4	Between core and annulus plus outside annulus	0.784	0.823	2.81

^aElectrical.

These results show that the reflector outside of the annulus improves performance slightly, but that the other reflected reactors have poorer performance. This behavior can be clarified by examining the power density distributions shown in Fig. M.1.

The reactor with the reflector outside the annulus shows a large peak in power in the annulus because of the large thermal flux from the reflector.

ORNL-LR-DWG. 69530

287

Fig. 1a

Unreflected - Case 1

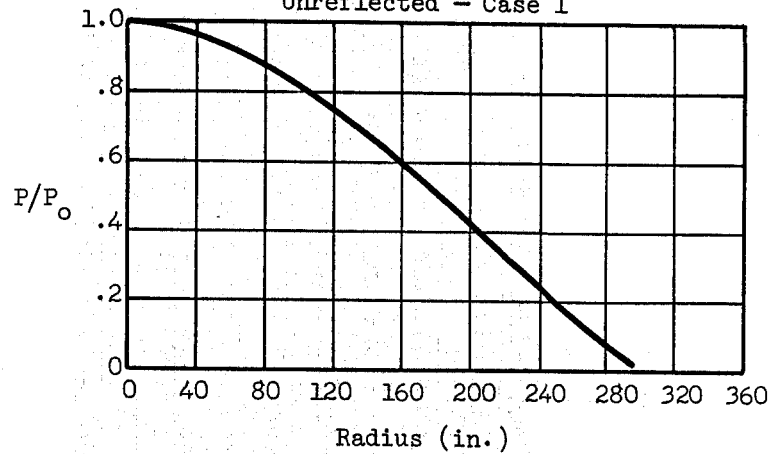


Fig. 1c

Reflector between core and annulus - Case 3

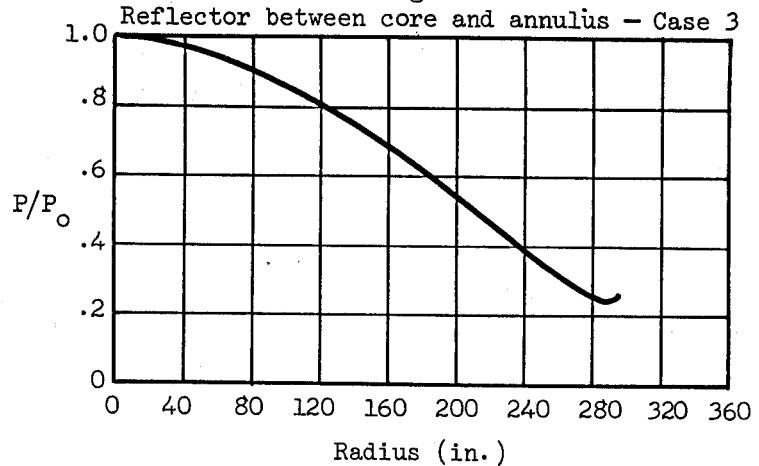


Fig. 1b

Reflector outside annulus - Case 2

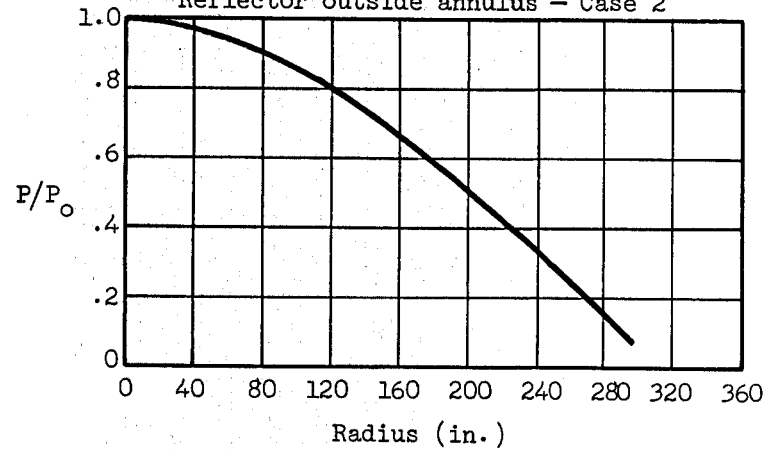


Fig. 1d

Reflector on both sides of annulus - Case 4

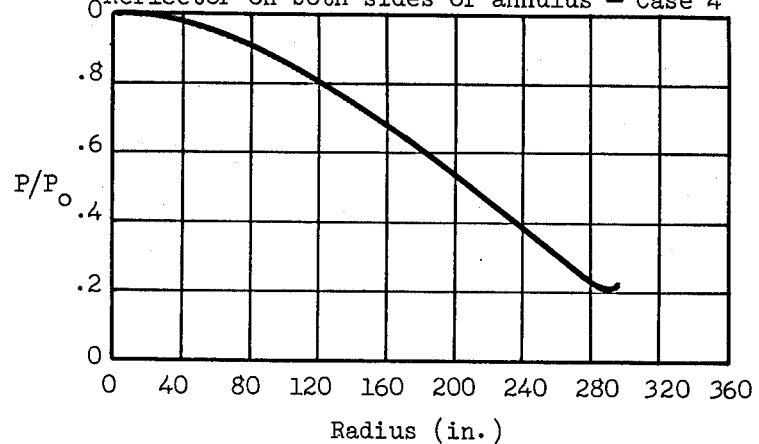


Fig. M.1. Power Density Distribution in MSCR.

Since a peak in the fission rate occurs, the source of neutrons aimed out of the reactor is increased; however, the reflector returns many of the neutrons leaving the annulus. The net effect, as shown in Table M.2, is a slight reduction in leakage.

The reactor with the reflector between the core and annulus experiences a considerable flattening of the power distribution. The fission rate in the annulus remains large and furnishes a large source of neutrons adjacent to the reactor periphery. This source is larger than for the unreflected case, and a higher leakage results.

The reactor with the graphite regions on each side of the annulus combines the bad features of cases 2 and 3. The fission rate is large in the annulus, giving a large source for neutrons to the reactor periphery.

Thus it is seen that the main reason that a reflector has such a small effect is the presence of the fuel annulus. Any addition of reflector increases the fission rate in this region. These fission neutrons are close to the reactor periphery, where they may be absorbed in the vessel or leak out of the reactor. A reflector would be much more beneficial if a design which eliminated the fuel annulus could be devised.

Conclusions

Use of a reflector in the MSCR improved the reactor performance only slightly [0.02 increase in conversion ratio and 0.04 mills/kwhr (electrical) decrease in fuel cycle costs]. Of the reflected-reactor configurations considered, the reactor with the reflector outside of the fuel annulus was the only one which improved performance. However, a method of pinning graphite to the vessel without leaving large cracks is unknown. Also, the extra cost of fabricating an INOR-8 vessel 2.5 ft larger is unknown. Therefore, in view of the slight benefit to be gained and the added design uncertainties and complexity, it appears that no reflector should be used in the MSCR study. If these uncertainties should be removed and slight improvements in performance become important, the gains available with a reflector should be exploited.

Appendix N

DETAILED ESTIMATE OF 1000 Mwe MSCR CAPITAL INVESTMENT*

C. H. Hatstat**

Summary

The cycle chosen for this analysis is shown in elementary form in Fig. 4.3. A 2500 Mwt reactor is cooled with a fuel-bearing molten salt, from which heat is transferred to an inert salt in eight vertical shell-and-tube heat exchangers; the heat in the inert salt is removed in a system of 16 shell-and-tube superheaters and eight reheaters, of a design similar to that of the superheaters. Approximately 63% of the superheated steam flows to a system of four Loeffler boilers, where it produces saturated steam by mixing with the turbine feed water. The remaining superheated steam is delivered at 2400 psi, 1000°F, to the throttle of the steam turbine. Exhaust steam from the high-pressure turbine elements is reheated to 1000°F in the reheaters and flows to the intermediate pressure turbine, from which it flows to a 6-flow low-pressure unit. Condensate is returned to the Loeffler boilers through eight stages of feed-water heating. The gross power output of the cycle is 1083 Mwe at a throttle steam flow of approximately 8×10^6 lb/hr and a condenser pressure of 1.5-in. Hg.

The plant design is based on an Atomic Energy Commission reference site in Western Massachusetts. The site is assumed to have an adequate source of circulating water for the turbine. Because of the low vapor pressure of the reactor coolant, high-pressure containment is not considered necessary; the reactor and its auxiliaries are contained in a sealed, steel lined concrete structure which forms a part of a subdivided biological shield with a total thickness of 10 feet.

The turbine-generator and the other components of the steam-condensate system are housed in a conventional steel frame building. The turbine

*Extracted from SL-1554, SL-1994.

**Sargent and Lundy, Engineers, Chicago, Illinois.

building and the reactor building are arranged so that one traveling bridge crane services both buildings.

Other structures on the site which are included in the cost estimate are the crib house, circulating water intake and discharge flumes and tunnels, waste disposal building and stack, and foundations for oil and condensate tanks. Road and rail access are also provided for the plant.

The cost estimate includes all systems and components necessary for a complete plant. In addition to the energy conversion components, the following equipment and/or systems are estimated in detail.

1. Radioactive waste treatment and disposal systems and building.
2. Cover gas supply and distribution system.
3. Reagent gas supply and disposal system.
4. UF_4 addition facility.
5. Fuel salt handling, sampling and storage systems.
6. Reactor vessel and primary pumps.
7. Thermal shield and cooling system.
8. Emergency shutdown cooling system.
9. Reactor control system.
10. Fuel salt chemical treatment system.
11. Intermediate salt chemical treatment system.
12. Intermediate salt handling, sampling and storage systems.
13. Coolant pump lubricating oil systems.
14. Hot sampling facilities.
15. Remote maintenance facility.
16. Subdivided shielded areas for reactor auxiliaries in the reactor building.

Investment Requirements

The capital investment required for the concept which is described in this report has been estimated on the basis of preliminary design and material quantities prepared by Oak Ridge National Laboratory and Sargent & Lundy. The estimating data for the heat cycle, auxiliary systems, and primary and intermediate system components were prepared by Oak Ridge

National Laboratory. The cost estimate was prepared by Sargent & Lundy, using accounting procedures specified by the U. S. Atomic Energy Commission in the Guide to Nuclear Power Cost Evaluation.

The direct construction cost and indirect cost are summarized below. The detailed estimate is presented on subsequent pages.

Estimated Direct Construction Cost	\$ 89,341,200
Indirect Costs	<u>48,582,600</u>
Total Capital Investment for Structures and Equipment	\$137,923,800
Coolant Salt Inventory plus 1.5% for Interest During Construction	10,951,800
Total Investment, Excluding Fuel Salt	<u>\$148,875,600</u>

Table N.1. 1000 MWe Molten Salt Converter
Reactor Plant - Estimate of Capital
Investment

ONE (1) 2500 MWt MOLTEN SALT REACTOR
ONE (1) 1000 MWe REHEAT TURBINE GENERATOR
UNIT C.C.6F 40" L.S.B.
(2400 Psi. - 1000°F - 1000°F)

(Prices as of 11-1-62 and Based on a 40 Hour Work Week)

		QUANTITY	MATERIAL OR EQUIPMENT	LABOR	TOTALS
<u>ACCOUNT 21 - STRUCTURES & IMPROVEMENTS</u>					
211	<u>Ground Improvements</u>				
.1	Access Roads for Permanent Use				
.11	Grading)				
.12	Surfacing)				
.13	Culverts)				
.14	Bridges & Trestles)	15 Miles			In Place
.15	Guards & Signs)				
.16	Lighting)				
.2	General Yard Improvements				
.21	Grading & Landscaping	Lot	\$6,000	\$19,200	\$25,200
.22	Roads Sidewalks & Parking Areas	47,000 SF	16,500	7,600	24,100
.23	Retaining Walls, Fences & Railings				
.231	Fence, Post, Gates	2,450 LF	8,500	3,200	11,700

Table N.1 (continued)

	QUANTITY	MATERIAL OR EQUIPMENT	LABOR	TOTALS
<u>ACCOUNT 21 - STRUCTURES & IMPROVEMENTS (Cont'd.)</u>				
211 <u>Ground Improvements (Cont'd.)</u>				
.2 General Yard Improvements (Cont'd.)				
.24 Outside Water Distribution Systems Including Fire Hydrants & Water Tanks for General Use				
.241 Domestic Water System				
.2411 500 G.P.M. Deep Wells,) Including Pump & Accessories)				
.2412 Storage Tank, 300 Gal.) & Controls)	Lot	13,000	17,600	30,600
.2413 Water Softener,) Piping & Controls)				
.2414 Piping)				
.242 Fire Protection System				
.2421 Water Storage Tank)				
.2422 2000 GPM Fire Pump & Motor Drive)				
.2423 Other Fire Protection Equipment)	Lot	27,500	27,500	55,000
.2424 Piping, Including Hydrants)				
.2425 Hose & Hose Houses)				

Table N.1 (continued)

	QUANTITY	MATERIAL OR EQUIPMENT	LABOR	TOTALS
ACCOUNT 21 - STRUCTURES & IMPROVEMENTS (Cont'd.)				
211 Ground Improvements (Cont'd.)				
.2 General Yard Improvements (Cont'd.)				
.25 Sewers & Drainage Systems:				
.251 Yard Drainage & Culverts	Lot	4,000	7,000	11,000
.252 Sanitary Sewer System				
.2521 Septic Tank)				
.2522 Dosing Syphon)	Lot	\$12,000	18,400	30,400
.2523 Distribution Box)				
.2524 Tile Field (Drainage))				
.253 Storm Sewer System:				
.2531 Excavation & Backfill)				
.2532 Vitrified Clay Tile)				
(6" & 8"))				
.2533 Reinforced Concrete Pipe)	Lot	13,000	11,200	24,200
(27" & 30"))				
.2534 Manholes)				
.2535 Outfall Structure)				
.26 Roadway & General Lighting				
.261 Security Fence Lighting)				
.262 Roadway Lighting)				
.263 Parkway Cable)	Lot	8,000	11,200	19,200
.264 Trenching for Parkway)				
Cable)				

294

Table N.1 (continued)

		QUANTITY	MATERIAL OR EQUIPMENT	LABOR	TOTALS
ACCOUNT 21 - STRUCTURES & IMPROVEMENTS (Cont'd.)					
211	<u>Ground Improvements (Cont'd.)</u>				
.3	Railroads				
.31	Off Site				
.311	Grading)				
.312	Bridges, Culverts & Trestles)	5 Miles	135,000	132,000	267,000
.313	Ballast & Track)				
.314	Signals & Interlocks)				
.32	On Site				
.321	Ballast & Track	265 LF	1,500	1,600	3,100
	TOTAL ACCOUNT 211		\$245,000	\$256,500	\$501,500
212	<u>Buildings</u>				
212A	<u>Turbine Generator Building</u>				
	<u>Including Office, Control Room,</u>				
	<u>Cable Room, Switch Gear Room</u>				
.1	Excavation & Backfill				
.11	Earth Excavation	11,500 CY	-	11,500	11,500
.12	Rock Excavation	5,650 CY	-	45,200	45,200
.13	Backfill	6,350 CY	2,000	9,400	11,400
.14	Disposal	10,800 CY	-	4,400	4,400
.15	Dewatering	Lot	-	75,000	75,000
.3	Substructure Concrete				
.31	Forms)				
.32	Reinforcing)				
.33	Concrete)				
.34	Waterproofing)	6,750 CY	232,000	218,400	450,400
.35	Patch & Finish)	Conc.			
.36	Miscellaneous Anchor Bolts,)				
	Sleeves Etc. Embedded in)				
	Concrete)				

Table N.1 (continued)

		QUANTITY	MATERIAL OR EQUIPMENT	LABOR	TOTALS
ACCOUNT 21 - STRUCTURES & IMPROVEMENTS (Cont'd.)					
212	<u>Buildings (Cont'd.)</u>				
<u>212A Turbine Generator Building</u>					
<u>Including Office, Control Room,</u>					
<u>Cable Room, Switch Gear Room (Cont'd.)</u>					
.4	Superstructure				
.41	Superstructure Concrete				
.411	Forms)				
.412	Reinforcing)	34,000 SF	\$57,500	\$49,000	\$106,500
.413	Concrete)	of Floor			
.42	Structural Steel &				
	Miscellaneous Metal				
.421	Structural Steel	1,650 T	535,000	128,000	663,000
.422	Stairs, Ladders, Railings, Walkways, Gratings, Etc.	Lot	55,000	24,000	79,000
.43	Exterior Walls				
.431	Masonry				
.432	Insulated Metal Siding	66,400 SF	134,000	46,400	180,400
.44	Roofing & Flashing				
.441	Pre-Cast Roof Slabs)				
.442	Built-Up Roofing & Flashing)				
.443	Poured Concrete Roof)	35,600 SF	32,000	36,000	68,000
.444	Deck)				
	Insulation)				

Table N.1 (continued)

	QUANTITY	MATERIAL OR EQUIPMENT	LABOR	TOTAL
ACCOUNT 21 - STRUCTURES & IMPROVEMENTS (Cont'd.)				
212 <u>Buildings (Cont'd.)</u>				
212A <u>Turbine Generator Building</u>				
<u>Including Office, Control Room,</u>				
<u>Cable Room, Switch Gear Room</u>				
.4 Superstructure (Cont'd.)				
.45 Interior Masonry & Partitions				
.451 Structural Tile	29,800 SF	\$15,100	\$20,300	\$35,400
.46 Doors & Windows				
.461 Doors	Lot	11,500	4,400	15,900
.462 Windows	12,600 SF	48,000	20,000	68,000
.47 Wall and Ceiling Finish				
.471 Glazed Tile)				
.472 Metal Ceiling)				
.473 Plastering Including) Lathing and Furring)	6,200 SF	5,000	4,400	9,400
.474 Acoustical Tile)				
.48 Floor Finish				
.481 Cement)				
.482 Tile)	Lot	30,000	38,100	68,100
.49 Painting Glazing and Insulation				
.491 Painting	Lot	10,500	32,400	42,900
.492 Glass and Glazing	-	-	-	Incl. 462
.5 Stack (Heating Boiler and Auxiliary Boiler)	1	4,000	1,600	5,600

Table N.1 (continued)

	QUANTITY	MATERIAL OR EQUIPMENT	LABOR	TOTALS
ACCOUNT 21 - STRUCTURES & IMPROVEMENTS (Cont'd.)				
212 <u>Buildings</u> (Cont'd.)				
212A <u>Turbine Generator Building</u>				
<u>Including Office Control Room,</u>				
<u>Cable Room, Switch Gear Room (Cont'd.)</u>				
.6 Building Services				
.61 Plumbing & Drainage Systems)				
.611 Plumbing)				
.612 Drainage)	Lot	\$60,000	\$32,000	\$92,000
.613 Duplex Sump Pump)				
.614 Domestic Cold Water Tank)				
.615 Domestic Hot Water Tank)				
.62 Heating Boiler & Accessories				
.621 Heating Boiler)				
.622 Unit Heaters)				
.623 Discharge Ducts)				
.624 Condensate Pump & Receiver)				
.625 Flash Tank)	Lot	77,000	50,400	127,400
.626 Piping)				
.627 Fuel Oil Transfer Pump)				
.628 Heating Oil Tanks - Day)				
& Storage)				
.6221 Berm for Fuel Oil Storage)				
Tank)				
.6222 Foundation for Heating Oil)				
Day Tank)				
.63 Ventilating System				
.64 Air-Conditioning System)				
.641 Air-Conditioning Control Room)	Lot	55,000	28,000	83,000
.642 Office Air-Conditioning)				
.643 Laboratory Air Conditioning)				

298

Table N.1 (continued)

		QUANTITY	MATERIAL OR EQUIPMENT	LABOR	TOTALS
ACCOUNT 21 - STRUCTURES & IMPROVEMENTS (Cont'd.)					
212	<u>Buildings (Cont'd.)</u>				
212A	<u>Turbine Generator Building</u>				
	<u>Including Office, Control Room,</u>				
	<u>Cable Room, Switch Gear Room (Cont'd.)</u>				
.6	Building Services (Cont'd.)				
.66	Lighting & Service Wiring				
.661	Control Panels & Cabinets)				
.662	Conduit)				
.663	Wiring)	Lot	\$46,500	\$39,200	\$85,700
.664	Fixtures Switches & Receptacles)				
.67	Fire Protection System (Water Lines, Hose, Sprinkler, Etc.)	Lot	<u>12,000</u>	<u>2,400</u>	<u>14,400</u>
	TOTAL ACCOUNT 212A		\$1,422,100	\$920,500	\$2,342,600
					299
212D	<u>Waste Disposal Building</u>				
.1	Excavation and Backfill				
.11	Excavation				
.111	Earth	85 c.y.	-	100	100
.112	Rock	-	-	-	-
.12	Backfill				
.121	Earth	45 c.y.	-	100	100
.13	Disposal				
.131	Earth)	.50 c.y.	-	50	50
.132	Rock)				
.15	Dewatering				
.151	Pumping	Lot	-	1,000	1,000
.3	Substructure Concrete				
	<u>Including, Forms, Anchored Steel</u>				
.31	Bottom Slab)				
.32	Walls to Grade)	100 c.y.	3,500	3,200	6,700

Table N.1 (continued)

		QUANTITY	MATERIAL OR EQUIPMENT	LABOR	TOTALS
<u>ACCOUNT 21 - STRUCTURES & IMPROVEMENTS (Cont'd.)</u>					
<u>212D Waste Disposal Building (Cont'd.)</u>					
.4	Superstructure				
.42	Structural Steel and Miscellaneous Steel				
.421	Structural Steel and Girts	105 Tons	\$34,000	\$8,000	\$42,000
.422	Miscellaneous Steel Galleries Stairs, Landing, Handrailing, Ladders, Etc.	Lot	4,500	2,000	6,500
.43	Exterior Walls				
.431	Insulated Metal Siding	6,800 s.f.	13,600	4,900	18,500
.44	Floors, Barriers, Including Reinforcing, Forms, Etc.				
.441	Walls Above Grade	135 c.y.	6,500	4,000	10,500
.442	Floors	80 c.y.	3,200	1,800	5,000
.4421	Pre-Cast Roof Slab	2,200 s.f.	2,000	2,000	4,000
.45	Interior Masonry and Partitions				
.46	Doors and Windows				
.461	Doors	Lot	2,000	1,000	3,000
.462	Windows	1,200 s.f.	4,500	2,000	6,500
.48	Floor Finish (Cement)	3,500 s.f.	500	1,500	2,000
.49	Exterior and Interior Finishes				
.491	Painting Floor and Walls				
.492	Painting Structural and Miscellaneous Steel)				
.493	Heavy Duty Coating)				
.494	Exterior Coating Below) Grade)	Lot	25,000	20,000	45,000

Table N.1 (continued)

		QUANTITY	MATERIAL OR EQUIPMENT	LABOR	TOTALS
ACCOUNT 21 - STRUCTURES & IMPROVEMENTS (Cont'd.)					
212D Waste Disposal Building (Cont'd.)					
.6	Building Services				
.61	Plumbing and Drainage System	Lot	\$4,800	\$2,200	\$7,000
.66	Lighting and Service Conduit	Lot	1,200	1,800	3,000
.67	Fire-Protection System	Lot	4,000	1,000	5,000
TOTAL ACCOUNT 212D			\$109,300	\$56,650	\$165,950
301					
212F Miscellaneous Structures					
.1	Gate House	Lot	\$5,500	\$5,200	\$10,700
.2	Electrical	Lot	3,000	2,800	5,800
.3	Waste Storage Pond	Each	2,800	5,200	8,000
TOTAL ACCOUNT 212F			\$11,300	\$13,200	\$24,500
212G Reactor Plant Building					
.1	Excavation & Backfill				
.11	Earth Excavation	5,655 c.y.	-	\$5,700	\$5,700
.12	Rock Excavation	1,090 c.y.	-	21,800	21,800
.13	Backfill	755 c.y.		1,200	1,200
.14	Disposal	5,990 c.y.	-	2,400	2,400
.15	Dewatering	Lot	-	55,000	55,000

Table N.1 (continued)

		QUANTITY	MATERIAL OR EQUIPMENT	LABOR	TOTALS
ACCOUNT 21 - STRUCTURES & IMPROVEMENTS (Cont'd.)					
212	<u>Buildings</u> (Cont'd.)				
212G	<u>Reactor Plant Building</u> (Cont'd.)				
.3	Substructure Concrete				
.31	Forms)				
.32	Reinforcing)				
.33	Concrete)				
.34	Waterproofing)	5,730 c.y.	\$200,000	\$185,000	\$385,000
.35	Patch & Finish)				
.36	Miscellaneous Anchor Bolts,) Sleeves Etc. Embedded in) Concrete)				
.4	Superstructure				
.41	Superstructure Concrete				
.411	Forms)				
.412	Reinforcing)	6,981 c.y.	365,000	225,000	590,000
.413	Concrete Interior)				
.42	Structural Steel & Miscellaneous Steel				
.421	Structural Steel & Reactor Supports	964 T	305,000	80,000	385,000
.422	Stairs, Ladders, Railings, Walkways, Grating, Etc.	Lot	30,000	14,500	44,500
.43	Exterior Walls				
.431	Masonry	-	-	-	-
.432	Insulated Metal Siding	54,100 s.f.	110,000	38,000	148,000
.433	Concrete Walls	5,150 c.y.	250,000	157,000	407,000

Table N.1 (continued)

	QUANTITY	MATERIAL OR EQUIPMENT	LABOR	TOTALS
<u>ACCOUNT 21 - STRUCTURES & IMPROVEMENTS (Cont'd.)</u>				
212 <u>Buildings</u> (Cont'd.)				
212G <u>Reactor Plant Building</u> (Cont'd.)				
.4 Superstructure (Cont'd.)				
.44 Roofing & Flashing				
.441 Pre-Cast Roof Slabs)				
.442 Built-Up Roofing & Flashing)	23,300 s.f.	\$21,000	\$21,600	\$42,600
.443 Insulation)				
.45 Interior Masonry & Partitions				
.451 Structural Tile	-	-	-	-
.453 Hot Cells	Lot	400,000	80,000	480,000
.46 Doors & Windows				
.461 Doors	Lot	2,500	1,200	3,700
.462 Windows	7,250 s.f.	27,000	12,000	39,000
.48 Floor Finish				
.481 Cement	35,000 s.f.	12,000	14,400	26,400
.49 Painting Glazing Insulation				
.491 Painting	Lot	7,000	18,500	25,500
.492 Glass and Glazing		Included .462		
.493 Insulation of Reactor Chamber			Incl. in Acct. 221.32	
.5 Stack (When Supported on Building)			Incl. in Acct. 212A	
.6 Building Services				
.61 Plumbing & Drainage System				
.611 Plumbing)				
.612 Drainage)	Lot	15,000	8,000	23,000
.613 Sump Pump)				

Table N.1 (continued)

		QUANTITY	MATERIAL OR EQUIPMENT	LABOR	TOTALS
ACCOUNT 21 - STRUCTURES & IMPROVEMENTS (Cont'd.)					
212	<u>Buildings</u> (Cont'd.)				
212G	<u>Reactor Plant Building</u> (Cont'd.)				
.6	<u>Buildings</u> (Cont'd.)				
.62	Cooling System)	Lot	\$130,000	\$70,000	\$200,000
.63	Ventilating System)				
.66	Lighting & Service				
.661	Control Panels &)				
	Cabinet)				
.662	Conduit)	Lot	17,000	19,600	36,600
.663	Wiring)				
.664	Fixtures, Switches)				
	& Receptacles)				
.67	Fire Protection System				
	(Water Lines, Hose,				
	Sprinkler, Etc.)	Lot	8,500	1,500	10,000
	TOTAL ACCOUNT 212G		\$1,900,000	\$1,032,400	\$2,932,400
	TOTAL ACCOUNT 212		\$3,442,700	\$2,022,750	\$5,465,450
218	<u>Stacks</u>				
218A	<u>Concrete Chimney</u>				
.1	Excavation and Backfill)				
.2	Substructure Concrete)	1	15,000	16,000	31,000
.4	Concrete Chimney)				
.6	Obstruction Lighting)				
	TOTAL ACCOUNT 218A		\$15,000	\$16,000	\$31,000
	TOTAL ACCOUNT 218		\$15,000	\$16,000	\$31,000
	TOTAL ACCOUNT 21		\$3,702,700	\$2,295,250	\$5,997,950

304

Table N.1 (continued)

		QUANTITY	MATERIAL OR EQUIPMENT	LABOR	TOTALS
ACCOUNT 22 - REACTOR PLANT EQUIPMENT					
221	<u>Reactor Equipment</u>				
.1	Reactor Vessel and Supports				
.11	Reactor Vessel Supports	Lot	\$15,000	\$8,000	\$23,000
.12	Vessel and Internals)				
.13	Pump Suction Columns)	Lot	7,540,000	560,000	8,100,000
.14	Graphite Rods)				
.15	Heaters		37,500	Included	37,500
.16	Insulation		7,000	6,400	13,400
.2	Reactor Controls				
.21	Reactor Control Salt Addition				
	Tank	1	6,200	100	6,300
.22	Reactivity Control Drain Tanks	2	42,400	800	43,200
.23	Drain Tank Condenser	1	1,200	100	1,300
.231	Condensate Pump	2	300	100	400
.24	BF ₃ Injection System				
.241	BF ₃ Cylinders			Not Included	
.25	Piping, Valves, Etc.			Incl. Account 228	
.3	Reactor Shielding				
.31	Thermal Shield System				
.311	Thermal Shield & Supports	1	75,000	16,000	91,000
.312	Surge Tank, 2000 Gal.	1	2,400	200	2,600
.313	Circulating Pumps	2	2,600	200	2,800
.314	Heat Exchanger	1	25,000	500	25,500
.315	Piping, Valves, and Insulation	Lot 1		Incl. Account 228	
.32	Biological Shielding -				
	Insulation, Shield Plugs,				
	Etc.	Lot	255,000	124,000	379,000
.34	Shield Cooling System				
.341	Closed Loop Liquid System				
.3411	Shield Cooling Heat				
	Exchanger (4000 Ft. 2				
	Surface - Admiralty)	2	35,000	2,500	37,500

Table N.1 (continued)

		QUANTITY	MATERIAL OR EQUIPMENT	LABOR	TOTALS
ACCOUNT 22 - REACTOR PLANT EQUIPMENT (Cont'd.)					
221	<u>Reactor Equipment (Cont'd.)</u>				
	.3 Reactor Shields (Cont'd.)				
	.34 Shield Cooling System (Cont'd.)				
	.341 Closed Loop Liquid System (Cont'd.)				
	.3412 Shield Cooling Circulating Pumps & Motors (2500 GPM 75 HP Motor)	3	\$7,500	800	8,300
	.3413 Piping & Valves	Lot	Included in Account 228		
	.3414 Cooling Coils Embedded in Concrete (16000 Ft. 1" Steel)	Lot	17,500	32,500	50,000
	.3415 H ₂ O Storage Tank 3000 Gallons	1	1,200	300	1,500
	.7 Reactor Plant Cranes & Hoists		Included in Account 251		
	TOTAL ACCOUNT 221		\$8,070,800	\$752,500	\$8,823,300
222	<u>Heat Transfer Systems</u>				
	.1 Reactor Coolant Systems				
	.11 Reactor Salt Circulating Pumps 9075 GPM Including 1600 HP Motors	8	2,768,000	25,000	2,793,000
	.12 Reactor Salt Piping	Lot	215,000	20,000	235,000
	.13 Insulation	Lot	5,000	5,600	10,600
	.2 Intermediate Coolant System				
	.21 Pumps Including Supports				
	.211 Coolant Salt Pumps - 13,900 GPM Including 2,000 HP Motors	8	3,640,000	30,000	3,670,000
	.212 Auxiliary Pumps and Drives	-			
	.213 Insulation		Included in Account 228		

Table N.1 (continued)

		QUANTITY	MATERIAL OR EQUIPMENT	LABOR	TOTALS
ACCOUNT 22 - REACTOR PLANT EQUIPMENT (Cont'd.)					
222	<u>Heat Transfer Systems</u> (Cont'd.)				
.2	Intermediate Coolant System (Cont'd.)				
.22	Intermediate Coolant Piping and Valves				
.221	Pipe, Valves, Supports, Etc.	Lot	\$1,925,000	172,000	\$2,097,000
.222	Insulation	Lot	50,000	48,000	98,000
.223	Coolant Salt Drain Tanks Including Heaters and Insulation	2	70,000	12,800	82,800
.23	Primary Heat Exchangers & Supports	8	2,320,000	28,000	2,348,000
.3	Steam Generators Superheaters & Reheaters				
.31	Loeffler Boilers	4	4,000,000	160,000	4,160,000
.32	Superheaters	16	6,350,000	48,000	6,398,000
.322	Steam Reheaters	8	1,400,000	10,000	1,410,000
.35	Auxiliary Start-up Boiler (300 Psi. 50,000 lb/hr. oil Fired)	1	60,000	5,000	65,000
.36	Insulation for Above Equipment				
.4	Reactor Coolant Receiving Supply and Treatment				Included in Account 228
.411	Fertile Salt Addition System				
.4111	Fertile Salt Addition Tank	1	1,200	50	1,250
.42	Reagent Gas System				
.421	H ₂ Supply				Not Included
.422	HF Supply				Not Included
.423	Piping				Included in Account 228
.431	Reactor Salt Purification System				
.4311	Chemical Treatment Tank	1	46,600	400	47,000
.4312	Fertile Salt Storage Tank	1	27,500	300	27,800

Table N.1 (continued)

		QUANTITY	MATERIAL OR EQUIPMENT	LABOR	TOTALS
<u>ACCOUNT 22 - REACTOR PLANT EQUIPMENT (Cont'd.)</u>					
222	<u>Heat Transfer Systems (Cont'd.)</u>				
.4	Reactor Coolant Receiving Supply and Treatment (Cont'd.)				
.431	Reactor Salt Purification System (Cont'd.)				
.4313	Radioactive Salt Sampler	Lot	\$67,500	\$1,600	\$69,100
.432	Intermediate Salt Purification System				
.4321	Chemical Treatment Tank	1	19,200	200	19,400
.44	Reactor Salt Charge System				
.441	Reactor Salt Preparation System				
.4411	Salt Melt Tank and Appurtenances	1	30,000	1,000	31,000
.4412	UF ₄ Addition System	1	3,000	500	3,500
.442	Intermediate Salt Charge System				
.4421	Intermediate Salt Preparation Tank and Appurtenances	1	30,000	1,000	31,000

308

Table N.1 (continued)

		QUANTITY	MATERIAL OR EQUIPMENT	LABOR	TOTALS
ACCOUNT 22 - REACTOR PLANT EQUIPMENT (Cont'd.)					
222	<u>Heat Transfer Systems</u> (Cont'd.)				
.4	Reactor Coolant Receiving Supply and Treatment (Cont'd.)				
.45	Cover Gas Supply and Purification System				
.4531	Dryer	2	200	50	250
.4532	Heater	2	400	100	500
.4533	O ₂ Removal Unit	2	3,000	200	3,200
.4534	Coolers	2	200	100	300
.4535	Pure H _e Reservoir	1	400	100	500
.4536	O ₂ Analyzer	1	7,000	500	7,500
.454	Piping		Included Acct. 228		
.5	Intermediate Coolant Storage Tanks, Etc.	2	70,000	2,000	72,000
	TOTAL ACCOUNT 222		\$23,039,200	\$570,500	\$23,609,700
223	<u>Fuel Handling and Storage Equipment</u>				
.31	Fuel Salt Drain and Storage System				
.311	Drain Tanks & Cooling Jacket	54	\$1,269,000	\$16,800	\$1,285,800
.312	Drain Tank Condenser	1	8,000	300	8,300
.3121	Condensate Pump	2	1,400	100	1,500
.313	Decay Storage Tank Including Cooling Jacket	5	55,000	1,000	56,000
.314	Fuel Withdrawal Transfer Tank	1	37,000	100	3,800

Table N.1 (continued)

	QUANTITY	MATERIAL OR EQUIPMENT	LABOR	TOTALS
ACCOUNT 22 - REACTOR PLANT EQUIPMENT (Cont'd.)				
223 Fuel Handling and Storage				
Equipment				
.321 Fuel Withdrawal Metering Tanks	1	\$6,200	\$300	\$6,500
.33 Flush Salt Storage Tanks	5	152,500	2,800	155,300
.34 Piping				Included in Account 228
TOTAL ACCOUNT 223		\$1,495,800	\$21,400	\$1,517,200
225 Radioactive Waste Treatment & Disposal				
.1 Liquid Waste Systems				
.11 High Level Storage Tank	1	12,400	600	13,000
.111 H.L. Storage Tank Pump	2	400	100	500
.112 H.L. Waste Evaporator	1	2,000	100	2,100
.113 H.L. Waste Condenser	1	600	50	650
.114 Evaporator Recycle Pump	2	400	100	500
.13 Demister	1	600	50	650
.14 H.L. Concentrated Waste Storage Tank	1	2,500	150	2,650
.15 KOH Scrubber	1	12,100	400	12,500
.151 KOH Make-up Tank & Pump	1	1,400	100	1,500
.16 H ₂ Burner	1	225	75	300
.161 H ₂ Burner Condenser	1	1,000	100	1,100
.17 Piping				Included in Account 228
.2 Gas Waste				
.21 Stack Blower	2	20,000	2,400	22,400
.211 Absolute Filter.	1	4,000	400	4,400
.212 Roughing Filter	1	1,200	200	1,400

Table N.1 (continued)

		QUANTITY	MATERIAL OR EQUIPMENT	LABOR	TOTALS
ACCOUNT 22 - REACTOR PLANT EQUIPMENT (Cont'd.)					
225	<u>Radioactive Waste Treatment & Disposal (Cont'd.)</u>				
.22	H.F. Absorbers Including				
	Charcoal	2	\$16,000	\$2,400	\$18,400
.221	Absorber Coolers	1	100	50	150
.222	Vacuum Pump	1	500	50	550
.223	H.F. Absorber Vacuum Tank	1	300	50	350
.23	Air Cooled Absorbers				
	Including Charcoal				
.231	1.5" Finned Tubes	2	3,600	400	4,000
.232	3" Finned Tubes	2	8,000	600	8,600
.233	6" Finned Tubes	2	15,000	800	15,800
.234	Dilution Air Duct & Dampers	1	8,000	3,200	11,200
.24	Water Cooled Absorbers				
.241	1/2" Tubes	4	23,200	800	24,000
.242	1" Tubes	4	60,400	1,900	62,300
.243	1-1/2" Tubes	4	51,400	1,900	53,300
.244	2" Tubes	4	49,600	1,800	51,400
.25	Decay Tank	1	12,500	800	13,300
.26	Absorber Cooling Water Condenser	1	900	100	1,000
.27	Helium Recycle Compressor	1	2,000	200	2,200
.28	BF ₃ Stripper	2	28,000	2,400	30,400
.281	Vacuum Pump	1	500	50	550
.29	Piping				
	TOTAL ACCOUNT 225		Included in Account 228		
		\$338,825	\$22,325		\$361,150
226	<u>Instrumentation and Controls</u>				
.1	Reactor		\$300,000	\$170,000	\$470,000
.2	Heat Transfer Systems		70,000	50,000	120,000

Table N.1 (continued)

		QUANTITY	MATERIAL OR EQUIPMENT	LABOR	TOTALS
ACCOUNT 22 - REACTOR PLANT EQUIPMENT (Cont'd.)					
226	<u>Instrumentation and Controls (Cont'd.)</u>				
.3	Service to Fuel Handling and Storage		\$120,000	\$80,000	\$200,000
.4	Service to Radioactive Waste & Disposal		60,000	50,000	110,000
.5	Radiation Monitoring		120,000	80,000	200,000
.6	Steam Generators			Included in Account 235	
.7	Control & Instrument Piping & Wiring			Included in Account 235	
.8	Electrical Connections			Included in Account 235	
.9	Other Miscellaneous			Included in Account 235	
	TOTAL ACCOUNT 226		\$670,000	\$430,000	\$1,100,000
227	<u>Feed Water Supply and Treatment</u>				
.1	Raw Water Supply	1 Lot		Included in Account 211	
.2	Make-up Water Treatment				
.21	Evaporator	-		-	-
.22	Ion Exchange Equipment, Filters, Etc.	1 Lot	\$45,000	\$10,000	\$55,000
.23	Acid & Caustic Transf. Pumps & Drives	2	600	200	800
.24	Demineralized Water Storage Tanks	2	30,000	Included	30,000
.25	Caustic Tank	1	2,200	400	2,600
.26	Acid Tank	1	2,200	400	2,600
.27	Foundation	1 Lot	3,500	2,500	6,000
.28	Piping & Valves	1 Lot		Included in Account 228	
.29	Insulation			Included in Account 228	
.3	Steam Generator Feed- Water Purification	-			

Table N.1 (continued)

		QUANTITY	MATERIAL OR EQUIPMENT	LABOR	TOTALS
ACCOUNT 22 - REACTOR PLANT EQUIPMENT (Cont'd.)					
227	<u>Feed Water Supply and Treatment</u>				
	(Cont'd.)				
.4	Feed-Water Heaters				
.41	Dearating Heaters - "E"				
	4,020,000 #/Hr. 150 Psig.	2	\$240,000	\$15,000	\$255,000
.42	Closed Heaters				
.421	L.P. Heater "A"	3	75,000	5,000	80,000
.422	L.P. Heater "B"	3	63,000	5,000	68,000
.423	L.P. Heater "C"	3	63,000	3,000	66,000
.424	L.P. Heater "D"	3	81,000	3,000	84,000
.425	H.P. Heater "F"	3	315,000	3,000	318,000
.426	H.P. Heater "G"	3	429,000	3,000	432,000
.427	H.P. Heater "H"	3	441,000	3,000	444,000
.5	Feed-Water Pumps and Drives				
.51	Feed-Water Pumps & Drives				
.511	6600 GPM Pumps - 2465 Psig Hd.	3	405,000	12,000	417,000
.512	11,300 H.P. - B.F. Pump Turbine Drive 5600 RPM	3	750,000	30,000	780,000
.52	Motor Driven Start-Up F.W. Pump				
.521	6000 GPM Pump 850 Psig. Hd.	1	70,000	3,000	73,000
.522	3500 H.P. Start-Up FW Pump Motor	1	55,000	2,000	57,000
.53	Heater "A" Drain Pumps and Drives				
.531	620 GPM Pump 285 Psig. Hd.)				
.532	125 H.P. Heater "A" Drain) Pump Motor)	3	22,500	1,500	24,000

313

Table N.1 (continued)

		QUANTITY	MATERIAL OR EQUIPMENT	LABOR	TOTALS
ACCOUNT 22 - REACTOR PLANT EQUIPMENT (Cont'd.)					
227	<u>Feed Water Supply and Treatment</u>				
	(Cont'd.)				
.5	Feed-Water Pumps and Drives (Cont'd.)				
.54	Heater "C" Drain Pumps and Drives				
.541	700 GPM Pumps 210 Psig. Hd.)				
.542	100 H.P. Heater "C" Drain) Pump Motor)	3	\$30,000	\$2,500	\$32,500
.55	Boiler Steam Circulators and Drives				
.551	5,300,000 #/Hr. Steam Circulator - 2500 #675°F	4	975,000	40,000	1,015,000
.552	5000 H.P. Turbine Drive for Steam Circulator 500 # Steam; 10,000 RPM	4	560,000	30,000	590,000
.553	5000 H.P. Motor for Steam Circulator Including Gear and Mag. Coupling	1	<u>100,000</u>	<u>7,000</u>	<u>107,000</u>
	TOTAL ACCOUNT 227		\$4,758,000	\$181,500	\$4,939,500
228	<u>Steam, Condensate, Feed Water, and all Other Piping, Valves Etc.</u>				
	<u>- For Turbine Plant, Crib House and Other Reactor Plant Auxiliaries</u>				
.1	Pipe, Valves, Fittings, Etc.				
.11	Turbine Plant)				
.12	Other Interior Piping)	1 Lot	\$4,025,000	\$2,575,000	\$6,600,000
.13	Yard Pipe Etc.)				

Table N.1 (continued)

		QUANTITY	MATERIAL OR EQUIPMENT	LABOR	TOTALS
ACCOUNT 22 - REACTOR PLANT EQUIPMENT (Cont'd.)					
228	<u>Steam, Condensate, Feed Water, and all Other Piping, Valves Etc. - For Turbine Plant, Crib House and Other Reactor Plant</u> <u>Auxiliaries (Cont'd.)</u>				
	.2 Insulation				
	.21 Piping Insulation	1 Lot	\$455,000	\$520,000	\$975,000
	.22 Equipment Insulation	1 Lot	155,000	195,000	350,000
	TOTAL ACCOUNT 228		\$4,635,000	\$3,290,000	\$7,925,000
229	<u>Other Reactor Plant Equipment</u>				
	.2 Remote Maintenance				
	Facilities	Lot	3,000,000	Included	3,000,000
	.4 Coolant Pump Lube Oil System				
	.41 Storage Tank)	1			
	.42 Pumps)	2			
	.43 Oil Coolers)	2	29,400	600	30,000
	.44 Filters)	2			
	.45 Piping	Lot		Included in Account 225	
	.62 Intermediate Salt Sampling System				
	.621 Sampler and Appurtenances	Lot	16,500	2,000	18,500
	TOTAL ACCOUNT 229		\$3,045,900	\$2,600	\$3,048,500
	TOTAL ACCOUNT 22			\$5,270,825	\$51,324,350

Table N.1 (continued)

		QUANTITY	MATERIAL OR EQUIPMENT	LABOR	TOTALS
<u>ACCOUNT 23 - TURBINE GENERATOR UNITS</u>					
231	<u>Turbine Generators</u>				
.1	Turbine Foundations				
.11	Concrete - Including Reinforcing Steel, Etc.	1 Lot	\$175,000	\$175,000	\$350,000
.12	Miscellaneous	1 Lot	10,000	10,000	20,000
.2	Turbine Generators				
.21	Turbine Generator Units - As Follows: 1000 MWe Reheat Turbine Generator Unit C.C.6F. 40" L.S.B. Complete with Accessories Steam Conditions 2400 Psi - 1000°F -1000°F Generators: 1,280,000 KVA Total .85 P.F. and .64 SCR	1	19,815,000	960,000	20,775,000
.22	Accessories - Other Than Standard			Included in Account 231.21	
.23	Generator			Included in Account 231.21	
.24	Exciter (Motor Driven)			Included in Account 231.21	
.3	Reserve Exciter	1	340,000	10,000	350,000
	TOTAL ACCOUNT 231		\$20,340,000	\$1,155,000	\$21,495,000
232	<u>Circulating Water System</u>				
.1	Pumping and Regulating Systems				
.11	Pumps, Drives & Controls				
.112	134,000 GPM Vertical Mixed Flow Circulating Water Pumps Head 30 ft.	6	360,000	18,000	378,000

316

Table N.1 (continued)

	QUANTITY	MATERIAL OR EQUIPMENT	LABOR	TOTALS
<u>ACCOUNT 23 - TURBINE GENERATOR UNITS (Cont'd.)</u>				
<u>232 Circulating Water System (Cont'd.)</u>				
.1 Pumping and Regulating Systems (Cont'd.)				
.11 Pumps, Drives & Controls (Cont'd.)				
.113 1250 H.P. Motor Drive for Circulating Water Pumps	6	\$270,000	\$10,000	\$280,000
.12 Traveling Screens, Etc.				
.121 Traveling Screens Complete with Motors	7	122,500	8,700	131,200
.122 1200 GPM Screen Wash Pumps 230 Ft. Discharge Head	2	5,000	1,000	6,000
.123 100 H.P. Motor for Screen Wash Pump	2	4,500	Included	4,500
.124 Trash Rake Complete with Appurtenances	1	27,500	2,500	30,000
.125 Pipe & Valves	1 Lot		Included in Account 228	
.2 Circulating Water Lines				
.21 Supply Lines - To Condenser				
.211 Circulating Water Piping, Valves, Fittings, Etc.				
.2111 Steel Circulating Water Piping, Valves Expansion Joints, Fittings, Etc.				
.22 Discharge Lines - From Condenser	1 Lot	155,000	70,000	225,000
.221 Circulating Water Piping, Valves, Fittings, Etc.				

317

Table N.1 (continued)

	QUANTITY	MATERIAL OR EQUIPMENT	LABOR	TOTALS
<u>ACCOUNT 23 - TURBINE GENERATOR UNITS (Cont'd.)</u>				
232 <u>Circulating Water System (Cont'd.)</u>				
.2 Circulating Water Lines (Cont'd.)				
.22 Discharge Lines - From Condenser (Cont'd.)				
.2211 Steel Circulating Water Piping Valves, Expansion Joints, Fittings, Etc.	1 Lot			Included in Account 232.21
.3 Intake and Discharge Structures				
.31 Intake Structures				
.311 River Dredging & Rock Removal	1 Lot	-	\$12,000	\$12,000
.312 Intake Flume				
.3121 Intake Flume Proper	1 Lot	-	45,000	45,000
.3122 Floating Boom	1	\$7,000	10,400	17,400
.3123 Concrete Retaining Walls	2	28,500	29,200	57,700
.313 Intake Crib House				
.3131 Substructure	1 Lot	140,000	135,000	275,000
.3132 Superstructure	-	-	-	-
.3133 Steel	35 T	11,000	4,000	15,000
.3134 Electrical Work	1 Lot	11,000	13,600	24,600
.32 Discharge				
.321 Seal Well & Discharge Tunnel	Lot	29,500	28,400	57,900
.322 Discharge Flume	Lot	4,500	22,400	26,900

Table N.1 (continued)

		QUANTITY	MATERIAL OR EQUIPMENT	LABOR	TOTALS
ACCOUNT 23 - TURBINE GENERATOR UNITS (Cont'd.)					
232	<u>Circulating Water System (Cont'd.)</u>				
.4	Fouling, Corrosion Control and Water Treatment				
.41	Chlorinating System				
.411	Chlorination Equipment	1 Lot	\$45,000	\$8,000	\$53,000
.412	Chlorine Handling Facilities	1 Lot	<u>3,000</u>	2,000	5,000
	TOTAL ACCOUNT 232		\$1,224,000	\$420,200	\$1,644,200
233	<u>Condensers and Auxiliaries</u>				
.1	Condensers				
.11	Foundations	3	\$7,000	\$6,400	\$13,400
.12	Condenser Shell and Appurtenances				
.121	225,000 Sq. Ft. Single Pass Condensers Complete with Appurtenances Including Shell, Water Boxes, Tube Sheets, Tube Supports, Hot Well, Extended Neck with Expansion Joint, Etc.	3	1,320,000	440,000	1,760,000
.13	50 Ft. Long Admiralty Condenser Tubes	3 Sets	1,053,000	Included	1,053,000
.17	Instruments & Accessories	3 Sets	15,000	Included	15,000
.2	Condensate Pumps				
.21	Pumps & Drives				
.211	1875 GPM Condensate Pumps Complete with Appurtenances, Discharge Head - 325 Ft.	6	87,000	6,000	93,000

Table N.1 (continued)

		QUANTITY	MATERIAL OR EQUIPMENT	LABOR	TOTALS
ACCOUNT 23 - TURBINE GENERATOR UNITS (Cont'd.)					
233	<u>Condensers and Auxiliaries (Cont'd.)</u>				
.2	Condensate Pumps (Cont'd.)				
.21	Pumps & Drives (Cont'd.)				
.212	400 H.P. Motors for Condensate Pumps	6	\$46,800	4,200	\$51,000
.22	Suction Piping	Lot		Included in Account 233.121	
.3	Air Removal Equipment and Piping				
.31	Steam Jet Air Ejector, with Inter & After Condensers	6	100,000	9,000	109,000
.32	Air Suction Piping	Lot		Included in Account 228	
.33	Priming Ejectors	Lot	10,500	Included	10,500
	TOTAL ACCOUNT 233		\$2,639,300	\$465,600	\$3,104,900
234	<u>Central Lubricating System</u>				
.1	Treating & Pumping Equipment	1 Lot	17,000	2,000	19,000
.2	Storage Tanks & Appurtenances	1 Lot	14,000	3,000	17,000
.3	Fire Protection	1 Lot		Included in Account 237	
	TOTAL ACCOUNT 234		\$31,000	\$5,000	\$36,000
235	<u>Turbine Plant Boards Instruments & Controls</u>				
.1	Control Equipment				
.11	Mechanical Control Boards)				
.12	Isolated Controller, Transmitters Etc.)	1 Lot	\$275,000	\$25,000	\$300,000
.2	Isolated Recording Gauges)				
	Meters & Instruments)				

Table N.1 (continued)

		QUANTITY	MATERIAL OR EQUIPMENT	LABOR	TOTALS
ACCOUNT 23 - TURBINE GENERATOR UNITS (Cont'd.)					
235	<u>Turbine Plant Boards Instruments & Controls</u>				
.3	Control & Instrument -				
	Piping & Tubing	1 Lot	\$20,000	\$55,000	\$75,000
.4	Electrical Connections	1 Lot	<u>18,000</u>	<u>33,600</u>	<u>51,600</u>
	TOTAL ACCOUNT 235		\$313,000	\$113,600	\$426,600
236	<u>Turbine Plant Piping</u>				
.1	Main Steam Between Stop Valves and Turbine Inlet				Included in Account 231.2
.2	Drip, Drain and Vent Piping and Valves				Included in Account 228
	TOTAL 236				<u>Included in Account 228</u>
237	<u>Auxiliary Equipment for Generators</u>				
.1	Excitation Panels, Switches & Rheostats				Included in Account 231.2
.2	Generator Cooling Water Systems				
.21	Lubricating Oil Cooling System)			
.22	Generator Hydrogen Cooling System)	Lot	60,000	12,000
.23	Generator Liquid Cooling System)			72,000

Table N.1 (continued)

		QUANTITY	MATERIAL OR EQUIPMENT	LABOR	TOTALS
<u>ACCOUNT 23 - TURBINE GENERATORS UNITS (Cont'd.)</u>					
237	<u>Auxiliary Equipment for Generators (Cont'd.)</u>				
.3	Central Hydrogen Cooling System	-	-	-	-
.4	Fire Extinguishing Equipment Including Piping and CO ₂) System Exclusively for Generators)	Lot	\$50,000	\$15,000	\$65,000
.5	Fire Extinguishing Equipment for Oil Room, Etc.)				
	TOTAL ACCOUNT 237		\$110,000	\$27,000	\$137,000
238	<u>Other Turbine Plant Equipment</u>				
.1	Gland Seal Water System	1		← Included in Account 228 →	
.2	Vacuum Priming System			← Included in Account 228 →	
	TOTAL ACCOUNT 238			← Included in Account 228 →	
	TOTAL ACCOUNT 23			2,186,400	\$26,843,700
<u>ACCOUNT 24 - ACCESSORY ELECTRIC EQUIPMENT</u>					
241	<u>Switchgear</u>				
.1	Generator Main and Neutral Circuits				
.11	Generator Potential Transformer Compartment	2	\$38,000	\$4,000	\$42,000
.12	Surge Protection Equipment	2	14,000	1,600	15,600
.13	Generator Neutral Equipment	1	6,000	800	6,800
.14	Miscellaneous Items	Lot	10,000	19,200	29,200

Table N.1 (continued)

		QUANTITY	MATERIAL OR EQUIPMENT	LABOR	TOTALS
ACCOUNT 24 - ACCESSORY ELECTRIC EQUIPMENT (Cont'd.)					
241	<u>Switchgear</u> (Cont'd.)				
.2	Station Service				
.21	13.8 KV Switchgear	Lot			
.22	4160 V. Switchgear	Lot	365,000	51,200	416,200
.23	480 V. Switchgear	Lot	110,000	17,600	127,600
	TOTAL ACCOUNT 241		\$543,000	\$94,400	\$637,400
242	<u>Switchboards</u>				
.1	Main Control Board	Lot	\$82,000	\$31,200	\$113,200
.2	Auxiliary Power Battery & Signal Board				
.21	Battery & Battery Charging Panels	1	15,000	5,600	20,600
.22	D.C. Control & Auxiliary Panels	2	18,000	4,800	22,800
.23	A.C. Control & Instrument Panels	1	7,000	1,600	8,600
.24	Motor Control Centers	Lot	80,000	13,600	93,600
.25	Miscellaneous Panels & Boards	Lot	16,000	11,200	27,200
	TOTAL ACCOUNT 242		\$218,000	\$68,000	\$286,000
243	<u>Protective Equipment</u>				
.1	General Station Grounding Equipment	Lot	\$60,000	\$48,800	\$108,800
.2	Fire Protection System	Lot	14,000	8,800	22,800
	TOTAL ACCOUNT 243		\$74,000	\$57,600	\$131,600

Table N.1 (continued)

		QUANTITY	MATERIAL OR EQUIPMENT	LABOR	TOTALS
ACCOUNT 24 - ACCESSORY ELECTRIC EQUIPMENT (Cont'd.)					
244	<u>Electrical Structures</u>				
.1	Concrete Cable Tunnels, Compartments and Cable Trenches in Earth	Lot	\$14,000	\$21,600	\$35,600
.2	Cable Trays & Supports	192,000 lb.	80,000	72,000	152,000
.3	Pipe and Steel Frames and Supports	Lot	7,000	8,000	15,000
.4	Foundations & Pads for Electrical Equipment	Lot	5,000	5,600	10,600
	TOTAL ACCOUNT 244		\$106,000	\$107,200	\$213,200
245	<u>Conduit</u>				
.1	Conduit				
.11	Power Conduit	Lot	\$25,000	\$61,200	\$86,200
.12	Control and Instrument Conduit	Lot	22,000	54,400	76,400
.2	Concrete Envelopes				
.21	10" Transite Pipe Duct Run	Lot	6,000	6,800	12,800
.22	Iron Conduit Enclosed in Concrete	Lot	9,000	15,200	24,200
.3	Manholes & Covers	5	5,000	5,600	10,600
	TOTAL ACCOUNT 245		\$67,000	\$143,200	\$210,200
246	<u>Power and Control Wiring</u>				
.1	Main Power Cables and Bus Duct				
.11	Isolated Phase Bus Duct (Generator)	Lot	\$576,000	\$49,600	\$625,600
.12	Main Power Cables	1	110,000	16,000	126,000

Table N.1 (continued)

		QUANTITY	MATERIAL OR EQUIPMENT	LABOR	TOTALS
ACCOUNT 25 - MISCELLANEOUS POWER PLANT					
<u>EQUIPMENT (Cont'd.)</u>					
251	<u>Cranes and Hoisting Equipment (Cont'd.)</u>				
.2	Miscellaneous Cranes and Hoists	Lot	\$23,000	\$2,000	\$25,000
	TOTAL ACCOUNT 251		\$173,000	\$22,000	\$195,000
252	<u>Compressed Air and Vacuum Cleaning System</u>				
.1	Compressors and Accessories				
.11	200 C.F.M. Station Air				
	Compressors Including Motor				
	Drives	2	\$13,500	\$1,200	\$14,700
.12	250 C.F.M. Control Air				
	Compressors including Motors	2	15,500	1,200	16,700
.13	Air Drying Equipment for				
	Control Air System	2	9,000	500	9,500
.14	Receivers				
.141	Station Air	2	1,300	300	1,600
.142	Control Air	2	1,300	300	1,600
.2	Pipe Valves and Fittings	Lot			
.3	Vacuum Cleaning System	Lot			
	TOTAL ACCOUNT 252		\$16,000	4,000	20,000
			\$56,600	\$7,500	\$64,100
253	<u>Other Power Plant Equipment</u>				
.1	Local Communication, Signal and Call System	Lot	\$50,000	\$44,800	\$94,800
.2	Fire Extinguishing Equipment				
.21	2000 GPM Fire Pump Including Drive and Accessories				Included in Account 211.24
.22	Other Fire Protection Equipment	Lot	\$19,000	\$1,000	\$20,000

Table N.1 (continued)

		QUANTITY	MATERIAL OR EQUIPMENT	LABOR	TOTALS
ACCOUNT 25 - MISCELLANEOUS POWER PLANT (Cont'd.)					
253	<u>Other Power Plant Equipment (Cont'd.)</u>				
.3	Furniture and Fixtures	Lot	\$10,000	-	\$10,000
.4	Lockers, Shelves, and Cabinets	Lot	7,000	-	7,000
.5	Cleaning Equipment	Lot	4,000	-	4,000
.6	Machine Tools & Other Station Maintenance Equipment	Lot	240,000	\$10,000	250,000
.7	Laboratory, Test & Weather Instruments				
.71	Radiation Monitoring Equipment	Lot	23,000	2,000	25,000
.72	Miscellaneous Laboratory, Test & Weather Instruments	Lot	20,000		20,000
.9	Diesel Generator Unit 1000 KW Including Oil Tank	1	100,000	10,000	110,000
	TOTAL ACCOUNT 253		\$473,000	\$67,300	\$540,800
	TOTAL ACCOUNT 25			\$97,300	\$799,900
	TOTAL DIRECT CONSTRUCTION COST		\$78,174,625	\$11,166,575	\$89,341,200
INDIRECT COSTS					
	Contractor's O'HD and Profit 20%				2,333,300
	SUB-TOTAL				\$91,674,500
	General and Administrative 6.3%				5,775,500
	SUB-TOTAL				\$97,450,000
	Miscellaneous Construction 1%				974,500
	SUB-TOTAL				\$98,424,500

326

Table N.1 (continued)

	QUANTITY	MATERIAL OR EQUIPMENT	LABOR	TOTALS
<u>ENGINEERING DESIGN AND INSPECTION</u>				
A - E Design and Inspection 11.1%				
SUB-TOTAL				\$10,925,000
Nuclear Engineering 3.8%				\$109,349,500
SUB-TOTAL				4,155,300
Start-up Costs				\$113,504,800
SUB-TOTAL				746,900
Land and Land Rights				\$114,251,700
SUB-TOTAL				360,000
Contingency 10%				\$114,611,700
SUB-TOTAL				11,461,200
Interest During Construction 9.4%				\$126,072,900
SUB-TOTAL				11,850,900
Fuel Charge				\$137,923,800
Intermediate Coolant Salt			Not Included	
Investment and 1.5% for Interest During Construction				10,790,000
				161,800
TOTAL CAPITAL INVESTMENT				\$148,875,600

Appendix O

DESIGN REQUIREMENTS FOR THE MSCR MODERATOR

L. G. Alexander

Introduction

The reactor vessel contains the moderator and holds it in a stable position during all phases of operation, provides for accepting fuel discharged from the heat exchangers, passage of fuel through the moderator, and discharge to the fuel pumps.

The reactor must be designed to expose the fuel to neutrons at a specified ratio of graphite volume to fuel volume. The graphite must be supported and restrained under all circumstances, including the drained condition. Allowance must be made for differential expansion between graphite and vessel. Provision must be made for distributing the flow of fuel over the core entrance, and for collecting the flow at the exit. A free surface in an expansion chamber must be provided somewhere in the fuel circuit, and circulation through the expansion chamber must be maintained. Provision must be made for preheating the reactor vessel prior to charging molten salt, and for cooling the reactor vessel during operation and after shutdown. This cooling must be accomplished without the generation of excessive thermal stresses. The vessel must be designed in conformance with the pressure vessel code. Means of sparging the fuel in the expansion chamber with an inert gas must be provided to remove xenon and other volatile materials. Excessive thermal stress in the graphite must be avoided, and it must be composed of pieces sufficiently small that differential shrinkage due to exposure to neutrons will be tolerable in each piece.

Stagnation of the fuel between adjacent blocks of graphite or between graphite and metal structure must be avoided if such stagnation leads to excessive temperatures or stresses in either the fuel, graphite, or metal structure. Temperature at the fuel-graphite interface should be below that at which chemical reaction, if any, takes place at an appreciable rate, and below the temperature at which any important constituent of the

salt (other than volatile fission products) has appreciable vapor pressure (e.g., if UF_4 were to vaporize appreciably and diffuse into pores in the graphite, this would be disadvantageous and perhaps hazardous). Temperature gradients in the graphite near stagnation areas should not exceed those corresponding to tolerable thermal stresses.

In the MSCR it is desirable, in order to reduce the graphite surface exposed to permeation by salt and fission product gases, to use moderator elements of larger diameter than in the MSRE. On the other hand, setting an allowable thermal strain of 0.001 imposes an upper limit. A diameter of about six to eight inches appears to be a suitable compromise between the conflicting requirements.

It would be desirable for the logs to extend the length of the core, but radiation damage may induce a tendency for the logs to bow outward and this would increase the volume fraction of fuel in the core. This increase is controlled and largely eliminated by using logs 24 in. long and stacking these in a vertical position. The ends are mated by means of pins and sockets. Differential shrinkage of the graphite is now accommodated by a slight rotation about the pins.

Fuel salt should permeate the graphite not more than 0.1% by volume. With this penetration, and 10 volume per cent of fuel in the core, about one per cent of the fuel will be in the pores in the graphite. This is probably tolerable, especially if the accessible pores are those near the surface, as seems to be the case.

Fuel stagnation in cracks between blocks and in pores in the blocks is closely related to the problem of afterheat, since the fuel so involved is probably not readily drainable. Means of flushing the fuel-salt thus retained must be provided if possible, and if this is not possible, means must be provided of removing the heat generated in the core after drainage.

Temperature rise and thermal stress in the reactor vessel must be limited to tolerable levels. Differential thermal expansion will leave a gap between the graphite structure and the reactor vessel not less than 1 in. in the radial direction. It will be necessary to provide some flow through this annulus not only to remove the heat generated there, but also to cool the reactor vessel.

It will be necessary to orifice the flow channels, or otherwise vary their width systematically in order to distribute the flow through the core compatibly with the power density distribution to achieve uniform temperature rise in all fuel channels.

Moderator

In the MSRE (1), the moderator is constructed of square graphite bars measuring 2 inches on the sides and 63 inches long. Channels 0.4 inches deep and 1.2 inches wide are machined into alternate faces of the bars, which are pinned loosely to beams lying across the bottom of the vessel. The channels occupy 22.5% of the volume of the matrix.

The shape, size, and spacing of the MSRE moderator elements are not suitable for the MSCR. The pieces need to be larger and the volume of fuel needs to be of the order of 10 percent.

The void fraction in a matrix formed by closely packed cylinders of uniform diameter is 0.093. Such a matrix appears to be structurally stable, is easily assembled in a close array, and provides a minimum of contact between individual pieces. This last is important in that the amount of stagnant fuel is probably roughly proportional to the total area of contact. Small variations in radius, circularity, and straightness of the cylinders can be tolerated, and a voidage as low as 10% still be achieved. Higher voidages can be obtained by machining away portions of the surface of the cylinders; in fact, the voidage can be systematically varied both radially and axially in this way. The relative positions of the logs are fixed by contact of the unmachined portions at the top and bottom. It should thus be possible to reduce power peaking in the reactor and, by a combination of orificing and power flattening, to obtain a good match between radial distributions of flow and power density and thus achieve approximate equal temperature rise in all fuel channels.

In the MSCR study, fuel-volume fractions in the range from 0.1 to 0.2 were investigated. The optimum fraction appears to be slightly

greater than 0.1. It appears undesirable to design a matrix having a fuel fraction much smaller than this. At low fuel fractions, dimensional tolerances in the machining of the logs and assembling of the matrix introduce uncertainties that become an appreciable fraction of the fuel volume. This uncertainty can be reduced somewhat by using logs of large cross section, but there are limits, viz.: (a) a limit on the size of log that can currently or in the foreseeable future be manufactured; (b) a limit imposed by thermal stress in the log, which becomes excessive with increasing size. Graphite logs measuring 16 inches in diameter can be made now (1962); while these are not of a grade satisfactory for use in the MSCR, it is not a great extrapolation of current technology to postulate the availability of graphite logs of satisfactory grade in sizes up to 8 inches in diameter, and this appears to be as large as thermal strain considerations will allow.

If the volume fraction of fuel in the core is small, then any slight variation in this volume fraction would have an appreciable effect on the reactivity and might result in power excursions. These variations might arise in any of a number of ways. For instance, radiation damage might result in the accumulation of stresses in the graphite which, upon sudden removal of external restraints (such as by the failure of the hoops, etc.) or by the yielding of the material itself, might result in gross movement of the matrix, and a sudden increase in reactivity.

Also, at very low volume fractions, the optimum concentrations of fissile and fertile isotopes in the fuel stream becomes high, and this imposes requirements on the design of the external system in regard to hold-up, velocities, etc., that are difficult to meet.

Permeation of Graphite by Salt

Graphite is not impervious to salt. The presence of an appreciable fraction of the salt in stagnant pockets introduces a number of problems (such as that associated with the fate of fission products generated in stagnant fuel). The "theoretical" density of graphite is 2.25 grams/cc. MSRE graphite has a bulk density of about 1.83, and thus the pore

fraction is about 0.16. The pores accessible to a wetting fluid, such as kerosene or a gas, however, amount to only 0.07% of the volume. Graphite is not wetted by molten fluoride salts, and the penetration is an order less than that of a wetting fluid. Treatment by any one of several methods (5) reduces the penetration further, either by filling the pores, by closing them, or by making the entrances smaller. Tests in which CGB-X graphite, newly proposed for the MSRE, was exposed to salt at 1300°F and 150 psi for 100 hours resulted in volume fraction permeations of 0.001 and 0.0002 (2, p. 93). The occlusions of salt lay mostly at the surface, and were presumably in reasonably good diffusional communication with the bulk fluid. The pieces tested were necessarily small, and the proportion of surface exposed was high. Estimates based on expected frequency of surface pores in larger pieces led to a prediction of a penetration not greater than 0.0016 in the MSRE graphite at 65 psi pressure in the salt (2, p. 91). Taking advantage of the fact that the number of surface pores can be reduced by proper orientation of the surface grains and that with larger bars the ratio of surface-to-volume is less, it appears plausible that a salt-accessible pore fraction of 0.001 can be assumed for MSCR graphite. Now, if the graphite occupies 90% of the matrix, salt-accessible pores in the graphite amount to roughly 0.1%, which is only 1% of the total fuel fraction. However, the fuel in these pores may be retained when the reactor is drained, and this may present a serious operational difficulty in regard to cooling the reactor after shutdown, especially if the core is drained shortly after operation at power.

Graphite Shrinkage

The graphite will, of course, be subjected to radiation damage, mostly from fast neutrons. At the temperatures anticipated in the MSCR, the graphite will shrink. Since that side of a log closest to the center of the core will absorb more radiation than the outer side, the logs will tend to bow outward, and increase the volume fraction of the fuel. These effects will take place slowly, of course, and can easily be

compensated, in respect to criticality, by increasing the concentration of thorium in the fuel or by decreasing that of the uranium. The breeding ratio will necessarily decrease, however, due to shifting of the C/Th/U ratio from the optimum. As mentioned above, the effect is minimized by the use of short logs.

Graphite Replacement

The precise effect of graphite shrinkage on the performance (as measured by the fuel cycle cost) has not been determined; however, if it proves to be serious, one or more of several countermeasures may be taken. The simplest would be to replace the graphite periodically. The excess sinking fund cost (@ 6.75%) over that corresponding to sinking fund amortization over a thirty-year life (1.11%, and which is charged off to capital costs) is listed below in Table 0.1 for several replacements periods.

Table 0.1. Power Cost Increment for Replacement
of Graphite* Moderator in MSCR

Replacement Period (years)	Incremental Power Cost (mills/kwhr)
1	0.58
5	0.096
10	0.037
15	0.018
20	0.008

*@ \$6/lb.

It is seen that, if the replacement occurs no oftener than once in ten years, the incremental cost is tolerable, being less than 10% of a typical fuel cost of 0.75 mills/kwhr.

If the shrinkage rate is such as to require replacement more often than this, then part of the fuel volume fraction increase might be avoided by restraining the core and preventing the bowing of the logs. Hoops of

molybdenum, which have a coefficient of thermal expansion very nearly equal to that of graphite (3) could be placed around the core (4, p. 32). Of course, should the hoops fail suddenly, an excursion in the power level might result. On the other hand, if the hoops held, accumulated stresses in the graphite might result in the formation of cracks in which the fuel might stagnate with deleterious effect.

The fuel volume fraction can be made self-preserving in spite of radiation induced shrinkage by use of interlocking blocks of graphite. The moderator elements are cubes having four holes, or sockets, in the four quadrants of the upper face and four corresponding pegs extending from the lower face. After a layer of blocks has been laid, the blocks of the next layer are positioned so that the axis of each block lies over the intersections of the fuel channel planes between adjacent blocks in the lower layer, with its pins fitting into sockets in four blocks in that layer. Thus each cube is pinned to four overlapping cubes in the layer above and four in the layer below. With cubes measuring 8 inches along an edge, and a void fraction of 10%, the thickness of the passage between adjacent cubes is approximately 0.4 inches when the blocks rest directly on the blocks below, and 0.3 inches when uniform clearance is provided on all six sides of the blocks. Now, as the blocks shrink, the fuel volume fraction is invariant, since this is determined by the spacing of the pegs and sockets and the dimensions of the blocks.

This arrangement, while solving one problem, introduces others, chief of which is a much increased resistance to flow of the fuel through the core, which may increase by a factor of perhaps 20. This would increase the pumping cost and the design requirements for pumps, heat exchangers and reactor vessel.

If difficulty with short-circuiting of the fuel through the annular gap between moderator and reactor vessel is encountered, this could be controlled by eliminating the gaps between the outer blocks of graphite so that the blocks fit tightly one against the other. The annulus thus becomes a channel unconnected to the voids in the moderator, and the flow through it could be orificed at the top where the pile floats up against the upper support grid.

The foregoing discussion of the problem of graphite shrinkage indicates some solutions that might be applied if the problem should prove to be serious, but it should not be inferred therefrom that the problem is known to be serious, for in fact, it may not be. There are indications (6) that radiation damage may anneal and saturate at the temperature of operation. In that event, the core would be designed so that, after the steady state is reached, the fuel volume fraction is at the desired value.

Differential Expansion

The coefficient of thermal expansion of graphite is smaller than that of INOR (compare Tables 3.2 and 3.1). Thus, in a 20-ft core with the graphite just filling the vessel at room temperature, there will be a gap about 2/3-in. wide between the graphite and the vessel wall at 1100°F. If further allowance is made for dimensional tolerances between metal and graphite during assembly, the gap cannot be much less than one inch thick at operating temperatures.

This gap will contain fuel salt, and this fact must be taken into account in evaluating the performance of the reactor and in the design of the core and the reactor vessel. In a 20 ft cylindrical core the volume of fuel in the annulus amounts to $\sim 100 \text{ ft}^3$, which is an appreciable fraction of the volume of fuel in the matrix ($\sim 600 \text{ ft}^3$). This fuel lies in a region of low neutron population so that it adds little to the reactivity. Also, it is nearly opaque to thermal neutrons which are absorbed, multiplied by η , and re-emitted as fast neutrons, thus increasing the leakage. This concentrated source of fast neutrons and concomitant gamma radiation adjacent to the reactor vessel wall introduces design problems. It may be necessary to provide a thermal shield between the fuel annulus and the wall. The most suitable material for this shield is INOR, but this must be cooled. The only available cooling medium in this situation is the fuel salt, and its use for this purpose further increases the nonactive inventory of valuable materials.

It may be possible to use the fuel annulus as a downcomer for fuel coming from the heat exchangers. This may or may not result in some saving in fuel inventory, depending on the location of the exchangers and their requirements for draining, etc. The annulus is so used in the MSRE (1).

References

1. A. L. Boch et al., The Molten-Salt Reactor Experiment, Power Reactor Experiments, Vol. I, pp. 247-292, International Atomic Energy Agency, Vienna, 1962.
2. Oak Ridge National Laboratory, MSRP Semiann. Progr. Rept. Feb. 28, 1962, USAEC Report ORNL-3282.
3. S. E. Beall et al., Molten-Salt Reactor Experiment Preliminary Hazards Report, USAEC Report ORNL CF-61-2-46 (with Addenda 1 and 2), Oak Ridge National Laboratory, February 1961.
4. Oak Ridge National Laboratory, MSRP Quarterly Progr. Rept. July 31, 1960, USAEC Report ORNL-3014.
5. J. W. H. Simmons, The Effects of Irradiation on the Mechanical Properties of Graphite, Proceedings of the Third Conference on Carbon, Sections E and F, Pergamon Press, 1959.

BIBLIOGRAPHY

1. L. G. Alexander et al., Nuclear Characteristics of Spherical, Homogeneous, Two-Region, Molten-Fluoride-Salt Reactors, USAEC Report ORNL-2751, Oak Ridge National Laboratory, September 1959.
2. L. G. Alexander et al., Experimental Molten-Salt-Fueled 30 Mw Power Reactor, USAEC Report ORNL-2795, Oak Ridge National Laboratory, March 1960.
3. L. G. Alexander et al., Thorium Breeder Reactor Evaluation - Part I - Fuel Yield and Fuel Cycle Costs in Five Thermal Breeders, USAEC Report ORNL-CF-61-3-9, Oak Ridge National Laboratory, March 1961, and USAEC Report ORNL-CF-61-3-9 (Appendices), Oak Ridge National Laboratory, March 1961.
4. Robert Avery et al., Report of the Fluid Fuel Reactors Task Force to the Division of Reactor Development, USAEC, USAEC Report TID-8507, United States Atomic Energy Commission, February 1959.
5. S. E. Beall et al., Molten-Salt Reactor Experiment Preliminary Hazards Report, USAEC Report ORNL-CF-61-2-46 (Addendum 1 and 2), Oak Ridge National Laboratory, February 1961.
6. E. S. Bettis et al., The Aircraft Reactor Experiment - Design and Construction, Nuclear Science Engineering, 2:804 (November 1957).
7. E. S. Bettis et al., The Aircraft Reactor Experiment - Operation, Nuclear Science Engineering, 2:841 (November 1957).
8. B. C. Blanke et al., Density and Viscosity of Fused Mixtures of Lithium, Beryllium, and Uranium Fluorides, USAEC Report MLM-1086, Mound Laboratory, March 1959.
9. J. O. Blomeke, Nuclear Properties of ^{235}U Fission Products, USAEC Report ORNL-1783, Oak Ridge National Laboratory, April 1957.
10. J. O. Blomeke and M. F. Todd, Uranium-235 Fission Product Production, USAEC Report ORNL-2127, Oak Ridge National Laboratory, November 1958.
11. C. M. Blood, Solubility and Stability of Structural Metal Difluorides in Molten Fluoride Mixtures, USAEC Report ORNL-CF-61-5-4, Oak Ridge National Laboratory, May 1961.
12. A. L. Boch et al., The Molten-Salt Reactor Experiment, Power Reactor Experiments, Vol. I, International Atomic Energy Agency, Vienna, 1962, pp. 247-292.
13. J. O. Bradfute et al., An Evaluation of Mercury Cooled Breeder Reactors, USAEC Report ATL-A-102, Advanced Technology Laboratory, October 1959.

14. R. C. Briant and A. M. Weinberg, Molten Fluorides as Power Reactor Fuels, Nuc. Sci. Eng., 2:797 (November 1957).
15. J. Bulmer et al., Fused Salt Fast Breeder, USAEC Report ORNL-CF-56-8-204 (Del.), Oak Ridge National Laboratory, August 1956.
16. D. O. Campbell and G. I. Cathers, Processing of Molten Salt Power Reactor Fuels, Ind. Eng. Chem., 52:41 (January 1960).
17. M. C. Cannon et al., Adsorption of Xenon and Argon on Graphite, USAEC Report ORNL-2955, Oak Ridge National Laboratory, November 1960.
18. W. H. Carr et al., Uranium-Zirconium Alloy Fuel Processing in the ORNL Volatility Pilot Plant, USAEC Report ORNL-2661, Oak Ridge National Laboratory, July 1962.
19. W. L. Carter, Thorium Utilization Program: A Survey of Processing Methods for Thorium Reactor Fuel, USAEC Report OTNL-TM-241, Oak Ridge National Laboratory, July 1962.
20. W. L. Carter, Thorium Utilization Program: Fuel Cycle Cost estimates for the Molten Salt Converter Reactor, USAEC Report ORNL-CF-62-12-55, Oak Ridge National Laboratory, December 1962.
21. W. L. Carter, R. P. Milford, and W. G. Stockdale, Design Studies and Cost Estimates of Two Fluoride Volatility Plants, USAEC Report ORNL-TM (in preparation), Oak Ridge National Laboratory, October 1962.
22. G. I. Cathers et al., The Fused Salt Fluoride Volatility Process for Recovering Uranium, USAEC Report ORNL-2661, Oak Ridge National Laboratory, April 1959.
23. G. I. Cathers et al., Use of Fused-Salt Fluoride Volatility Process With Irradiated Urania Decayed 15-30 Days, USAEC Report ORNL-2380, Oak Ridge National Laboratory, September 1962.
24. S. I. Cohen et al., A Physical Property Summary for ANP Fluoride Mixtures, USAEC Report ORNL-2150 (Declassified), Oak Ridge National Laboratory, August 1956.
25. S. I. Cohen and T. N. Jones, A Summary of Density Measurements on Molten Fluoride Mixtures and a Correlation for Predicting Densities of Fluoride Mixtures, USAEC Report ORNL-1702 (Declassified), Oak Ridge National Laboratory, July 1954.
26. J. K. Davidson and W. L. Robb, A Molten-Salt Thorium Converter for Power Production, USAEC Report KAPL-M-JKD-10 (Declassified), Knolls Atomic Power Laboratory, October 1956.
27. R. W. Davies et al., 600 Mw Fused Salt Homogeneous Reactor Power Plant, USAEC Report CF-56-8-208 (Deleted), Oak Ridge National Laboratory, August 1956.

28. J. H. DeVan and R. B. Evans III, Corrosion Behavior of Reactor Materials in Fluoride Salt Mixtures, USAEC Report ORNL-TM-328, Oak Ridge National Laboratory, September 19, 1962.
29. Lawrence Dresner, Tables for Computing Effective Resonance Integrals, Including Doppler Broadening of Nuclear Resonances, USAEC Report ORNL-CF-55-9-74, Oak Ridge National Laboratory, September 1955.
30. T. A. Eastwood and R. D. Werner, The Thermal Neutron Capture Cross Section and Resonance Capture Integral of Protactinium-233, Can Jr. Phys., 38:751 (June 1960).
31. W. K. Ergen et al., The Aircraft Reactor Experiment - Physics, Nuc. Sci. Eng., 2:826, November 1957.
32. W. H. Farrow, Jr., Radiochemical Separations Plant Study, Part II. Design and Cost Estimates, USAEC Report DP-566, E. I. du Pont de Nemours and Co., March 1961.
33. D. E. Ferguson, Fuel Cycle Development: Semiannual Progress Report, USAEC Report ORNL-3142, Oak Ridge National Laboratory, July 1961.
34. R. L. Ferguson and G. D. O'Kelley, A Survey and Evaluation of ^{233}U Fission Yield Data, USAEC Report ORNL-CF-62-3-71, Oak Ridge National Laboratory, March 1962.
35. J. D. Gabor et al., Spray Fluorination of Fused Salt as a Uranium Recovery Process, USAEC Report ANL-6131, Argonne National Laboratory, March 1960.
36. E. R. Gaerttner and M. L. Yeater, Reports to the AEC Nuclear Cross Section Advisory Group, USAEC Report WASH-194, Nuclear Cross Sections Advisory Group, AEC, February 1958.
37. J. D. Garrison and B. W. Roos, Fission Product Capture Cross Sections, Nuc. Sci. Eng., 12:115 (January 1962).
38. P. F. Gorman, 1000 Mw Unit Conceptual Design Supercritical Double Reheat Coal Fired, (No document number), Jackson and Moreland, Inc., New York, January 1962.
39. C. R. Greenhow and E. C. Hansen, Thermal and Resonance Fission-Product Poisoning for ^{235}U System, USAEC Report KAPL-2172, Knolls Atomic Power Laboratory, October 1961.
40. W. R. Grimes et al., Reactor Chemistry Division Annual Progress Report for Period Ending January 31, 1960, USAEC Report ORNL-2931, pp. 87-88, Oak Ridge National Laboratory, April 1960.
41. C. E. Guthrie, Fuel Cycle Costs in a Graphite Moderated ^{235}U -Th Fueled Fused Salt Reactor, USAEC Report ORNL-CF-59-2-82, Oak Ridge National Laboratory, February 1959.

42. R. Gwin and D. W. Magnuson, Determination of Eta by Comparison of ^{233}U and ^{235}U in a Flux Trap Critical Assembly, Nuc. Sci. Eng., 12(3): 359, March 1962.
43. R. Gwin and D. W. Magnuson, The Measurement of Eta and Other Nuclear Properties of ^{233}U and ^{239}Pu in Critical Aqueous Solutions, Nuc. Sci. Eng., 12(3):364, March 1962.
44. J. A. Harvey, Oak Ridge National Laboratory, personal communication to C. W. Nestor, Oak Ridge National Laboratory, March 1960.
45. E. C. Hensen, A Critical Examination of the Uncertainties in Predicted Gross Fission Product Poisoning, USAEC Report KAPL-M-ECH-8, Knolls Atomic Power Laboratory, March 1962.
46. E. C. Hensen and C. R. Greenhow, An Improved Generalized Analysis of Fission Product Poisoning and Thermal and Resonance Fission Fragment Cross Sections, USAEC Report KAPL-M-ECH-7, Knolls Atomic Power Laboratory, September 1960.
47. D. J. Hughes and R. B. Schwartz, Neutron Cross Sections, USAEC Report BNL-325, Brookhaven National Laboratory, July 1958.
48. The Industrial Graphite Engineering Handbook, National Carbon Company, Division of Union Carbide Corporation, 30 East 42nd Street, New York 17, New York, 1962.
49. T. Jarvis et al., Reactor Design and Feasibility Problem, USAEC Report ORNL-CF-53-10-26 (Cassified), Oak Ridge National Laboratory, August 1953.
50. L. V. Jones et al., Phase Equilibria in the LiF-BeF₂-UF₄ Ternary Fused Salt System, USAEC Report MLM-1080, Mound Laboratory, June 1957.
51. Kaiser Engineers Division, Steam-Cooled Power Reactor Evaluation, Capital and Power Generation Costs, USAEC Report TID-12747, H. J. Kaiser Co., March 1961.
52. Kaiser Engineers, Guide to Nuclear Power Cost Evaluation, USAEC Report TID-7025 (Vol. 1-5), Kaiser Engineers, March 1962.
53. B. W. Kinyon and G. D. Whitman, Steam Generator-Superheater for Molten Salt Power Reactor, Paper No. 61-WA-228, Am. Soc. Mech. Engrs., November 1961.
54. B. W. Kinyon and F. E. Romie, Two Thermodynamic Systems for Molten Fluoride Reactors, Trans. Am. Inst. Chem. Engrs. Preprint No. 177, Third Nuclear Science and Engineering Conference, March 1958.
55. W. E. Knabe and G. E. Putnam, Activity of Fission Products of ^{235}U , USAEC Report APEX-448, General Electric Atomic Products Division, October 1958.

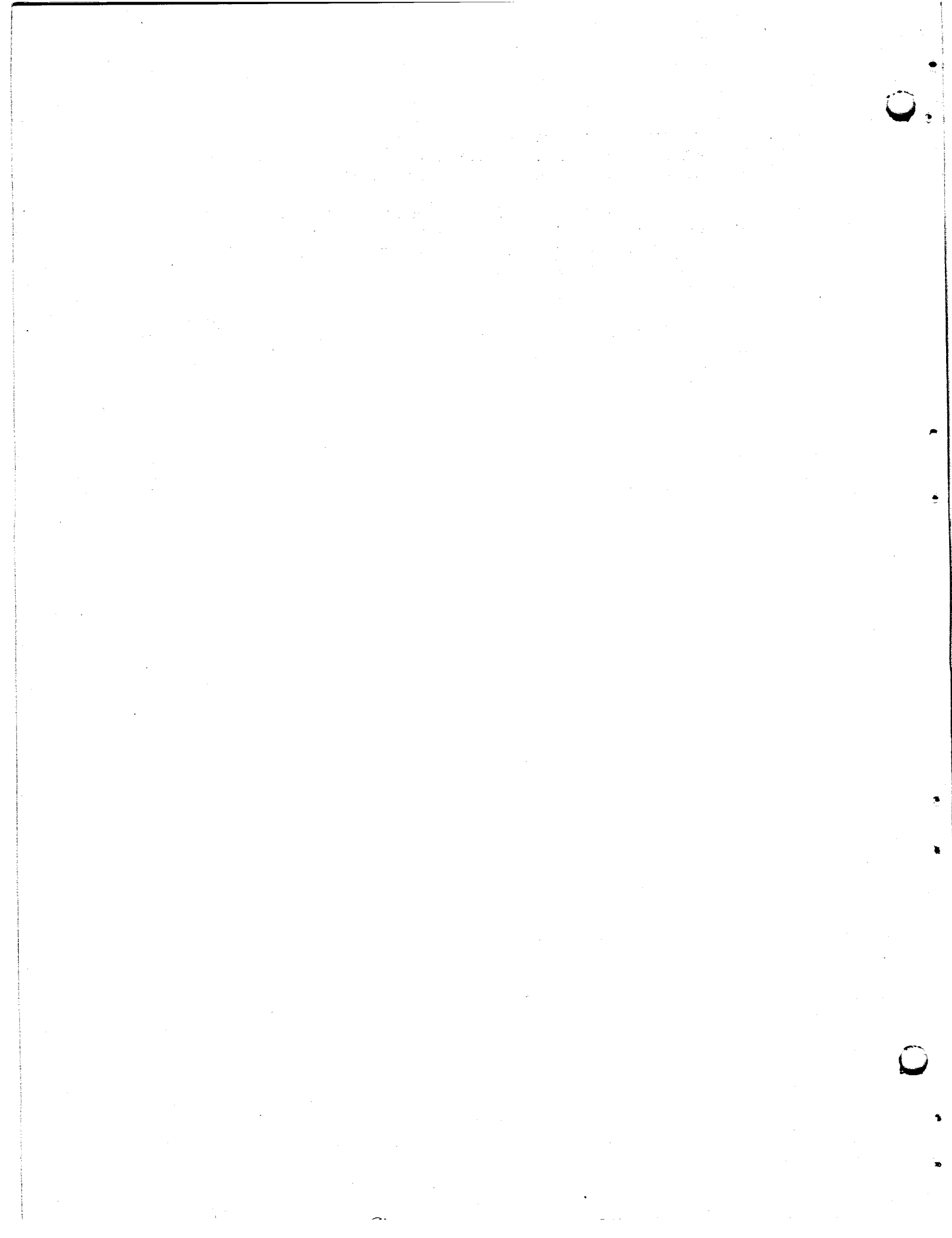
56. J. A. Lane, H. G. MacPherson, and F. Maslan (editors), *Fluid Fuel Reactors*, Addison-Wesley Publishing Company, Reading, Massachusetts, 1958.
57. H. G. MacPherson, *Molten Salts for Civilian Power*, USAEC Report ORNL-CF-57-10-41, Oak Ridge National Laboratory, October 1957.
58. H. G. MacPherson et al., *A Preliminary Study of Molten Salt Power Reactors*, USAEC Report CF-57-4-27 (Rev., Del.), Oak Ridge National Laboratory, April 1957.
59. H. G. MacPherson et al., *Molten Salt Reactor Program Status Report*, USAEC Report ORNL-2634, Oak Ridge National Laboratory, November 1958.
60. H. G. MacPherson et al., *A Preliminary Study of a Graphite-Moderated Molten Salt Power Reactor*, USAEC Report CF-59-1-26, Oak Ridge National Laboratory, January 1959.
61. H. G. MacPherson, *Optimizing the Molten-Salt Reactor for Minimum Doubling Time*, p. 335 of Proceedings of the Conference on the Physics of Breeding, USAEC Report ANL-6122, Argonne National Laboratory, October 1959.
62. H. G. MacPherson, *Molten-Salt Breeder Reactors*, USAEC Report ORNL-CF-59-12-64 (Revised), Oak Ridge National Laboratory, December 1959.
63. H. G. MacPherson, *Molten-Salt Reactors: Report for 1960 Ten-Year Plan Evaluation*, USAEC Report ORNL-CF-60-6-97, Oak Ridge National Laboratory, June 1960.
64. B. Manowitz, *Fuel Reprocessing Costs*, Nucleonics, 20(2):60, February 1962.
65. W. B. McDonald and C. I. McGlothlan, *Remote Maintenance of Molten Salt Reactors*, USAEC Report ORNL-2981, Oak Ridge National Laboratory (in preparation September 1962).
66. R. P. Milford et al., *Recovering Uranium Submarine Reactor Fuels*, Ind. Eng. Chem., 53:357, May 1961.
67. J. W. Miller, *Thorium Resonance Cross-Sections for Thermal Breeder Reactor Study*, USAEC Report ORNL-CF-61-1-26, Oak Ridge National Laboratory, January 1961.
68. E. C. Moncrief, *Corrosion of the Volatility Pilot Plant INOR-8 Hydrofluorinator and L-Nickel Fluorinator after 21 Nonradioactive Dissolution Runs*, USAEC Report ORNL-TM-186, Oak Ridge National Laboratory, March 1962.
69. M. S. Moore, MTR Nuclear Physics Group, personal communication to C. W. Nestor, Oak Ridge National Laboratory, March 1960.

70. J. P. Murray et al., Economics of Unirradiated Processing Phases of Uranium Fuel Cycles, Proceedings of the Second International Conference on the Peaceful Uses of Atomic Energy, Geneva, 1958, Vol. 13, Paper No. Pp439, p. 582, United Nations, New York, 1958.
71. E. A. Nephew, Thermal and Resonance Absorption Cross Section of the ^{233}U , ^{235}U , ^{239}Pu Fission Products, USAEC Report ORNL-2869, Oak Ridge National Laboratory, March 1960.
72. C. W. Nestor, Multigroup Neutron Cross Sections, USAEC Report ORNL-CF-61-6-87 (Rev.), Oak Ridge National Laboratory, June 1961.
73. Oak Ridge National Laboratory, Chemical Technology Division Unit Operations Section Monthly Progress Report, USAEC Report ORNL-TM-34, p. 44 (7.0 Volatility) Oak Ridge National Laboratory, June 1961.
74. Oak Ridge National Laboratory, Reactor Chemistry Division Annual Progress Report for Period Ending January 21, 1951, USAEC Report ORNL-3127.
75. Oak Ridge National Laboratory, Molten-Salt Reactor Program Quarterly Progress Report for Period Ending October 31, 1957, USAEC Report ORNL-2431.
76. Oak Ridge National Laboratory, Molten-Salt Reactor Program Quarterly Progress Report for Period Ending June 31, 1958, USAEC Report ORNL-2551.
77. Oak Ridge National Laboratory, Molten-Salt Reactor Program Quarterly Progress Report for Period Ending October 31, 1958, USAEC Report ORNL-2626.
78. Oak Ridge National Laboratory, Molten-Salt Reactor Project Quarterly Progress Report for Period Ending January 31, 1959, USAEC Report ORNL-2684.
79. Oak Ridge National Laboratory, Molten-Salt Reactor Project Quarterly Progress Report for Period Ending April 30, 1959, USAEC Report ORNL-2723.
80. Oak Ridge National Laboratory, Molten-Salt Reactor Program Quarterly Progress Report for Period Ending July 31, 1959, USAEC Report ORNL-2799.
81. Oak Ridge National Laboratory, Molten-Salt Reactor Program Quarterly Progress Report for Period Ending October 31, 1959, USAEC Report ORNL-2890.
82. Oak Ridge National Laboratory, Molten-Salt Reactor Program Quarterly Progress Report for Periods Ending January 31 and April 30, 1960, USAEC Report ORNL-2973.

83. Oak Ridge National Laboratory, Molten-Salt Reactor Program Quarterly Progress Report for Period Ending July 31, 1960, USAEC Report ORNL-3014.
84. Oak Ridge National Laboratory, Molten-Salt Reactor Program Progress Report for Period from August 1, 1960 to February 28, 1961, USAEC Report ORNL-3122.
85. Oak Ridge National Laboratory, Molten-Salt Reactor Program Progress Report for Period from March 1 to August 31, 1961, USAEC Report ORNL-3215.
86. Oak Ridge National Laboratory, Molten-Salt Reactor Program Semiannual Progress Report for Period Ending February 28, 1962, USAEC Report ORNL-3282.
87. Oak Ridge National Laboratory, Molten-Salt Reactor Program Semiannual Progress Report for Period Ending August 31, 1962, USAEC Report ORNL-3369.
88. Organization for European Economic Cooperation, Nuclear Graphite, OEEC Dragon Project, Proceedings of the Symposium Held at Bournemouth, G.B. Europ. Nuclear Energy Agency, p. 259 Session I-V, NP-11221, November 1959.
89. R. G Orrison, Union Carbide Nuclear Company (Y-12 Plant), personal communication to L. G. Alexander, Oak Ridge National Laboratory, December 1959.
90. J. J. Pattenden, Fission Product Poisoning Data, USAEC Report ORNL-2778, Oak Ridge National Laboratory, October 1959.
91. W. D. Powers and G. C. Blalock, Enthalpies and Heat Capacities of Solid and Molten Fluoride Mixtures, USAEC Report ORNL-1956, Oak Ridge National Laboratory, January 1956.
92. C. C. Randall et al., Study of Mercury Binary Cycles for Nuclear Power Plants, Report WCAP-1832, Westinghouse Electric Corp., July 1961.
93. J. E. Ricci, Guide to the Phase Diagrams of the Fluoride Systems, USAEC Report ORNL-2396, Oak Ridge National Laboratory, November 1958.
94. Sargent and Lundy, Engineers, Power Cost Normalization Studies, Civilian Power Reactor Program - 1959, USAEC Report SL-1674, January 1960.
95. Sargent and Lundy, Engineers, Capital Cost Evaluation 1000 Mwe Molten Salt Converter Reactor Power Plants, USAEC Report SL-1954, June 1962.
96. Sargent and Lundy, Engineers, Capital Investment for 1000 Mwe Molten Salt Converter Reference Design Power Reactor, USAEC Report SL-1994, December 1962.

97. J. H. Shaffer, W. R. Grimes, and G. M. Watson, Boron Trifluoride as a Soluble Poison in Molten Salt Reactor Fuels, Nuclear Sci. Eng., 12:337, March 1962.
98. J. W. H. Simmons, The Effects of Irradiation on the Mechanical Properties of Graphite, in Proceedings of the Third Conference on Carbon, Sections E and F, Pergamon Press, 1959.
99. I. Spiewak and L. F. Parsly, Evaluation of External Hold-up of Circulating Fuel Thermal Breeders as Related to Cost and Feasibility, USAEC Report ORNL-CF-60-5-93, Oak Ridge National Laboratory, May 1960.
100. P. E. Spivak et al., Measurement of Eta for ^{233}U , ^{235}U , and ^{239}Pu with Epithermal Neutrons, J. Nuc. Energy, 4:70, January 1957.
101. R. E. Thoma, Crystallization Reactions in the Mixture $\text{LiF-BeF}_2\text{-ThF}_4$ (67.5-17.5-15 mole %) BELT-15, USAEC Report ORNL-CF-59-4-49, Oak Ridge National Laboratory, April 1959.
102. R. E. Thoma (Editor) Phase Diagrams of Nuclear Reactor Materials, USAEC Report ORNL-2548, Oak Ridge National Laboratory, November 1959.
103. R. E. Thoma and W. R. Grimes, Phase Equilibrium Diagrams for Fused Salt Systems, USAEC Report ORNL-2295 (Decl.), Oak Ridge National Laboratory, June 1959.
104. USAEC, Summary Report: AEC Reference Fuel Processing Plant, USAEC Report WASH-743, October 1957.
105. W. T. Ward et al., Rare Earth and Yttrium Fluorides - Solubility Relations in Various Molten NaF-ZrF_4 and $\text{NaF-ZrF}_4\text{-UF}_4$ Solvents, USAEC Report ORNL-2421, Oak Ridge National Laboratory, January 1958.
106. W. T. Ward et al., Solubility Relations Among Rare-Earth Fluorides in Selected Molten Fluoride Solvents, USAEC Report ORNL-2749, Oak Ridge National Laboratory, October 1959.
107. G. M. Watson and R. B. Evans III, Xenon Diffusion in Graphite: Effects of Xenon Absorption in Molten Salt Reactors Containing Graphite, USAEC Report ORNL-CF-61-2-59, Oak Ridge National Laboratory, February 1961.
108. C. F. Weaver et al., Phase Equilibria in Molten Salt Breeder Reactor Fuels, I - The System $\text{LiF-BeF}_2\text{-ThF}_4$, USAEC Report ORNL-2896, Oak Ridge National Laboratory, December 1960.
109. D. B. Wehmeyer et al., Study of a Fused Salt Breeder Reactor for Power Production, USAEC Report ORNL-CF-53-10-25, Oak Ridge National Laboratory, September 1953.

110. C. H. Wescott, Effective Cross Section Values for Well-Moderated Thermal Reactor Spectra, Canadian Report CRRP-787, Chalk River, Ontario AECL-670, August 1, 1958 (Rev. 1958).
111. N. F. Wikner and S. Jaye, Energy-Dependent and Spectrum-Averaged Thermal Cross Sections for the Heavy Elements and Fission Products for Various Temperatures and C:²³⁵U Atom Ratios, USAEC Report GA-2113, General Atomic Division, General Dynamics Corporation, June 1961.
112. H. U. Woelk, Molten Salts in Nuclear Technology, Chemie-Ingenieur-Technik, 32:765, 1960. AEC-TR-4774 by A. R. Saunders and H. H. Stone, Oak Ridge National Laboratory, August 1961.



Internal Distribution

- | | |
|-------------------------|---|
| 1. T. D. Anderson | 68. C. G. Lawson |
| 2-20. L. G. Alexander | 69. R. B. Lindauer |
| 21. H. F. Bauman | 70. J. L. Lucius |
| 22. S. E. Beall | 71. M. I. Lundin |
| 23. L. L. Bennett | 72. R. N. Lyon |
| 24. E. S. Bettis | 73. H. G. MacPherson |
| 25. F. F. Blankenship | 74. H. C. McCurdy |
| 26. E. P. Blizzard | 75. W. B. McDonald |
| 27. A. L. Boch | 76. H. F. McDuffie |
| 28. E. G. Bohlmann | 77. R. P. Milford |
| 29. C. J. Borkowski | 78. A. J. Miller |
| 30. R. B. Briggs | 79. R. L. Moore |
| 31. F. R. Bruce | 80. J. C. Moyers |
| 32. D. O. Campbell | 81. R. W. Olson |
| 33. S. Cantor | 82. H. R. Payne |
| 34. W. L. Carter | 83. A. M. Perry |
| 35. G. I. Cathers | 84. B. E. Prince |
| 36. R. H. Chapman | 85. R. C. Robertson |
| 37. R. S. Carlsmith | 86. M. W. Rosenthal |
| 38. C. W. Collins | 87. H. W. Savage |
| 39. W. H. Cook | 88. A. W. Savolainen |
| 40. C. W. Craven | 89. D. Scott |
| 41. F. L. Culler | 90. J. H. Schaffer |
| 42. S. G. Delene | 91. M. J. Skinner |
| 43. J. H. DeVan | 92. I. Spiewak |
| 44. R. G. Donnelly | 93. W. G. Stockdale |
| 45. D. A. Douglas | 94. A. Taboada |
| 46. J. R. Engel | 95. J. R. Tallackson |
| 47. W. K. Ergen | 96. R. E. Thoma |
| 48. A. P. Fraas | 97. D. B. Trauger |
| 49. J. H. Frye, Jr. | 98. J. W. Ullman |
| 50. W. R. Gall | 99. D. R. Vondy |
| 51. E. H. Gift | 100. R. Van Winkle |
| 52. H. E. Goeller | 101. G. M. Watson |
| 53. W. R. Grimes | 102. A. M. Weinberg |
| 54. A. G. Grindell | 103. J. H. Westsik |
| 55. C. E. Guthrie | 104. G. D. Whitman |
| 56. R. P. Hammond | 105. K. J. Yost |
| 57. P. N. Haubenreich | 106. Gale Young |
| 58. E. C. Hise | 107. Biology Library |
| 59. H. W. Hoffman | 108-109. Reactor Division Library |
| 60. D. B. Janney (K-25) | 110-111. MSRP Director's Office,
Room 219, Building 9204-1 |
| 61. W. H. Jordan | 112-113. ORNL Y-12 Technical Library,
Document Reference Section |
| 62. P. R. Kasten | 114-115. Central Research Library |
| 63. R. J. Kedl | 116-145. Laboratory Records Department |
| 64. M. T. Kelley | 146. Laboratory Records, ORNL,
R.C. |
| 65. T. W. Kerlin | |
| 66. J. A. Lane | |
| 67. C. E. Larson | |

External Distribution

147. G. Beasley, TVA, EGCR Site, Oak Ridge, Tennessee
148. W. R. Cooper, TVA, EGCR Site, Oak Ridge, Tennessee
- 149-150. D. F. Cope, AEC, ORO
151. W. E. Dean, Jr., TVA, Chattanooga, Tennessee
152. Division of Research and Development, AEC, ORO
153. J. Ebersole, TVA, EGCR Site, Oak Ridge, Tennessee
154. W. F. Emmons, TVA, Knoxville, Tennessee
155. R. W. Garrison, AEC, Washington, D. C.
156. R. Harris, AEC, ORO
- 157-158. C. A. Hatstat and W. Chittenden, Sargent and Lundy, Chicago, Illinois
159. S. Jaye, General Atomic, San Diego, California
160. R. W. McNamee, Manager, Research Administration, UCC, New York, N. Y.
161. G. P. Palo, TVA, Knoxville, Tennessee
162. R. E. Pahler, AEC, Washington, D. C.
163. P. F. Pasqua, University of Tennessee, Knoxville, Tennessee
164. R. L. Phillipone, Reactor Division, AEC, ORO
165. H. M. Roth, Division of Research and Development, AEC, ORO
166. F. P. Self, AEC, Washington, D. C.
167. W. L. Smalley, Research Division, AEC, ORO
168. J. M. Vallance, AEC, Washington, D. C.
169. M. J. Whitman, AEC, Washington, D. C.
170. J. Wett, AEC, Washington, D. C.
- 171-185. Division of Technical Information Extension (DTIE)